
Imaging of the dynamics of Eph receptors and their ephrin ligands in mature hippocampal neurons

Jenny Köhler



München 2005

For Amalia Casselmann

Imaging of the dynamics of Eph receptors and their ephrin ligands in mature hippocampal neurons

Dissertation
an der Fakultät für Biologie
der Ludwig–Maximilians–Universität
München

vorgelegt von
Jenny Köhler
aus Hanau

München, den 02.06.2005

Erstgutachter:

Zweitgutachter:

Tag der mündlichen Prüfung:

PD Dr. Rüdiger Klein

Prof. Dr. Tobias Bonhoeffer

13.09.2005

Erklärung

Ich versichere, daß ich die Dissertation "Imaging of the dynamics of Eph receptors and their ephrin ligands in mature hippocampal neurons" selbstständig und ohne unerlaubte Hilfe angefertigt habe. Ich habe mich dabei keiner anderen als der von mir ausdrücklich bezeichneten Hilfen und Quellen bedient.

Die Dissertation wurde in der jetzigen oder ähnlichen Form bei keiner anderen Hochschule eingereicht und hat noch keinen sonstigen Prüfungszwecken gedient.

(Ort, Datum)

(Jenny Köhler)

Contents

1. Abbreviations	1
2. Publication from the work presented in this dissertation	7
3. Summary	9
4. Introduction	11
4.1. The synapse	12
4.1.1. Glutamate receptors	12
4.1.2. The postsynaptic density	13
4.2. Synaptic plasticity	15
4.3. Glial cells	17
4.3.1. Properties and functions of neuroglial cells	18
4.4. Eph receptors and their ephrin ligands	19
4.4.1. The Eph class of receptor tyrosine kinases	20
4.4.2. Ephrin ligands	21
4.4.3. Structure of Eph RTKs and ephrin ligands	22
4.4.3.1. Receptor structure	22
4.4.3.2. Ligand structure	22
4.4.4. Bi-directional signalling between Eph receptor and ephrin ligands	24
4.4.4.1. Binding and activation of Eph/ephrins	24
4.4.4.2. Mechanisms of Eph receptor forward signalling	26
4.4.4.3. Signal transduction through ephrin reverse signalling	29
4.4.5. Repulsion and adhesion in cell-to-cell contact	32
4.4.5.1. Cleavage of ephrin ligands	32
4.4.5.2. Regulated endocytosis of Eph-ephrin complexes	33

4.5.	Eph receptors in the adult brain	35
4.5.1.	Expression patterns of ephrins/Ephs in the adult hippocampus	35
4.5.2.	Dendritic spine morphogenesis during development and plasticity	36
4.6.	The thesis project	41
5.	Materials and Methods	43
5.1.	Materials	43
5.1.1.	Chemicals, enzymes and commercial kits	43
5.1.2.	Equipment	45
5.1.3.	Consumable material	47
5.1.4.	Oligonucleotides	49
5.1.5.	Bacteria	50
5.1.6.	Plasmids	51
5.1.6.1.	EphB2 expression constructs	51
5.1.6.2.	EphB2-ExFP expression constructs	52
5.1.6.3.	Thy1-EphB2-EYFP expression constructs for injection	54
5.1.6.4.	ExFP-HA-ephrinB1 and -ephrinB2 expression constructs	54
5.1.7.	Cell lines	55
5.1.8.	Antibodies	55
5.1.8.1.	Primary antibodies	55
5.1.8.2.	Secondary antibodies	57
5.1.9.	Media and standard solutions	58
5.1.9.1.	Media and antibiotics for bacterial culture	60
5.1.9.2.	Media and supplements for tissue culture	60
5.1.9.3.	Media and supplements for primary cell culture	61
5.1.9.4.	Reagents for primary culture of astrocytes	62
5.1.9.5.	Media and solutions for cell transfection	62
5.1.9.6.	Reagents for live-cell imaging	63
5.1.9.7.	Solutions and buffers for western blot analysis	63
5.1.9.8.	Solutions for embedding of vibratome sections	66
5.1.9.9.	Solutions for <i>in situ</i> hybridization	66
5.1.9.10.	Reagents for electrophysiology	68
5.2.	Methods	69
5.2.1.	Molecular Biology	69

5.2.1.1.	Preparation of plasmid DNA	69
5.2.1.2.	Enzymatic treatment of DNA	69
5.2.1.3.	Separation of DNA on agarose gels	70
5.2.1.4.	Purification of DNA	70
5.2.1.5.	Preparation of competent <i>E.coli</i>	71
5.2.1.6.	Transformation of competent <i>E. coli</i> using calcium chloride . .	71
5.2.1.7.	Transformation of competent <i>E. coli</i> by electroporation	71
5.2.1.8.	Screening bacterial colonies using X-gal and IPTG	72
5.2.1.9.	Polymerase chain reaction (PCR) & TOPO cloning	72
5.2.1.10.	Mutagenesis	73
5.2.1.11.	Cloning and generation of <i>in situ</i> probes	73
5.2.1.12.	Extraction of genomic DNA and genotyping using PCR	74
5.2.1.13.	Generation of transgenic mice	75
5.2.2.	Cell culture	77
5.2.2.1.	Propagation and freezing of mammalian cells	77
5.2.2.2.	Primary culture of hippocampal neurons	77
5.2.2.3.	Primary culture of glia	78
5.2.2.4.	Transfection of cell lines, primary neurons	79
5.2.2.5.	Stimulation of cells with Eph receptors or ephrin ligands . . .	80
5.2.2.6.	Time lapse imaging	80
5.2.2.7.	Chemical stimulation of neurons	81
5.2.3.	Biochemistry	81
5.2.3.1.	Cell lysis and immunoprecipitation of proteins	81
5.2.3.2.	Immunoblotting	82
5.2.4.	Mouse work	82
5.2.5.	Histology	82
5.2.5.1.	Cryosections	82
5.2.5.2.	Vibratome sections	83
5.2.5.3.	Antibody staining	83
5.2.5.4.	Immunocytochemistry	84
5.2.5.5.	<i>in situ</i> hybridization	85
5.2.6.	Electrophysiology	86
5.2.6.1.	Organotypic acute hippocampal slices	86
5.2.6.2.	Electrophysiological recordings	86

5.2.6.3. Data analysis	87
5.3. Ordering information	88
6. Results	91
6.1. Generation of fluorescently tagged EphB2 receptors	91
6.1.1. Analysis of tagged EphB2 receptors	92
6.1.1.1. Expression	92
6.1.1.2. Tyrosine phosphorylation	93
6.1.2. Cluster behaviour of the different EphB2-ExFP receptors	96
6.1.3. Clustering of fluorescently tagged EphB2-C1 receptors	97
6.1.4. Cluster formation of EphB2-C1 in young and old cultures	99
6.1.5. Specificity of EphB2-C1 clustering	102
6.1.6. Localization of EphB2-C1 in the neuron	103
6.1.7. Localization of fluorescently tagged EphB2 receptors in filopodia and other dendritic protrusions	106
6.1.8. Cytoplasmic clusters of fluorescently tagged EphB2 receptors	108
6.2. Live cell imaging of tagged EphB2 receptors	110
6.3. Generation and analysis of transgenic mice	115
6.3.1. Patterns of transgene expression	116
6.3.1.1. Full-length EphB2-C1-EYFP (line A-N, P-W)	116
6.3.1.2. Kinase-dead EphB2-C1-EYFP (line Ka-Kh)	117
6.3.1.3. C-terminal truncated EphB2-C1-EYFP (line Da-Dk)	119
6.3.2. <i>In situ</i> hybridization data of different transgenic <i>thy1-EphB2-C1</i> mice . .	123
6.3.3. Overexpression of EphB2-C1 or EphB2- Δ C in transgenic mice does not affect CA3-CA1 hippocampal LTP	125
6.4. Transcytosis of EphB2-C1 receptors	127
6.4.1. Reverse transcytosis of EphB2-C1 receptors in mature primary hippocam- pal cultures	127
6.4.2. Reverse transcytosis of EphB2-C1-EYFP proteins followed by persistent retraction of the neuronal protrusion	130
6.4.3. Transcytosis is not a general phenomenon among the Eph and ephrin classes of protein families	132
6.4.4. Reverse transcytosis of EphB2-C1 in mature primary hippocampal low- density cultures	133

6.5. Supplementary information on CD-Rom	136
7. Discussion	139
7.1. Transcytosis of EphB2 receptors in primary hippocampal cultures	139
7.1.1. Overexpression of full-length EphB2-C1-EYFP receptors lead to transcytosis in primary hippocampal cultures	139
7.1.2. What could be the <i>in vivo</i> relevance of Eph receptor transcytosis by glial cells?	146
7.2. Generation and analysis of the different fluorescently tagged EphB2 receptors .	148
7.3. Transgenic mice expressing EphB2-C1 variants driven by the Thy-1.2 expression cassette	151
7.3.1. Patterns of transgene expression and their fluorescent intensities	151
7.3.2. Overexpression of full-length or C-terminal truncated EphB2-C1-EYFP receptor does not affect synaptic plasticity	153
8. Acknowledgements	175
A. Curriculum vitae	177

List of Figures

4.1. Ultrastructure of the synapse	14
4.2. Long-term potentiation in the hippocampus	15
4.3. Astrocytes as regulators of synaptic activity, synaptogenesis & neurogenesis	17
4.4. The Eph class of receptor tyrosine kinases and their ligands	20
4.5. Domain structure of Eph receptor and ephrin ligands	23
4.6. Mechanism of Eph receptor activation and the initiation of bi-directional signalling	25
4.7. Molecular mechanisms of cytoskeletal regulation downstream of EphA forward signalling	28
4.8. Summary of ephrinB signal transduction pathway described in the text . . .	30
4.9. Repulsion and adhesion in cell-to-cell contact	33
4.10. EphB receptors drive dendritic spine morphogenesis	38
4.11. NMDA and EphB2 receptor and their possible role during synapse formation, maturation and synaptic plasticity	40
6.1. Schematic view of the ExFP insertions sites in the EphB2 receptor	91
6.2. Expression of fluorescently tagged EphB2 receptors and ephrinB1	92
6.3. Tyrosine phosphorylation of EphB2 receptors	93
6.4. Interaction of EphB2-ExFP receptors with NR1 and GRIP2	95
6.5. Comparison of the different EphB2-ExFP proteins before and after ephrinB stimulation	96
6.6. Clustering of EphB2-C1 before and after ephrinB1 stimulation in 6-day-old neuronal cultures	98
6.7. Comparison of control-stimulated versus ephrinB1-stimulated EphB2-C1 expressing neurons in young and older cultures	101

6.8. Clusters of the EphB2 receptor are visible in dendritic spines of old neurons (DIV23) without ephrinB stimulation	101
6.9. Stimulation of EphB2-C1 expressing hippocampal neurons with different Fc fusion proteins	102
6.10. EphB2-C1 is located in axons and dendrites of control-stimulated hippocampal neurons	104
6.11. EphB2-C1 is expressed in axons and dendrites of ephrinB-stimulated hippocampal neurons	105
6.12. Fluorescently tagged EphB2 receptors are located at filopodia and other dendritic protrusions	106
6.13. EphB2 receptors are located at the surface of filopodia and other dendritic protrusions	108
6.14. Cytoplasmic clusters of fluorescently tagged EphB2 receptors in neurites	109
6.15. Schematic diagram of the EphB2-C1 variants	110
6.16. Comparison of unstimulated versus ephrinB2-stimulated young neurons expressing one variant of EphB2-C1-EYFP during live-cell imaging	111
6.17. Comparison of unstimulated versus ephrinB2-stimulated more mature neurons expressing one variant of EphB2-C1-EYFP during live-cell imaging	113
6.18. Summary of the effects observed during live-time imaging of young and more mature hippocampal neurons expressing one variant of the different EphB2-C1 receptors	114
6.19. Transgene expression in the hippocampal formation of adult Thy-EphB2-C1-EYFP mice	117
6.20. Sparse expression of EphB2-C1-EYFP in the adult transgenic mouse	119
6.21. Expression pattern of kinase-deficient EphB2-C1-EYFP in the hippocampal formation of adult transgenic mice	121
6.22. Expression pattern of C-terminal truncated EphB2-C1-EYFP in the hippocampal formation of adult transgenic mice	122
6.23. Comparison of <i>in situ</i> hybridization data with the fluorescent signal of hippocampal sections of different transgenic lines	123
6.24. <i>In situ</i> hybridization analysis of hippocampal sections of <i>thy1-YFP</i> transgenic mice and a wild type animal	124
6.25. LTP was not affected in hippocampal neurons overexpressing full-length or C-terminal truncated EphB2-C1 in adult transgenic mice	126

6.26. Reverse transcytosis of EphB2-C1-EYFP in a primary neuronal culture during live-cell imaging after neuron-to-cell contact	128
6.27. Reverse transcytosis of EphB2-C1-EYFP into adjacent cells of a mature primary hippocampal culture after neuron-to-cell contact	130
6.28. Reverse transcytosis of EphB2-C1-EYFP followed by retraction of a neuronal protrusion from the dendritic shaft	131
6.29. Quantification of percentage of transcytosis in transfected neuronal high-density cultures	132
6.30. Reverse transcytosis of EphB2-C1-EYFP from an axonal filopodium into a glial process is followed by withdrawal of glia	135

List of Tables

1.1. Abbreviations	1
5.1. Chemicals & commercial kits	43
5.2. Equipment	45
5.3. Consumable materials	47
5.4. Oligonucleotides	49
5.5. Bacterial strains	50
5.6. Vectors	51
5.7. Primary antibodies	55
5.8. Secondary antibodies	57
5.9. Order Information	88

1. Abbreviations

Units were abbreviated using the International System of Units (SI). The single letter code was used for amino acids and nucleotides and abbreviations according to common words the dictionary was used.

Table 1.1. Abbreviations

aa	amino acid(s)
Abi-1	Abl interacting protein-1
Abl	Abelson
ACSF	artificial cerebrospinal fluid
ADAM	A-Disintegrin-And-Metalloprotease
AF-6	Acute myeloid leukemia-1/chromosome 6 fusion protein/afadin-6
Amp	ampicillin
AMP	adenosine 5'-monophosphate
AMPA	α -amino-3-hydroxy-5-methyl-4-isoxazole propionic acid
AP	alkaline phosphatase
APS	ammonium persulfate
APV	2-amino-5-phosphonovaleric acid
Arg	Abelson-related gene
Arp2/3	actin-related protein 2/3
ATP	adenosine 5'-triphosphate
Borax	sodium tetraborate
BBS	BES buffered saline
BCIP	5-bromo-4-chloro-3-indolyphosphate
BES	N,N-bis[2-hydroxyethyl]-2-aminoethanesulfonic acid
bp	base pairs
BSA	bovine serum albumin

1. Abbreviations

CA	Cornu ammonis
CAM	cell-adhesion protein
CamKII	Ca ²⁺ /Calmodulin-dependent kinase II
cAMP	cyclic AMP
CAP	c-Cbl associated protein
CHAPS	3-[(3-Cholamidopropyl)dimethylammonio]-1-propanesulfonate
cDNA	complementary DNA
CMV	cytomegalovirus
CNS	central nervous system
CREB	Ca ²⁺ /cAMP-responsive element binding protein
C-terminus	carboxy terminus
CXCR	chemokine receptor of CXCR-family
Da	Dalton (g/mol)
DG	dentate gyrus
DIG	digoxigenin
DIV	days <i>in vitro</i>
DMEM	Dulbecco's modified Eagle's medium
DMSO	dimethylsulfoxide
DNA	desoxyribonucleic acid
dNTPs	deoxyribonucleoside triphosphates
dsDNA	double strand DNA
DTT	1,4-Dithio-DL-threitol
E	embryonic day
ECFP	enhanced cyan/blue fluorescent protein
ECL	enhanced chemoluminescence
<i>E. coli</i>	<i>Escherichia coli</i>
EDTA	ethylenediaminetetraacetic acid
Eph	erythropoietin-producing hepatocellular
ephrin	Eph receptor interacting
EGF	epidermal growth factor
EGFP	enhanced green fluorescent protein
EGFR	epidermal growth factor receptor
EPSP	excitatory postsynaptic potential
Erk	extracellular-signal regulated kinase

EtOH	ethanol
ExFP	ECFP, EGFP or EYFP
EYFP	enhanced yellow fluorescent protein
FAK	focal adhesion kinase
FBS	fetal bovine serum
fEPSP	field EPSP
fig.	figure
FNIII	fibronectin type III
G protein	GTP-binding protein
GAP	GTPase-activating protein
GDP	guanosine diphosphate
GEF	guanine nucleotide exchange factor
GluR	glutamate receptor subunit
GPI	glycosylphosphatidylinositol
Grb	growth-factor receptor bound
GRIP	glutamate receptor interacting protein
GTP	guanosine triphosphate
HEPES	N-2-hydroxyethylpiperanzine-N'-2-ethanesulfonic acid
HEK	human embryonic kidney
HeLa	Henrietta Lacks
HBSS	Hank's balanced salt solution
HC	heavy chain
HRPO	horseradish peroxidase
HS	horse serum
HUVEC	human umbilical cord venous endothelial cell
IF	immunofluorescence
Ig	immunoglobulin
IHC	immunohistochemistry
IP	immunoprecipitation
IPTG	isopropyl β -D-thiogalactopyranoside
KA	kainate receptor subunit
Kan	kanamycin monosulfate
kb	kilo bases
KD	kinase dead

1. Abbreviations

Kuz	Kuzbanian
<i>lacZ</i>	gene encoding β -galactosidase
LB	Luria-Bertani
LC	light chain
LMW-PTP	low molecular weight phosphotyrosine phosphatase
LTD	long-term depression
LTP	long-term potentiation
MAP	mitogen-activated protein
MAP2	microtubule-associated protein 2
MAPK	mitogen-activated protein kinase
MB	mushroom body
MEM	minimal essential medium
mGluR	metabotropic glutamate receptor
MOPS	3-(N-Morpholino)propanesulfonic acid, 4-Morpholinepropanesulfonic acid
NBT	nitroblue tetrazolium
Nck	noncatalytic region of tyrosine kinase
NGF	nerve growth factor
NMDA	N-methyl-D-aspartate
NMJ	neuromuscular junction
NP-40	Nonidet P-40
NR	NMDA receptor subunit
N-terminus	amino terminus
N-WASP	neural Wiskott-Aldrich syndrome protein
OD	optical density
O/N	over night
P	postnatal day
p.a.	per analysis
PAGE	polyacrylamide-gel-electrophoresis
Pak	p21 activated kinase
PBS	phosphate-buffered saline
PBST	PBS with Tween
PCR	polymerase chain reaction
PDZ	postsynaptic density-95/discs-large/zona occludens 1
PDZ-RGS	PDZ-regulator of heterotrimeric G-protein signalling

PFA	paraformaldehyde
pH	<i>potentium hydrogenii</i>
PHIP	pleckstrin-homology-domain interacting protein/ ephrin interacting protein
PI3K	phosphatidylinositol 3-kinase
PICK	protein interacting with C kinase
PKA	protein kinase A
PKC	protein kinase C
PMSF	phenylmethylsulfonyl fluoride
PP	protein phosphatase
PPF	paired-pulse facilitation
PSD	postsynaptic density
PSD-95	postsynaptic density protein 95
PTP	post tetanic potentiation
PTP1B	protein tyrosine phosphatase-1B
PTP-BL	protein tyrosine phosphatase-basophil-like
pY	phospho-tyrosine
RasGAP	Ras-GTPase activation protein
Ref.	reference
RNA	ribonucleic acid
rpm	rounds per minute
RT	room temperature
RTK	receptor tyrosine kinase
Ryk	receptor-like tyrosine kinase
SAM	sterile α -motif
SDF-1	stromal-cell-derived factor-1
SDS	sodium dodecyl sulfate
SEM	standard error of the mean
SFK	src family kinase
SH	src homology
SHEP	SH2 domain-containing Eph receptor-binding protein
SLAP	Src-like adaptor protein
SSC	sodium salt citrate
src	sarcoma virus transforming gene product
TAE	Tris-acetate EDTA

1. Abbreviations

TBS	thetaburst stimulation
TE	Tris-EDTA
TEMED	N,N,N',N'-Tetramethylethylenediamine
tet	Tetracycline
TK	tyrosine kinase
TNF- α	tumour necrosis factor- α
Tris	Tris[hydroxymethyl]aminomethane
TX-100	Triton X-100
U	unit(s)
UV	ultra-violet
WB	western blot
wt	wild type
X-gal	5-Bromo-4-chloro-3-indolyl- β -D-galactopyranoside

2. Publication from the work presented in this dissertation

Zimmer M., Palmer A., Köhler J., and Klein R.

EphB-ephrinB bi-directional endocytosis terminates adhesion allowing contact mediated repulsion.

Nature Cell Biology (2003) 5(10):869-878

3. Summary

The Eph receptors comprise the largest subfamily of receptor tyrosine kinases (RTKs) with important roles during neuronal development. Unlike other RTKs, these receptors can be activated by their membrane bound ligands, the ephrins. Recent evidence strongly suggests that Eph receptors and their ligands also contribute to synapse formation and synaptic plasticity in the postnatal brain. However, the details of the mechanisms still remain unclear.

In order to better understand the role of EphB2 receptors during these processes in living cells, EphB2 receptors were visualized. Therefore, one variant of the enhanced blue, green, or yellow fluorescent protein (E(C/G/Y)FP) was fused to the receptor. For this, ExFP was inserted in one of three different positions of EphB2: the N-terminus (EphB2-N), a site close to the juxtamembrane region (EphB2-C1) and between two functional relevant domains of the cytoplasmic tail (EphB2-C2). The different EphB2-ExFP receptors, EphB2-N, EphB2-C1 and EphB2-C2, were exogenously expressed in cell lines and showed intense fluorescence at the plasma membrane, comparable to other described transmembrane ExFP fusion proteins. Biochemical methods were used to test functionality of the different EphB2-ExFP proteins concerning tyrosine phosphorylation and interaction with known proteins, such as NR1 and GRIP2, and showed no obvious impairment. Surprisingly, however, the cluster behaviour of the EphB2-ExFP variants transiently expressed in neurons was different, only the EphB2-C1 proteins revealed a proper cluster formation after ephrinB stimulation, indicating that the ExFP insertion at the N- and C-terminus impaired the clustering.

In order to study the dynamics of trafficking, insertion and cluster behaviour of fluorescently tagged EphB2 receptors in living neurons, hippocampal cultures were transfected with these constructs. EphB2-C1 expressing neurons revealed two pools of fluorescent clusters, one pool was static, representing EphB2 receptors at the plasma membrane, whereas the other pool was trafficking along neurites, presumably reflecting EphB2 proteins in transport vesicles. In addition, the subcellular distribution of these receptors was analyzed, revealing that e.g. EphB2 clusters are present at the tips of filopodia and in growth cones. Filopodia are highly dynamic structures, which explore the environment and therefore have to extend and retract a lot. Our

3. Summary

group recently described a new mechanism of how an adhesive Eph-ephrin interaction between filopodia of immature growth cones and EphB2-expressing cell lines can be turned into a retraction response by bi-directional EphB/ephrinB-triggered trans-endocytosis. Intrigued by these findings, we were interested whether bi-directional transcytosis also exists in mature hippocampal cultures, presumably being involved in the dynamics of filopodia. The present thesis could show that after contact of mature neurons with cells, most-likely glial cells, the exogenous expression of fluorescently tagged EphB2 receptors in neurons induces a retrograde transcytosis into the interacting neighbouring cell. This reverse transcytosis of EphB2-C1 proteins was often followed by persistent retraction of the neuronal protrusion. This could have a potential role in axon pruning or in morphological plasticity in mature neurons, thereby adjusting the proper connectivity.

In a second approach, *thy1-EphB2-C1-EYFP* transgenic mice were generated to gain insights into the *in vivo* behaviour of these fluorescently tagged proteins and to have a closer look in the dynamics and cluster behaviour of EphB2 receptors during synaptogenesis and in spines of more mature neurons. Contrary to our expectations, both the fluorescent intensities and the distribution of the EphB2-C1-EYFP proteins in these transgenic mice were not bright nor sparse enough for conclusive imaging experiments.

4. Introduction

The human brain is a complex structure. It consists of trillions of cells, about roughly 10^{12} cells are nerve cells (neurons) and at least 10^{13} cells are glial cells (Haydon, 2001). These cells are interconnected and build up the complex brain architecture. The neuronal network is superbly organized in brain areas that construct our perceptions of the external world, fix our attention and control the machinery of our actions. These brain structures and regions have to develop a correct cellular organization and synaptic connectivity. During embryonic development of the nervous system, precursor cells produce through extensive cell proliferation postmitotic neurons and glial progenitor cells. These cells then migrate to build the different brain structures. An important next step is the correct wiring and the establishment of proper interconnections of these neurons among and within different brain areas. To achieve this, neurons extend axons tipped with growth cones that explore the environment, navigate along specific pathways, recognize their appropriate targets and then form synaptic connections by elaborating terminal arbors. Growth cone navigation is controlled by long- and short-range attractive and repulsive guidance cues. Upon arrival at the target region, functional synaptic contacts are rapidly formed. However, this initial connectivity is not rigid, but needs to be refined throughout early development and also later during adult life.

During our lifetime we experience and learn continuously to adapt to our environment. The basis behind this is the functional and anatomical modifiability of neuronal connections due to activity-dependent plasticity. How exactly these cellular events are regulated and which molecules contribute to it, will be the focus of this study with particular emphasis on the Eph/ephrin system.

I will first introduce some of the morphological structures and molecular components responsible for synaptic plasticity. I will then describe the Eph receptors and the ephrin ligands and their bi-directional signalling. Finally, a description of transcytosis and the resulting cell detachment as a possible mechanism for axon guidance in early development, e.g. through axon repulsion will be presented.

4.1. The synapse

Densely packed neuronal and glial cells are interconnected in systems and form a net: the central nervous system (CNS) - with over 10^{15} synaptic and even more extrasynaptic connections. The CNS is an active assembly of cells that continuously receives information, analyzes it, perceives it and makes decisions. In the brain, information is communicated between neurons in the form of electrical signals. This communication occurs at highly specialized sites of contact between a presynaptic nerve terminal and a postsynaptic neuron – the synapse.

A typical neuron has four morphologically defined regions: the dendrites, the cell body, the axon and the presynaptic terminals. The branched dendrites are the main apparatus for receiving incoming signals from other cells. In contrast, the usually long axon is the main conducting unit for carrying signals to other neurons or target organs. The information is transmitted in the form of chemical transmitters released from synaptic vesicles in the presynaptic terminal of the axon into the synaptic cleft (~ 25 nm wide). After rapid diffusion across the synaptic cleft, the neurotransmitters bind to their specific receptors (transmitter-gated ion channels) in the postsynaptic membrane of the dendrite, where the message is processed, integrated and propagated. Depending on the kind of transmitter and the ion channel, an electric signal can cause an inhibitory or excitatory synaptic input in the target cell. The postsynaptic site of many synapses is specialized in a thorny-like protrusion called a spine (Cajal, 1888).

4.1.1. Glutamate receptors

The amino acid glutamate is the most important and prevalent excitatory neurotransmitter in the mammalian brain and spinal cord and acts through the binding on different types of glutamate receptors: the ionotropic receptors and the metabotropic receptors. Ionotropic receptors form ion channels (glutamate-gated cation channels) and are the most common of all transmitter-gated channels in the brain. According to their different sensitivities to glutamate analogues and sequence similarities, they can be divided into three functionally distinct subclasses: N-methyl-D-aspartate (NMDA) receptors, α -amino-3-hydroxy-5-methyl-4-isoxazole propionic acid (AMPA) receptors and kainate receptors (Hollmann and Heinemann, 1994; Dingledine et al., 1999). The channels are multimeric complexes composed of a combinatorial assembly of two to four subunits. These subunits NR1 and NR2A through NR2D are involved in the formation of NMDA receptors. AMPA receptors are assembled from another set: GluR1 through GluR4 (GluRA-GluRD) and kainate receptors are combinations of the subunits KA1-KA2 and GluR5-GluR7 (Wisden and Seeburg, 1993; Bettler and Mülle, 1995). The subunit com-

position of glutamate receptors varies, creating great structural and functional heterogeneity. This heterogeneity is further increased by alternative splicing and RNA editing. AMPA receptors in the adult hippocampus are composed of mainly GluR2 with either GluR1 or GluR3 (Wenthold et al., 1996). During postnatal development, NMDA receptor subunit composition changes from mainly NR1/NR2B to mainly NR1/NR2A, which has a significant effect on the time course of the NMDA-mediated excitatory postsynaptic potential (EPSC) (Flint et al., 1997).

Postsynaptic AMPA receptors mediate the majority of the fast excitatory synaptic transmission in the CNS. Kainate receptors contribute to the postsynaptic responses at some excitatory synapses (Castillo et al., 1997; Vignes et al., 1998) and can also modulate presynaptic neurotransmitter release (Chittajallu et al., 1996; Contractor et al., 2000). These non-NMDA receptors open for Na⁺ or K⁺ influx. The postsynaptic NMDA receptors are unique among the ionotropic channels in that they are in addition voltage-dependent. At resting membrane potentials, NMDA receptors are blocked by extracellular magnesium-ions and are only relieved from this Mg²⁺ block when the membrane is depolarized. Thus, both membrane depolarization and glutamate binding are needed to open the NMDA receptors for Ca²⁺ influx (= coincidence receptors), which contributes only to the late component of the EPSP. These inflowing calcium-ions can activate downstream calcium-dependent signal transduction processes, thereby modulating the excitatory synaptic transmission of the neuron. The metabotropic glutamate receptors link glutamate release to GTP-binding (G) protein-mediated signalling cascades in the postsynaptic membrane (Pin and Duvoisin, 1995).

4.1.2. The postsynaptic density

Glutamate receptors are an essential component of the postsynaptic density (PSD). Ultrastructural studies of this disk-shaped postsynaptic membrane undercoat in excitatory synapses have revealed an electron-dense thickening that marshals more than seventy proteins (Husi et al., 2000; Walikonis et al., 2000). The PSD has been proposed to be a protein lattice that localizes and organizes the various ion channels, receptors, scaffold and adaptor proteins, cytoskeleton proteins, kinases, phosphatases and other signalling proteins (Pawson and Scott, 1997; Ziff, 1997; Kennedy, 1998). Many of these proteins contain postsynaptic density-95/disc-large/zona occludens 1 (PDZ)-domains, which are protein-interaction domains that bind to the PDZ-binding motif usually at the cytoplasmic carboxyl (C-)termini of membrane proteins, including ionotropic glutamate receptors, Eph receptors, neuroligins, stargazin, thereby clus-

4. Introduction

tering and anchoring proteins at high density in the PSD (Doyle et al., 1996; Songyang et al., 1997; Scannevin and Huganir, 2000; Sheng, 2001). Structurally, proteins in the PSD are in close proximity to glutamate receptors and other signalling proteins, which allow rapid responses of the synapse once glutamate has been released (Kennedy, 1998). The PDZ scaffold proteins are well-positioned to link the postsynaptic membrane with the underlying actin cytoskeleton and couple spine morphology and actin dynamics to postsynaptic receptor activation (Figure 4.1).

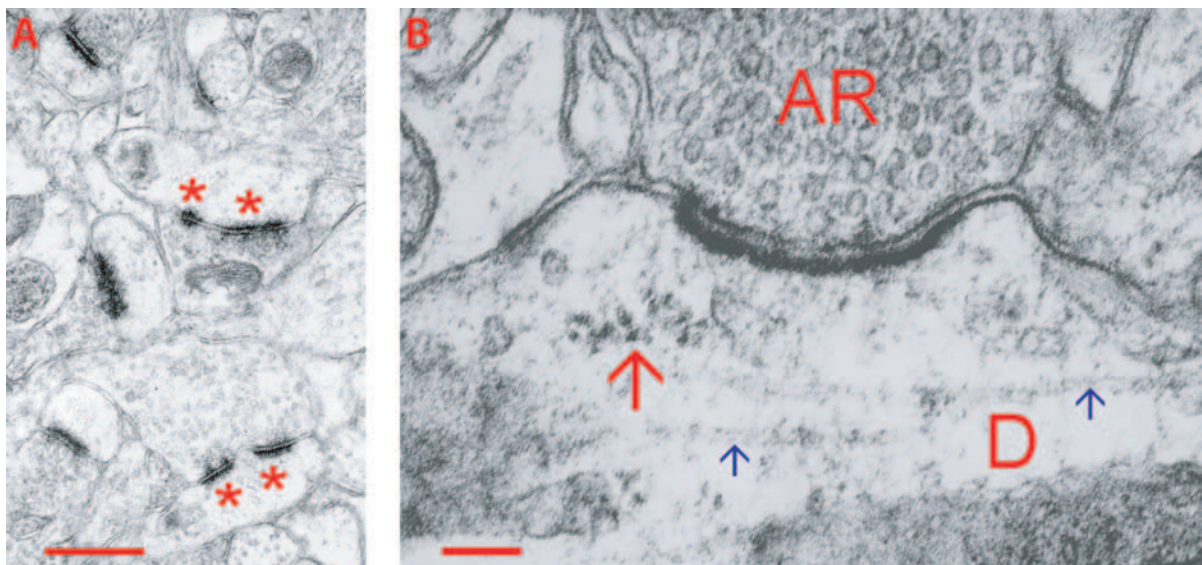


Figure 4.1. **Ultrastructure of the synapse.** (A) The PSDs (red asterisks) of chemical synapses are darkly stained and are in contrast with all other, much lighter structures in the mouse neocortex. Scale bar = 1 μm . (Ref. http://synapses.mcg.edu/atlas/1_6_1.stm) (B) Electron micrograph of a synapse between an axon terminal (AR) and a dendritic spine (D) with polyribosomes (red arrow) and microtubules (blue arrows) present in the subsynaptic cytoplasm. The presynapse contains numerous synaptic vesicles. The PSD is visible as a thick membrane undercoat postsynaptically in the rat hippocampus. Scale bar = 200 nm. (Ref. http://synapses.mcg.edu/atlas/1_6_37.stm)

The best characterized of the PDZ scaffold proteins is postsynaptic density-95 (PSD-95) protein, an abundant component of the PSD. This multidomain scaffold protein is capable of forming a macromolecular signalling complex by binding to subunits of the NMDA receptor and other molecules (Scannevin and Huganir, 2000; Sheng, 2001). Overexpression of PSD-95 promotes spine growth in cultures (El-Husseini et al., 2000) and potentiates AMPA receptor-mediated EPSCs in brain slices (Béïque and Andrade, 2003; Stein et al., 2003; Ehrlich and Malinow, 2004). The synaptic potentiation induced by the ectopic expression of PSD-95 in brain slices seems to mimic long-term potentiation (LTP), in that it converts silent synapses

into functional synapses, drives GluR1 into synapses, occludes LTP and enhances long-term depression (LTD) (Béïque and Andrade, 2003; Stein et al., 2003; Ehrlich and Malinow, 2004). Another class of proteins included in the postsynaptic membrane are the cell-adhesion proteins (CAMs), such as cadherins, syndecans and neuroligins. The transmembrane CAMs are needed for the formation and maintenance of the synaptic junction through interaction with their presynaptically expressed partners via their extracellular domains.

4.2. Synaptic plasticity

Certain excitatory synapses in the brain can dynamically regulate their strength and structure in response to afferent activity. This property, also called synaptic plasticity, is believed to underlie a variety of neuronal processes, such as brain development, learning and memory (Bliss and Collingridge, 1993). The most widely studied examples of synaptic plasticity are LTP and LTD in the hippocampus.

The hippocampus has three major afferent pathways: The perforant fiber pathway from the entorhinal cortex forms connections with the granule cells of the dentate gyrus (DG). The granule cells send axons that form the mossy fiber pathway, which synapse on the pyramidal cells in the Cornu ammonis 3 (CA3) region of the hippocampus. The pyramidal cells of the

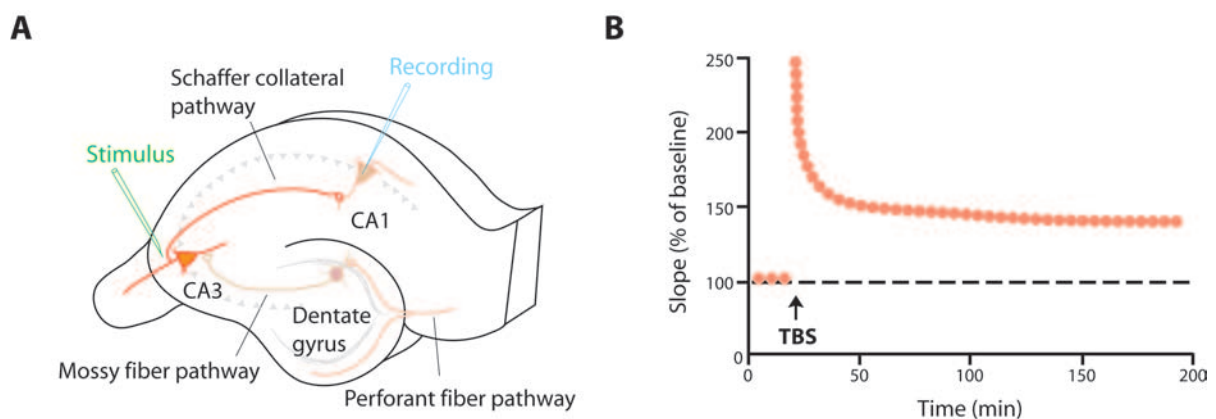


Figure 4.2. **Long-term potentiation in the hippocampus.** (A) Schematic view of a hippocampal slice showing the perforant fibers from the subiculum, which forms excitatory connections with the granule cells of the dentate gyrus. The mossy fiber axons synapse on pyramidal cells in area CA3 of the hippocampus. The Schaffer collateral fiber pathway connects the pyramidal cells of the CA3 region with the pyramidal cells in the CA1 region. LTP occurs at each of the three major synaptic pathways in the hippocampus. (B) Thetaburst stimulation (TBS) of the Schaffer collateral pathway causes an increase in the amplitude of the synaptic response recorded in CA1 neurons, lasting for up to several hours *in vitro*.

4. Introduction

CA3 regions send excitatory Schaffer collaterals to the pyramidal neurons in the CA1 region of the hippocampus (Freund and Buzsáki, 1996). LTP has been studied most extensively at the Schaffer collateral pathway to the CA1 region in hippocampal slices, which was also the focus for the experiments in this work (Figure 4.2A).

The first description of LTP was in 1973, when Bliss and Lømo (Bliss and Lomo, 1973) showed that brief repetitive activation of hippocampal excitatory synapses causes a persistent enhancement in synaptic strength for several hours or, under some circumstances, for days or weeks. They called this facilitation LTP. LTP in the Schaffer collateral and perforant pathway is associative and requires simultaneous firing in postsynaptic and presynaptic neurons, supporting Hebb's theory: In 1949, the psychologist Donald O. Hebb proposed that synapses are strengthened when pre- and postsynaptic elements are synchronously active (Hebb, 1949).

LTP can be subdivided temporally in early LTP (E-LTP), lasting for 1-3 hours and late LTP (L-LTP) that lasts for at least 6-8 hours. E-LTP does not involve *de novo* protein synthesis, in contrast to the L-LTP, for which protein synthesis is an important component (Figure 4.2B) (Kandel, 2001).

At most central synapses, activation of NMDA receptor and subsequent Ca^{2+} influx into the postsynaptic cell are critical for the induction of synaptic plasticity. The NMDA receptor antagonist 2-amino-5-phosphonovaleric acid (APV) can block LTP and LTD of the CA1 region of the hippocampus (Collingridge et al., 1983; Fujii et al., 1991; Mulkey and Malenka, 1992). Interestingly, following LTP induction most studies demonstrate a selective increase in the AMPA receptor EPSPs and little change in NMDA receptor EPSPs (Kauer et al., 1988; Muller and Lynch, 1988). In addition, AMPA receptors can be inserted into the postsynaptic site in an activity-dependent manner (Shi et al., 2001). Taken together, these data show that potentiation or strengthening of excitatory synapses is associated with the specific recruitment and insertion of AMPA receptors from intracellular pools into the postsynaptic membrane (Lledo et al., 1998; Shi et al., 1999). Similarly, frequent activation that causes synaptic depression or weakening of synaptic strength is correlated with AMPA receptor endocytosis from the postsynaptic membrane (Daw et al., 2000; Man et al., 2000). In most cases, the insertion and removal of AMPA receptors (= trafficking) is triggered by Ca^{2+} influx through NMDA receptors. Therefore, AMPA receptors are suggested to be responsible for mediating synaptic plasticity, whereas NMDA receptors are controlling plasticity (Montgomery and Madison, 2004).

4.3. Glial cells

Glial cells are divided into two major classes: microglia, which are phagocytes and macroglia composed of oligodendrocytes, Schwann cells and astrocytes. Oligodendrocytes and Schwann cells are responsible for the myelination in the central and peripheral nervous system, respectively. Astrocytes are the most numerous glial cell type and account for nearly one-half of the cells in a human brain (Peters et al., 1991; Laming et al., 1998). Morphologically, astrocytes are in close association with neurons and have extensive contacts with endothelial cells (Simard et al., 2003). Each hippocampal astrocyte in the mouse brain defines a territory that is free of processes from neighbouring astrocytes and only the most peripheral processes overlap with one another (less than 5%) (Ogata and Kosaka, 2002). Originally, these little cells were thought to be passive glue that connects and supports neurons. During the last decade, however, there has been mounting evidence that neuroglial cells are important modulators of synaptic transmission (Nedergaard et al., 2003).

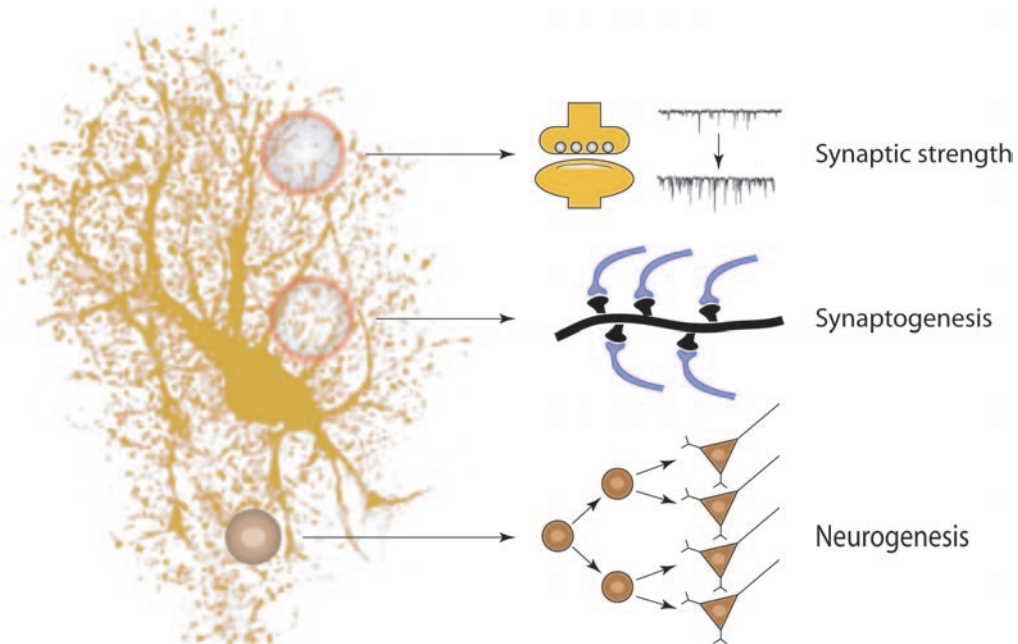


Figure 4.3. **Astrocytes as regulators of synaptic activity, synaptogenesis and neurogenesis.** Astrocytes transmit signals to neurons that can directly modulate synaptic strength in the CNS by releasing glutamine, for instance (illustrated here by an increase in spontaneous excitatory postsynaptic currents). Moreover, astrocytes are potent inducers of synaptogenesis and crucial for maturation of synapses. In addition, astrocytes are involved in the regulation of neurogenesis from endogenous progenitor populations, at least in the dentate gyrus of adult rats (scheme taken from Nedergaard et al. (2003)).

4.3.1. Properties and functions of neuroglial cells

Astrocytic processes intimately associate with synapses, the ideal place to synchronize neuronal network activity. Many synapses in the brain are ensheathed by astrocytes and it has been estimated that an individual astrocyte in the adult rodent brain may surround and interact with as many as 10,000 synapses (Bushong et al., 2003, 2004).

One of the functions of the ensheathing glial cell is to clear neuronal waste, including metabolic byproducts and released neurotransmitters (e.g. glutamate) during synaptic transmission. Most synapses lack extracellular enzymes for glutamate inactivation and therefore the rapid reuptake of this transmitter from the synaptic cleft via glutamate transporters with fast kinetics is very important (Bergles et al., 1999; Danbolt, 2001). The fast uptake by perisynaptic glia is crucial to terminate the postsynaptic response and prevent excitotoxicity by excess glutamate. It also enhances spatial specificity of signalling and partially shields synapses from each other by preventing glutamate spillover.

In the absence of glia, neurons in culture form few and functionally immature synapses. Cocultures with astrocytes or glia-conditioned medium, increase the number of synapses and enhance synaptic efficacy (Pfrieger and Barres, 1997; Ullian et al., 2001). Glia secrete molecules, such as cholesterol and tumour necrosis factor- α (TNF- α) that are crucial for synaptogenesis and maturation of synapses. Cholesterol is a component of lipid rafts, which are important for the formation and stability of neuronal synapses (Hering et al., 2003) and TNF- α enhances synaptic efficacy by increasing the surface expression of AMPA receptors in neurons (Beattie et al., 2002).

Recent studies demonstrated that there is a dynamic bi-directional communication between glia and neurons at this tripartite synapse. Release of neurotransmitter from the presynaptic terminal also stimulates the perisynaptic glial cell via metabotropic glutamate receptors. The activated glial cell, in turn releases gliotransmitter (e.g. glutamine) from vesicles by a calcium-dependent mechanism that can directly stimulate the postsynaptic neuron and can feed back to the presynaptic terminal to either enhance or depress further release of neurotransmitters (Volterra et al., 2002). Thus, surrounding astrocytes function as active partners by transmitting signals to neurons, through which synaptic strength in the hippocampus, cortex and thalamus is directly modulated (Kang et al., 1998; Haydon, 2001; Newman, 2003). In addition, astrocytes return the released glutamate in the form of glutamine to neurons. Neuronal reuptake of glutamine seems to be important because continued release of glutamate depends on astrocytic glutamine synthetase activity (Norenberg and Martinez-Hernandez, 1979; Pow and Robinson,

1994; Laake et al., 1995). In contrast to astrocytes, neurons lack the enzyme pyruvate carboxylase and therefore cannot perform net synthesis of glutamate from glucose but can hydrolyze glutamine to form glutamate (Yu et al., 1983; Shank et al., 1985; Waagepetersen et al., 2001).

Interestingly, recent work in the larvae brain of *Drosophila melanogaster* demonstrated that neuron-glia signalling triggered by the steroid hormone ecdysone is required to actively recruit glia to the appropriate axonal segments for the selective pruning process. Processes of the surrounding glia first infiltrate bundles of larval axon branches and then engulf clusters of axonal varicosities – interpreted to be synaptic boutons – prior to their degeneration. At the time of axonal pruning, glial cells remove axon branches by phagocytosis and accumulate acidic degenerative organelles (Awasaki and Ito, 2004; Watts et al., 2004).

In addition, astrocytes are involved in the maintenance of the blood-brain barrier, as well as in the regulation of neurogenesis from endogenous progenitor populations (Horner and Palmer, 2003). Thus, the multitask functions of astrocytes are essential for higher brain function (Figure 4.3).

4.4. Eph receptors and their ephrin ligands

Eph receptors and their ligands are found in a wide variety of cell types in developing and mature tissue with reciprocal or overlapping expression patterns. In case of the complementary expression of interacting Eph receptors and ephrins, the activation occurs at the interface of their expression domains (Gale et al., 1996). Due to the nature of the membrane-anchored ligands, the interactions between Eph receptors and ephrins activate a bi-directional signalling cascade transducing the signal in the Eph-receptor expressing cell as well as in the ephrin-expressing cell. Therefore, the Eph/ephrin interaction mediates a cell-to-cell communication that has important roles in the establishment of neuronal and vascular networks during embryonic development, which involves diverse processes like (neuronal) cell migration, axon guidance, (neo-)angiogenesis and tissue patterning (e.g. topographic mapping, segmental patterning) (Palmer and Klein, 2003).

The findings from the last years are changing the conventional view of these proteins to function predominantly in a developmental context (Dalva et al., 2000; Ethell et al., 2001; Grunwald et al., 2001; Henderson et al., 2001; Contractor et al., 2002; Takasu et al., 2002; Henkemeyer et al., 2003; Penzes et al., 2003; Grunwald et al., 2004). The new essential function of these molecules lies in the regulation of structural and physiological functions of excitatory synapses through multiple mechanisms in the adult brain. Besides, they have been found

4. Introduction

to be involved in nerve generation, cancer progression and pathological angiogenesis in the adult (Palmer and Klein, 2003).

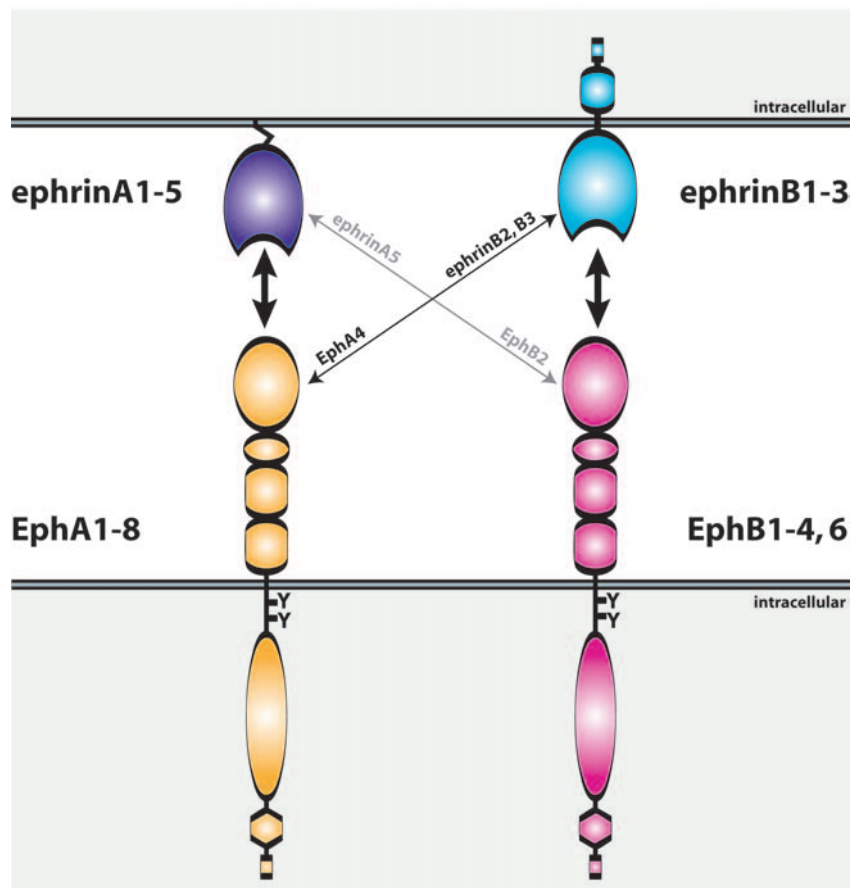


Figure 4.4. **The Eph class of receptor tyrosine kinases and their ligands.** Eph receptors can be subdivided according to their binding affinities to their ephrin ligands and to sequence similarities. The B-subclass (in mammals: EphB1-B4, EphB6) binds preferentially to ephrinB1-B3, whereas EphA receptors bind promiscuously to ephrinA1-A5. There are two exceptions to this subclass discrimination: (i) EphA4 receptors can bind to ephrinAs as well as to ephrinB2 and -B3 and (ii) EphB2 can also interact with ephrinA5.

4.4.1. The Eph class of receptor tyrosine kinases

In 1987, the first member of the Eph receptors, EphA1, was identified in a screen for tyrosine kinases involved in cancer (Hirai et al., 1987). This new receptor was named Eph, after “erythropoietin-producing human hepatocellular” carcinoma cell line from which its cDNA

was isolated. The Eph receptors form the largest known subfamily of receptor tyrosine kinases (RTKs) (Orioli and Klein, 1997; Flanagan and Vanderhaeghen, 1998). Today, it is known that vertebrates have at least 14 members (van der Geer et al., 1994; Murai and Pasquale, 2004) that are related to Eph receptors by sequence and by general characteristics of their kinase and extracellular domain (Holder and Klein, 1999). Invertebrates like the fruitfly *Drosophila melanogaster* and the nematode *Caenorhabditis elegans* have only a single Eph receptor: Vab-1 and Dek, respectively (George et al., 1998; Scully et al., 1999). Thus, the diversity in this subfamily of RTKs among vertebrates must have arisen through more recent gene duplications and this might also explain the high degree of functional overlap between family members and interspecies homologous from quite distantly related organisms, like humans and zebrafish (Oates et al., 1999; Kullander and Klein, 2002). Based on sequence similarity and ligand affinity mammalian Eph receptors can be divided into an A-subclass, which contains eight members (EphA1-A8) and a B-subclass, which consists of five members (EphB1-B4, EphB6). Chicken expresses an additional EphB receptor, EphB5 (Wilkinson, 2001). Binding specificity within a subclass is low. There are two preferred binding specificity subclasses: EphA receptors (EphA1-A8) bind promiscuously to the glycosylphosphatidylinositol(GPI)-linked A-type ephrins (ephrinA1-A5), whereas EphB1 to EphB3 receptors bind to the transmembrane B-type ephrins (ephrinB1-B3). In contrast to this A- or B-subclass discrimination: EphA4 receptor has also been found to bind ephrinB2 (Flanagan and Vanderhaeghen, 1998) and ephrinB3 (Gale et al., 1996). Additionally, a recent study showed EphB2 receptors to interact with ephrinA5 (Figure 4.4)(Himanen et al., 2004). In addition, there are also Eph receptors with less or no binding specificity: EphB5 does not bind any of the known ephrins. Suggesting that there might be other ligands for the Eph receptors. Finally, EphB4 can be only activated by ephrinB2 binding (Brambilla et al., 1995; Gerety et al., 1999).

4.4.2. Ephrin ligands

Identification of the ligands lagged several years behind that of the receptors. In 1994, soluble receptor affinity methods were used to identify the first Eph ligands, namely the ephrins (ephrinA1) (Bartley et al., 1994). The name ephrin derived from **Eph** receptor **interacting** protein or from the ancient Greek word *ephoros*, meaning an overseer or controller (Eph Nomenclature Committee, 1997). Homologues of ephrin ligands have been identified in vertebrate and invertebrate. The nine ephrins in vertebrates have been subdivided into an A-subclass (ephrinA1-A5) and B-subclass (ephrinB1-B3), according to their affinities for each other, sequence con-

4. Introduction

servation and the mode of ephrin membrane attachment (Gale et al., 1996; Eph Nomenclature Committee, 1997).

EphrinA ligands are tethered to the cell surface by a GPI-anchor, whereas ephrinB ligands are single pass transmembrane proteins, which possess a short cytoplasmic region. In invertebrates the nematode *Caenorhabditis elegans* has four GPI-anchored ephrin genes (EFN1-4)(Chin-Sang et al., 1999; Wang et al., 1999), whereas the fruitfly *Drosophila melanogaster* has only one gene encoding for ephrin (Dephrin) (Dai, 1999; Bossing and Brand, 2002). Dephrin has unusual structural features compared to other ephrins. Although the amino (N-)terminal part of the ligand shares similarities with vertebrate ephrins, the Dephrin encoding sequence instead predicts three transmembrane domains and a cytoplasmic part with some sequence similarity to vertebrate ephrinBs (Bossing and Brand, 2002).

4.4.3. Structure of Eph RTKs and ephrin ligands

4.4.3.1. Receptor structure

The extracellular region of the transmembrane Eph receptors consists of a N-terminal ligand-binding globular domain (\sim 180 amino acids (aa)), adjacent to a cysteine-rich epidermal growth factor(EGF)-like region, which is followed by two fibronectin type III (FNIII) repeats (Figure 4.5). One FNIII repeat (\sim 90 aa) is a long stretch that is repeated 15-17 times in the fibronectin protein. It is a common motif in many cell-surface proteins.

The single transmembrane spanning region is followed by the cytoplasmic part, which can be divided into four functional units: the juxtamembrane region that contains two conserved tyrosine (Y) residues, a classical protein tyrosine kinase (TK) domain, a sterile α -motif (SAM) and a postsynaptic PDZ-domain binding motif. The TK domain catalyses phosphoryl transfer from adenosine 5'-triphosphate (ATP) to tyrosine residues in protein substrates. The aa of the SAM domain are roughly conserved and are thought to participate in protein-protein interactions forming dimers or oligomers. Another protein-protein interaction motif – the PDZ-binding motif – are the C-terminal 4-5 aa residues containing a consensus binding sequence that includes a hydrophobic residue (usually valine or isoleucine) at the very carboxyl terminus. This C-terminal PDZ-domain target site might bind scaffolding proteins.

4.4.3.2. Ligand structure

Ephrins are characterized by the presence of a unique N-terminal receptor-binding domain, which is separated from the membrane via a linker of \sim 40 aa. EphrinA ligands are attached

to the exoplasmic leaflet of the cell membrane by a GPI-anchor, whereas B-subclass ephrins possess a single-pass transmembrane helix, followed by a short but highly conserved 83-90 aa cytoplasmic region containing 5-6 conserved tyrosine residues and a C-terminal PDZ-binding motif (Figure 4.5).

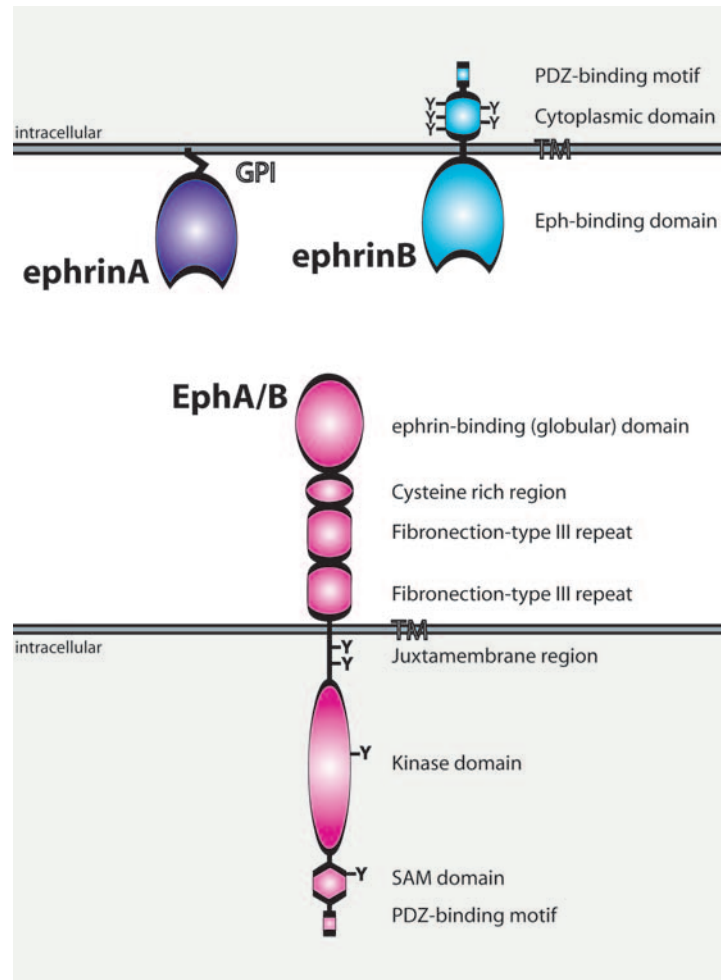


Figure 4.5. **Domain structure of Eph receptor and ephrin ligands.** The transmembrane **EphA/B receptors** are multidomain RTKs and consist of an N-terminal ephrin-binding domain, followed by two fibronectin-type III repeats and a transmembrane region (TM). Intracellularly, the juxtamembrane region, containing two important tyrosine residues (Y), is followed by a tyrosine kinase domain, a SAM domain and a PDZ-domain binding site. The GPI-anchored **ephrinAs** are composed only of a N-terminal receptor-binding domain, whereas the transmembrane **ephrinB** ligands have a cytoplasmic domain with conserved tyrosine phosphorylation sites (Y) and a C-terminal PDZ-domain binding motif.

4.4.4. Bi-directional signalling between Eph receptor and ephrin ligands

Unlike most RTKs that bind their cognate soluble ligands, the Eph receptor family members are activated through the binding of membrane-bound proteins. Therefore, interaction between receptor and ligand requires cell-to-cell contact (trans-interaction), which makes Eph/ephrin ideal signalling molecules in developmental processes, such as boundary formation and axon guidance (Holland 1998). This trans-interaction leads to multimerization of both receptor and ligand to distinct clusters in their respective plasma membrane. This initiates a so-called bi-directional signalling cascade where the Eph receptor TK domain transduces the forward signal into the Eph-expressing cell and the ephrin transduces the reverse signal into the other cell, acting each as both “receptor” and “ligand” simultaneously (Figure 4.6A-B).

The outcome of the activation of the bi-directional signal-transduction cascade can differ depending on the subclass-expression of Eph/ephrin and from the cell types. As an example, a repulsion of neighbouring cells or growth cones can follow. In a few cases, the activation lead to an increased attraction. In molecular terms, many signalling pathways that are downstream of Eph/ephrin converge to regulate the cytoskeleton.

4.4.4.1. Binding and activation of Eph/ephrins

Prior to cell-to-cell contact, unbound ephrins and Eph receptors may form low-affinity homodimers at the surface (Toth et al., 2001; Himanen and Nikolov, 2003), probably in lipid rafts (Brückner et al., 1999). It is thought that cell-to-cell contact leads to a repositioning of these homodimers so that ligands and receptors bind each other with a 1:1 stoichiometry in large aggregates known as patches (Figure 4.6D-E).

So far, the clustering mechanism has been revealed by structural studies of the complex formed between the ligand-binding globular domain of EphB2 and the complete extracellular part of ephrinB2 (Himanen et al., 2001). Structural information on the ephrin-binding globular domain obtained from the EphB2-ephrinB2 complex reveals two distinct ephrin-binding sites located on opposite sides of the domain. These sites interact with separate regions of distinct ephrinB2 molecules with different affinities. Biophysical studies in solution indicate that EphB2 interacts with EphrinB2 in a two-step process: in the first step, one receptor and one ligand bind with high affinity and specificity to form a heterodimer dominated by the insertion of an extended ephrin loop into a channel of the globular domain. In the next step, these heterodimers interact with each other through a lower affinity interaction to form ring-like tetramers, in which each receptor interacts with two ephrins and *vice versa* (Figure 4.6D). In

these complexes the Eph/ephrin proteins are precisely positioned and orientated, promoting higher-order aggregates that are believed to initiate the bi-directional signalling cascade (Figure 4.6C, E)(Kullander and Klein, 2002; Murai and Pasquale, 2003). In the high-order clustering, other Eph/ephrin domains are probably involved, like the SAM domain (Stapleton et al., 1999; Thanos et al., 1999) and the cysteine-rich region of the receptors (Lackmann et al., 1998), as well as the C-terminal PDZ-domain binding site from Eph receptors and ephrinB ligands (Hock et al., 1998b; Torres et al., 1998; Brückner et al., 1999; Buchert et al., 1999; Lin et al., 1999; Cowan et al., 2000).

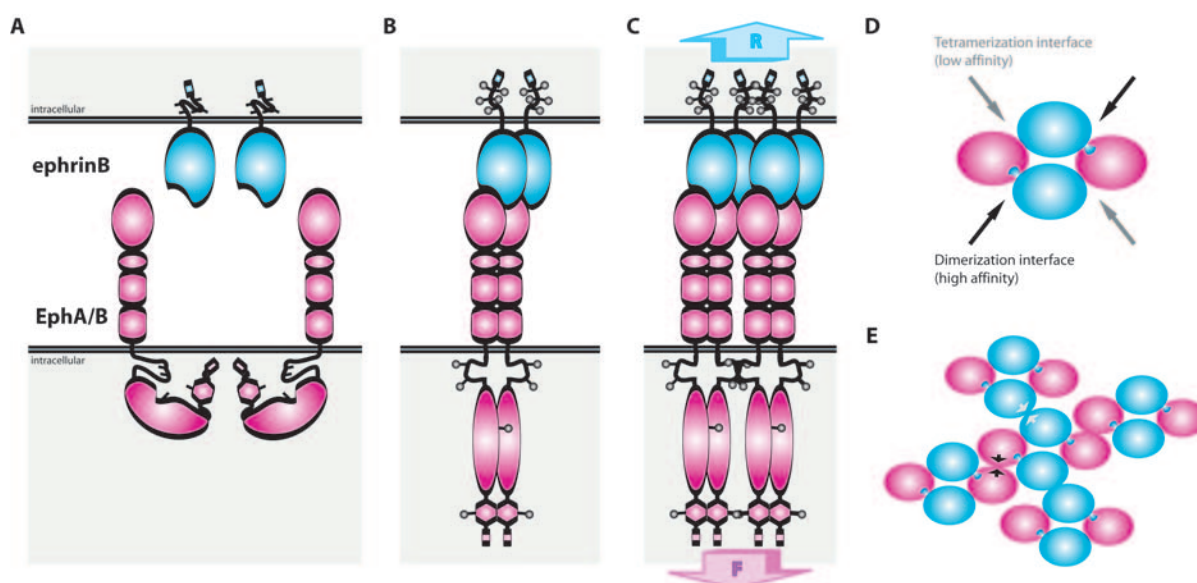


Figure 4.6. **Mechanism of Eph receptor activation and the initiation of bi-directional signalling.** **(A)** Prior to cell contact, Eph receptors and ephrins are inactive. The unbound Eph receptor is in a close conformation held by a fold in the juxtamembrane region. **(B)** Cell-to-cell contact induces dimerization of receptor and ligand. The cytoplasmic tails of the Eph receptors are now juxtapposed, which facilitates trans-phosphorylation by basal activity of tyrosine residues (grey circles). Phosphorylation of the activation loop within the kinase domain stimulates kinase activity. Phosphorylated tyrosines (pYs) causes changes in the structure of the ephrinB cytoplasmic tail and the Eph receptor juxtamembrane domain, thus relieving inhibitory constraints on the kinase domain. **(C)** Eph-ephrin binding results in high-order clustering by the lateral aggregation of multiple Eph-ephrin complexes. The pYs provide binding sites for many signalling and adaptor proteins, thereby inducing (i) forward (F) signalling into the Eph-expressing cell or (ii) reverse (R) signalling into the ephrin-expressing cell or bi-directional signalling into both cells. **(D)** Dimerization and tetramerization interfaces of the tetrameric complex of ephrins (blue) and Eph receptors (red). One ephrin-binding domain of a receptor and one Eph-binding domain of a ligand initially form a high-affinity heterodimer dominated by the insertion of an extended ephrin loop into a channel of the globular domain (black arrows). Two heterodimers then join to form a tetramer through a lower affinity interaction (grey arrows), in which each ligand interacts with two receptors. **(E)** Possible high-order side-by-side clustering of the ring-like tetrameric Eph/ephrin complexes might occur via the SAM domains in the receptors and the C-terminal PDZ-domain binding-sites in ephrins (grey arrows) and Ephs (black arrows).

4.4.4.2. Mechanisms of Eph receptor forward signalling

The catalytic activity of RTKs is tightly regulated by several mechanisms because it controls crucial cellular events, including growth, differentiation, migration, metabolism and survival (Himanen and Nikolov, 2003; Hubbard, 2004). In the absence of ligand binding, Eph receptors, like all RTKs, are either monomeric or dimeric on the cell surface and in an inactive state. Binding of ephrin induces stabilization and clustering of Eph receptors, thereby allowing the receptor kinase domain to trans-phosphorylate the tyrosine residues in the cytoplasmic tail of the neighbouring receptor through the spacial proximity (Figure 4.6A-B)(Schlessinger, 2000; Ullrich and Schlessinger, 1990). Cis-phosphorylation might occur, but it is believed to be also a downstream event of the ligand-binding. The activation of Eph receptors leads to phosphorylation of ten or more specific tyrosine residues in the cytoplasmic domain (Kalo and Pasquale, 1999), several of which are involved in the upregulation of TK activity (Choi and Park, 1999; Binns et al., 2000; Zisch et al., 2000).

The most general mechanism for stimulating kinase activity involves the phosphorylation of the so-called activation loop within the kinase domain, which in its non-phosphorylated form blocks the kinase active site (Johnson et al., 1996). In addition, for a subset of RTKs like Eph, the highly conserved juxtamembrane region is known to negatively regulate the catalytic activity of the TK. The EphB2 crystal structure of the intracellular region reveals that the kinase domain is auto-inhibited by the non-phosphorylated juxtamembrane region (Wybenga-Groot et al., 2001). Trans-phosphorylation of the two juxtamembrane tyrosine residues is thought to destabilize the autoinhibitory conformation of the juxtamembrane region because steric and electrostatic forces push the phosphorylated juxtamembrane region away from the kinase domain, leading to upregulation of TK activity (Figure 4.6) (Wybenga-Groot et al., 2001). The exposed phosphorylated juxtamembrane tyrosine residues now become available for the recruitment to the cell membrane of many different downstream signalling proteins bearing src homology-2 (SH2) domains, resulting in the assembly of signalling complexes, which initiate intracellular signal transduction cascades (Figure 4.6-7). At least four phosphotyrosines in the Eph receptor serve as docking sites for a number of SH2-domain containing proteins, including Ras-GTPase activation protein (RasGAP), the src family kinases (SFKs) Src and Fyn, non-receptor TKs Abl-related gene (Arg) and Abelson (Abl), low molecular weight phosphotyrosine phosphatase (LMW-PTP), phospholipase C γ , phosphatidylinositol 3-kinase (PI3K), SH2 domain-containing Eph receptor-binding protein 1 (SHEP1) and adaptor proteins Src-like adaptor protein (SLAP), growth-factor receptor bound 2 (Grb2), Grb10, Crk and noncatalytic

region of tyrosine kinase (Nck) (Krull et al., 1997; Zisch and Pasquale, 1997; Gao et al., 1998a). Furthermore, PDZ binding motifs at the C-terminus of the Eph receptors bind to PDZ-domain containing proteins such as Acute myeloid leukemia-1/chromosome 6 fusion protein/afadin-6 (AF6), a receptor-like tyrosine kinase (Ryk) receptor TK interacting protein, protein interacting with C kinase (Pick) 1, Syntenin, a syndecan-interacting protein and two glutamate receptor interacting proteins 1 (GRIP1) and GRIP2 (Hock et al., 1998a,b; Torres et al., 1998; Brückner et al., 1999; Kullander and Klein, 2002).

Two conserved tyrosine residues of the EphB receptors are not present in EphA receptors. This may be important for the EphA and EphB receptors to trigger distinct responses. For example, during the establishment of visual system topography, EphA receptors mediate axon repulsion, whereas EphB receptors appear to provide a stop signal to the growth cone (Hindges et al., 2002; Mann et al., 2002).

In many cell types a unique feature of Ephs among the family of RTKs is their inability to mediate signals leading to proliferation and differentiation (Klein, 2001; Miao et al., 2001). One recent study could show that EphA receptors direct the differentiation through a mitogen-activated protein kinase (MAPK)-dependent pathway in mammalian neuronal precursor cells (Aoki et al., 2004). Many of the signalling proteins identified in the Eph signalling pathways, are known to be involved in the regulation of the cell attachment, shape and mobility.

Cytoskeletal regulation

Cell migration and adhesion require a dynamic reorganization of the actin cytoskeleton. An important regulator of the actin cytoskeleton is the Rho family of small GTPases, which includes Rho, Rac and Cdc42 (Hall and Nobes, 2000). Activated Rho promotes stress fiber formation and growth cone collapse, whereas activated Rac and Cdc42 mediate the extension of filopodia and lamellopodia formation, respectively. The activity of Rho family GTPases is controlled by guanine nucleotide exchange factors (GEFs) that promote the exchange from guanosine diphosphate (GDP) to GTP. The identification of the novel Rho GEF Eph-interacting exchange factor (Ephexin) provided a direct link between EphA receptors and Rho family GTPases (Figure 4.7)(Shamah et al., 2001). Ephexin is preferentially expressed in the nervous system and interacts directly with the kinase domain of EphA4. EphrinA-mediated activation of Eph receptors activates Rho on the one hand and inhibits Rac and Cdc42 on the other hand, shifting the actin dynamics to increased contraction and reduced extension. Expression of dominant-negative form of Ephexin and the use of specific inhibitors of Rho GTPases inhibit or reduce ephrinA-induced growth-cone collapse, respectively (Wahl et al., 2000; Shamah

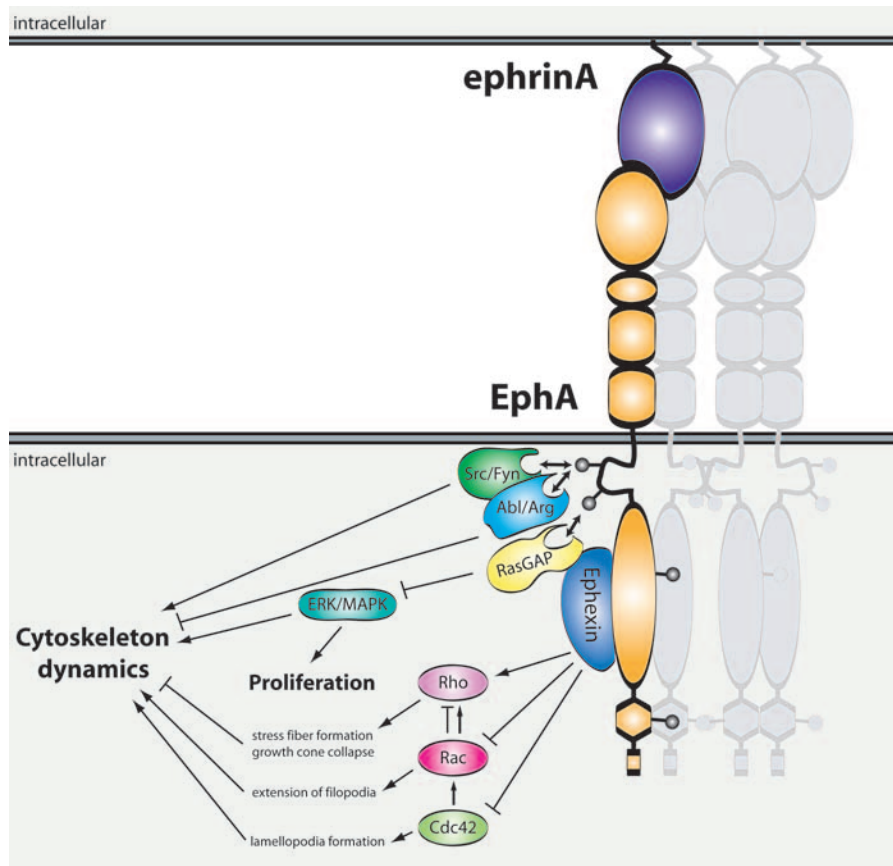


Figure 4.7. **Molecular mechanisms of cytoskeletal regulation downstream of EphA forward signalling.** Activation of EphA receptors by ephrinA binding leads to the recruitment and activation of SFKs (Src and Fyn) to the juxtamembrane tyrosines. SFKs regulate cytoskeleton dynamics, which may be required for growth cone collapse. Activation of the cytoplasmic tyrosine kinases Abl promotes neurite outgrowth, which is inhibited by Eph receptor activation. The recruitment of RasGAP inhibits the extracellular-signal regulated kinase (ERK)/MAPK pathway, which reduces its impact on actin cytoskeleton motility and might be the reason for the missing proliferative response following Eph receptor activation. The Rho guanine nucleotide exchange factor Ephexin shifts the balance of Rho family GTPase activity towards Rho thereby inducing growth cone collapse.

et al., 2001).

Other known downstream targets of Eph receptors, such as Abl and Src kinases, are regulators of the actin cytoskeleton and might also contribute to Eph-mediated actin reorganization (Zisch et al., 1998; Yu et al., 2001; Takasu et al., 2002; Battaglia et al., 2003). The non-receptor TKs, Abl and Arg, were identified as new binding partners of EphB2 and EphA4 in a yeast-two hybrid screen and interact with EphB2 independently of phosphorylation through their C-terminal tail and to tyrosine phosphorylated motifs of EphB2 through their SH2 domain (Yu et al., 2001). A third interaction between Abl and Eph requires tyrosine phosphorylated

EphB2 and is probably mediated by a SKF, as these are known to regulate Abl kinase activity (Plattner et al., 1999) and are well-characterized interactors with Eph receptors (Zisch et al., 1998). Abl and Ephs are localized in the neuronal growth cone. Activation of endogenous EphB2 receptors through stimulation with ephrinB1 decreases Abl kinase activity in a neuronal cell line (Yu et al., 2001). In contrast, activation of Abl in cultured neurons promotes neurite outgrowth (Zukerberg et al., 2000). These findings are consistent with the known opposite effects of these kinases on neurite outgrowth and providing a conceivable explanation of why Abl promotes neurite outgrowth and activated Eph receptor growth cone collapse.

4.4.4.3. Signal transduction through ephrin reverse signalling

Eph receptor binding leads to clustering and activation of the membrane attached ephrinA or ephrinB, which enable ephrins to transduce signals into the cell, resulting in a cellular response (Henkemeyer et al., 1996; Holland et al., 1996; Brückner et al., 1997; Davy et al., 1999; Wang et al., 1999; Davy and Robbins, 2000). But so far, little is known about the signal pathway that act downstream of ephrin ligands.

EphrinB

In case of the ephrinB proteins, activation leads to phosphorylation of the conserved tyrosine residues in the cytoplasmic domains by the cytoplasmic SFK Src (Holland et al., 1996; Brückner et al., 1997; Palmer et al., 2002), thereby generating docking sites for SH2-containing adaptor proteins such as Grb4 (Cowan and Henkemeyer, 2001). Grb4 (Nck2) is a SH2-SH3 adaptor protein, which was the first identified interactor in a modified yeast two-hybrid screen of tyrosine-phosphorylated ephrinBs (Cowan and Henkemeyer, 2001). The Grb4 SH3 domains can bind to several polyproline-containing proteins, including Abl interacting protein-1 (Abl-1), axin, a scaffold protein in the Wnt signalling pathway and c-Cbl associated protein (CAP). These and other Grb4 binding adaptors could function as potential links to modify cell morphology through reorganization of the actin cytoskeleton, but a role in synapses has not been discovered. Activation of cells overexpressing ephrinB1 increases focal adhesion kinase (FAK) activity, thereby recruiting the FAK-binding protein Paxillin from the plasma membrane, causing reduction of actin stress fibers and disassembly of integrin-mediated focal adhesion, eventually resulting in a detachment of the cells from the substratum (Figure 4.8) (Cowan and Henkemeyer, 2001).

The C-terminal PDZ-binding motif (YKV) mediates association with several distinct PDZ-domain proteins. Some of them, such as GRIP1, GRIP2 and syntenin are adaptor proteins

4. Introduction

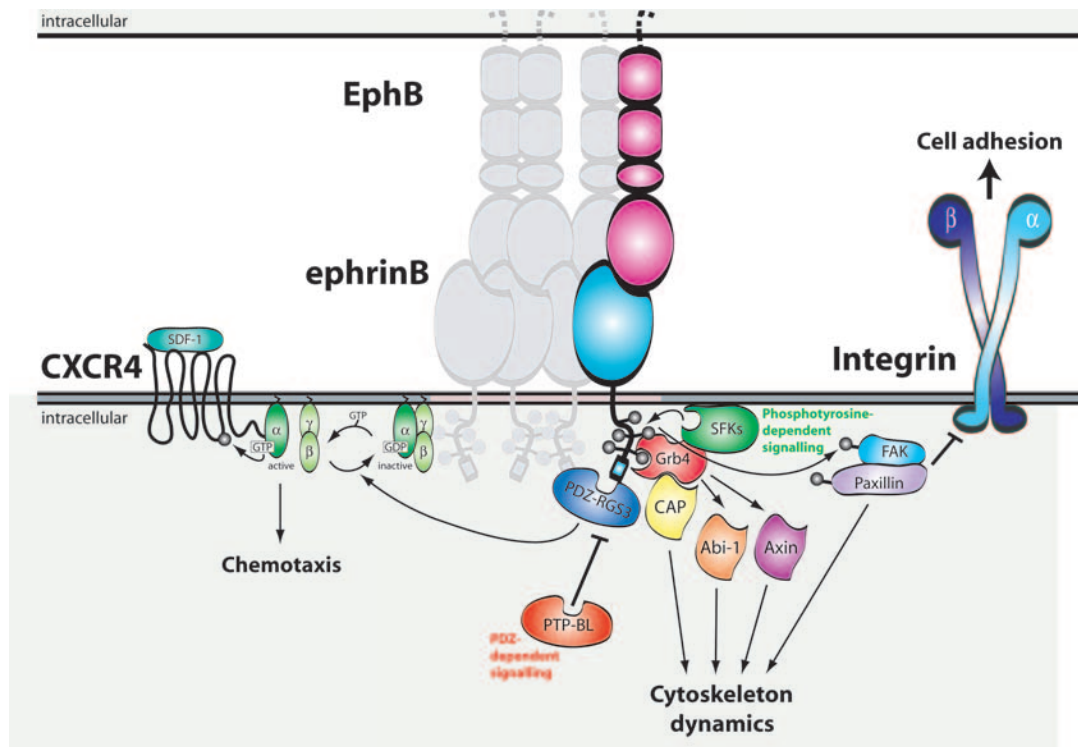


Figure 4.8. **Summary of ephrinB signal transduction pathway described in the text.** Activation of ephrinB leads to the recruitment and activation of SFKs that phosphorylate the tyrosine residues of ephrinB and concomitant recruitment of Grb4 and its SH3-binding partners, such as Abl-1, Axin and CAP. These proteins initiate a cascade of signalling events that regulate cytoskeleton dynamics. Additionally, the phosphorylation of FAK recruits Paxillin from the cell membrane, thereby inhibiting integrin-mediated focal adhesion. The delayed recruitment of the phosphatase PTP-BL might cause a switch from the phosphotyrosine- to the PDZ-domain-dependent signalling. PDZ-RGS3 inhibits cell migration mediated by SDF-1/CXCR4.

that contain only PDZ-domains. Others are linked to a functional subunit, including PDZ-regulator of heterotrimeric G-protein signalling (PDZ-RGS3), PICK1, pleckstrin-homology-domain interacting protein/ephrin interacting protein (PHIP) and protein tyrosine phosphatase-basophil-like (PTP-BL) (Torres et al., 1998; Brückner et al., 1999; Lin et al., 1999; Lu et al., 2001; Palmer et al., 2002). PTP-BL is recruited to ephrinB membrane clusters with delayed kinetics, thereby acting as a negative regulator of ephrinB phosphorylation and Src activity, suggesting a switch from the phosphotyrosine-dependent signalling to the PDZ-domain-dependent signalling (Palmer et al., 2002).

Like the EphB receptors, ephrinBs can regulate signals downstream of heterotrimeric G-proteins coupled receptors. PDZ-RGS3, a GTPase-activating protein (GAP) for heterotrimeric G-proteins (Lu et al., 2001), binds constitutively to the PDZ-binding motif of ephrinB1. Following activation of ephrinB1 by EphB2 in cellular granule neurons, PDZ-RGS3 inhibits chemoat-

traction by the chemokine stromal-cell-derived factor-1 (SDF-1). The chemoattractant SDF-1 activates the serpentine receptor CXCR4. This G-protein coupled receptor acts then as a GTP exchange protein by inducing the $G\alpha$ subunit to catalysing the replacement of bound GDP by GTP, causing a dissociation of the heterotrimeric $G\alpha\beta\gamma$ -protein complex into a $G\beta\gamma$ and a GTP- $G\alpha$ subunit. These subunits can then activate downstream effectors. EphrinB reverse signalling via PDZ-RGS3 interferes with the SDF-1/CXCR4 activation because its RGS domain promotes the hydrolysis of GTP to GDP by its "GAP" activity, thereby acting as a negative regulator of the G-protein signalling (Figure 4.8). During cerebellar development, ephrinB1-activation may mediate inhibition of the chemotactic response of cerebellar granule cells to SDF-1, contributing to the correct layering of these cells in the cerebellum (Lu et al., 2001).

EphrinA

Although ephrinA ligands lack a cytoplasmic tail, they are still able to mediate signal transduction. Signalling through ephrinA ligands may be mediated by the recruitment of adaptor proteins. It has been shown that ephrinA are localized to lipid rafts, which contain other signalling proteins, indicating that ephrinA ligands may activate a number of signalling pathways (Huai and Drescher, 2001).

Lipid rafts are small plasma membrane microdomains (\varnothing 50-100 nm), rich in cholesterol and sphingolipids. These subcompartments within the plasma membrane are enriched in GPI-anchored proteins (such as ephrinA), transmembrane proteins (such as ephrinB), as well as doubly acylated proteins (such as SFKs). Therefore, rafts acts as platforms for the signal transduction and lateral clustering can lead to fusion of dispersed rafts to larger patches, thereby forming higher order signalling units (Simons and Ikonen, 1997; Brown and London, 1998, 2000; Simons and Toomre, 2000). EphrinAs and ephrinBs are localized to lipid rafts, but in contrast to the ephrinAs, which are permanently localized to this membrane microdomains, the localization of ephrinBs critically depends on the cytoplasmic tail and its associated proteins (Brückner et al., 1999; Huai and Drescher, 2001). Clustering of ephrinA5 by the soluble EphA5 receptor ectodomain recruits and activate the SFK Fyn to lipid rafts (Davy and Robbins, 2000). This is accompanied by tyrosine phosphorylation of a 120 kDa lipid raft protein and prolonged activation of the MAPK Erk1 and Erk2. At the cellular level, the redistribution of vinculin, a cytoskeletal protein (binds to actin filaments), to focal adhesion complexes and increased cell substrate adhesion through β 1 integrin is induced by ephrinA activation (Davy et al., 1999; Davy and Robbins, 2000; Huai and Drescher, 2001). Therefore, ephrinA ligands are capable of transducing signals that influence actin dynamics, attachment and migration.

4.4.5. Repulsion and adhesion in cell-to-cell contact

The ephrin/Eph interaction-induced signal transduction generally results in a repulsive response after cell-to-cell contact. A growth cone encountering an ephrin-expressing cell via its Eph receptors, responds with a collapse. At the cellular level, this involves retraction of lamellipodia and filopodia mediated by depolymerization of the actin cytoskeleton. The questions that remain to be solved are about how the initially high-affinity adhesive interaction between ephrins/Ephs turned into a repulsive effect. Recent data by our group and others are now providing two possible answers: first, the proteolytical cleavage of ephrinA by a metalloprotease and second, the regulated receptor-ligand internalization from juxtaposed cell surfaces (Hattori et al., 2000; Mann et al., 2003; Marston et al., 2003; Zimmer et al., 2003). Thus, signalling and adhesive forces generated by binding of ephrins to Eph receptors can be modulated by ephrin cleavage or Eph receptor-ephrin internalization.

4.4.5.1. Cleavage of ephrin ligands

EphrinA reverse signalling may be modulated through its constitutive association with the metalloprotease A-Disintegrin-And-Metalloprotease (ADAM)-10/Kuzbanian (Kuz). Binding of EphA-ephrinA activates cleavage of ephrinA by the Kuz protease, thus releasing ephrinA from the cell surface and allowing the receptor-bearing cell to withdraw (Figure 4.9A) (Hattori et al., 2000). In contrast, EphA receptor expressing axons encounter cells expressing an ectopically uncleavable form of ephrinA2, causing a great delay in growth cone collapse and repulsion of the axon in an *in vitro* assay (Hattori et al., 2000).

The cleavage of endogenous ephrinB ligands by metalloprotease is induced by phorbol ester treatment, a stimulus that promotes the ectodomain shedding of a variety of transmembrane proteins. However, ephrinB cleavage upon EphB receptor stimulation is very inefficient in primary cells and sometimes not detectable (G.A. Wilkinson, R.K., unpublished).

A mechanism to maintain adhesive contacts between ephrinAs and EphAs could be the inhibition of ephrinA cleavage. Interestingly, a splice variant of ephrinA1 – ephrinA1b – has been found to strongly inhibit the proteolysis of the cleavable form of ephrinA1 after the interaction with their receptors by coexpression of ephrinA1 and ephrinA1b in human embryonic kidney (HEK) 293 cells (Finne et al., 2004). It is not clear yet if the cleavage mechanism terminates cell surface signalling of ephrinA.

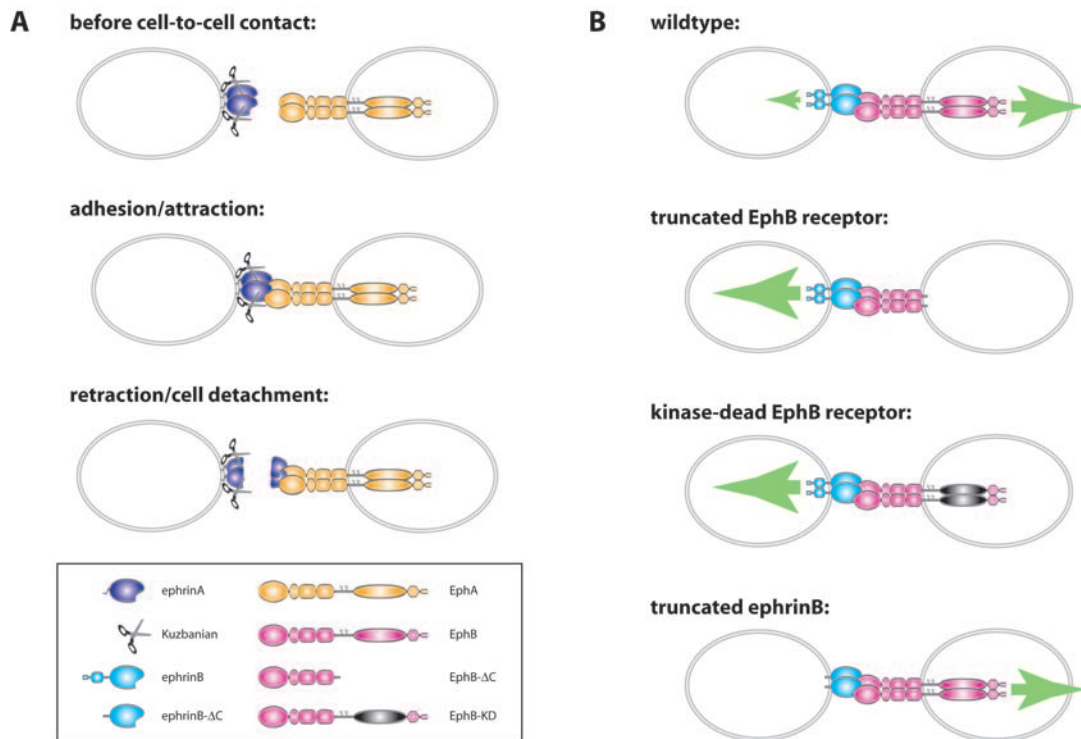


Figure 4.9. **Repulsion and adhesion in cell-to-cell contact.** (A) An ephrinA-expressing cell comes in close proximity with an EphA receptor-expressing cell (**upper panel**) and attaches by forming an adhesive complex (**middle panel**), thereby initiating signal transduction in the cells. Activation of the ephrinA-associated metalloprotease Kuzbanian by some of these signals leads to cleavage of the ligand ectodomain, thereby allowing the cells to detach (**lower panel**). (B) Contact between EphB- and ephrinB-expressing cells leads to bi-directional endocytosis, preferentially in the EphB-expressing cell (**top panel**). C-terminal truncation or inactivation of the kinase domain of the EphB receptor completely inhibits forward endocytosis, but strengthens reverse endocytosis into the ligand-expressing cell (**second panel** and **third panel**). C-terminal truncation of the ligand abolishes reverse endocytosis but does not affect forward endocytosis (**bottom panel**).

4.4.5.2. Regulated endocytosis of Eph-ephrin complexes

When Henrietta Lacks (HeLa) cells expressing fluorescently tagged ephrinB1 (enhanced cyan fluorescent protein, ECFP) were seeded and juxtapositioned next to fluorescently tagged EphB2 (enhanced yellow fluorescent protein, EYFP) expressing cells, clusters of EphBs and ephrinBs are initially formed locally at site of cell-to-cell contact and EphB2-ephrinB complexes are rapidly trans-endocytosed bi-directionally into adjacent cells (Figure 4.9B).

This event requires signalling through their respective cytoplasmic domains because ephrinB1 or EphB2 endocytosis can be blocked by C-terminal truncation of ligand and receptor in the ectopically expressing cell, respectively. For example, when ephrinB1 encounters truncated EphB2, endocytosis of both proteins occurs only uni-directional into the ephrinB1-expressing

4. Introduction

cell. In addition, the kinase-dead (KD) version of EphB2 could only be transcytosed into the ephrinB1-expressing cell and also causes abnormal adhesion. Remarkably, the uni-directional endocytosis of EphB2-expressing cells after interaction with truncated ephrinB1 have a stronger repulsion response than cells that show bi-directional endocytosis. Interaction between truncated forms of ephrinB1s and truncated forms of EphB2s are not endocytosed from juxtaposed cell surfaces into the expressing cells, causing enlarged ephrin-Eph clusters on the cell surface and resulting in an abnormally prolonged adhesion between the cells (Zimmer et al., 2003). Therefore, removing Eph-ephrin complexes from the cell surface requires uni-directional or bi-directional endocytosis, thereby enabling cells to detach and separate from each other.

Endocytosis has been considered merely as a mechanism for signal termination by downregulation of the activated receptors such as epidermal growth factor receptors (EGFR) and other RTKs, at the plasma membrane and their degradation in the lysosomes. However, internalized EGF and nerve growth factor (NGF) receptors are still able to signal (Burke et al., 2001; Barker et al., 2002). Endocytosed EGFR are phosphorylated and can be sorted to the surface of the endoplasmic reticulum, where they become dephosphorylated by the protein tyrosine phosphatase-1B (PTP1B)(Haj et al., 2002). EphB2s in intracellular vesicles are phosphorylated (Marston et al., 2003), suggesting that EphB2s may also contribute to signalling after endocytosis.

Both the internalization of the receptor-ligand complex and the subsequent cell retraction event are dependent on actin-polymerization, which in turn is dependent on Rac signalling within the receptor-expressing cell. EphrinB-EphB clusters do not colocalize with known markers of endocytic pathways, such as clathrin and caveolin (Marston et al., 2003; Zimmer et al., 2003), therefore the underlying mechanism of EphB2 endocytosis may resemble phagocytosis (Chimini and Chavrier, 2000) or macropinocytosis (Nichols and Lippincott-Schwartz, 2001).

Full-length ephrinB together with portions of the plasma membrane are transferred into the EphB4-expressing cell after binding to Eph receptor (Marston et al., 2003). Other proteins, such as the ion channels could also be removed by the endocytosis of the Eph receptor from the cell surface, when the Eph-complexes are incorporated into endocytic vesicles containing plasma membrane fragments, thereby influencing synaptic transmission.

Recent data by Marston et al. (2003) indicate that prolonged cell-to-cell contact may favour forward endocytosis by receptor-expressing cells using Swiss 3T3 and primary endothelial cells (human umbilical cord venous endothelial cells, HUVECs). Very immature primary neurons

from mouse forebrain show little forward, but rather pronounced ephrinB reverse endocytosis (Zimmer et al., 2003). Similar results were obtained with primary neurons from embryonic *Xenopus* retina when stimulated with soluble ectodomain fusion proteins (Mann et al., 2003). On the cell biological level, bi-directional transcytosis of two full-length transmembrane proteins is a new phenomenon.

These mechanisms provide conceivable explanations for the differences observed after Eph-ephrin interactions resulting in either (i) an adhesive effect by inhibiting the endocytosis or by expressing the splice variant of ephrinA1 or (ii) in a repulsive response through bi-directional endocytosis or the proteolytic cleavage of ephrinAs.

4.5. Eph receptors in the adult brain

In the past few years it has been shown that Eph receptors and their ligands are important in the adult nervous system, for example during the development of excitatory synapses, dendritic spine formation, and activity-dependent synaptic plasticity (Dalva et al., 2000; Ethell et al., 2001; Grunwald et al., 2001; Henderson et al., 2001; Contractor et al., 2002; Irie and Yamaguchi, 2002; Takasu et al., 2002; Henkemeyer et al., 2003; Penzes et al., 2003; Grunwald et al., 2004).

4.5.1. Expression patterns of ephrins/Ephs in the adult hippocampus

This work mainly concentrates on EphB2 and its binding partners in the hippocampus and only their expression patterns will be described. Ephs/ephrins are expressed at high levels in the embryonic nervous system (Flanagan and Vanderhaeghen, 1998). Many Eph receptors and their ligands continue to be expressed in the adult brain and Eph receptors can be localized to postsynaptic sites in the hippocampus (Torres et al., 1998; Buchert et al., 1999; Dalva et al., 2000; Murai and Pasquale, 2003). Interestingly, some Eph receptors change their localization from axonal to dendritic compartments with dendritic maturation (Henderson et al., 2001). Using immunogold electron microscopy, EphB2, EphB3 and EphA7 receptors are localized at the postsynaptic densities of the CA1 region in the adult rat hippocampus (Buchert et al., 1999).

In situ hybridization experiments demonstrated that EphB2 and EphA4 mRNAs are detectable at high levels in all regions of the hippocampus (Grunwald et al., 2001). While, EphB1 mRNA is expressed at middle levels in the DG, highly enriched in the CA3 and absent in the CA1

region; EphB3 mRNA shows a complementary expression pattern: absent in the DG, barely detectable in CA3 and high levels in CA1 region. EphrinB ligand mRNA is absent or barely detectable in the CA3 region. EphrinB3 mRNA has prominent levels in the DG and CA1, whereas ephrinB1 mRNA was found at low levels in the DG. EphrinB2 mRNA expression was mostly confined to CA1 and weak in the DG (Grunwald et al., 2001). At the CA1-CA3 synapse, mRNAs of EphB2 and EphA4 are most-likely both expressed pre- and postsynaptically, whereas EphB3 is mainly postsynaptic and EphB1 exclusively presynaptic. In addition, the mRNA of the ligands ephrinB2 and ephrinB3 are expressed mainly if not exclusively at the postsynaptic CA1 site (Grunwald et al., 2001). EphrinA5 is expressed in mature neurons in the DG (Gao et al., 1998b). Recent evidence suggests that ephrinBs are presynaptic in mossy fiber-CA3 synapses but postsynaptic in CA3-CA1 synapses of the hippocampus (Grunwald et al., 2001; Henderson et al., 2001; Contractor et al., 2002; Klein, 2004). In addition, ephrinA3 and EphA4 are also expressed in astrocytes that surround synapses (Murai et al., 2003; Goldshmit et al., 2004).

The Eph/ephrinB are expressed in overlapping and specific patterns, suggesting multiple sites of interaction and redundancy throughout the hippocampal formation.

4.5.2. Dendritic spine morphogenesis during development and plasticity

Dendritic spine formation

In the rat hippocampus, first synapses are formed as early as postnatal day 1 (P1) (Fiala et al., 1998) and the density of synapses gradually increases during the following weeks – doubling from P7 to P15 and from P15 to adulthood (Harris and Stevens, 1989; Harris et al., 1992). In dissociated hippocampal neuronal cultures, synapse development follows roughly in a similar time course: during the second week the synapse number doubles or triples and keeps increasing until the third week, after which it tends to fall (Papa et al., 1995; Boyer et al., 1998). Synapses are frequently found on filopodia (long thin protrusions), on stubby spines and on dendritic shafts in the brain (Miller and Peters, 1981; Fiala et al., 1998); they are later gradually replaced by or converted to, synapses on mushroom-like spines that have a well-defined head (Harris, 1999). Filopodia are remarkably more motile than mushroom-shaped spines and with a mean lifetime of only \sim 10 minutes versus hours and days. These thin protrusions are more transient than mature dendritic spines in culture (Dailey and Smith, 1996; Ziv and Smith, 1996). Filopodial motility might help to contact the “right” axon and can therefore be related to synaptogenesis (Ziv and Smith, 1996; Bonhoeffer and Yuste, 2002). Filopodia

have been proposed to be the precursors of mature mushroom-shaped spines (Ziv and Smith, 1996; Harris, 1999; Bonhoeffer and Yuste, 2002) and once formed, synapses are not rigid. During development, synaptic connections undergo an activity-dependent remodelling (Katz and Shatz, 1996; Shatz, 1996) and also in the adult brain synapses undergo long-term modifications (synaptic plasticity) that are believed to be the basis of information storage (learning and memory) (Bonhoeffer and Yuste, 2002; Li and Sheng, 2003).

The polymerization of actin, the main cytoskeletal element of the spine, is necessary for the shape and motility of the spine (Matus et al., 2000; Bonhoeffer and Yuste, 2002). As described in more detail before, many signalling proteins downstream of Eph receptors are known regulators of actin dynamics and therefore the activation of these receptors is required for spine development and maintenance.

Kalirin & Intersectin

EphB2 also promotes dendritic spine development through the activation of the GEFs Kalirin and Intersectin, which activate the two Rho family GTPases, Rac1 and Cdc42, respectively (Irie and Yamaguchi, 2002; Penzes et al., 2003). In the first pathway, long-term activation of EphB2 by ephrinB1-Fc induces clustering, phosphorylation and synaptic translocation of the endogenous Rho-GEF Kalirin to the postsynaptic site in immature hippocampal neurons and promotes spine morphogenesis. Unlike Intersectin and Ephexin, Kalirin binds only to activated EphB2 receptors. EphB2 activation also upregulates the activation of the serine/threonine kinase p21 activated kinase (Pak), a Rac1 downstream effector that promotes actin cytoskeleton rearrangement. Transfection of dominant negative forms of Kalirin, Rac1 and the Pak inhibitory domain all prevent spine morphogenesis in response to ephrinB1 stimulation, suggesting that Kalirin regulates Rac1 activation downstream of activated EphB2 receptors (Penzes et al., 2003). The second downstream pathway that link EphB2 to spine morphogenesis involves Intersectin and Cdc42. Intersectin, an exchange factor for Cdc42, is predominantly expressed in neurons and associated in an activity-independent manner with the kinase-domain of EphB2, but not EphA4. EphB2 cooperates synergistically with neural Wiskott-Aldrich syndrome protein (N-WASP) to activate Intersectin, which in turn activates Cdc42. N-WASP bind to the actin-related protein 2/3 (Arp2/3) complex in the presence of activated Cdc42 and activate Arp2/3-mediated polymerization of branched actin filaments (Irie and Yamaguchi, 2002). Transfection of dominant-negative forms of Cdc42, Intersectin and N-WASP inhibit spine morphogenesis (Figure 4.10). Thus, this pathway provides a direct link between EphB receptor activation and actin dynamics and has been proposed to promote branching of actin

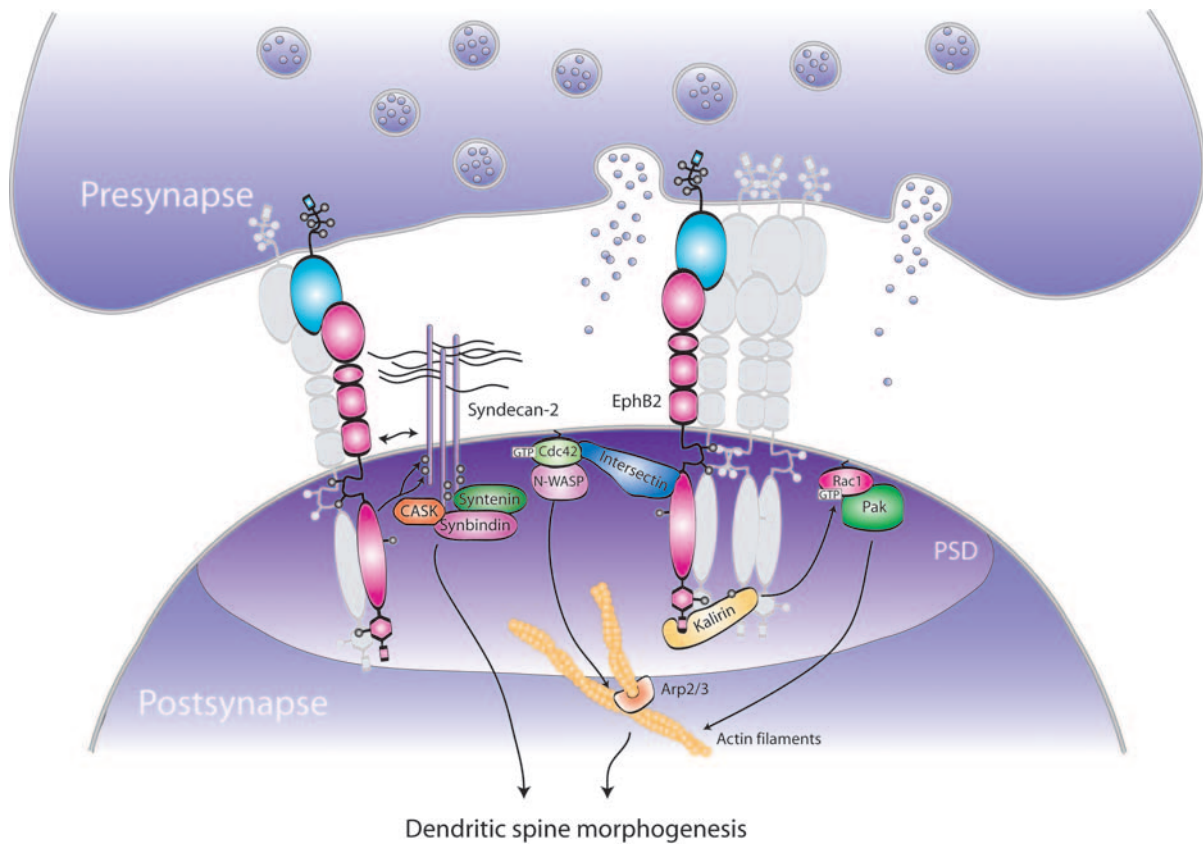


Figure 4.10. **EphB receptors drive dendritic spine morphogenesis.** Phosphorylation of the proteoglycan syndecan-2 downstream of activated EphB2 receptors is critical for promoting dendritic spine formation. Activated EphB2 receptors also activate the Rho-GEF proteins, Intersectin and Kalirin, which in turn activate the Rho family GTPases, Cdc42 and Rac1, respectively. The activated GTPases interact with downstream effector proteins which induce actin rearrangements, thereby promoting the EphB2-induced spine morphogenesis. The phosphorylation of syndecan-2 downstream of EphB2 is critical to induce association with EphB2 and its clustering. Clustered syndecan-2 recruits its cytoplasmic ligands toward subsynaptic localization, thereby promoting the morphological maturation of spines.

filaments, leading to the enlargement of the spine head.

Syndecan-2

Ethell et al. found that clustering of the cell surface proteoglycan syndecan-2 promotes dendritic spine maturation (Ethell and Yamaguchi, 1999). In a follow-up study they could demonstrate that tyrosine phosphorylation of syndecan-2 downstream of EphB2 receptor activation, but not EphAs, induces syndecan clustering and transforms immature filopodia-like dendritic protrusions into mature, mushroom-shaped dendritic spines in cultured hippocampal neu-

rons. EphB2 phosphorylates syndecan-2 on two cytoplasmic tyrosines and this phosphorylation is necessary for the association of both proteins (Ethell et al., 2001). Clustered syndecan-2 recruits cytoplasmic proteins, such as CASK, syntenin and Synbindin through the interaction of the C-terminal EFYA sequence, leading to the morphological maturation of spines (Figure 4.10)(Ethell and Yamaguchi, 1999).

NMDA receptor

Four recent studies demonstrate the involvement of Eph receptors forward signalling in the assembly of postsynaptic complexes at the excitatory synapses (Dalva et al., 2000; Ethell et al., 2001; Takasu et al., 2002; Penzes et al., 2003). The activation of the EphB receptor by soluble preclustered ephrinB1-Fc induces the direct association of EphB2 receptors with the NR1 subunit of the NMDA glutamate receptor in large raft-like patches within one hour in young immature cultured neurons. This interaction is mediated by the extracellular regions of the two receptors. Although this interaction is independent from the kinase activity of EphB receptors, the authors showed that forward signalling via EphB2 is required for further steps in synapse formation. This is all very important because the NMDA receptor plays a central role in synaptic plasticity and is known to be the first recruited glutamate-gated ion channel to the immature synapse. Ca^{2+} /Calmodulin-dependent kinase II (CamKII) and Grb10 were also found to colocalize with NR1 and EphB2 following ephrinB stimulation (Dalva et al., 2000). More recent data showed that EphB2 recruits and activates the cytoplasmic tyrosine kinase Src, which in turn phosphorylates subunits of the NMDA receptor (Grunwald et al., 2001; Takasu et al., 2002). Phosphorylation of the NR2B subunit enhances Ca^{2+} influx through the NMDA receptor in response to glutamate and increases phosphorylation of the transcription factor Ca^{2+} /cAMP-responsive element binding protein (CREB) and CREB-dependent transcriptional events that may affect synapse formation, maturation and plasticity (Grunwald et al., 2001; Takasu et al., 2002).

***EphB*-knockout mice**

Consistent with these *in vitro* findings, EphB2 null mice show reduced levels of NR1-containing NMDA receptors in hippocampal synapses (Henderson et al., 2001) and show deficits in activity-dependent synaptic plasticity (LTP and LTD). Targeted expression of a truncated kinase-deficient form of EphB2 rescued the *EphB2*-knockout phenotype, suggesting that ephrinB reverse signalling might play a role at the synapse. However, *EphB2*-knockout mice have normal hippocampal synapse morphology and density, which indicates that EphB2 is

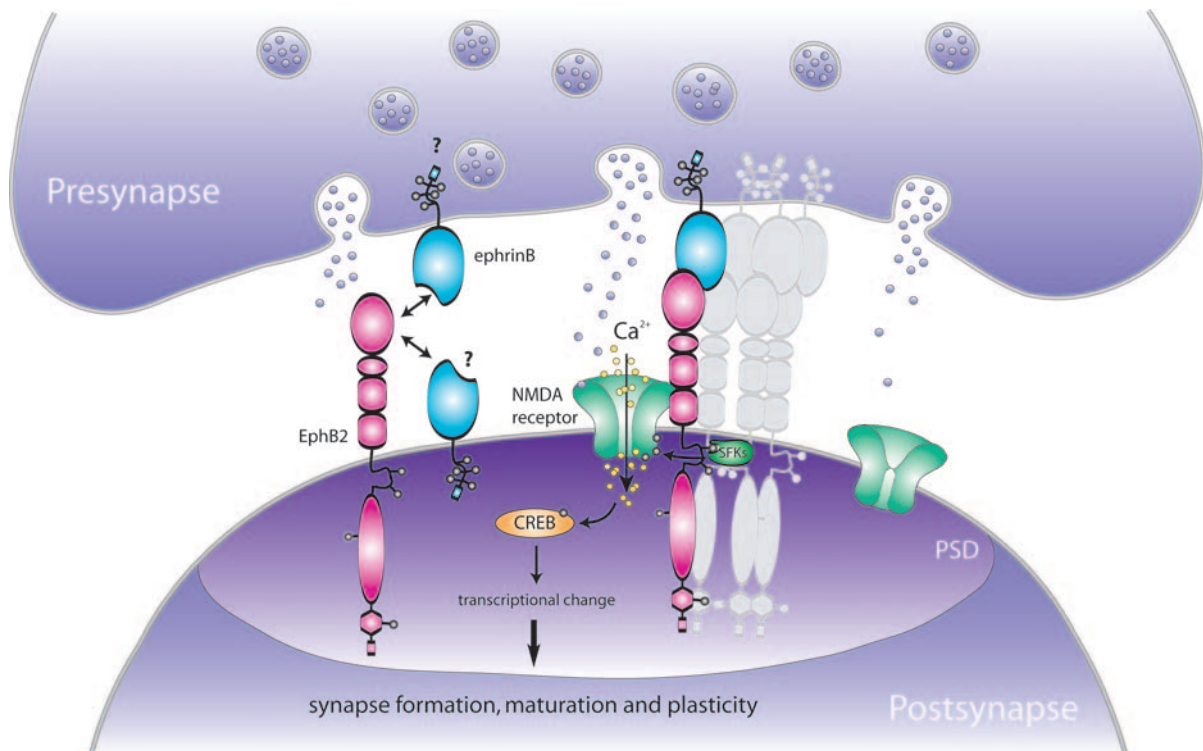


Figure 4.11. **NMDA and EphB2 receptor and their possible roles during synapse formation, maturation and synaptic plasticity.** EphB2 receptor activation leads to the recruitment of SFKs, direct interaction with the NR1 subunit and clustering of the NMDA receptor (in young cultures). The activated SFKs phosphorylate the NMDA receptor subunits NR2B (grey spheres), which enhances Ca²⁺ influx through the ion channel after glutamate (pink spheres) stimulation and potentiates phosphorylation (grey spheres) of the transcription factor CREB. CREB-dependent transcriptional events and other EphB2 downstream signalling cascades may influence synapse formation, maturation and synaptic plasticity. The site of ephrin localization has not yet been addressed (question marks).

not critically required for most aspects of synapse development (Grunwald et al., 2001; Henderson et al., 2001). In contrast, overexpression of kinase-deficient EphB2 in dissociated hippocampal neurons (one week old) that presumably block phosphorylation of multiple EphB family members (EphB1-B3), results in a decrease of synapse density (Dalva et al., 2000) and dendritic protrusions remain filopodial in old cultures (three weeks old) (Ethell et al., 2001). Hippocampal neurons from triple *EphB1/EphB2/EphB3*-knockout mice fail to form spines *in vitro* and develop abnormal spines *in vivo*, indicating that multiple EphB receptors cooperate to promote spine morphogenesis and synapse formation in the hippocampus (Henkemeyer et al., 2003). Thus, EphB receptor signalling pathways are required for spine morphogenesis.

Glia-dendritic spine formation

EphA4 activation by application of ephrinA3-Fc induces a marked spine shortening in slices of adult hippocampus. *EphA4*-knockout mice or mice ectopically expressing kinase-deficient EphA4 show irregularly shaped dendritic spines that are longer than normal. EphrinA3 was found to be highly expressed on astrocyte processes near synaptic terminals. This evidence suggests that astrocyte ephrinA3 and neuronal EphA4 interaction, leads to forward signalling in the synapse that stabilizes spine morphology and possibly synapses in the hippocampus (Murai et al., 2003).

4.6. The thesis project

Recent evidence strongly suggests that Eph receptor tyrosine kinases and their ligands contribute to synapse formation and synaptic plasticity (Dalva et al., 2000; Ethell et al., 2001; Grunwald et al., 2001; Henderson et al., 2001; Contractor et al., 2002; Irie and Yamaguchi, 2002; Takasu et al., 2002; Henkemeyer et al., 2003; Penzes et al., 2003; Grunwald et al., 2004). EphB2 receptors were found to be highly enriched in synapses and to specifically interact with the NR1 subunit of the NMDA receptor (Dalva et al., 2000). Furthermore, clustering of the receptors and interaction with NMDA receptor can be rapidly induced upon stimulation with ephrinB ligands, possibly mimicking initial steps of excitatory synapse formation. Additionally, EphB2 receptor activation leads to phosphorylation of syndecan-2 (Ethell et al., 2001), a protein that is involved in spine formation and spine morphogenesis. Moreover, our groups and others could demonstrate that lack of EphB2 leads to the impairment of two forms of synaptic plasticity in the hippocampus, namely LTD and LTP (Grunwald et al., 2001; Henderson et al., 2001). These initial findings strongly indicate a role for this receptor family in plasticity and synapse formation. However, the details of the mechanisms remain unclear.

The aim of this study was therefore to visualize EphB2 receptors in the living cell to understand their role during synapse formation. We therefore decided to generate fluorescently tagged EphB2 receptors (EphB2-ExFP) as a tool to study their dynamics of trafficking, insertion and clustering in neurons *in vitro* and *in vivo*.

For the *in vitro* approach, hippocampal cultures were transfected to exogenously express the fluorescently tagged EphB2 receptors and to analyze their motility and clustering behaviour in neurons.

For the *in vivo* approach, EphB2-EYFP transgenic mice were generated to monitor the *in vivo* behaviour of these fluorescently tagged proteins. Slices of these transgenic mice should allow

4. Introduction

a closer look into the dynamics and cluster behaviour of EphB2 receptors during synaptogenesis and also in spines and synapses of more mature neurons.

Recent findings by our lab and others could demonstrate that an adhesive contact between interacting cells can be turned into a retraction response by bi-directional EphB/ephrinB-triggered trans-endocytosis in cell lines and in immature growth cones upon contact with EphB2-expressing HeLa cells (Zimmer et al., 2003; Marston et al., 2003). A second major aim of this study was therefore to demonstrate the existence and relevance of Eph/ephrin-mediated transcytosis in mature hippocampal cultures.

5. Materials and Methods

5.1. Materials

5.1.1. Chemicals, enzymes and commercial kits

Chemicals were purchased in the highest purity from the companies Merck, Serva, Sigma, Fluka and Roth. The water used to prepare all solutions was filtered with the “Milli-Q-Water-System” from Millipore. Restriction enzymes were purchased from the companies: Roche and New England Biolabs (NEB). Other suppliers and kits used are mentioned in the methods section. Company contact details are given under 5.3 (see ordering information).

Table 5.1. Chemicals & commercial kits

Chemicals & commercial kits	ordering information	supplier
30% (w/v) Acrylamide:0.8% (w/v) Bisacrylamide stock solution (37.5:1), ProtoGel®	#EC-890	National Diagnostics
Aprotinin	#A-4529	Sigma
β -Mercaptoethanol	#M-7522	Sigma
BES	#B-6420	Sigma
Bovine albumin powder	#A-7906 (WB), #A-3294 (IHC)	Sigma
DMSO	#41641	Fluka
DNA ladder (Ready-load 1 kb plus)	#12308-011	Invitrogen
Complete EDTA-free, Protease inhibitor cocktail tablets	#1873580	Roche
ECL Western blot detection reagent	#RPN2132	Amersham
EphB2-Fc chimera, mouse	#467-B2-200	R&D

5. Materials and Methods

EphrinB1/B2-Fc chimera, mouse	#473-EB-200, #496-EB-200	R&D
Gel/Mount	#MØ1	Biomeda
Human IgG Fc-fragment	#009-000-008	Dianova
Films, Kodak BioMax MS Film	#Z363049-50EA	Sigma
Mouse-laminin, natural	#23017-015	Invitrogen
Nonidet P-40 (IGEPAL CA-630)	#I-3021	Sigma
Normal donkey serum	#017-000-121	Jackson ImmunoRe- search
Normal goat serum	#005-000-121	Jackson ImmunoRe- search
Normal sheep serum	#013-000-121	Jackson ImmunoRe- search
Orange G	#O-1625	Sigma
Paraffin, non caking, solidification point 57-60°C	#107158	Merck
PMSF	#P-7626	Sigma
Poly-D-lysine	#P-7886	Sigma
Poly-L-lysine	#P-2636	Sigma
Poly-DL-ornithine	#P-8638	Sigma
PonceauS solution	#33427	Serva
Precision Plus Protein™ Standards	#161-0373	Bio-Rad
Protein A-sepharose 4B	#17-0780-01	Amersham
Protein G-sepharose 4B	#17-0618-01	Amersham
QuikChange™ Site-directed mutagenesis kit	#200518 or -19	Stratagene
QuikChange™ XL Site-directed mutagenesis kit	#200516 or -17	Stratagene
TOPO TA Cloning®kit	#K4660-40	Invitrogen
TEMED	#161-0801	Bio-Rad
Triton X (TX)-100 solution	#93443	Serva

Tween®20 (Polyoxyethylene sorbitan monolaurate)	#170-6531	Bio-Rad
---	-----------	---------

5.1.2. Equipment

Table 5.2. Equipment

Equipment	Model	Supplier
Centrifuge	SORVALL RC 5Bplus	Kendro
Centrifuge	Varifuge 3.0R	Kendro
Centrifuge	Centrifuge 5810	Eppendorf
Rotor	GSA rotor & type 3	Sorvall
Table centrifuge	Centrifuge 5415 D	Eppendorf
Mini centrifuge	Quickspin Minifuges, C-1200	International Labnet
Hybridisation oven	Model U	Memmert
Incubator shaker	Unitron-Pro	Infors
Water bath	Type 3043	Köttermann
Water bath	Type 1083	GFL
Thermo mixer	Thermomixer comfort	Eppendorf
Balance	XT2220M-DR	Precisa
Fine balance	XT2220A-FR	Precisa
Magnetic stirring bar	50 × 8 mm	Brand
pH Meter	Inolab, pH Level 1	WTW
Electrophoresis power supply	EPS 301	Amersham
Water purification system	Milli-Q Biocel A10	Millipore
PCR machine	Peltier Thermal Cycler, PTC-225	MJ Research
Shaker	IKA Schüttler MTS 4	IKA® Werke
Shaker	POLYMAX 2040	Heidolph
Magnetic stirrer with heating	IKAMAG®Ret	IKA® Werke

5. Materials and Methods

Hood	HERASafe	Kendro
Laminar air flow hood	HERAGuard	Kendro
CO ₂ incubator	HERAcell® 240	Kendro
Spectrophotometer	Ultrospec 3000	Amersham
Pipettes	P2, P20, P100, P1000	Gilson
Multi pipette	Multipette® plus	Eppendorf
Multi channel pipette	20-200 µl, Transferpette-8	Brand
Multi channel pipette	0.5-10 µl, research	Eppendorf
Pipette help	Pipetboy acu	Integra Biosciences
Vacuum sucking system	VacuSafe	Integra Biosciences
Burner	Fireboy ecu	Integra Biosciences
Sequencer	ABI Prism 377 DNA sequencer	Applied Biosystems
Vortexer	VF2	IKA® Werke
Hemocytometer	Neubauer improved (depth 0.100 mm, 0.0025 mm ²)	Brand
Epifluorescence microscope	Zeiss Axioplan	Zeiss
Digital camera	SpotRT	Diagnostics Instruments
for Western Blot analysis:		
Semidry blotting apparatus		Pharmacia
Electrophoresis power supply	Power Pac 200, Power Pac 300	Bio-Rad
Bio-Rad gel system		Bio-Rad
Dissection instruments:		
Straight forceps, Biology tip	Dumont #5 (#11252-20)	Fine Science Tools
Vannas-Tübingen spring scissors	#15003-08	Fine Science Tools
Fine iris scissor	11 cm (#14090-11)	Fine Science Tools

Extra fine iris scissor, model "Bonn"	8.5 cm (#14084-08)	Fine Science Tools
Bent forceps, Biologie tip	Dumont #7 (#11297-10)	Fine Science Tools
Dissection stereomicroscope	Stemi SV 11	Zeiss
Dissection lamp	KL 1500 LCD	Leica
Equipment for time lapse imaging:		
Inverted epifluorescence microscope	Zeiss Axiovert 200M	Zeiss
CO ₂ -incubation chamber		EMBL
Digital camera	CoolSNAP-fx	PhotoMetrics

All other instruments used are mentioned with the methods.

5.1.3. Consumable material

Table 5.3. Consumable materials

Material	Type	Supplier
Live-cell dishes with a glass bottom	∅ 3.5 cm (#P35G-0-14-C)	MatTek
Coverslips, glass	∅ 10 mm, 13 mm	Marienfeld
Syringe	5 ml, 10 ml, 50 ml	Becton Dickinson
Combitips plus	5 ml, 10 ml, 0.5 ml	Eppendorf
Injection needles, disposable	20G, 22G, 23G, 26G, 27G	Terumo
Tissue culture plastic dishes, Nunclon™Δ	∅ 6 cm	Nunc
Tissue culture plastic dishes, Falcon®	∅ 3.5 cm, 6 cm, 10 cm	Becton Dickinson
Conical bottom, screw-top tube, Falcon®	15 ml, 50 ml	Becton Dickinson
Conical bottom, screw-top tube	15 ml, 50 ml	Greiner
Pasteur pipettes, glass, Volac	length 150 mm	Poulten & Graf

5. Materials and Methods

Multiwell cell culture plates, Falcon®	6 well, 12 well	Becton Dickinson
Multiwell cell culture plates, Costar	24 well	Corning
Plastic pipettes, Falcon	1 ml, 2 ml	Becton Dickinson
Plastic pipettes, Cellstar®	5 ml, 10 ml, 50 ml	Greiner
Exam gloves, powder-free, nitrile	SAFESKIN, Purple Nitrile, Size S	Kimberly-Clark
Parafilm®	Parafilm® "M"	American National Can
Tissue culture flasks, Nunclon™Δ	75 cm ²	Nunc
Tissue culture flasks, Falcon®	50 ml, 250 ml	Becton Dickinson
Cryo tubes	1.5 ml	Nunc
Reaction tubes, safelock	1.5 ml, 2 ml	Eppendorf
Pipette tips	20 μl, 200 μl, 1000 μl	PESKE
Reaction tubes, safelock	1.5 ml, 2 ml	Eppendorf
PCR lids	8-lid-strips (#7-9717)	NeoLab
PCR reaction tubes	Thermo-Fast 48 (#AB-0648)	ABgene
Precision wipes	KIMTECH Science	Kimberly-Clark
PVDF membrane	Immobilon	Millipore
Nitrocellulose membrane	0.45-μm pore size, Protran	Schleicher & Schüll
Blotting paper	3 mm Chr	Whatman
Filter systems:		
Syringe driven filter unit, Millex®-GV	0.22 μm	Millipore
Steritop, bottle top filter	250 ml, 500 ml (0.22 μm)	Millipore
Stericup, filtration system	250 ml, 500 ml (0.22 μm)	Millipore

All other consumable materials are mentioned with the methods.

5.1.4. Oligonucleotides

All oligonucleotides were synthesized by Metabion (www.metabion.de). Desalted or HPLC-purified oligonucleotides were used for sequencing reaction or mutagenesis, respectively. All sequences are shown from their 5' to their 3' end.

Table 5.4. Oligonucleotides

S: Sequencing reaction, IS: *in situ*, M: Mutagenesis, GT: Genotyping

Name	Oligonucleotide sequence	Use
T7 universal primer	TAATACGACTCACTATAGGG	S, IS
T3 promoter primer	ATTAACCCTCACTAAAGGGA	S
SP6	ATTTAGGTGACACTATAG	S, IS
BGH_reverse	TAGAAGGCACAGTCGAGG	S
pAdlox_afterMCS_rev (pExFP)	GGTTCAGGGGGAGGTGTGGG	S
CMV_sense_II (pExFP, pcDNA3)	CCATCCGCACATGCCACCCCTCC	S
EGFP-N (Clontech)	CGTCGCCGTCCAGCTCGACCAG	S
EGFP-C (Clontech)	CATGGTCCTGCTGGAGTTCGTG	S
5'vor_ATG_EphB2	GGACCTGGGAGTGGACACCTGTGG	S
5'mEphB2(356)	AACCTCTACTACTATGAGGC	S
5'mEphB2(841)	CATCAGGAACCTTCAAGGC	S
3'mEphB2(1507)	ACAGTGACTGTGTTGGTGG	S
3'mEphB2(1973)	TACAAAGATCTCTCTTTGCC	S
EphB2(2122)	CTCCTGTGTCAAGATTGAGC	S
3'mEphB2(2535)	CGTTGATTACGTCTTGATTGG	S
5'EphB2(3132-3153)	GCGTTGGGGTCACTCTAGCTGG	S
EphB2_afterCDR_rev	CGACGTAGGGGCTCAGGGG	S
5'ephrinB2_1713-1731	CCAAGATGTGAAATTCACC	S
3'ephrinB2_2098-2116	GGATGGATCATCTTCATCG	S
5'FgB2c3_HindIII_to_EcoRV	C GACTCACTATAGGGAGACCCgAtaTcGAGGTGTGGCAGGC	M
3'FgB2c3_HindIII_to_EcoRV	G CCTGCCACACCTCgAtaTcGGGTCTCCCTATAGTGAGTCG	M
5'ExFP_ClaI_Stop	C GAGCTGTACAAGggcggcgagcatcatgTAAAGCGGCCGCG	M
3'ExFP_ClaI_Stop	C GCGGCCGCTTTAategatgctgccgccCTTGACAGCTCG	M
5'EphB2_Y604F_Y610F	G GCATGAAGATCTtTATAGATCCTTTCACCTtTGAAGATCC	M
3'EphB2_Y604F_Y610F	G GATCTTCAaAGGTGAAAGGATCTATAaAGATCTTCATGCC	M
5'FgB2c3_NheI_344_ClaI	G GGGCCCTGATGctagcggcgcatcatgGACTCTACGACAGC	M
3'FgB2c3_NheI_344_ClaI	G CTGTTCGTAGAGTCatcatgcccccctagCATCAGGGGCC	M
5'FgB2c3_NheI_1999_ClaI	G CCGACTCAGAGctagcggcgcatcatgTACACGGACAAGC	M
3'FgB2c3_NheI_1999_ClaI	G CTTGTCCGTGTAtcatgcccccctagCTCTGAGTCGGC	M
5'FgB2c3_NheI_2958_ClaI	C CATGGCACCCCTGctagcggcgcatcatgTCCTCTGGCATCAACC	M
3'FgB2c3_NheI_2958_ClaI	G GTTGATGCCAGAGGAatcatgcccccctagCAGGGGTGCCATGG	M

5. Materials and Methods

5'deletion_PDZ_motif_EphB2	CCAGATCCAGTCTTGACATTCGCCTGCC	M
3'deletion_PDZ_motif_EphB2	GGCAGGCGAATGTCAAGACTGGATCTGG	M
5'K660R(FgB2c3_K630R)	GAGATCTTTGTAGCCATCAgGACCCCTCAAGTCAGG	M
3'K660R(FgB2c3_K630R)	CCTGACTTGAGGGTcTGATGGCTACAAAGATCTC	M
5'KOZAK_EphB2	CATTCTGATCGACGgcCAcCATGgACTTTATCCCAGTCG	M
3'KOZAK_EphB2	CGACTGGGATAAAGTcCATGgTGgcCGTCGATCAGAAATG	M
Nt_HindIII_HA-ephrinB2	AAGCTTGCCTACCCATACGATGTCCAGATTACGCTatctccagatcgatagt tta-gagcc	PCR
Ct_HindIII_HA-ephrinB2	GCGGCCGCCAGTGTGATGGATATCTGCAGAAAtcagacctttagtaaattt ggc	PCR
5'ephrinB2_DC_EcoRV	ccacagcacagcaccacgTGAGATATCctgtctcagcacactgg	M
3'ephrinB2_DC_EcoRV	ccagtgtgctgagagacagGATATCTCAcgtggctgtgtgtgtgg	M
Thy1F1 (Feng et al., 2000)	TCTGAGTGGCAAAGGACCTTAGG	GT
3'EphB2_358-340	CGTTGCTGTCGTAGAGTCC	GT

5.1.5. Bacteria

Table 5.5. Bacterial strains

Strain	relevant genotype
XL1-Blue	<i>supE44 hsdR17 recA1 endA1 gyrA46 thi relA1 lac⁻</i>
XL2-Blue MRF'	$\Delta(mcrA)183 \Delta(mcrCB-hsdSMR-mrr)173 endA1 supE44 thi-1 recA1 gyrA96 relA1 lac[F' proAB lacI^qZ\Delta M15 Tn10 (Tet^r) Amy Cam^r]$
XL10-Gold	$Tet^r \Delta(mcrA)183 \Delta(mcrCB-hsdSMR-mrr)173 endA1 supE44 thi-1 recA1 gyrA96 relA1 lac Hte$
TOP10	$F^- mcrA \Delta(mrr-hsdRMS-mcrBC) \Phi80 lacZ \Delta M15 \Delta lacX74 recA1 ara\Delta139 \Delta(ara-leu7697) galU galK rpsL (Str^r) endA1 nupG$
DH5 α	<i>supE44 $\Delta lacU169$ ($\Phi80 lacZ \Delta M15$) hsdR17 recA1 endA1 gyrA96 thi-1 relA1</i>
K12 (dam minus)	<i>supE44 $\Delta lacU169$ ($\Phi80 lacZ \Delta M15$) hsdR17 recA1 endA1 gyrA96 thi-1 relA1</i>

Table 5.6. Vectors

Plasmid	Size (kb)	Resistance	Supplier
pBluescriptII SK/KS	3.0	Amp	Stratagene
pcDNA3.1 plus	5.5	Amp	Invitrogen
pExFP-N1	4.7	Kan	Becton Dickinson
pExFP-C1/C2/C3	4.7	Kan	Becton Dickinson
pCRII-TOPO	3.9	Amp & Kan	Invitrogen
pCR2.1-TOPO	3.9	Amp & Kan	Invitrogen

5.1.6. Plasmids

5.1.6.1. EphB2 expression constructs

Expression constructs encoding full-length (FgB2c3) and truncated mouse flagEphB2 (FgB2Trc2) are described in Dalva et al. (2000). For more information see GenBank accession number NM_010142 (www.ncbi.nlm.nih.gov).

EphB2-EcoRV (pJK1):

In the FgB2c3 plasmid the *Hind*III cloning site upstream of the coding sequence of the signal peptide was changed by site-directed mutagenesis using the primer pairs 5'FgB2c3_HindIII_to_EcoRV & 3'FgB2c3_HindIII_to_EcoRV to an *Eco*RV restriction site. After the mutagenesis it was possible to clone the coding sequence of EphB2 in other constructs by using, e.g. *Eco*RV and *Not*I as restriction enzymes.

EphB2-KD (pJK2):

An expression construct encoding kinase-deficient EphB2 was generated by site-directed mutagenesis leading to exchange of lysine (aa660) to arginine using the primer pairs 5'K660R(FgB2c3_K630R) & 3'K660R(FgB2c3_K630R) with the Stratagene QuikChange™ kit.

EphB2-2F (pJK3) & EphB2-KD-2F (pJK4):

The two tyrosine residues, aa603 and aa609, of the juxtamembrane region were mutated to phenylalanine by site-directed mutagenesis using the primer pairs 5'EphB2_Y604F_Y610F & 3'EphB2_Y604F_Y619F of the kinase-active (pJK1) and the kinase-deficient (pJK2) construct, respectively, encoding the full-length flagEphB2.

EphB2- Δ PDZ (pJK5):

The C-terminal PDZ-motif VEV in the full-length kinase-active EphB2 (pJK1) was removed by site-directed mutagenesis using the primer pairs 5'deletion_PDZ_motif_EphB2 & 3'deletion_PDZ_motif_EphB2.

5.1.6.2. EphB2-ExFP expression constructs

Strategy:

In fluorescent fusion proteins the ExFP-protein is usually fused to the N- or the C-terminus of the protein. Because of EphB2 structural features we wanted to generate fusion proteins with the insertion of ExFP was between domains. As a control we decided to construct a N-terminal fusion protein, being aware that the ligand binding ability of the domain could be impaired.

The crystal structure of EphB2 was studied. The aim was to find ideal insertion sides, where the protein structure could still be intact after the ExFP-insertion between the protein domains. For the N-terminal fusion (EphB2-N-ExFP) we chose an insertion site downstream of the signal peptide. The two C-terminal insertions were designed close to the juxtamembrane region or between the kinase and the SAM domains.

pExFP-N1-ClaI-STOP (pJKm1-pJKm3):

To insert a glycine-serine linker followed by a *ClaI* cloning site into the expression constructs pEGFP-N1, pEGFP-N1 and pEYFP-N1 (pExFP-N1) by site-directed mutagenesis, the following primer pairs were used: 5'ExFP_ClaI_Stop & 3'ExFP_ClaI_Stop.

EphB2-Nhe1-344/1995/2958-ClaI (pJKm4-pJKm6):

NheI and *ClaI* restriction site were inserted by mutagenesis using the primer pairs: 5'FgB2c3_NheI_344_ClaI & 3'FgB2c3_NheI_344_ClaI for EphB2-Nhe1-344-ClaI (pJKm4), 5'FgB2c3_NheI_1999_ClaI & 3'FgB2c3_NheI_1999_ClaI for EphB2-Nhe1-1995-ClaI (pJKm5) and 5'FgB2c3_NheI_2958_ClaI & 3'FgB2c3_NheI_2958_ClaI for EphB2-Nhe1-2958-ClaI (pJKm6).

EphB2-N-ExFP (pJK7-pJK9):

To generate an expression construct encoding EphB2-N-ExFP, EphB2-Nhe1-344-ClaI (pJKm4) and pExFP-N1-ClaI-STOP (pJKm1-pJKm3) were cleaved with *NheI* and *HindIII*. The most N-

terminal *NheI* restriction site of the multiple cloning site (MCS) from the ExFP-N1 plasmids was used. The MCS can act as a linker increasing the likelihood that the fusion proteins will be functional (personal communication with Becton Dickinson). ExFP fragments were cloned in frame in the N-terminal region of EphB2, resulting in the following amino acid sequence: (ExFP)-DSTTATAE... .

EphB2-C1-ExFP (pJK10-pJK12):

An expression construct encoding EphB2-C1-ExFP was generated, as described above, by cloning the ExFP-N1 fragment (from pJKm1-pJKm3) in frame into the juxtamembrane region of EphB2 (pJK5). The flanking aa sequence of the EphB2 juxtamembrane region is ...GFERADSE-(ExFP)-YTDKLQHY... .

EphB2-C2-ExFP (pJK13-pJK15):

The EphB2-C1-ExFP construct was generated, as described above, by cloning the ExFP-N1 fragment (from pJKm1-pJKm3) in frame between the kinase and the SAM domain of EphB2 (pJK5). The aa sequence of the EphB2-ExFP fusion protein at the site of the insertion is ...PNSLKAMAPL-(ExFP)-SSGINLPLLD... .

EphB2-ΔC-ExFP (pJK16-pJK18):

To generate an expression construct encoding EphB2-ΔC-ExFP, almost all the cytoplasmic sequence from EphB2-C1-ExFP was replaced by ExFP. For this, both pJK10-12 and pExFP-N1 were cleaved with *NheI* and *NotI* and the ExFP-fragment was cloned in frame into the cut EphB2 construct. The remaining aa sequence of the EphB2 cytoplasmic domain is GFERADSE followed by the ExFP sequence.

EphB2-C1-KD-ExFP (pJK25-27):

The sequence for the ATP-binding site in the kinase domain of the pJK10-12 plasmids was mutated by site-directed mutagenesis using the primer pairs 5'K660R(FgB2c3_K630R) & 3'K660R(FgB2c3_K630R) in order to generate expression constructs encoding kinase-deficient EphB2-C1-ExFP (see EphB2-KD (pJK2)).

5.1.6.3. Thy1-EphB2-EYFP expression constructs for injection

The Thy-1.2 construct (pUC18-Thy-1.2) containing the mouse Thy-1.2 expression cassette was kindly provided by Dr. Pico Caroni (Friedrich Miescher Institute, Switzerland). It contains 6.5 kb of the murine *thy-1.2* gene, extending from the promoter to the intron following exon 4, but lacking exon 3 and its flanking regions and is described in Caroni (1997).

KOZAK-EphB2-C1-EYFP (pJK19-21):

A kozak in the plasmids pJK12 (EphB2-C1-EYFP), pJK27 (EphB2-C1-KD-EYFP), pJK18 (EphB2- Δ C-EYFP) was generated by site-directed mutagenesis using the primer pairs: 5'KOZAK_EphB2 & 3'KOZAK_EphB2.

Thy1-EphB2-C1-EYFP (pJK22), Thy1-EphB2-C1-KD-EYFP (pJK23), Thy1-EphB2- Δ C-EYFP (pJK24):

To put full-length, kinase-deficient and C-terminal truncated EphB2-C1-EYFP under the control of the Thy-1.2 expression cassette, the corresponding EphB2 construct were first cleaved with *NotI*. The 3' overhang was filled in with dNTPs and the fragments were then incubated with the restriction enzyme *XmnI*. These blunt-ended fragments were cloned into the blunt-ended *XhoI* site of the opened pUC18-Thy-1.2 plasmid.

5.1.6.4. ExFP-HA-ephrinB1 and -ephrinB2 expression constructs

E(C/Y)FP-HA-ephrinB1 (pJK30, pJK31) & ExFP-HA-ephrinB1 Δ C (pJK32, pJK33):

To generate expression constructs encoding a blue or yellow fluorescent HA-ephrinB1 (pJK30, pJK31) or HA-ephrinB1 Δ C (pJK32, pJK33), the E(C/Y)FP coding region was cloned into pJP136 or pJP139 (Brückner et al., 1999) using *SalI* and *BsRGI* restriction sites.

ExFP-HA-ephrinB2 (pJK36-pJK38):

The coding region for ephrinB2 was amplified from a pcDNA3.1-ephrinB2 plasmid (from George Wilkinson) using the primer pairs: Nt_HindIII_HA-ephrinB2 & Ct_HindIII_HA-ephrinB2 and cloned into the pCR2.1-TOPO plasmid. To generate expression constructs coding for ExFP-HA-ephrinB2, ephrinB2 was cloned in place of the ephrinB1 sequence in the ExFP-HA-ephrinB1 constructs (pJK30, pJP136 & pJK31) by cleaving these plasmids and the pCR2.1-TOPO-ephrinB2 (pJK35) with *HindIII* and *NotI*.

ExFP-HA-ephrinB2ΔC (pJK42-pJK44):

To generate expression constructs coding for ExFP-HA-ephrinB2ΔC an *EcoRV* restriction site was inserted by site directed mutagenesis into ExFP-HA-ephrinB2 plasmids (pJK36-pJK38) using the primer pairs 5'ephrinB2_DC_EcoRV & 3'ephrinB2_DC_EcoRV. The sequence encoding most of the cytoplasmatic domain was cleaved with *EcoRV*. The remaining aa sequence of the ephrinB2ΔC is ...RKHSPQHSTT.

5.1.7. Cell lines**Human embryonic kidney (HEK) 293 cells**

organism: *Homo sapiens* (human)

ATCC number: CRL-1573

For more information: www.atcc.org

5.1.8. Antibodies

(IHC: Immunohistochemistry, IP: Immunoprecipitation, WB: Western Blotting, d: donkey, g: goat, m: mouse, r: rabbit, h: human, minX: minimal crossreactivity)

5.1.8.1. Primary antibodies

Table 5.7. Primary antibodies

Antibodies	Dilutions
Preclustering of Fc-fusion proteins	
g anti-human Fc γ , minX (#109-005-098, Jackson ImmunoResearch)	Fc-clustering: 1/10 (w/w)
m anti-human Fc γ , minX (#209-005-098, Jackson ImmunoResearch)	Fc-clustering: 1/10 (w/w)
c-Myc tag	
m ascites anti-c-Myc (#1 667 149 (9E10), Roche)	WB: 1:1000
r anti-c-Myc agarose beads (#A7470, Sigma)	IP: 40 μ l/IP (= 10 μ l beads)

5. Materials and Methods

HA tag m anti-HA [0.4 $\mu\text{g}/\mu\text{l}$] (#1 583 816 (12CA5), Roche)	IHC: 8 $\mu\text{g}/\text{ml}$, WB: 1:1000, IP: 4 $\mu\text{g}/\text{IP}$
FLAG tag m anti-FLAG M2 [4 $\mu\text{g}/\mu\text{l}$] (#F3165, Sigma)	IHC: 1:2000, WB: 1:2000, IP: 1 $\mu\text{l}/\text{IP}$
GFP m anti-JL-8 (ExFP) [1 $\mu\text{g}/\mu\text{l}$] (#8371-2, Clontech) r anti-GFP [1 $\mu\text{g}/\mu\text{l}$] (#RDI-GRNFP4abr, RDI)	IHC: 2-5 $\mu\text{g}/\text{ml}$, WB: 1:1000, IP: 2 $\mu\text{g}/\text{IP}$ IHC: 1:1000, WB: 1:2000, IP: 1 $\mu\text{g}/\text{IP}$
NMDA1 receptor m anti-NR1 [2 $\mu\text{g}/\mu\text{l}$] (#60021A, PharMingen) m anti-NR1 [1 $\mu\text{g}/\mu\text{l}$] (#114011 (M 68), SySy)	WB: 1:1000, IP: 5 $\mu\text{l}/\text{IP}$ IHC: 1:1000
AMPA receptor r anti-GluR2/3 [0.1 $\mu\text{g}/\mu\text{l}$] (#AB1506, PharMingen) r anti-GluR1 [0.1 $\mu\text{g}/\mu\text{l}$] (#AB1504, PharMingen)	IHC: 1:30 - 1:100, WB: 1:1000, IP: 2 $\mu\text{g}/\text{IP}$ IHC: 1:30 - 1:100, WB: 1:1000, IP: 2 $\mu\text{g}/\text{IP}$
MAP2 m ascites anti-MAP2 (#M4403 (HM-2), Sigma)	IHC: 1:12000
PSD95 m anti-PSD95 (#P-246 (7E3-IB8), Sigma)	IHC: 1:200, WB: 1:2000, IP: 3-4 $\mu\text{l}/\text{IP}$
Synaptophysin r anti-Synaptophysin (#101002, SySy) m anti-Synaptophysin (#S-5768 (SVP-38), Sigma) m anti-Synaptophysin [1 $\mu\text{g}/\mu\text{l}$] (#MAB5258 (Sy 38), Chemicon)	IHC: 1:50 - 1:100 IHC: 1:100 IHC: 1:500 - 1:1000, WB: 1:1000
Synapsin r anti-Synapsin (#AB1543, Chemicon)	IHC: 1:500

Phosphotyrosine m anti-Phosphotyrosine [1 $\mu\text{g}/\mu\text{l}$] (#05-321 (4G10), UBI)	WB: 1:5000
ephrinB r serum anti-ephrinB, #200 (Brückner et al., 1999)	IHC: 1:100
ephrinB1/2 g anti-m ephrinB1 [0.1 $\mu\text{g}/\mu\text{l}$] (#AF473, R&D) r anti-m/h ephrinB1-B3 [0.2 $\mu\text{g}/\mu\text{l}$] (#C-18, Santa Cruz) rat anti-m ephrinB1 [0.5 $\mu\text{g}/\mu\text{l}$] (#MAB473, R&D)	IHC: 1:50 IHC: 1:50 IHC: 1:250
ephrinB2 g anti-m ephrinB2 [0.1 $\mu\text{g}/\mu\text{l}$] (#AF496, R&D)	IHC: 0.4 $\mu\text{g}/\text{ml}$ (1:250)
EphB2/3 g anti-m EphB2 [0.1 $\mu\text{g}/\mu\text{l}$] (#AF467, R&D) g anti-m EphB3 [1 $\mu\text{g}/\mu\text{l}$] (#AF, R&D)	IHC: 4 $\mu\text{g}/\text{ml}$ (1:25) IHC: 1:250
EphA4 g anti-m EphA4 [0.1 $\mu\text{g}/\mu\text{l}$] (#AF641, R&D) r anti-m/h EphA4 [0.2 $\mu\text{g}/\mu\text{l}$] (#S-20, Santa Cruz)	IHC: 1:50 IHC: 1:50

5.1.8.2. Secondary antibodies

Table 5.8. Secondary antibodies

Antibodies	Dilutions
Anti-Mouse <i>d anti-m-Cy3, -Cy5, minX</i> [0.75 $\mu\text{g}/\mu\text{l}$] (#715-165-151, #715-175-151, Jackson ImmunoResearch)	IHC: 1:200 - 1:400
<i>g anti-m-Alexa488</i> [2 $\mu\text{g}/\mu\text{l}$] (#A11001, Molecular Probes)	IHC: 1:400
<i>d anti-m-Texas Red, minX</i> [0.70 $\mu\text{g}/\mu\text{l}$] (#715-075-150, Jackson ImmunoResearch)	IHC: 1:50 - 1:100
<i>sheep anti-m-HRPO conjugate</i> (#NA931V, Amersham)	WB: 1:3000

5. Materials and Methods

Anti-Rabbit <i>d anti-r-Cy3, -Cy5, minX</i> [0.75 µg/µl] (#711-165-152, #711-175-152, Jackson ImmunoResearch) <i>d anti-r-Alexa488, minX</i> [2.0 µg/µl] (#A21206, Molecular Probes)	IHC: 1:200 - 1:400 IHC: 3.75 µg/ml
Anti-Goat <i>d anti-g-Cy3, minX</i> [0.75 µg/µl] (#705-165-147, Jackson ImmunoResearch) <i>d anti-g-HRPO conjugate</i> [0.75 µg/µl] (#705-035-147, Jackson ImmunoResearch)	IHC: 1:200 - 1:400 WB: 1:3000
Anti-Rat <i>d anti-rat-Cy3, minX</i> [0.75 µg/µl] (#712-165-153, Jackson ImmunoResearch)	IHC: 1:200 - 1:400
Protein A <i>HRPO-labelled Protein A</i> (#NA9120, Amersham)	WB: 1:3000

5.1.9. Media and standard solutions

Dulbeccos Phosphate-buffered saline (D-PBS)

137 mM NaCl	→ NaCl	8 g
2.7 mM KCl	→ KCl	0.2 g
8 mM Na ₂ HPO ₄	→ Na ₂ HPO ₄	1.15 g
1.5 mM KH ₂ PO ₄	→ KH ₂ PO ₄	0.24 g

Dissolve all ingredients in 800 ml of distilled water. Adjust to pH 7.4 with HCl and adjust volume to 1 l. Sterilize by autoclaving and store at room temperature (RT).

10× D-PBS

1.37 M NaCl	→ NaCl	80 g
27 mM KCl	→ KCl	2 g
81 mM Na ₂ HPO ₄	→ Na ₂ HPO ₄	11.5 g
15 mM KH ₂ PO ₄	→ KH ₂ PO ₄	2.4 g

Dissolve all ingredients in 800 ml of distilled water. Adjust to pH 7.4 with HCl and adjust volume to 1 l. Sterilize by autoclaving and store at RT.

0.5 M EDTA, pH 8.0

disodium EDTA-2H₂O 186.1 g

Dissolve all ingredients in 800 ml of distilled water. Adjust to pH 7.4 with HCl and adjust volume to 1 l. Sterilize by autoclaving and store at RT.

1 M Tris-HCl, pH 7.4 or 8.0

Tris base 121.1 g

pH 7.4 → HCl 70 ml

pH 8.0 → HCl 42 ml

Dissolve Tris base in 800 ml of distilled water. Adjust pH to the desired value by adding concentrated HCl. Adjust volume to 1 l. Sterilize by autoclaving and store at RT.

Tris-EDTA (TE) buffer, pH 8.0

10 mM Tris-HCl

1 mM EDTA

Adjust to pH 8.0 by adding concentrated HCl. Adjust volume to 1 l. Sterilize by autoclaving and store at RT.

50× Tris-acetate-EDTA (TAE) electrophoresis buffer

Tris base 242 g

Glacial acetic acid 57.1 ml

0.5 M EDTA (pH 8.0) 100 ml

Add distilled water to 1 l. The pH should be ~8.3. Store at RT. Dilute the concentrated stock buffer prior to use and prepare both the gel solution and the electrophoresis buffer from this concentrated stock solution.

6× Agarose gel-loading buffer

50% Glycerol (v/v) → 87% Glycerol 57 ml

1× TAE buffer → 50× TAE buffer 2 ml

0.2% Orange G (w/v) → Orange G 0.2 g

Add distilled water to 100 ml and store at RT.

4% Paraformaldehyde (PFA)

PFA (w/v) 20 g

D-PBS 500 ml

5N NaOH 200 μl

HCl, min. 37% 75 μl

Heat D-PBS to approximately 70°C, add PFA powder and stir at high speed. Add NaOH to dissolve the PFA completely and HCl, min. 37% to pH 7.3. Store in 50-ml aliquots at -20°C.

5. Materials and Methods

5.1.9.1. Media and antibiotics for bacterial culture

Luria-Bertani (LB) medium

Bacto-Tryptone	10 g
Bacto-Yeast extract	5 g
NaCl	5 g

Add distilled water to 1 l. The pH should be 7.5. Sterilize by autoclaving and store at RT.

LB plates

LB media	1 l
Bacto-Agar	15 g

Autoclave and store at 4°C.

Psi broth

Bacto-Tryptone	20 g
Bacto-Yeast extract	5 g
MgSO ₄	5 g

Add distilled water to 1 l. Adjust to pH 7.6 with 1N KOH. Sterilize by autoclaving and store at RT.

Antibiotics

1000× stock solutions:

<i>Ampicillin</i>	100 mg/ml
<i>Kanamycin monosulfate</i>	50 mg/ml

400× stock solutions:

<i>Tetracycline</i>	5 mg/ml in 100% EtOH
---------------------	----------------------

Dissolve in distilled water and sterilize by filtration. Store in aliquots at -20°C.

5.1.9.2. Media and supplements for tissue culture

DMEM-FBS medium

DMEM (Sigma, #D-5523)	500 ml
FBS, heat-inactivated (#10270-106, Invitrogen)	50 ml
Penicillin/Streptomycin (5000 U/ml, 100 µg/ml)(#15070-063, Invitrogen)	5 ml
200 mM L-Glutamine (100×)(#25030-024, Invitrogen)	5 ml
100 mM Sodium pyruvate (100×)(#11360-039, Invitrogen)	5 ml

Store at 4°C.

5.1.9.3. Media and supplements for primary cell culture

Borate buffer

Boric acid 1.24 g

Borax (#B-3545, Sigma) 1.90 g

Dissolve in 400 ml of distilled water. The pH should be 8.5, filter-sterilize and store at 4°C.

Neurobasal-B27 medium

Neurobasal medium (#21103-049, Invitrogen) 500 ml

B27 supplement (#17504-044, Invitrogen) 10 ml

Store at 4°C.

DMEM-FBS

DMEM (#61965-026, Invitrogen) 100 ml

FBS, heat-inactivated (#F-7524, Sigma) 10 ml

Sterilize by filtration through a 0.22- μ m membrane and store at 4°C.

1M MgCl₂

MgCl₂·6H₂O 20.33g

Dissolve in 100 ml of distilled water, filter-sterilize and store in small aliquots because of its hygroscopic property.

Store at RT.

1M HEPES

HEPES, free acid (#9105.2, Roth) 23.83 g

Dissolve in 100 ml of distilled water. The pH should be 7.3, filter-sterilize and store at 4°C.

Dissection medium (cooled on ice before use)

HBSS (Invitrogen, #24020-091) 500 ml

Penicillin/Streptomycin (5000 U/ml, 100 μ g/m)(Invitrogen, #15070-063) 5 ml

1M MgCl₂, pH 7.3 5 ml

1M HEPES 3.5 ml

200 mM L-Glutamine (100 \times)(Invitrogen, #25030-024) 5 ml

Store at 4°C.

5. Materials and Methods

5.1.9.4. Reagents for primary culture of astrocytes

5.5% NaHCO₃ (w/v)

NaHCO₃ 5.5 g

Dissolve in 100 ml of distilled water. Sterilize by filtration through a 0.22- μ m membrane and store at 4°C.

20% Glucose (w/v)

D(+)-Glucose 20 g

Dissolve in 100 ml of distilled water. Sterilize by filtration through a 0.22- μ m membrane and store at 4°C.

NMEM-B27 medium (Goetze et al., 2003)

10 \times MEM (#21430-020, Invitrogen)	50 ml
5.5% NaHCO ₃	20 ml
20% glucose	15 ml
100 mM sodium pyruvate (100 \times)(#11360-039, Invitrogen)	5 ml
200 mM L-Glutamine (100 \times)(#25030-024, Invitrogen)	5 ml
B27 supplement (#17504-044, Invitrogen)	10 ml

Add distilled water to 500 ml. Sterilize by filtration through a 0.22- μ m membrane. Store at 4°C and use within 10 days.

MEM-HS medium (de Hoop et al., 1998)

10 \times MEM (#21430-020, Invitrogen)	50 ml
50 \times MEM amino acids (#11130-036, Invitrogen)	10 ml
100 \times MEM non-essential amino acids (#1140-035, Invitrogen)	5 ml
5.5% NaHCO ₃	20 ml
20% glucose	15 ml
100 mM sodium pyruvate (100 \times)(#11360-039, Invitrogen)	5 ml
200 mM L-Glutamine (100 \times)(#25030-024, Invitrogen)	5 ml
Horse serum, heat-inactivated (#16050-122, Invitrogen)	50 ml

Mix all ingredients with approximately 350 ml distilled water. Adjust to pH 7.4 with 1N NaOH and adjust volume to 500 ml. Sterilize by filtration through a 0.22- μ m membrane. Store at 4°C and use within 2 weeks.

5.1.9.5. Media and solutions for cell transfection

1M CaCl₂

CaCl₂·2H₂O 2.94g

Add distilled water to 20 ml. Sterilize by filtration through a 0.22- μ m membrane and store 1-ml aliquots at -20°C.

2× BES-buffered saline (2×BBS)

50 mM BES → BES 1.07 g

280 mM NaCl → NaCl 1.6 g

1.5 mM Na₂HPO₄·2H₂O → Na₂HPO₄·2H₂O 0.027 g

Dissolve in 90 ml of distilled water. Adjust the pH with NaOH to 6.96-7.22. The optimal pH changes according to different sizes and preparations of plasmid DNA, then adjust the volume to 100 ml. Sterilize by filtration through a 0.22- μ m membrane and store in 1-ml aliquots at -20°C.

5.1.9.6. Reagents for live-cell imaging**External solution (Bi and Poo, 1998)**

145 mM NaCl → NaCl 8.474 g

3 mM KCl → KCl 0.224 g

10 mM HEPES → HEPES 2.383 g

3 mM CaCl₂ → CaCl₂·2H₂O 0.441 g2 mM MgCl₂ → MgCl₂·6H₂O 0.407 g8 mM D(+)-Glucose → D(+)-Glucose ·1H₂O 1.585 g

Dissolve one ingredient after another in approximately 900 ml distilled sterile water. Adjust to pH 7.3 with 1N NaOH and adjust volume to 1 l. Use within 1 day.

50 mM KCl-stimulation solution (Bi and Poo, 1998)

98 mM NaCl → NaCl 2.864 g

50 mM KCl → KCl 1.864 g

10 mM HEPES → HEPES 1.191 g

3 mM CaCl₂ → CaCl₂·2H₂O 0.221 g2 mM MgCl₂ → MgCl₂·6H₂O 0.203 g8 mM D(+)-Glucose → D(+)-Glucose ·1H₂O 0.793 g

Dissolve one ingredient after another in approximately 400 ml distilled sterile water. Adjust to pH 7.3 with 1N NaOH and adjust volume to 500 ml. Use within 1 day.

5.1.9.7. Solutions and buffers for western blot analysis**6× Sample buffer for reducing conditions**

12% SDS → SDS 3.6 g

300 mM Tris-HCl, pH 6.8 → 1.5 M Tris 6 ml

600 mM DTT → DTT 2.77 g

0.6% Bromophenol blue → bromophenol blue 0.18 g

60% Glycerol → 18 ml

Add distilled water to 30 ml. Store in aliquots at -20°C.

5. Materials and Methods

Lysis buffer

50 mM Tris-HCl, pH 7.5	→ 1M Tris, pH 7.5	5 ml
150 mM NaCl	→ 5M NaCl	3 ml
0.5-1% Triton X(TX)-100	→ TX-100	0.5-1 ml

Add distilled water to 100 ml. Store at 4°C.

Add fresh to 100 ml:

1 mM Sodium ortho vanadate (Na_3VO_4)	→ 100 mM Na_3VO_4	1 ml
10 mM NaPPi	→ NaPPi	0.45 g
20 mM NaF	→ NaF	0.084 g
Protease inhibitor cocktail tablets (complete)	→	2 tablets

4% Laemmli stacking gel, 10 ml

30% w/v Acrylamid/bisacrylamide	1.3 ml
0.5 M Tris-HCl (pH 6.8), 0.4% SDS	2.6 ml
H ₂ O	6.1 ml
10% APS	100 μ l
TEMED	10 μ l

Always prepare fresh.

7.5% Laemmli separating gel, 10 ml

30% (w/v) Acrylamide/bisacrylamide	2.5 ml
1.5 M Tris-HCl (pH 8.8), 0.4% SDS	2.6 ml
H ₂ O	4.85 ml
10% APS	50 μ l
TEMED	5 μ l

Always prepare fresh.

10% Laemmli separating gel, 10 ml

30% (w/v) Acrylamide/bisacrylamide	3.3 ml
1.5 M Tris-HCl (pH 8.8), 0.4% SDS	2.6 ml
H ₂ O	4.05 ml
10% APS	50 μ l
TEMED	5 μ l

Always prepare fresh.

5× Laemmli electrophoresis buffer

Tris base 154.5 g

Glycine 721 g

SDS 50 g

Add distilled water to 10 l. Store at RT.

10× Transfer buffer

Tris base 60.5 g

Glycine 281.5 g

SDS 25 g

Add distilled water to 2.5 l. Store at RT.

⇒ Add 20% methanol to the 1× Transfer buffer before use.

Sodium phosphate buffer, pH 7.2

1 M Na₂HPO₄ 68.4 ml

1 M NaH₂PO₄ 31.6 ml

2% SDS

Add distilled water to 1 l. Store at RT.

PBS-Tween (PBST)

1× D-PBS

0.1% Tween®20

Store at RT.

Blocking solution (w/v)

PBST

7.5% Milk powder, non-fat (Roth, #T145.2)

Always prepare fresh for use.

Stripping buffer

5 mM Sodium phosphate buffer, pH 7-7.4

2 mM β-Mercaptoethanol

2% SDS

Always prepare fresh for use.

5. Materials and Methods

5.1.9.8. Solutions for embedding of vibratome sections

0.1 M Acetate buffer, pH 6.5

1 M Sodium acetate 99 ml

1 M Acetic acid 960 μ l

Adjust to pH 6.5 and adjust volume to 1 l. Store at RT.

Embedding solution

1) Ovalbumin (Sigma, #A-S253) 90 g

0.1 M Acetate buffer, pH 6.5 200 ml

Dissolve albumin in acetate buffer by stirring for several hours at RT. Filter the solution with gauze to remove air bubbles and big clumps of undissolved albumin.

2) Gelatin 1.5 g

0.1 M Acetate buffer, pH 6.5 100 ml

Dissolve gelatin in acetate buffer by short heating. Let the solution cool down to RT! Mix the two solutions (1+2) without making air bubbles. Store 11-ml aliquots at -20°C.

5.1.9.9. Solutions for *in situ* hybridization

5% CHAPS (w/v)

Chaps (#C-3023, Sigma) 0.25 g

Distilled water (#W-3500, Sigma) 5 ml

Always prepare fresh for use.

Formamide deionized (deio)

Formamide (#K31880384 318, Merck) 500 ml

Resin (AG 501-X8 (D)) (#142-6425, Bio-Rad) 25 g

Stir for 45 min, filtrate and store in 50-ml aliquots at -20°C.

Heparin solution, 50 mg/ml (w/v)

Heparin 500 mg

Distilled water (#W-3500, Sigma) 10 ml

Store in 500- μ l aliquots at -20°C.

Proteinase K solution, 20 mg/ml (w/v)

Proteinase K 100 mg

Distilled water (#W-3500, Sigma) 5 ml

Store in 50- μ l aliquots at -20°C.

Prehybridization buffer

50% Formamide deio

0.2% Tween@20

0.5% Chaps

5 mM EDTA, pH 8.0

50 µg/ml Heparin

50 µg/ml tRNA (#R-5636, Sigma)

5× SSC, pH 4.5

0.2% Blocking reagent

Add distilled water (#W-3500, Sigma) to 50 ml, dissolve at 70°C and store at 20°C.

Solution I

50% Formamide deio

5× SSC, pH 4.5

0.2% Tween@20

0.5% Chaps

Add distilled water (#W-3500, Sigma) to 50 ml. Always prepare fresh for use.

Solution II

50% Formamide deio

2× SSC, pH 4.5

0.2% Tween@20

0.1% Chaps

Add distilled water (#W-3500, Sigma) to 50 ml. Always prepare fresh for use.

Solution III

2× SSC, pH 4.5

0.2% Tween@20

0.1% Chaps

Add distilled water (#W-3500, Sigma) to 50 ml. Always prepare fresh for use.

5× Maleic acid buffer (MAB)

Maleic acid 58 g

NaCl 44 g

Adjust to pH 7.5 first with 25 to 30 g NaOH pellets, then with 5N NaOH. Add distilled water (#W-3500, Sigma) to 1 l. Store at -4°C.

5. Materials and Methods

MAB-Tween (MABT)

1× MAB

0.1% Tween®20

Store at RT.

Blocking solution (w/v)

1× MABT

0.2% Blocking reagent (#1 096 176, Roche)

Incubate at 70°C until blocking reagent is dissolved (4 to 5 hours), then put on ice. Always prepare fresh for use.

NTMT

5 M NaCl 4 ml

1M Tris-HCl (pH 9.5) 20 ml

1M MgCl₂ 10 ml

Tween®20 200 µl

Add distilled water (#W-3500, Sigma) to 200 ml. Always prepare fresh for use.

20× SSC, pH 4.5

Sodium citrate 69.2 g

Citric Acid 13.7 g

NaCl 175 g

Adjust to pH 4.5 and adjust volume to 1 l. Store at RT.

5.1.9.10. Reagents for electrophysiology

Artificial Cerebrospinal Fluid (ACSF)

124 mM NaCl → NaCl 7.25 g

3 mM KCl → KCl 0.224 g

1.25 mM KH₂PO₄ → KH₂PO₄ 0.17 g

26 mM NaHCO₃ → NaHCO₃ 2.184 g

2.5 mM CaCl₂ → CaCl₂·2H₂O 0.368 g

2 mM MgSO₄ → MgSO₄·7H₂O 0.493 g

10 mM D(+)-Glucose → D(+)-Glucose ·1H₂O 1.98 g

Dissolve one ingredient after another in approximately 900 ml distilled sterile water. Adjust volume to 1 l. Saturate ACSF with 95% O₂ and 5% CO₂. Use within 1 day.

5.2. Methods

5.2.1. Molecular Biology

5.2.1.1. Preparation of plasmid DNA

Plasmid DNA was purified from small-scale (5 ml, minipreparation) or from large-scale (300 ml, maxipreparation) bacterial cultures. Hereby, single colonies of transformed bacteria or from a bacterial glycerol stock were picked each into LB medium containing 100 $\mu\text{g}/\text{ml}$ ampicillin or kanamycin and grown overnight (O/N) at 37°C with vigorous shaking. The bacterial suspension was pelleted by centrifugation at 4,000 rpm for 5 min at RT. The pellet was resuspended in buffer P1 (QIAGEN). Mini- and Maxipreparation of plasmid DNA were carried out according to the QIAGEN protocol using lysis of the cells and binding of the plasmid DNA to a special resin. After washing, elution and precipitation the plasmid DNA was redissolved in a suitable volume of buffer EB (QIAGEN) for minipreparation or pure water (#W-3500, Sigma) for maxipreparation. DNA concentration was measured in a UV spectrometer at 260 nm. The following formula was used:

dsDNA: $\text{OD} \times 50 \times \text{dilution factor} = X \mu\text{g}/\text{ml}$

5.2.1.2. Enzymatic treatment of DNA

Cleavage of plasmid DNA: Approximate 2-6 μg of DNA was cut in 30 μl of the appropriate buffer and 2 to 5 units (U) restriction enzyme for 1 to 2 hours (hrs) at an appropriate temperature.

Dephosphorylation of DNA fragments: For the dephosphorylation of DNA fragments 10 \times buffer, pure water (#W-3500, Sigma) and 1 U (1 μl) of calf intestine alkaline phosphatase (#713 023, Roche) was added to the restriction enzyme reaction to get a total reaction volume of 40 μl , incubated for 20 min at 37°C and heat-inactivated at 75°C for 15 min. Subsequently the dephosphorylated DNA fragments were purified from the reaction mix (see purification of DNA).

Generation of blunt-end DNA fragments: To generate blunt-ends of DNA fragments by *filling in the 5' overhang*, 5 U (1 μl) of Klenow (fragment of the DNA polymerase I)(#M0210S, NEB) was incubated with the DNA fragments (see cleavage of DNA) at 37°C for 20 min in the presence of 2 μl of dNTPs (25 mM each, Amersham). The enzyme was then inactivated at

5. Materials and Methods

75°C for 10 min. Subsequently the filled in DNA fragments were purified from the enzymatic reaction (see purification of DNA).

To generate blunt-ends of DNA fragments by **removing the 3' overhang**, the DNA-fragments (whole reaction from "cleavage of DNA") were incubated with 5 U (1 μ l) of Klenow polymerase (#M0210S, NEB) at RT for 20 min. The enzyme was then inactivated at 75°C for 10 min. Subsequently the blunt-ended DNA fragments were purified from the reaction mix (see purification of DNA).

Ligating vector and target DNA fragments: A 10 μ l reaction containing purified linearized vector (approximate 0.1 μ g) and DNA fragments ("insert") in an 1:5 ratio, 0.5 μ l of T4 DNA ligase (#M0202L, NEB), ligation buffer (10 \times T4 DNA ligase buffer, NEB) was incubated O/N at 16°C or at RT for 2 hrs, followed by 30 min at 37°C for sticky end ligations. Then the whole reaction was used to transform competent bacteria.

5.2.1.3. Separation of DNA on agarose gels

The DNA mix and circa one sixth of the volume of 6 \times loading buffer were loaded onto an 0.8-2% agarose gel in TAE buffer containing ethidium bromide (#2218.2, Roth; use 6 μ l per 100 ml) and run for approximate 30 to 35 min at 100-180 V. After electrophoresis a photograph of the gel was taken in the transilluminator on a UV light box and printed.

In a **preparative gel**, the DNA band was excised from the agarose gel with a clean, sharp scalpel and purified (see purification of DNA).

5.2.1.4. Purification of DNA

From agarose gel: Following extraction, purification of DNA fragments from agarose gels was carried out using the QIAquick Gel Extraction Kit (#28704, QIAGEN) as recommended by the manufacturer. The DNA was eluted in 30 μ l of buffer EB (QIAGEN).

From enzymatic reactions: To clean-up DNA fragments or oligonucleotides (\geq 17 nucleotides) from salts, enzymes, unincorporated nucleotides, the QIAquick Nucleotide Removal Kit (#28104, QIAGEN) was used according to the protocol of QIAGEN. The DNA was eluted in 30 μ l of buffer EB (QIAGEN).

5.2.1.5. Preparation of competent *E. coli*

The *E. coli* XL2-Blue supercompetent cells (Table 5.5) were streaked on a LB-tetracycline (tet) agar plate and incubated O/N at 37°C. One single colony of *E. coli* was picked into 10 ml of LB-tet medium, and cultured O/N at 37°C with vigorous shaking. The bacterial suspension was added to 1 l Psi broth without tet and grown for 2.5 to 3 hrs at 37°C until the OD reached ≥ 0.48 at 600 nm. To harvest, the flask was chilled on ice for 20 to 30 min and centrifuged in a cold rotor at 3,000 rpm for 15 min at 4°C. The pellet was gently resuspended in a total of 400 ml of ice-cold TFBI (30 mM potassium acetate, 100 mM KCl, 10 mM CaCl₂, 50 mM MnCl₂, 15% glycerol, adjusted to pH 5.8 with acetic acid and filter-sterilized) and kept on ice for 15 min. After re-centrifugation, the bacterial pellet was gently resuspended in 20 ml of ice-cold TFBII (10 mM MOPS, 10 mM KCl, 75 mM CaCl₂, 15% glycerol, adjust to pH 6.5 with KOH and filter-sterilized) and incubated on ice for 15 min. Then the *E. coli* suspension was frozen in 200 μ l-aliquots in liquid nitrogen, and stored at -80°C.

5.2.1.6. Transformation of competent *E. coli* using calcium chloride

50 μ l of chemical competent bacteria were gently thawed on ice and mixed with the ligation product. The tube was incubated on ice for 30 min. A heat shock was given by incubation at 42°C for 1 min. The tube was immediately placed back on ice for 2 min. Then 0.5 ml of LB medium was added, incubated at 37°C for 15 to 60 min with shaking at 225-250 rpm, plated on LB agar plates containing the appropriate antibiotic for the plasmid vector and incubated at 37°C O/N.

5.2.1.7. Transformation of competent *E. coli* by electroporation

50 μ l of electro competent bacteria were gently thawed on ice, mixed with 3-5 μ l of the ligation product and placed on ice for 1 min. Sterile 0.2 cm (green) cuvettes were placed on ice. Gene pulser apparatus (Bio-Rad) was set at 25 μ F and to 2.5 kV; the pulse controller to 200 Ω . The mixture of bacteria and DNA was transferred to a cold electroporation cuvette and shaken to the bottom of the cuvette. The cuvette was placed in the chamber slide, pushed into the chamber and pulsed once at the above settings. 1 ml LB medium was immediately added to the cuvette. The cells were resuspended, transferred to a reaction tube and incubated at 37°C for 15 to 60 min with shaking at 225-250 rpm. The bacteria were then plated on LB agar plates containing the appropriate antibiotic for the plasmid vector and incubated at 37°C O/N.

5.2.1.8. Screening bacterial colonies using X-gal and IPTG

For blue-white colour screening the LB agar plate containing the appropriate antibiotic was prepared 30 min prior to plating of the transformations. Hereby, 20 μ l of 10% (w/v in Dimethylformamide) X-gal and 20 μ l of 100 mM IPTG were pipetted into a 100 μ l pool of LB medium, and then the mixture was spread across the plate. If mixed before adding to LB medium IPTG and X-gal may precipitate. The transformation was spread and incubated O/N at 37°C. If the gene of interest was successfully cloned into the *lacZ* gene of the pBluescriptII SK/KS, plasmid the β -galactosidase reading frame is shifted or interrupted and *E. coli* cells appear then white instead of blue on the LB plates.

5.2.1.9. Polymerase chain reaction (PCR) & TOPO cloning

ExFP-HA-ephrinB2:

100 ng of plasmid DNA (ephrinB2-pcDNA3, kindly provided by George Wilkinson) were mixed with each 500 ng of 5' primer Nt-HindIII-HA-ephrinB2 and 3' primer Ct-HA-ephrinB2, 0.4 μ l of dNTPs (25 mM each), 5 μ l of 10 \times Expand High Fidelity System buffer and 2.5 U (=1 μ l) of *PfuTurbo* DNA polymerase (#600250, Stratagene) and pure distilled water (#W-3500, Sigma) was added to a volume of 50 μ l.

PCR cycling parameters:

Segment	Cycles	Temperature	Time
1	1	95°C	2 min
2	5	95°C	1 min
		60°C	30 sec
		72°C	1 min (1 min/kb)
3	25	95°C	1 min
		60°C + 0.5°C /cycle	30 sec
		72°C	70 sec
4	1	72°C	10 min
5	1	10°C	forever

→ 5 μ l of the PCR product were loaded on an 1% agarose gel and revealed a predicted band of approximately 1 kb in size.

TOPO cloning:

The TOPO mix contained 4 μl of PCR product, 1 μl diluted (1:4) salt solution and 1 μl of TOPO Vector (pCR2.1-TOPO). It was incubated for 30 min at RT. Chemical competent bacteria were transformed with 2 μl of the TOPO reaction and spread on a X-gal and IPTG treated LB-kanamycin plate for blue-white colour screening. White colonies were picked and DNA preparations were checked by restriction analysis and sequenced.

5.2.1.10. Mutagenesis

All mutagenesis (see plasmids) were performed with the QuikChange Site-Directed Mutagenesis Kit according to the protocol of Stratagene. All desired mutations were verified by sequencing procedure (Mrs. Thyrlas, Max-Planck-Institute of Neurobiology).

5.2.1.11. Cloning and generation of *in situ* probes**Cloning of the EYFP *in situ* RNA probe**

To generate a pCRII-TOPO-EYFP construct the insert encoding exon 12 of c-Ret (kindly provided by Laura Knott) was replaced by EYFP. For this, both pCRII-TOPO-cRet-ex12 and pEYFP-N1 were cleaved with *HindIII* and *XbaI* and the EYFP-fragment was cloned into the cut pCRII-TOPO plasmid.

Generation of the EYFP *in situ* RNA probe

Plasmid digestion: The primers (Sp6 or T7) for the RNA amplification must be chosen, depending on the direction of the insert in the TOPO vector. Here, the insert's 5' end was located next to the SP6 RNA polymerase sequence and the 3' end next to the T7 RNA polymerase. The vector had to be cleaved to linearize the plasmid upstream of the insert for the antisense probes produced by the T7 RNA polymerase and downstream for the sense probes transcribed by the SP6 RNA polymerase.

5 μg of pCRII-TOPO-EYFP plasmid were first digested with *HindIII*, which cleaves upstream of the insert (for the antisense probe) and then cut downstream of the insert with *XbaI* (for the sense probe). 20 U (2 μl) of each enzyme in the appropriate 10 \times buffer were used. The reaction was carried out with a final volume of 30 μl and incubated at 37°C for 1 hr. 2 μl of the reaction were loaded on an agarose gel to check if digestion was complete. In the case of complete lin-

5. Materials and Methods

earization, the DNA was purified with the PCR Purification Kit (#28104, QIAGEN) and eluted in 30 μ l buffer EB (QIAGEN). DNA concentration was measured with a spectrophotometer at 260 nm.

Labelling reaction (for 20 μ l):

- 300 ng linearized DNA
- 2 μ l 10 \times Transcription Buffer (#1 465 384, Roche)
- 2 μ l 0.1 M DTT
- 2 μ l 10 \times DIG RNA labeling mix (#1 277 073, Roche)
- 1 μ l RNase inhibitor (RNasin) (#3 335 399, Roche)
- 1 μ l specific RNA polymerase (SP6 (#810 274, Roche) or T7 (#881 767, Roche))
- to 20 μ l distilled water, RNase free (#W-3500, Sigma)

The reaction was incubated for 3 hrs at 37°C with gentle rocking. After the incubation, 2 μ l were loaded on an agarose gel to check the transcription efficiency.

In order to precipitate the RNA probe 100 μ l of TE buffer, 10 μ l 4M LiCl and 300 μ l EtOH were added. Samples were spun for 20 min at 4°C with 13,000 rpm. After two washing steps with 70% EtOH, the pellets were dried on ice. Subsequently, the dried pellet was resuspended in 100 μ l TE buffer and stored in 50- μ l aliquots at -80°C.

5.2.1.12. Extraction of genomic DNA and genotyping using PCR

DNA preparation:

DNA was prepared from mouse tail by treatment with NaOH. 100 μ l of 50 mM NaOH was added to each approximate 2 mm mouse tail, which was placed at 95°C for 20 min and returned to 10°C in the PCR machine for 2-3 times and vortexed thoroughly in between the boiling steps. Before neutralization with 100 μ l 10 mM Tris-HCl (pH 6.8), the tubes were shortly centrifuged (4-15C, Sigma) at 5,000 rpm to avoid mixing of fluids. The samples were vortexed and shortly centrifuged.

PCR:

1 μ l per 51 μ l reaction of DNA was used for PCR amplification to check the DNA for the presence of the transgene.

PCR master mix:

5.1 μ l	10 \times PCR buffer (NEB)
0.4 μ l	dNTPs (25 mM each)
1 μ l	33 μ M 5' primer (Thy1F1)
1 μ l	33 μ M 3' primer (3'EphB2_358-340)
2-5 μ l	homemade <i>Taq</i> polymerase or 0.5 μ l T4- <i>Taq</i> polymerase (#M0267L, NEB)
1 μ l	genomic DNA
to 51 μ l	add distilled water

The master mix was filled into the wells of a 48-well or 96-well PCR plate. Then 1 μ l of DNA was added and mixed thoroughly. The samples were placed into the PCR machine and the program with following PCR cycling parameters was started:

Segment	Cycles	Temperature	Time
1	1	95°C	2 min
2	35	95°C	1 min
		68°C	1 min
		72°C	1 min (1 min/kb)
3	1	10°C	forever

The PCR product was mixed with 6 \times loading buffer, loaded on a 1% agarose gel and then electrophoresed for approximate 30 min at 200 V. After electrophoresis, a photograph was taken under UV light.

5.2.1.13. Generation of transgenic mice

Vector sequences, particularly prokaryotic promoter and origin (*ori*) sequences impair the expression of the transgene. Therefore, single cutting restrictions sites should flank the final DNA fragment and this should be taken into consideration during design of the construct.

Purification of DNA fragments for pronuclear injection:**Plasmid digestion:**

Plasmids Thy1-EphB2-C1-EYFP (pJK22), Thy1-EphB2-C1-KD-EYFP (pJK23) and Thy1-EphB2- Δ C-EYFP (pJK24) (see plasmids) were purified from large-scale bacterial cultures using the Endofree Plasmid Kit (#12362, QIAGEN). About 25 μ g of each plasmid were digested with 30

U of the restriction enzymes *PvuI* and *NotI*. 1 μ l of the reaction mix was loaded and run on an agarose gel to check if digestion was complete.

Gel electrophoresis:

In the case of complete linearization, the cut DNA was loaded onto a 0.8% preparative agarose gel with a comb width of at least 5 cm in TAE buffer (in a clean gel running chamber) containing 10 mg (0.8 μ l) ethidium bromide per 100 ml agarose solution and run for approximately 4 to 5 hrs at 140 to 180 V. DNA size marker should not be used in order to prevent cross contamination with the DNA fragment!

Electroelution:

After separation of the specific DNA fragment from the vector backbone, the fragment of interest was cut out of the agarose gel with a fresh scalpel under low intensity UV light with a wavelength of 320 nm to avoid DNA damage. The DNA-agarose piece was transferred in a dialysis tube (#132 111, Spectra/Por-7 dialysis membrane, Spectrum Laboratories) sealed on one end by a plastic clamp. The dialysis bag was then filled with running buffer, closed by a second plastic clamp and fixed in the running chamber across the electric field (e.g. with a glass plate). The electrophoresis was continued for approximately 1 hr at 80 V to elute the DNA fragment out off the agarose gel piece. Subsequently, the polarity was changed for 30 sec to force the eluted DNA back from the dialysis membrane into the solution. The electroelution was controlled under low density UV light. At least 90% of the DNA should be eluted in the dialysis bag. The DNA solution was transferred, free of any agarose particles, into a 15 ml tube with the help of a 5 ml-syringe with a needle connected to the bag.

Purification of the DNA fragment:

The DNA fragment was purified with the Elutip-D minicolumns (#10462615, Elutip-D-Column-Set, NA010/0, Schleicher & Schuell). The Elutip-D column were equilibrated with 5 ml low salt buffer (0.2 M NaCl, 20 mM Tris-HCl, 1 mM EDTA, pH 7.4). After cutting off the column's tip, removing the protection cap and connecting the column to a syringe, the buffer was gently pressed through the column with a flow rate of 0.5 to 1.0 ml per min.

The DNA solution was diluted with two volumes of low salt buffer and gently pressed through the column with a flow rate of 1 ml per min (= 1 drop per second) to absorb the DNA to the column matrix. The column was washed twice with 5 ml of low salt buffer and then the DNA was eluted with 400 μ l of high salt buffer (1 M NaCl, 20 mM Tris-HCl, 1 mM EDTA, pH 7.4)

in an eppendorf reaction tube.

In order to precipitate the DNA 1 ml of 100% EtOH was added and mixed. The samples were then spun for 15 min at 13,000 rpm. The pellet was washed three times with ice-cold 70% EtOH and then dried at 50°C. Subsequently, the DNA pellets were resuspended in a small volume (25 μ l) of injection buffer (10 mM Tris-HCl, 0.2 mM EDTA, pH 7.5; in water of highest purity (#W-3500, Sigma)). DNA concentration was determined by UV spectrophotometry and adjusted to 100 ng/ μ l. Additionally the DNA concentration was checked by gel electrophoresis. 50 ng, 100 ng and 200 ng DNA per lane were loaded and compared with reference DNA of known concentration.

Pronuclear injection:

The pronuclear injection was carried out by the transgenic mice service (Michael Bösel, Max-Planck-Institute of Neurobiology). The DNA solution was injected into fertilized oocytes from FVB mice (FVB/NCrlMpi, animal house, Max-Planck-Institute of Neurobiology) which were implanted in pseudo pregnant females.

5.2.2. Cell culture

5.2.2.1. Propagation and freezing of mammalian cells

HEK293 cells were grown at 37°C with 5% CO₂ in DMEM-FBS medium. To harvest adherent cells, plates were washed once with D-PBS and treated with Trypsine/EDTA (#25300-054, Invitrogen) until cells deattached. Cells were usually seeded at a 1:8 ratio.

Cells were frozen in 8% DMSO/92% FBS, stored shortly on ice and then transferred to -80°C or liquid nitrogen. Cells were thawed quickly in 10 ml DMEM-FBS medium, pelleted, resuspended in DMEM-FBS medium and seeded.

5.2.2.2. Primary culture of hippocampal neurons

Before preparation coverslips and live-cell dishes were precoated with 1mg/ml Poly-D-lysine in borate buffer for at least 4 hrs at 37°C. Dishes were washed twice with sterile water and dried in a sterile hood. After coating O/N at 37°C with 5 μ g/ml mouse laminin in D-PBS, dishes were washed twice with D-PBS. For high-density cultures, D-PBS was replaced with Neurobasal-B27 medium and for low-density cultures with DMEM-B27. Media were left to equilibrate for at least 1 hr in the incubator with a 5% CO₂ atmosphere.

Hippocampal neurons were taken from pregnant CD1 mice (MpiCrlIcr:CD1, animal house,

5. Materials and Methods

Max-Planck-Institute of Neurobiology) at embryonic day 16.5 (E16.5) or from pregnant Wistar rats (MpiChbb:Thom, animal house, Max-Planck-Institute of Neurobiology) at E18.5. Pregnant rat was deeply anesthetized using diethyl ether. After decapitation (rat) or cervical dislocation (mouse), embryos were obtained and kept in ice-cold dissection medium. The preparation was then continued under an open sterile hood. Embryo heads were cut off and the skull opened to take out the brain. Embryonic brains were placed in fresh dissection medium and dissected under a stereomicroscope. Brain cortices were removed from the midbrain and brainstem and the meninges were pulled off. The striatum was cut out. The hippocampus was separated from the cortex and placed in fresh 15 ml dissection medium on ice. After removing the medium, hippocampi were incubated in 1.5 ml 0.25% Trypsin/1mM EDTA-HBSS-solution (#25200-056, Invitrogen) for 20 min at 37°C. The digestion reaction was stopped first by carefully removing Trypsin/EDTA-HBSS-solution and then by washing hippocampi three times with 3 ml DMEM-FBS. Then the tissue was triturated approximately 20 times with the help of a fire-polished glass pasteur pipette until the suspension was homogeneous. Subsequently, the cell suspension was centrifuged for 5 min at 80g to remove debris. Pellet was resuspended in 2 ml Neurobasal-B27 medium. Cells were counted in a hemacytometer and plated on coated glass coverslips in a 24-well plate at a density of 45,000 cells per well (high-density) or on coated glass bottom live-cell dishes. Depending on the length of culture, different numbers of cells were plated and incubated for 3-28 days *in vitro* (DIV) at 37°C in a humidified incubator with an atmosphere of 5% CO₂.

For time lapse experiments, glass bottom live-cell dishes were coated as described above. For high-density cultures 160,000 cells and for low-density cultures 40,000 cells were seeded in 2 ml of growing medium, respectively. After 14 DIV the hippocampal cultures were transfected using the Calcium-phosphate-DNA precipitation procedure.

5.2.2.3. Primary culture of glia

Preparation of astrocytes

Cerebral hemispheres (without meninges) were collected when preparing the hippocampi from pregnant Wistar rats (MpiChbb:Thom, animal house, Max-Planck-Institute of Neurobiology) at E17.5 to E18.5. The hemispheres were kept in dissection medium at 37°C during trypsinization of the hippocampi. After replacing the dissection medium with 5 ml of 0.25% Trypsin/1mM EDTA-HBSS-solution (#25200-056, Invitrogen), the tissue was incubated for 15 min at 37°C. The digestion reaction was first stopped by removing carefully Trypsin/EDTA-

HBSS-solution and then by washing three times with dissection medium or MEM-HS medium. Subsequently, the hemispheres were triturated approximately 20 times in 5 ml MEM-HS with the help of a fire-polished glass pasteur pipette until the suspension was homogeneous. To grow astrocytes, cells were plated at a density of approximately 60,000 cells per cm² onto untreated Nunc tissue culture flasks (approximately 5 million cells per 75 cm², approximately 4-5 hemispheres) containing MEM-HS. The next day, after cell attachment, the medium was changed completely to remove cell debris. When the cells reached about 80% confluency (7-10 days), they were trypsinized and split at 1:3 ratio. The astrocyte cultures can be passed up to four times.

Preparation of feeder layer for neuronal low density cultures

For low-density cultures hippocampal neurons were seeded as described above. After three days in culture the astrocytes feeding-layer and conditioned medium were put into the live-cell dishes.

One week before plating the neurons, twelve coverslips (Ø 10-mm) with paraffin dots are placed onto one Ø 6-cm tissue culture dish to maximize the glass surface. 80% confluent glia cells from one flask were trypsinized, resuspended in 30 ml MEM-HS and plated onto six Ø 6-cm tissue culture dishes with the coverslips. One day later the medium was replaced with fresh MEM-HS. On the day of preparation of the neuronal cultures MEM-HS was replaced with NMEM-B27 medium in order to let glia cells secrete survival factors in the medium. Three days after plating of the hippocampal low-density cultures, the coverslips with approximately 80% confluent astrocytes were grabbed using sterile forceps and flipped over into the dishes containing the neurons (1 to 2 coverslips/Ø 3-cm dish). Half of the NMEM-B27 medium (approximately 1 ml) in the neuronal dish was then replaced with the conditioned NMEM-B27 medium from the astrocytes. Every 10 days half of the old medium was replaced with fresh NMEM-B27.

5.2.2.4. Transfection of cell lines, primary neurons

HEK293 cells were transiently transfected using Effectene (QIAGEN) according to the protocol.

For the calcium phosphate transfection method all solutions were warmed to room temperature. The plasmid DNAs were briefly spun down in a mini centrifuge. For transfection of neurons growing (i) in live-cell dishes, part of the medium was removed, leaving 0.9 ml medium in the dish and (ii) on coverslips (Ø 13-mm) in a 24-well plate, leaving 0.25 ml. The remaining

5. Materials and Methods

medium was collected, filter-sterilized and kept at 37°C in a humidified incubator with an atmosphere of 5% CO₂. For 1 ml transfection solution 3-7.5 µg DNA (depending on the plasmid size) were slowly added to freshly diluted 250 mM CaCl₂ solution by stirring with the pipette tip, the final volume being 50 µl. 50 µl of 2× BBS was added drop wise to the DNA-CaCl₂ solution. The reaction tube was gently shaken each time after addition of three drops of 2× BBS. The solution was then thoroughly mixed. The CaCl₂-DNA-BBS mixture was added drop wise to the hippocampal neurons and the dishes gently swirled in order to mix medium and transfection mixture and to ensure a homogeneous formation of the DNA-calcium phosphate precipitation.

For the transfection of neurons on coverslips the CaCl₂-DNA-BBS mixture was added drop wise to 0.9 ml medium in a polystyrene-tube (Falcon) while vortexing. After collecting the remaining medium from 2 to 4 wells, 250 µl of the transfection solution was immediately added to each well. The collected medium was filter-sterilized and again kept in the incubator.

Cells were incubated at 37°C in a humidified incubator with an atmosphere of 5% CO₂ for the desired transfection time (2-4 hrs). If the formation of precipitate was too strong, the transfection medium was removed and cultures were washed with prewarmed HBSS (#14025-050, Invitrogen) until the DNA-calcium phosphate precipitation was completely washed off from the cells, subsequently they were incubated in the “old” kept culture medium. The expression time for time lapse experiments was typically 2 to 3 days and up to 10 days for some immunohistochemistry experiments.

5.2.2.5. Stimulation of cells with Eph receptors or ephrin ligands

Activation of the Ephs and ephrins was induced with clustered multimeric ligands or receptors, respectively. Hereby, ephrin-Fc, Eph-Fc or as a control Fc were multimerized for at least 30 min at room temperature using 1/10 (w/w) anti-human Fcγ. In Immunohistochemistry experiments, a concentration of 4 µg/ml of preclustered ligands was used to stimulate Eph receptors and 1-2 µg/ml to activate the ephrin ligands.

5.2.2.6. Time lapse imaging

Live-cell imaging was performed with a Zeiss Axiovert 200M microscope equipped with a temperature-controlled CO₂-incubation chamber set to 37°C, 60-70% humidity, 5% CO₂ and a FluoArc system (Zeiss, Germany) set to 30-50%. Images were acquired using a 63× oil immer-

sion objective with a CoolSNAP-fx camera. Sequential couples of EYFP and phase contrast images were taken at a rate of 1-2 frames per minute and processed using MetaMorph (Visitron, Germany) and ImageJ software (rsb.info.nih.gov/ij/download.html).

5.2.2.7. Chemical stimulation of neurons

For KCl-stimulation experiments of transfected neurons the live-cell dishes were transferred to the above described "time lapse setup". Before starting the live-cell imaging, cultures were constantly perfused (speed=5.2, Minipuls 3, Gilson) for at least 30 min with external solution Bi and Poo (1998). YFP images were taken at a rate of 1 frame per min. After 15 to 20 min the neuronal cultures were stimulated with 50 mM KCl or 50 μ M glutamate for 4 to 5 min by washing in and out (speed=8) the KCl-stimulation solution. Time-lapse imaging was continued for about 1 hr.

5.2.3. Biochemistry

5.2.3.1. Cell lysis and immunprecipitation of proteins

Cell lysis Transiently transfected HEK293 cells were washed once with ice-cold D-PBS and lysed in lysis buffer on ice for approximately 5 min. After scraping off and collecting the cells from the dish, the cell lysate was centrifuged at 10,000g for 15 min at 4°C to remove insoluble material (nuclei, cytoskeletal components and insoluble membranes). The supernatant was placed in a fresh eppendorf tube and directly loaded onto a SDS-Polyacrylamide (PA) gel or purified further (see below). Before loading on a gel, samples were boiled in 2 \times sample buffer for 5 min to denature the proteins.

Immunoprecipitation of proteins Depending on the specific immunoprecipitation X μ g of the antibody against the protein of interest (see table secondary antibodies) was prebound to 20 μ l of protein A-sepharose (for rabbit polyclonal antibodies) or 20 μ l of protein G-sepharose (for mouse monoclonal and goat polyclonal antibodies) for 30 min on ice. The total lysate from the different samples was added and incubated for 2 to 3 hrs on a rotating wheel at 4°C. Subsequently, the mixture was spun down at 3,000 rpm for 5 min at 4°C. The supernatant was discarded and the beads were washed three times with lysis buffer to remove traces of unbound proteins. 20 μ l of 2 \times sample buffer was added to the beads and the mix was then heated to 95°C for 5 min to elute the proteins and antibodies from the beads. The full sample

was loaded on a SDS-PAGE gel under reducing conditions and further processed, typically using SDS-PAGE and western blot analysis.

5.2.3.2. Immunoblotting

Protein samples derived from the procedures described above were separated by 7.5% or 10% SDS-PAGE and transferred to nitrocellulose or PVDF membranes by semi-dry blotting (1 mA per cm² for 1 to 1.5 hrs). Membranes were blocked at least for 1 hr at RT or O/N at 4°C in blocking solution. Following the blotting, membranes were incubated either 1-3 hrs at RT or O/N at 4°C with a primary antibody diluted in blocking solution. Subsequently, membranes were washed three times for 10 min in PBST at RT. Secondary antibodies linked to horseradish peroxidase (HRPO) were used to specifically recognize the primary antibody diluted in blocking solution. After incubation for 1 hr at RT, membranes were washed three times for 10 min in PBST. To visualize signals, the membrane was incubated with ECL solution for 1 min at RT and exposed to films (BioMax MS/MS, Kodak). The films were developed in an Optimax (Typ TR, MS Laborgeräte). For reprobing, membranes were stripped with stripping buffer.

5.2.4. Mouse work

Transgenic mice were crossed in a C57/Black6 (C57BL/6NCrlMpi, animal house, Max-Planck-Institute of Neurobiology) genetic background. For experiments with adult mice, mice were separated from their parents at the age of about three weeks, males and females were housed separately. Tail biopsies were taken and mice were ear tagged using six-digit number eartags from the Nationalband & Tag company. For all experiments a heterozygous transgenic male was crossed with wild type females and the mice of one litter were compared. For experiments with embryos, breedings were set up with one male and two females. Vagina plugs were checked starting on the next morning from the start of breeding. A plug was counted as pregnancy for 0.5 days. Embryos were taken according to experimental procedures, but typically at E16.5.

5.2.5. Histology

5.2.5.1. Cryosections

Cryosections were used to analyze the different founder lines from the transgenic mice or for immunostainings on floating sections. Therefore, transgenic mice (age: P50 to P120)

were shortly anesthetized with diethyl ether and decapitated with a guillotine (Max-Planck-Institute of Neurobiology). The head was opened and the whole brain quickly dissected out of the skull and placed into 15 ml ice-cold D-PBS for 2 min to eliminate blood. Brains were then fixed in 4% paraformaldehyde (PFA)/4% sucrose for 2.5 to 4 hrs. Subsequently brains were transferred in 30% sucrose in D-PBS and incubated O/N at 4°C.

For cryosections the brain was cut at the midline with a razor blade (between left and right hemisphere) and one half was frozen in embedding medium (Tissue-Tek O.C.T. compound, #4583, Sakura Finetek) on a cooling platform (cortex side down, cut side up). Sagittal sections were cut at a thickness of 20 μm to 100 μm on a sliding microtome (HM400, MICROM). Single sections were picked up with a fine brush and immersed in PBS.

5.2.5.2. Vibratome sections

In situ analysis of expression in adult brain was carried out using vibratome sections. Therefore, brains which were left O/N in 4% PFA at 4°C were washed three times with D-PBS and then immersed in a mixture of gelatin and ovalbumin in acetate buffer (see embedding solution). For embedding, a 11-ml aliquot was thawed at 37°C and cooled down at RT. A base was prepared by adding 100 μl of glutaraldehyde (25%, Sigma) to 2 ml embedding medium, mixed quickly and poured into the molds. After polymerization of the embedding medium the half brain was placed on top of it. Liquid was carefully removed with tissue paper and 350 μl of glutaraldehyde (25%, Sigma) were added to the remaining 7 ml of embedding medium, then mixed quickly and poured on the sample. For complete solidification the polymerized sample was stored 1 hr at 4°C in PBS.

For vibratome sections a small block including the brain tissue was cut out of the mould with a razor blade and glued to the holder (Leica). 80 μm and 100 μm sagittal sections were cut on a microtome (VT1000S, Leica), immersed in D-PBS and immediately processed further for *in situ* hybridization.

5.2.5.3. Antibody staining

20 μm to 40 μm cryosections were incubated for 1 hr at RT in 10% serum (typically from the same animal species used for the production of secondary antibody) in D-PBS, 0.2% TX-100 (blocking solution). The primary antibody was diluted in blocking solution and incubated O/N at 4°C. After washing three times with D-PBS for about 30 min, slices were incubated with fluorescent labeled secondary antibody diluted in D-PBS for 2 hrs at RT. After 3 washes

with D-PBS slices were mounted in Gel/Mount media and dried at RT.

5.2.5.4. Immunocytochemistry

Immunostaining of cells

For normal immunocytochemistry of total protein distribution, neurons grown on coverslips were fixed with 4% PFA/4% sucrose in D-PBS for 13 min at RT, washed once with D-PBS, then incubated with 50 mM ammonium chloride in D-PBS for 10 min at RT and washed again before permeabilization for 5 min with ice-cold 0.1% TX-100 in D-PBS at 4°C. After washing, coverslips were blocked for about 30 min at RT or O/N at 4°C with 2% bovine albumin (#A-3294, Sigma) and 4% serum (depending on the secondary antibody used: donkey, goat, sheep and/or rat serum, Jackson ImmunoResearch) in PBS. After blocking, coverslips were transferred into a dark moist chamber, face up. Primary antibodies for total stainings were incubated for at least 60 min at RT in 50 μ l blocking solution. After 3 washing steps with D-PBS for 5 min, secondary antibodies, previously diluted in 50 μ l of blocking solution, were added to the coverslips for 30 min at RT in the dark. After washing, samples were mounted in Gel/Mount media and dried at RT. Images were acquired using an epifluorescence microscope (Zeiss) equipped with a digital camera (SpotRT, Diagnostic Instruments) and the MetaMorph software (Visitron Systems).

Immunofluorescence internalization assay

Cells were fixed with 4% PFA/ 4% sucrose in D-PBS for 13 min at RT, washed once with D-PBS, then incubated with 50 mM ammonium chloride in D-PBS for 10 min at RT and rinsed again before blocking for about 30 min at RT with 2% bovine albumin (#A-3294, Sigma) and 4% serum (depending on the secondary antibody used: donkey, goat, sheep and/or rat serum, Jackson ImmunoResearch) in PBS. Primary antibodies for surface labeling were applied for 60 min at RT in blocking solution. Cells were washed three times for 5 min with D-PBS and then permeabilized for 5 min with ice-cold 0.1% TX-100 in D-PBS at 4°C. After washing, the coverslips were blocked for 30 min at RT or O/N at 4°C. Primary antibodies for total stainings were applied for at least 60 min at RT in blocking solution. After three washing steps with D-PBS for 5 min, secondary antibodies, diluted in blocking solution, were applied to the coverslips for 30 min at RT in the dark. After washing, samples were mounted in Gel/Mount media and let dry at RT. Images were acquired using an epifluorescence microscope (Zeiss) equipped with a digital camera (SpotRT, Diagnostic Instruments) and the MetaMorph software (Visitron Systems).

5.2.5.5. *in situ* hybridization

Brain sections were prepared with the vibratome and processed directly *in situ* hybridization using a whole mount protocol. All solutions used were RNase free. 80 μm sections were collected in D-PBS and subsequently dehydrated in methanol diluted in D-PBS (25% for 5 min, 50% for 5 min, 75% for 5 min, 100% for twice 5 min). Sections were stored for up to several months at -20°C in 100% methanol or further processed after at least 2 hrs at -20°C . Sections were then placed into a solution made out of 80% methanol and 20% of a 30% H_2O_2 solution (final concentration of 6% H_2O_2) for 1 hr at RT. Rehydration was carried out in 50% methanol in D-PBS for 5 min followed by 25% methanol in D-PBS for 5 min. Finally, the samples were washed three times in PBST for 5 min at RT. To remove proteins from RNA, sections were treated with Proteinase K (20 $\mu\text{g}/\text{ml}$ in D-PBST) for 13 min at RT. In order to stop the reaction, sections were washed twice with PBST on ice. Subsequently, sections were refixed in fresh 4% PFA containing 0.2% glutaraldehyde for 40 min at RT. Following two washes in PBST, sections were gently rocked in prehybridization buffer for at least 1 hr at 70°C . DIG-labeled RNA probes (= 12.5 $\mu\text{l}/\text{ml}$) were diluted in prehybridization buffer, preheated for 7 min to 70°C , and incubated with the sections O/N at 70°C .

The next day, sections were first rinsed for 5 min and then washed three times for 30 min in Solution 1 at 70°C . From this point on, RNase-free solutions were no longer required. Following 5-min rinsing and three 30-min washes in Solution 2 at 66°C , sections were initially rinsed for 5 min and then washed three times for 30 min in Solution 3 once at 66°C and twice at 68°C . Subsequently, sections were washed twice with MABT for 5 min at RT and then twice for 30 min at 70°C . Unspecific antibody binding was prevented using blocking solution for 1.5 hrs at RT. To detect DIG-labeled RNA, sections were incubated O/N at 4°C with an anti-DIG Fab fragment conjugated with alkaline phosphatase (AP) (1:2000 in blocking solution, #1 093 274, Roche).

The next day, sections were washed 8 to 10 times with MABT for 30 min to get rid of unbound or unspecifically bound Fab fragments and to prevent endogenous AP activity. After washing, sections were rinsed once in freshly made NTMT and then equilibrated in NTMT for 10 to 20 min. Developing solution was added (1.4 μl nitroblue tetrazolium (NBT) and 1.1 μl 5-bromo-4-chloro-3-indolyphosphate (BCIP) per ml NTMT) to give a dark purple color. Reaction and sample were kept in the dark. Sections were left in substrate solution at 37°C until enough staining was obtained. Upon development, sections were washed in PBST and postfixed in 4% PFA O/N. The sections were then mounted and stored in a solution made of 1 part 4%

PFA and 1 part glycerol.

5.2.6. Electrophysiology

Electrophysiological experiments were conducted by Dr. Martin Korte and Volker Staiger in the laboratory of Prof. Dr. Tobias Bonhoeffer at the Max-Planck-Institute of Neurobiology, Martinsried, Germany.

5.2.6.1. Organotypic acute hippocampal slices

Mice were shortly anesthetized using diethyl ether. After decapitation, embryonic brains were quickly dissected out and placed into ice-cold artificial cerebrospinal fluid (ACSF) for 2 min. To ensure constant pH and oxygen levels the ACSF was constantly aerated with Carbogen (95% O₂ and 5% CO₂). After cooling for a few minutes, the hemispheres were separated and the hippocampus was isolated. Intact hippocampi were cut with a so-called “egg-slicer” (Katz, 1987). The egg-slicer separates 400- μ m thick transverse hippocampal sections via a fine wire-net that acts in a guillotine-like fashion. The sections were then separated with the help of a pair of fine forceps and maintained in ACSF for several hrs before and during the experiments.

5.2.6.2. Electrophysiological recordings

The Thy1-EphB2-EYFP^{+/-} (A line) and Thy1-EphB2- Δ C-EYFP^{+/-} (Df line) transgenic mice were between P41 and P60 for LTP (E-LTP, L-LTP) experiments. The ACSF was saturated with 95% O₂ and 5% CO₂. The hippocampi were cut as described above. Slices were maintained in ACSF at RT for at least 1.5 hrs before recording. Recordings were started after a 20-min equilibration phase in the recording chamber. Synaptic responses were evoked in the CA3 region of the mouse hippocampus by stimulating Schaffer collaterals with 0.1 ms pulse through a monopolar tungsten electrode. Field excitatory postsynaptic potentials (fEPSPs) were recorded extracellularly in the *striatum radiatum* of the CA1 pyramidal cell region (approximately 100 μ m below slice surface) using glass microelectrodes (borosilicate: 1.0 mm OD \times 0.58 mm ID + inner filament, Clark) filled with 3 M NaCl (8-10 M Ω). For baseline recordings slices were stimulated at 0.1 Hz for 20 min at stimulation intensities that resulted in half-maximal fEPSP-amplitudes (30-180 mA). Paired-pulse facilitation (PPF) was tested by

applying two pulses separated by intervals ranging from 10-160 ms.

LTP was induced by applying thetaborst stimulation (TBS): TBS consists of three bursts (10-s interval), each of them composed of 10 trains (5 Hz) with four pulses each (100 Hz).

5.2.6.3. Data analysis

Electrophysiological data were sampled at 5 kHz on a personal computer using a customized LabView program (National Instruments), which was also used for offline analysis. All measurements were carried out and analyzed in a strictly blind fashion. Therefore, the genotype of the slices was revealed after the measurement and its analysis had been completed. As an indicator of synaptic strength the initial slope of the evoked fEPSPs was measured, averaged across 6 or 7 consecutive measurements and expressed as percentages relative to the baseline mean. The normalized data of each experiment were then time-matched, averaged across experiments and expressed as means (\pm SEM). PPF was expressed as the increase in initial slope of the second fEPSP relative to the first. Post tetanic potentiation (PTP) was measured as the mean fEPSP-slope during the first 3 min after the application of TBS relative to baseline.

5.3. Ordering information

Table 5.9. Order Information

COMPANY	(WEB) ADDRESS
ABgene Germany	www.abgene.com
Amersham Biosciences Europe GmbH	www4.amershambiosciences.com
Applied Biosystems	www.appliedbiosystems.com
Becton Dickinson and Company	www.bdbiosciences.com
Biomeda Corporation.	www.biomeda.com
Bio-Rad Laboratories	www.bio-rad.com
Brand GmbH & Co.KG	www.brand.de
Carl Zeiss AG Deutschland	www.zeiss.de
Chemicon Europe	www.chemicon.com
Clark, Electromedical Instruments	PO Box 8 Pangbourne, Reading RG8 7HU, UK
Corning Incorporated	www.corning.com
Diagnostics Instruments, Inc.	www.diaginc.com
Dianova GmbH	www.dianova.de
EMBL	www.embl-heidelberg.de
Eppendorf AG	www.eppendorf.de
Fine Science Tools GmbH	www.finescience.com
Fluka	www.sigma-aldrich.com
GFL - Gesellschaft für Labortechnik mbH	www.gfl.de
Gilson, Inc.	www.gilson.com
Greiner Bio-One GmbH	www.gbo.com/bioscience
Heidolph Instruments GmbH & Co. KG	www.heidolph.com
IKA® Werke GmbH & Co. KG	www.ika.net
International Labnet Co.	www.labnetlink.com
Integra Biosciences AG	www.integra-biosciences.com
Invitrogen GmbH	www.invitrogen.com
Infors GmbH	www.infors-ht.com
Jackson ImmunoResearch	www.jacksonimmuno.com
Kendro Laboratory Products GmbH	www.kendro.com
Kimberly-Clark Europe	www.kimberly-clark.com
Köttermann GmbH & Co.KG	www.koettermann.de
Labnet International	www.labnetlink.com
Leica Mikrosysteme Vertrieb GmbH	www.leica.com , www.leica-microsystems.com

MatTek Corporation	www.mattek.com
Memmert GmbH & Co.KG	www.memmert.com
Merck KGaA	www.merckeurolab.de
Metabion	www.metabion.de
MICROM International GmbH	www.microm.de
Millipore Corporate Headquarters	www.millipore.com
MJ Research	www.aibltd.com
Molecular Probes	www.probes.com
MS Laborgeräte	www.ms-l.de
Nationalband & Tag company	www.nationalband.com
National Diagnostics	www.nationaldiagnostics.com
National Instruments (LabView)	www.ni.com
NeoLab	www.neolab.de
New England Biolabs GmbH, NEB	www.neb-online.de
Nunc GmbH & Co.KG	www.nunc.de
Paul Marienfeld GmbH & Co. KG	www.superior.de
PESKE, Medizintechnik/Laborbedarf	Beratung und Vertrieb, Von Schaezler Str. 18 D-86447 Aindling, Germany
PharMingen	www.pharmingen.com
PhotoMetrics, Inc	www.photomet.com
Poulsen & Graf GmbH, Volac	Am Bildacker 3-7, D-97877 Wertheim, Germany
Precisa Instruments AG	www.precisa.com
QIAGEN GmbH	www.qiagen.com
R&D	www.RnDSystems.com
RDI, Research Diagnostics, Inc.	www.researchd.com
Roche	www.roche.com
Roth	www.carl-roth.de
Sakura Finetek Europe	www.sakura-america.com
Santa Cruz	www.scbt.com
Schleicher & Schuell BioScience GmbH	www.schleicher-schuell.com
Serva	www.serva.de
Sigma-Aldrich Chemie GmbH	www.sigma-aldrich.com
Spectrum Laboratories	www.spectrapor.com
Stratagene	www.stratagene.com
Synaptic Systems, SySy	www.sysy.com
TERUMO Deutschland GmbH	www.terumo-europe.com

5. *Materials and Methods*

Upstate Biotechnology, UBI

www.upstate.com, www.upstatebiotech.com

Visitron Systems GmbH

www.visitron.de

Whatman

www.whatman.com

WTW

www.wtw.com

6. Results

6.1. Generation of fluorescently tagged EphB2 receptors

In order to better understand the role of EphB2 receptors and to study their trafficking dynamics, insertion and clustering in neurons during synapse formation and synaptic plasticity, the EphB2 receptor was fluorescently tagged with blue (ECFP), green (EGFP) or yellow fluorescent protein (EYFP) (generally indicated as: ExFP). Eph receptors interact N-terminally with their different ephrin ligands via their globular domain and C-terminally with a large number of signalling proteins via their PDZ-motif. Thus N- or C-terminal tagging could negatively influence important protein-protein interaction. Surprisingly, it has been shown by our group that the N-terminal fusion of ExFP to ephrinB1 does not affect the clustering of ephrinB1 (Brückner et al., 1999; Zimmer et al., 2003).

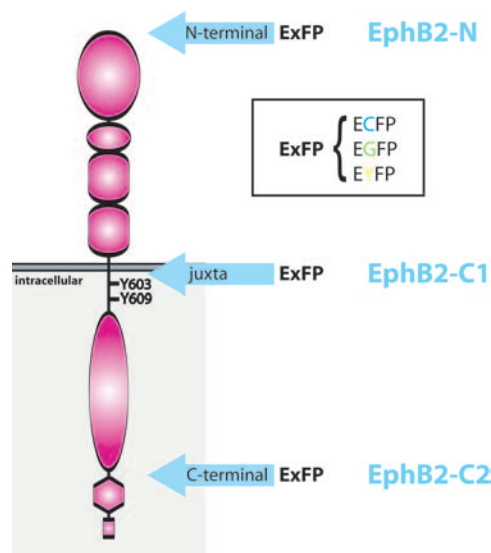


Figure 6.1. **Schematic view of the ExFP insertions sites in the EphB2 receptor.** To visualize the EphB2 receptors one variant of the enhanced blue, green or yellow fluorescent protein (ExFP) was fused to the receptor. ExFP was inserted in one of the three different positions (blue arrows) of the EphB2 receptor: the N-terminus (EphB2-N), a site close to the juxtamembrane domain (EphB2-C1) and between two functional relevant domains of the cytoplasmic part of EphB2 (EphB2-C2).

6. Results

The crystal structure of EphB2 was analyzed to find ideal insertion sites, where the protein structure could still be intact after the ExFP-insertion, for example between the functional protein domains. Three different tagging sites were chosen: (i) the N-terminus, (ii) a site adjacent to the juxtamembrane region or (iii) between the kinase domain and the SAM domain (Figure 6.1). According to the EGFP-ephrinB1 and other N-terminal fusion proteins the N-terminally tagged ExFP-EphB2 (named EphB2-N) was expected to be the most likely functionally intact fusion protein and was therefore generated as a “control” fusion protein, however with the potential caveat that the ligand binding ability of the domain could be impaired. The two intracellularly tagged EphB2 receptor versions, EphB2-C1 and EphB2-C2, have unconventional ExFP insertions into the receptor sequence and were therefore more unpredictable concerning receptor function and fluorescence properties (for details see Material and Methods/Plasmids/EphB2-ExFP expression constructs).

6.1.1. Analysis of tagged EphB2 receptors

6.1.1.1. Expression

HEK293 cells can be readily and very efficiently transfected with plasmid DNA. The three different EphB2-ExFP receptors, EphB2-N, EphB2-C1 and EphB2-C2, were expressed in HEK293 cells and showed intense fluorescence at the membrane level (Figure 6.2A-C). Compared to only ExFP-expressing cells, the fluorescently tagged EphB2 receptors are less bright (data not shown), but bright enough for live-cell imaging or in combination with immunostaining experiments. The fluorescence intensity was comparable to EGFP-ephrinB1 or EGFP-ephrinB1- Δ C overexpressing HEK293 cells (Figure 6.2).

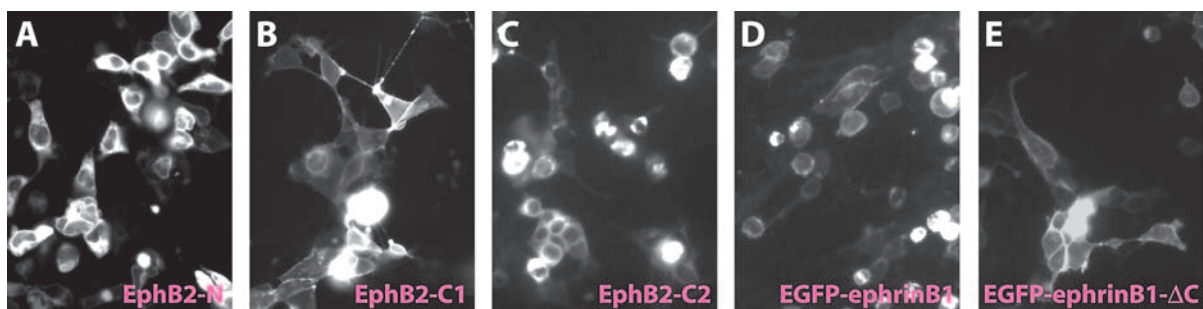


Figure 6.2. **Expression of fluorescently tagged EphB2 receptors and ephrinB1.** HEK293 cells were transfected with plasmid DNA encoding EphB2-N (A), EphB2-C1 (B), EphB2-C2 (C), EGFP-ephrinB1 (D) or EGFP-ephrinB1- Δ C (E). Images were taken two days after transfection.

6.1.1.2. Tyrosine phosphorylation

Activation of Eph receptors induces autophosphorylation on multiple residues, including the two tyrosines within a highly conserved juxtamembrane motif and a tyrosine in the kinase activation segment (Dodelet and Pasquale, 2000). In the absence of exogenous ephrin ligands overexpressed Eph receptors are constitutively autophosphorylated in HEK293 cells (Kullander et al., 2001).

To analyze the autophosphorylation potential of fluorescently tagged EphB2 receptors, kinase-active and kinase-deficient versions of non-fluorescently tagged and fluorescently tagged EphB2 receptors were expressed in HEK293 cells. All of the different EphB2 receptors carried an N-terminal FLAG-epitope tag. EphB2 proteins were immunoprecipitated with monoclonal anti-FLAG antibodies from cell lysates. Immunoprecipitations (IPs) were analyzed by SDS-PAGE and immunoblotted (WB) with anti-phosphotyrosine (pY) antibodies (Figure 6.3, upper panel). The blot was stripped and reprobed with anti-FLAG antibodies to determine protein levels (Figure 6.3, lower panel). Like the wild type (wt) receptor, the fluorescently tagged

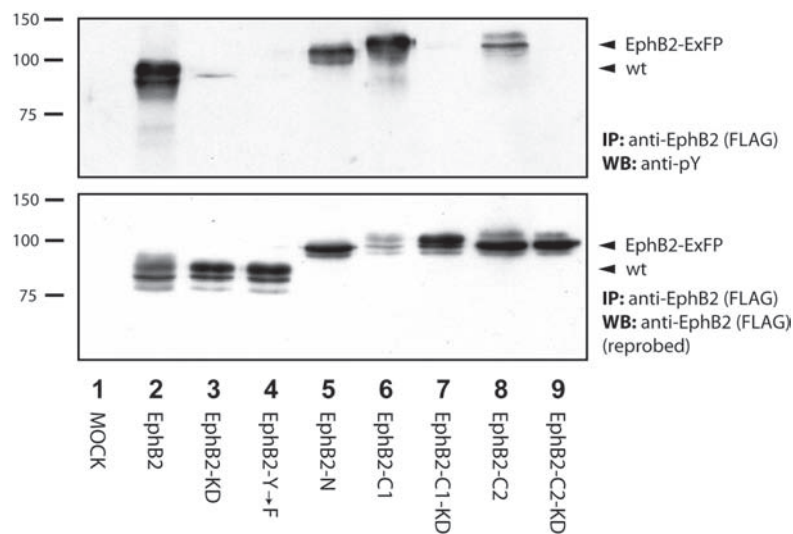


Figure 6.3. Tyrosine phosphorylation of EphB2 receptors. Untransfected HEK293 cells (MOCK, lane 1) or HEK293 cells transfected with expression vectors encoding epitope-tagged (FLAG) wild type EphB2 (EphB2, lane 2), kinase-deficient FLAG-EphB2 (EphB2-KD, lane 3), FLAG-EphB2 with mutated juxtamembrane tyrosine residues to phenylalanine (EphB2-Y→F, lane 4), fluorescently-tagged FLAG-EphB2-N (EphB2-N, lane 5), fluorescently-tagged FLAG-EphB2-C1 (EphB2-C1, lane 6), fluorescently-tagged kinase-deficient FLAG-EphB2-C1 (EphB2-C1-KD, lane 7), fluorescently-tagged FLAG-EphB2-C2 (EphB2-C2, lane 8) or fluorescently-tagged kinase-deficient FLAG-EphB2-C2 (EphB2-C2-KD, lane 9). Cell lysates were immunoprecipitated (IP) with monoclonal anti-FLAG antibody and then immunoblotted (WB) with monoclonal antibodies against phosphotyrosine (anti-pY) (**upper panel**). The stripped blot was reprobed with antibodies against FLAG to visualize expression levels (**lower panel**). The migration positions of molecular size marker (in kilodaltons) are indicated on the left.

6. Results

EphB2 receptors were autophosphorylated and migrated with an apparent molecular mass of \sim 140 kDa (Figure 6.3, lane 5-6 and 8). Wt EphB2, EphB2-N and EphB2-C1 proteins gave high levels of tyrosine phosphorylation. The EphB2-C2 fusion protein showed somewhat reduced tyrosine phosphorylation (Figure 6.3, compare lane 2, 5-6 with 8). In contrast, drastically reduced levels of tyrosine phosphorylation or even no tyrosine phosphorylation were detected as expected in kinase-deficient EphB2 mutants, generated by a replacement of lysine (aa660) to arginine in the kinase domain (= mutated ATP binding site) (Figure 6.3, lane 3, 7 and 9). As in the EphA4 receptor, substitution of the two conserved juxtamembrane tyrosines in EphB2 with phenylalanine inhibited autophosphorylation of non-fluorescent EphB2 (Figure 6.3, lane 4)(Kullander et al., 2001).

Interaction partners

Unlike EphA4 receptors, EphB2 receptors interact via the extracellular part with the NMDA receptor subunit NR1 upon ephrinB stimulation in cultured cortical neurons. NR1 and EphB2, could be co-immunoprecipitated when expressed in HEK293T cells or from cortical lysates (Dalva et al., 2000). In addition, the C-terminal PDZ motif of EphB2 interacts with the synaptic protein GRIP (Figure 6.4A) (Torres et al., 1998).

To test whether the fluorescently tagged EphB2 receptor is capable of interacting with known proteins, such as NR1 and GRIP2, HEK293 cells were transiently transfected with expression constructs encoding one of the variants of the EphB2 receptors or in combination with vectors coding for NR1 or MYC-epitope tagged GRIP2. Before lysis cells were stimulated with preclustered fusion bodies of Fc fragments (Fc) with ephrinB2 ectodomains (ephrinB2-Fc) or Fc for 10 min. EphB2 and NR1 proteins were immunoprecipitated with anti-FLAG and anti-NR1 antibodies, respectively. After stripping, blots were reprobed with anti-FLAG or anti-NR1 antibodies (Figure 6.4B-D, lower panels). IPs were resolved by SDS-PAGE and probed with anti-FLAG or anti-NR1 antibodies to visualize protein levels (Figure 6.4B-C, upper panels). As shown in figure 6.4B, NR1 was co-precipitated with anti-FLAG antibodies only from cell lysates overexpressing both proteins (Figure 6.4B, compare lanes 2-5 with lanes 6-9). In the reverse experiment, co-immunoprecipitation of EphB2 proteins with NR1 could also be observed (Figure 6.4C, lanes 3-6).

In case of the interaction partner GRIP2, wt and fluorescently tagged EphB2 receptors could be co-immunoprecipitated with MYC-GRIP2 protein only from cells that had been co-transfected with an expression plasmid encoding GRIP2, albeit with low efficiency. In the converse experiment, presumably due to technical reasons, co-IP of EphB2 with MYC-GRIP2 protein could

6.1. Generation of fluorescently tagged EphB2 receptors

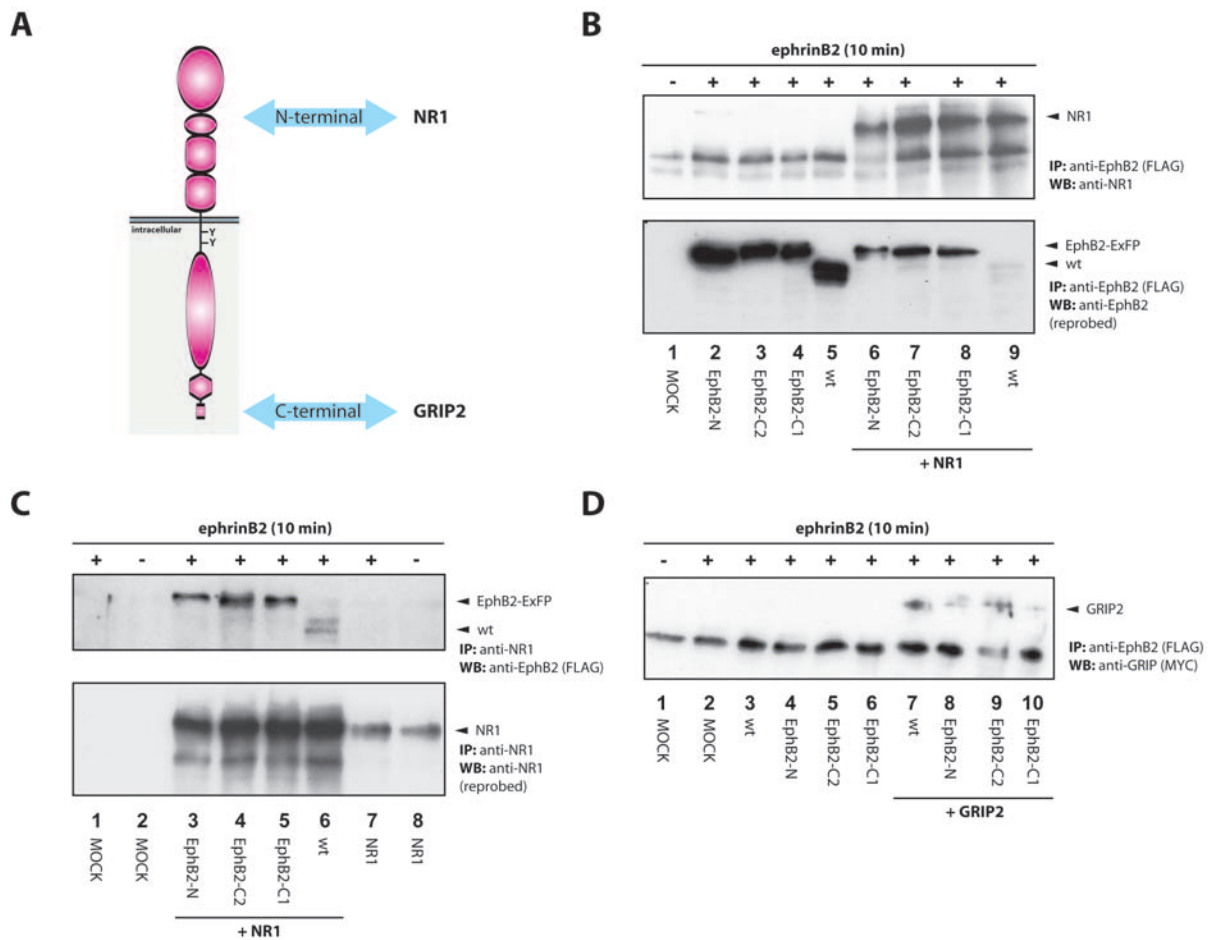


Figure 6.4. Interaction of EphB2-ExFP receptors with NR1 and GRIP2. (A) Schematic representation of the regions of EphB2 interacting with NR1 and GRIP2. (B) Co-precipitation of EphB2 with NR1. HEK2993 cells overexpressing wt EphB2 (wt, lane 5 and 9) or EphB2-ExFP (EphB2-N, lane 2 and 6; EphB2-C2, lane 3 and 7; EphB2-C1, lane 4 and 8), either alone or in combination with NR1 (lane 6-9) were stimulated with ephrinB2-Fc (+) for 10 min before lysis. IPs using anti-FLAG antibodies were analyzed with SDS-PAGE and immunoblotted (WB) with anti-NR1 antibodies (upper panel). Blot was stripped and reprobbed with anti-FLAG antibodies to visualize EphB2 protein levels (lower panel). (C) Reverse experiment of (B) with IPs using anti-NR1 antibodies and immunoblotted with anti-FLAG antibodies. The stripped blot was reprobbed with anti-NR1 antibodies. (D) GRIP2 interacts with EphB2. HEK2993 cells were transfected and stimulated as indicated above and under each panel. IPs were performed using anti-FLAG antibodies and then immunoblotted with anti-MYC to visualize MYC-GRIP2 protein levels.

not be detected, suggesting that the MYC-tag of GRIP2 is less accessible (data not shown).

Taken together, fluorescently tagged EphB2 fusion proteins interact with the NR1 subunit of the NMDA receptor and with the PDZ-domain containing protein GRIP2.

6.1.2. Cluster behaviour of the different EphB2-ExFP receptors

Binding of Eph receptors to their ephrin ligands results in high-order clustering by the aggregation of multiple Eph-ephrin complexes, thereby initiating downstream signalling into both the Eph receptor and ephrin ligand expressing cell. In the biochemical experiments used to test the binding of interaction partners of EphB2-ExFP receptors, cells had been stimulated

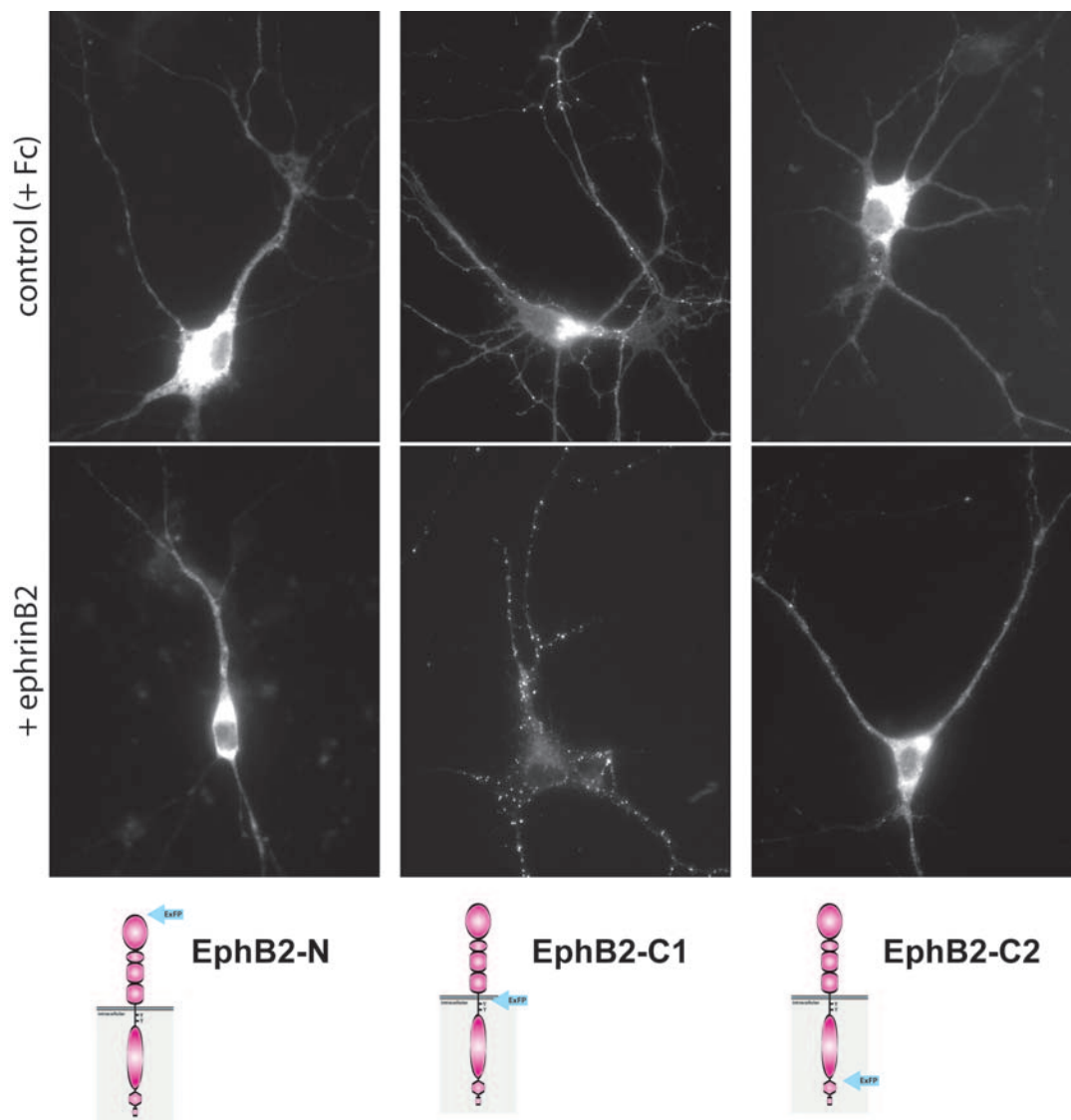


Figure 6.5. **Comparison of the different EphB2-ExFP proteins before and after ephrinB stimulation.** Hippocampal neurons were transfected at day 5 *in vitro* (DIV5) with expression constructs encoding EphB1-N, EphB2-C1 or EphB2-C2. Two days later (DIV5+2), neurons were stimulated with preclustered ephrinB2-Fc (**lower panel**) or as a control with preclustered Fc (**upper panel**) before fixation. 63-times magnification.

with preclustered ephrinB2-Fc. The aim of the ephrinB2-Fc application was to induce the cluster formation of the different variants of fluorescently-tagged EphB2 receptors, thereby associating activated receptors with their interaction partners. In contrast to young cultured neurons, Eph receptors and NR1 are capable of interacting in the absence of exogenously applied ephrinB-Fc in cell lines (HEK293T). This may be due to overexpression of EphB2 or by the presence of ephrins within the serum-containing media (Dalva et al., 2000). Therefore, the addition of ephrinB-Fc to stimulate EphB2-expressing HEK293 cells was perhaps not required to induce the association of different EphB2-ExFP receptors with their interaction partners in the biochemical experiments. The next step was therefore to analyze in the cell type we were interested in – the neurons – if cluster formation of fluorescently-tagged Eph receptors could be induced upon stimulation with preclustered ephrinB-Fc. For this, young rat hippocampal neurons were transfected at day 5 *in vitro* (DIV5) with one of the three different expression constructs encoding fluorescently tagged EphB2 proteins (EphB2-N, EphB2-C1 or EphB2-C2). Two days later neurons were treated with preclustered ephrinB2-Fc or with preclustered Fc in the control experiment before fixation. Treatment of EphB2-C1 expressing neurons with clustered ephrinB2 resulted in a dramatic increase of cluster formation. In contrast, only few clusters were visible in the neurons treated with Fc alone as a control (Figure 6.5, middle row). Surprisingly, EphB2-N or EphB2-C2 expressing neurons showed no visible clusters upon ephrinB2 stimulation, indicating that the insertion of the fluorescent protein at the N-terminus or between the kinase domain and the SAM domain impaired the clustering behaviour of the tagged molecules.

6.1.3. Clustering of fluorescently tagged EphB2-C1 receptors

The next step was to further investigate cluster formation of the fluorescent EphB2-C1 protein in neuronal cultures. To do this, hippocampal neurons were transfected on DIV3 with plasmids encoding EphB2-C1-YFP and ECFP. ECFP was co-transfected to highlight the structure of neurons expressing EphB2-C1-EYFP, which is recruited into clusters after ephrinB stimulation (Figure 6.5, middle column, control versus ephrinB2). At DIV6 preclustered Fc or ephrinB1-Fc was added to the cultures for 1 hour before fixation. In Fc-stimulated neurons only few clusters of EphB2-C1 were visible and fluorescent receptors were more evenly distributed in the neuron (Figure 6.6A-D). In contrast, ephrinB1-Fc treatment of neurons expressing EphB2-C1-EYFP induced dramatic clustering of the tagged EphB2 receptors mainly along all neuronal processes (Figure 6.6E-J). EphB2-clusters were present on the shaft of dendrites

6. Results

and axons and on the tips of filopodia. These results indicate that despite the presence of the ExFP “domain” fluorescently tagged EphB2-C1 receptors interact and cluster normally in response to ephrinB1-Fc stimulation.

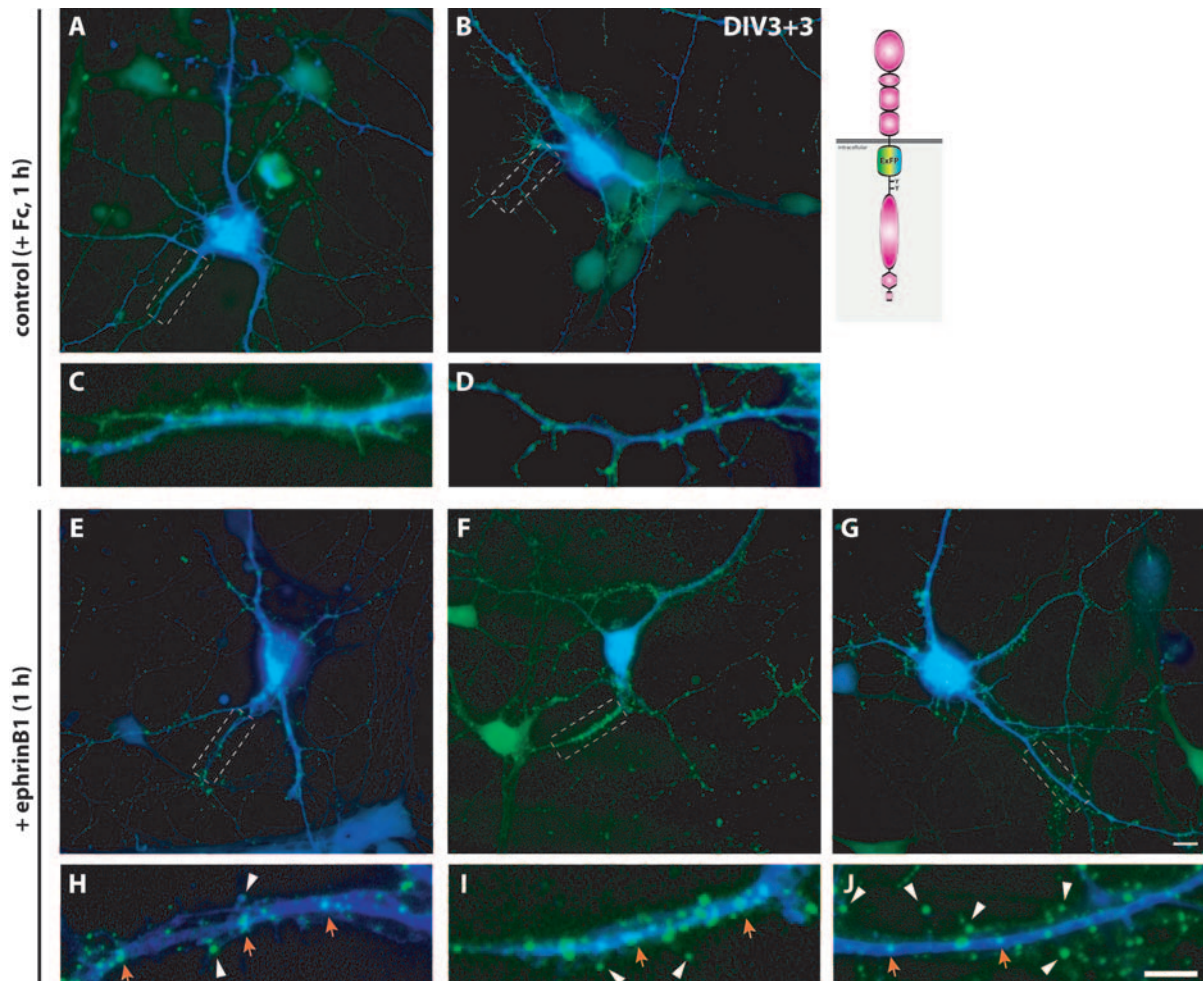
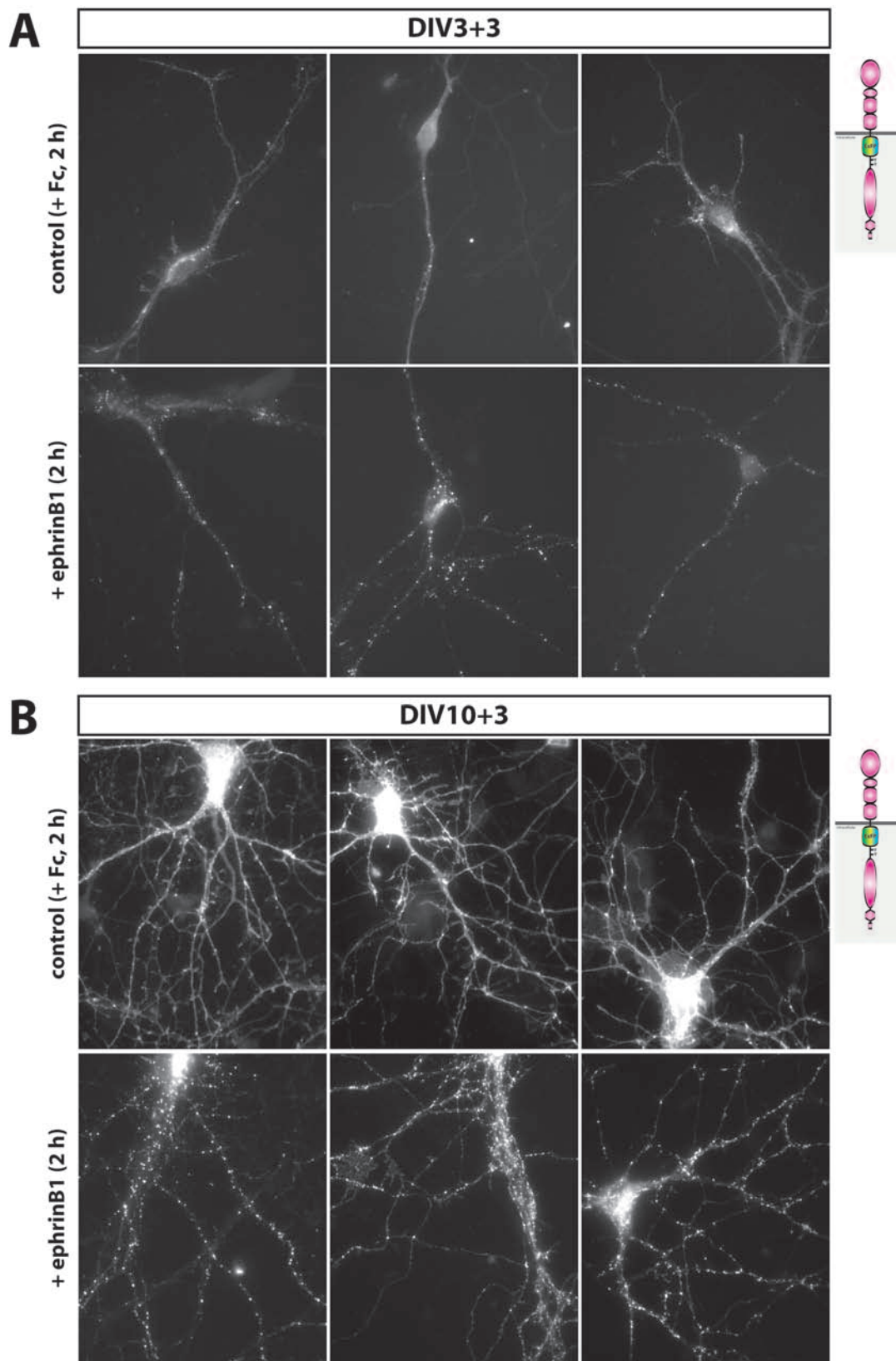


Figure 6.6. **Clustering of EphB2-C1 before and after ephrinB1 stimulation in 6-day-old neuronal cultures.** After 3 days in culture hippocampal neurons were co-transfected with expression constructs containing an EphB2-C1-EYFP cDNA and to visualize the cell morphology with ECFP cDNA. All panels show the merge of the two fluorescent signals with EphB2-C1 in green and ECFP in blue. Neurons were stimulated with either preclustered Fc (A-D) or ephrinB1-Fc (E-J) for 1 hour before fixation. Dashed boxes in panels A-B and E-G indicate the areas that are magnified (C-D) and (H-J), respectively. White arrowheads indicate filopodial EphB2 clusters; red arrows indicate shaft EphB2 clusters. Scale bars represent 10 μm and 5 μm for the enlargement.

6.1.4. Cluster formation of EphB2-C1 in young and old cultures

In young hippocampal cultures EphB2-ExFP expressing neurons displayed little cluster formation before ephrinB stimulation. These cultures were immature and had less arborization, few contacts with other neurons and showed many filopodia-like protrusions. To answer the question whether clustering of EphB2-C1 receptors before and after stimulation with the ligand differs in some ways in young and mature cultures, hippocampal neurons were transfected with the EphB2-C1 construct at DIV3 and DIV10. Three days later either preclustered Fc or ephrinB1-Fc was added for 2 hours to the cultures before fixation.

In comparison to young cultures, old neurons showed smaller clusters without ephrinB stimulation (Figure 6.7A-B, upper panels). Application of preclustered ephrinB induced a dramatic increase in cluster size and number in both 6-day-old and 13-day-old cultures (Figure 6.7A-B, lower panels). Without any exogenous stimulation, older neurons (approximately 3-4 weeks old cultures) showed a higher number of clusters compared to young neurons (Figure 6.8). In mature neurons that had already developed spines, clusters were often localized at the head of a spine (Figure 6.8). This suggests that ligands provided by the interaction with other cells may also induce the formation of EphB2 clusters possibly associated with synaptic sites. In addition, many EphB2 clusters were always visible in the proximity of the cell body and along the dendritic shaft. As will be demonstrated in this thesis, most of these clusters represent endogenous vesicle-trafficking (i) from the production site (in general the cell body) to the target site in the dendrite or axon and perhaps (ii) *vice versa* from the plasmalemma to either degradative compartments or recycled to the cell membrane for reuse (Figure 6.14; supplementary information on CD Rom, movies 4-7).



6.1. Generation of fluorescently tagged EphB2 receptors

Figure 6.7. **Comparison of control-stimulated versus ephrinB1-stimulated EphB2-C1 expressing neurons in young and older cultures.** 3-day-old (A) and 10-day-old (B) hippocampal neurons were transfected with expression constructs encoding EphB2-C1. Three days later, cultures were stimulated with either preclustered Fc (A-B, upper panel) or ephrinB1-Fc (A-B, lower panel) for 2 hours before fixation. 63-times magnification.

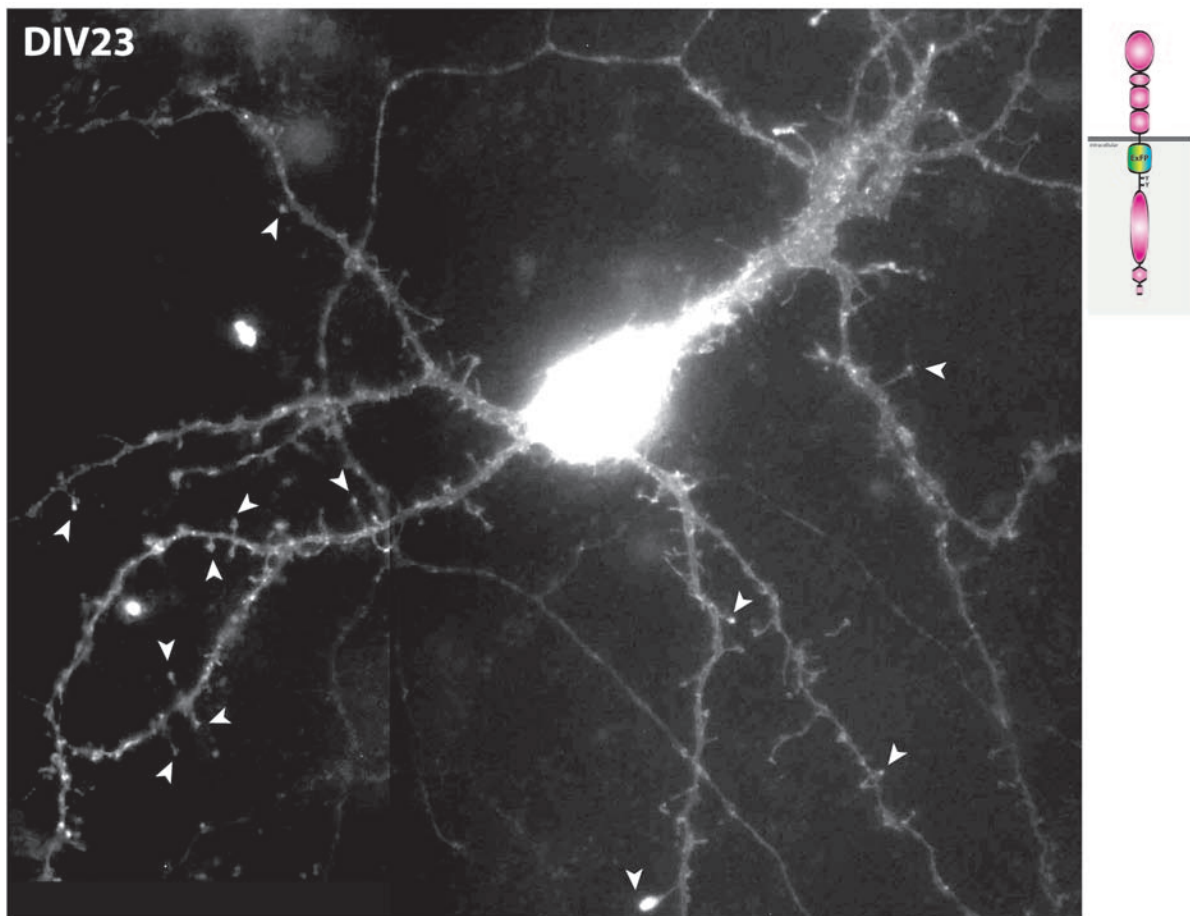


Figure 6.8. **Clusters of the EphB2 receptor are visible in dendritic spines of a mature neuron (DIV23) without ephrinB stimulation.** The 23-day-old hippocampal neuron expressing EphB2-C1 shows clusters located to several dendritic spine heads without stimulation indicated by arrowheads. 100-times magnification.

6.1.5. Specificity of EphB2-C1 clustering

In order to test the specificity of EphB2-ExFP clustering, EphB2-C1 expressing hippocampal neurons were stimulated on DIV14 with preclustered ephrinB1, ephrinB2, EphB2 or Fc for two hours before fixation (Figure 6.9). As expected, the known EphB2 ligands, ephrinB1 and ephrinB2, revealed strong cluster formation of EphB2-C1 (Figure 6.9A-B), whereas stimulation with EphB2 and Fc caused no effect (Figure 6.9C-D). In addition, another non-interacting ligand of EphB2, ephrinA1, showed no clustering effect of EphB2 (data not shown). As a summary, only known ligands of EphB2 induced clustering of the fluorescently tagged EphB2-C1 receptor.

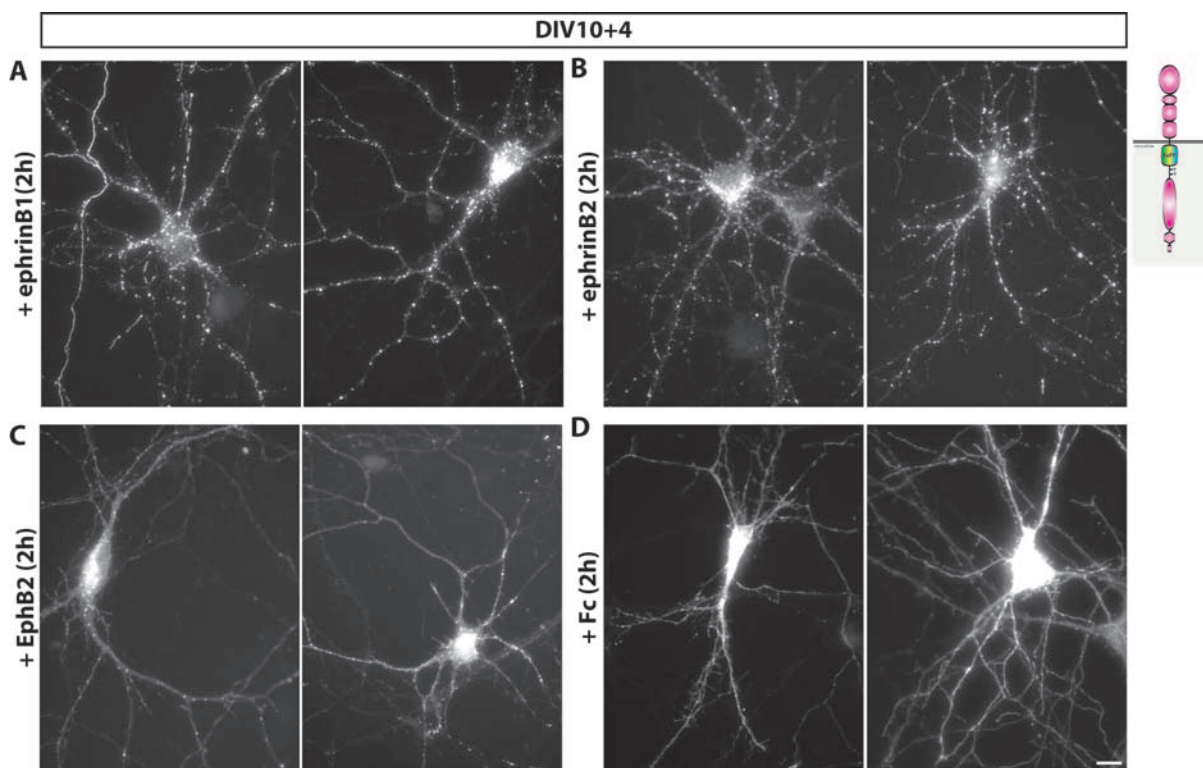


Figure 6.9. **Stimulation of EphB2-C1 expressing hippocampal neurons with different Fc fusion proteins.** Hippocampal neurons transfected at DIV10 with expression constructs containing an EphB2-C1 gene were stimulated at DIV14 with either preclustered ephrinB1-Fc (A), ephrinB2-Fc (B), EphB2-Fc (C) or Fc (D) for 2 hours before fixation. Scale bar = 10 μm .

6.1.6. Localization of EphB2-C1 in the neuron

To determine the subcellular localization of EphB2-C1 in neurons, dissociated hippocampal neurons were transfected with EphB2-C1 expression plasmid at DIV10. At DIV14, the neuronal cultures were stimulated with preclustered ephrinB1-Fc or ephrinB2-Fc or as a control with preclustered EphB2-Fc or Fc for two hours, respectively (Figure 6.10 and 6.11). Fixed cultures were stained with antibodies against the cytoskeletal microtubule-associated protein 2 (MAP2), which is widely used as dendritic marker and is present in the somata and dendrites of most neurons, but virtually absent from most axons (Banker and Goslin, 1998). Comparing the EphB2-C1 fluorescent signal with the MAP2 staining revealed that EphB2-C1 is present in axons, dendrites and neuronal cell bodies in both ephrinB- and control-stimulated neurons. Clusters of EphB2-C1-EYFP could be induced in all three compartments upon ephrinB1/2-stimulation, but surprisingly also in EphB2-stimulated neurons. In contrast, application of Fc as a control showed a more homogeneous distribution of EphB2-C1 in the entire neuron.

6. Results

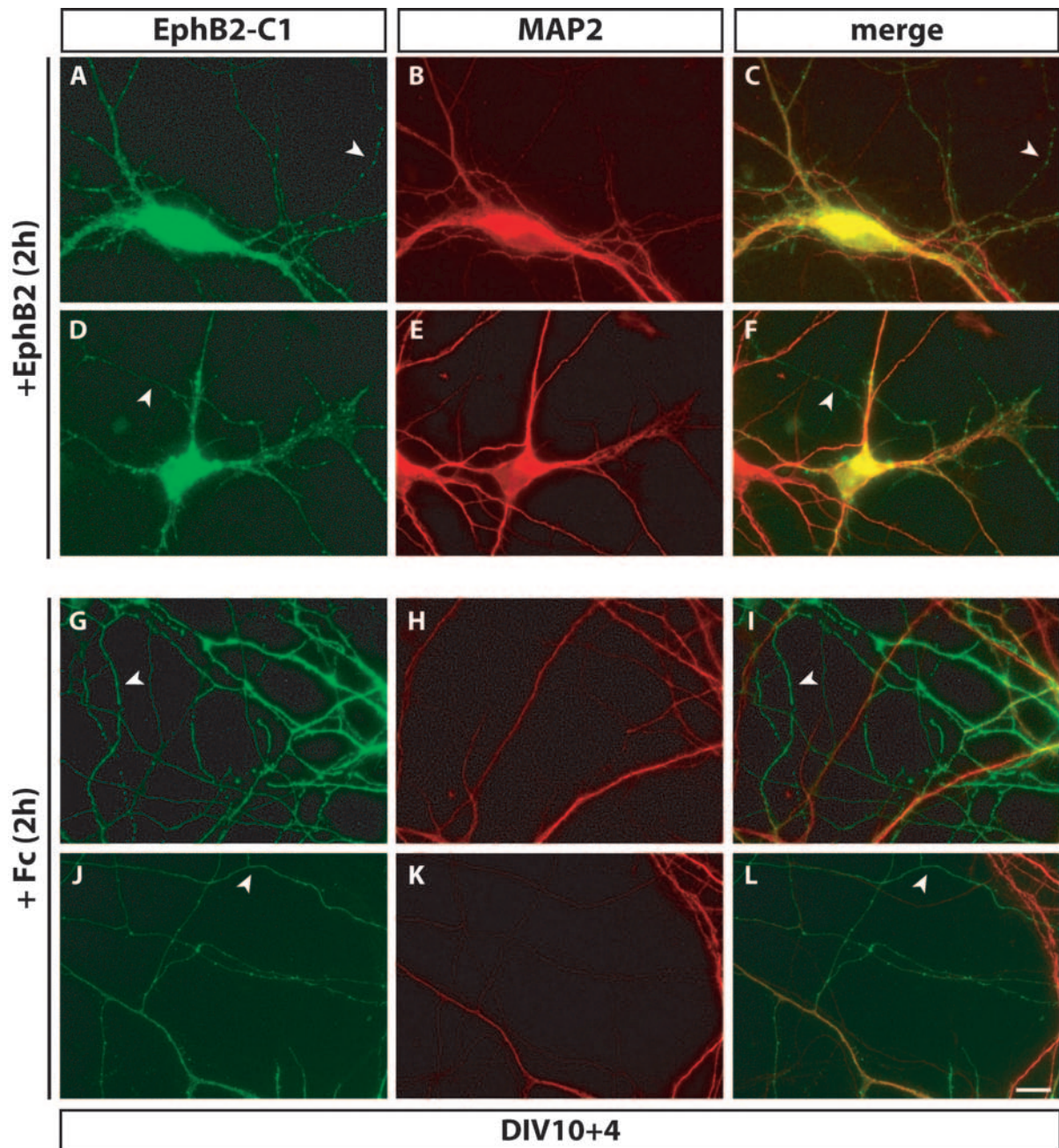


Figure 6.10. **EphB2-C1 is located in axons and dendrites of control-stimulated hippocampal neurons.** Hippocampal neurons transfected at DIV10 with EphB2-C1 expression constructs were stimulated on DIV14 with preclustered EphB2-Fc (A) or Fc (B) for 2 hours prior fixation. Fluorescence images of EphB2-C1-EYFP expressing neurons are shown in the **left panel**. Antibodies against MAP2 revealed neuronal cell bodies and their dendrites (**middle panel**). The merge of the two signals with EphB2-C1 fluorescence in green and anti-MAP2 stainings in red is shown in the **right panel**. Arrowheads indicate the axonal expression of EphB2-C1. Scale bar = 10 μ m

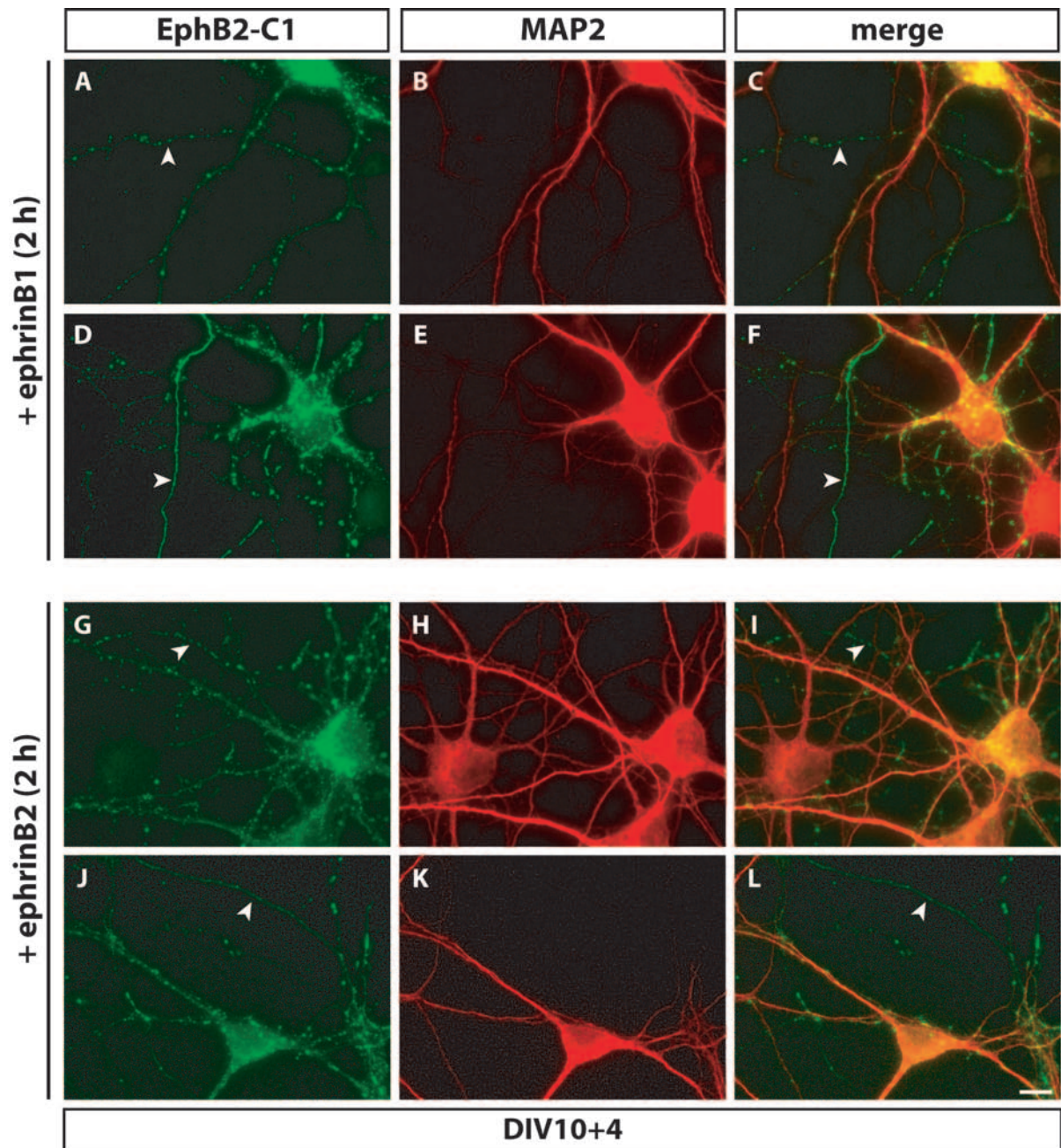


Figure 6.11. **EphB2-C1 is expressed in axons and dendrites of ephrinB-stimulated hippocampal neurons.** Hippocampal neurons transfected at DIV10 with expression constructs encoding EphB2-C1 were stimulated on DIV14 with preclustered ephrinB1-Fc (**A**) or ephrinB2-Fc (**B**) for 2 hours prior fixation. Fluorescence images of EphB2-C1-EYFP expressing neurons are shown in the **left panel**. Antibodies against MAP2 revealed neuronal cell bodies and their dendrites (**middle panel**). The merge of the two signals with EphB2-C1 fluorescence in green and anti-MAP2 stainings in red is shown in the **right panel**. Arrowheads indicate the axonal expression of EphB2-C1. Scale bar = 10 μm

6. Results

6.1.7. Localization of fluorescently tagged EphB2 receptors in filopodia and other dendritic protrusions

So far, stimulation with preclustered ephrinBs indicated that EphB2-C1 receptors were expressed on the plasma membrane of neurons similar as seen before in cell lines (HEK293). To investigate in more detail if EphB2-C1 receptors are inserted into the neuronal cell membrane, dissociated hippocampal neurons were transfected at DIV13 with expression plasmids

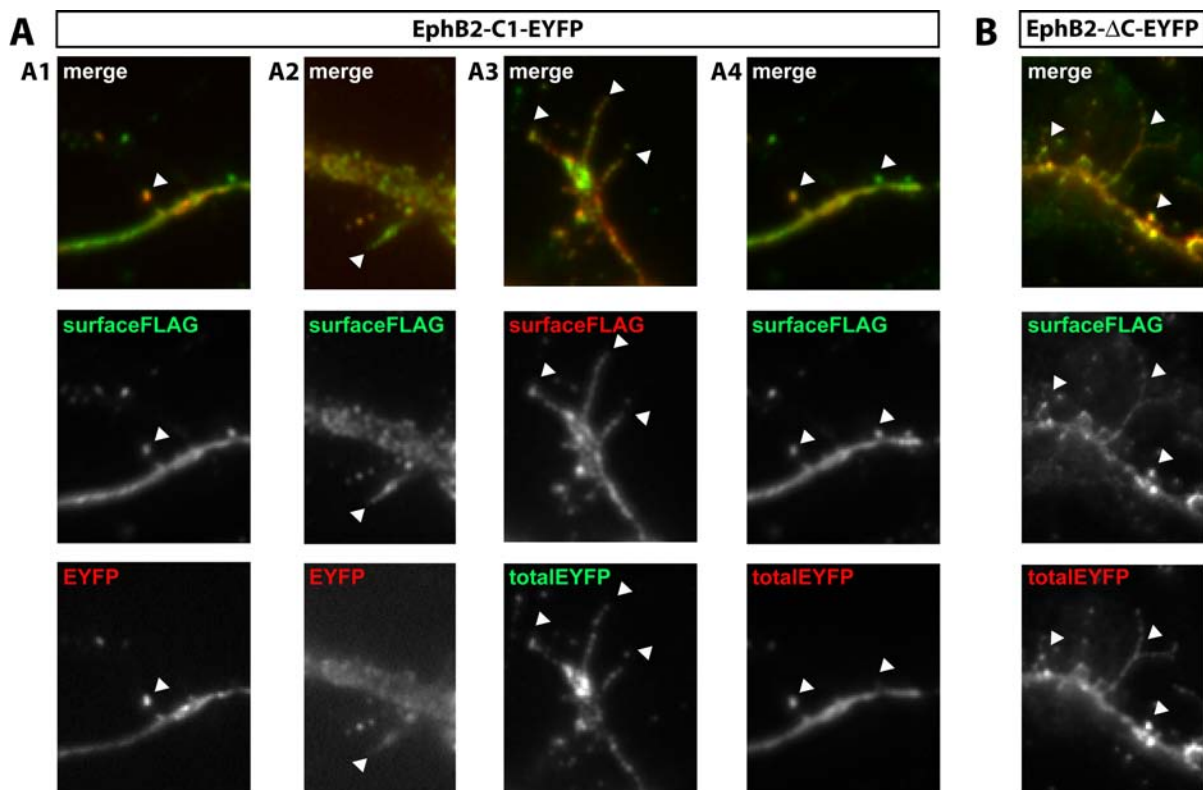


Figure 6.12. **Fluorescently tagged EphB2 receptors are located in filopodia and other dendritic protrusions.** 13-day-old dissociated hippocampal neurons were transfected with expression constructs encoding EphB2-C1-EYFP (A) or EphB2-ΔC-EYFP (B). At DIV15 cultures were fixed and immunostained with antibodies against the FLAG-tag to reveal surface expression of EphB2-C1-EYFP or EphB2-ΔC-EYFP (A-B, middle panel, surfaceFLAG). After permeabilization the total distribution of the overexpressed EphB2 versions were visualized with an antibody directed against the C-terminal EYFP protein of EphB2-C1-EYFP or EphB2-ΔC-EYFP (A2-A3 and B, lower panel, totalEYFP). The merge of the anti-surfaceFLAG stainings and the EphB2-C1 fluorescence (A1-A2, lower panel, EYFP) or total anti-totalEYFP stainings (A3-A4 and B, lower panel, totalEYFP) is shown in the upper panel. The label colour from images of the middle and lower panel indicate the colour of this image in the merge. Arrowheads indicate the surface expression of fluorescent EphB2 receptors in dendritic protrusions (A1-2, A4, B) and a growth cone (A3). 63-times magnification.

coding for EphB2-C1-EYFP or EphB2- Δ C-EYFP. Two days later, cultures were fixed in absence of detergents (pre-permeabilization) and immunostained for the N-terminal FLAG-tag of EphB2 proteins to reveal surface expression of EphB2-C1-EYFP or EphB2- Δ C-EYFP (Figure 6.12, middle panel, surfaceFLAG). After permeabilization (post-permeabilization), cultures were stained with antibodies against the intracellular EYFP protein of the EphB2 fusion proteins to determine the total pool of the overexpressed EphB2 versions (Figure 6.12A3-A4 & B, lower panel, totalEYFP). The fluorescent signals of EphB2-EYFP proteins (Figure 6.12A1-A2, lower panel, EYFP) were compared with the signals of the totalEYFP stainings to analyze fluorescence intensity of fusion proteins without immunostaining and specificity of the totalEYFP stainings.

The surfaceFLAG immunostaining revealed that EphB2-C1 is located on the surface of dendrites and filopodia (Figure 6.12A-B), even on the tip of thin filopodia (Figure 6.12A3). Comparing the surface expression of EphB2-C1 with its total distribution showed that the majority of the EphB2-C1 proteins were inserted into the membrane (yellow colour in figure 6.12, upper panel, merge). The growth cone in figure 6.12A3 showed an internal pool of EphB2-EYFP in the central core of the growth cone (green staining in merge). As expected, the fluorescent signal of EphB2-C1 is almost identical to the totalEYFP staining of EphB2 proteins (Figure 6.12, compare A1 (EYFP) with A4 (totalEYFP)). Interestingly, the C-terminal truncation of EphB2 does not seem to alter the described localization and surface expression of EphB2- Δ C-EYFP in transfected neurons (Figure 6.12B).

In addition, immunostaining of total surface EphB2 (endogenous and exogenous) was carried out with an antibody against its N-terminus in neurons expressing EphB2-C1 before permeabilization (Figure 6.13A-B, middle panel, surfaceEphB2). After permeabilization the expressed EphB2-C1 proteins were immunostained with an antibody against EYFP (Figure 6.13A-B, lower panel, totalEYFP).

In comparison to the total EphB2-C1 stainings (totalEYFP) from figure 6.12 the surface EphB2-immunostaining gave a stronger signal in EphB2-C1 overexpressing neurons. This was expected because the preEphB2 immunostaining also stained endogenous EphB2 receptors. In addition to the cytoplasmic EphB2-EYFP receptors (Figure 6.13A, merge, green colour), a strong staining of surface EphB2 receptors (endogenous and exogenous) along the plasma membrane was visible (Figure 6.13A, yellow colour in merge).

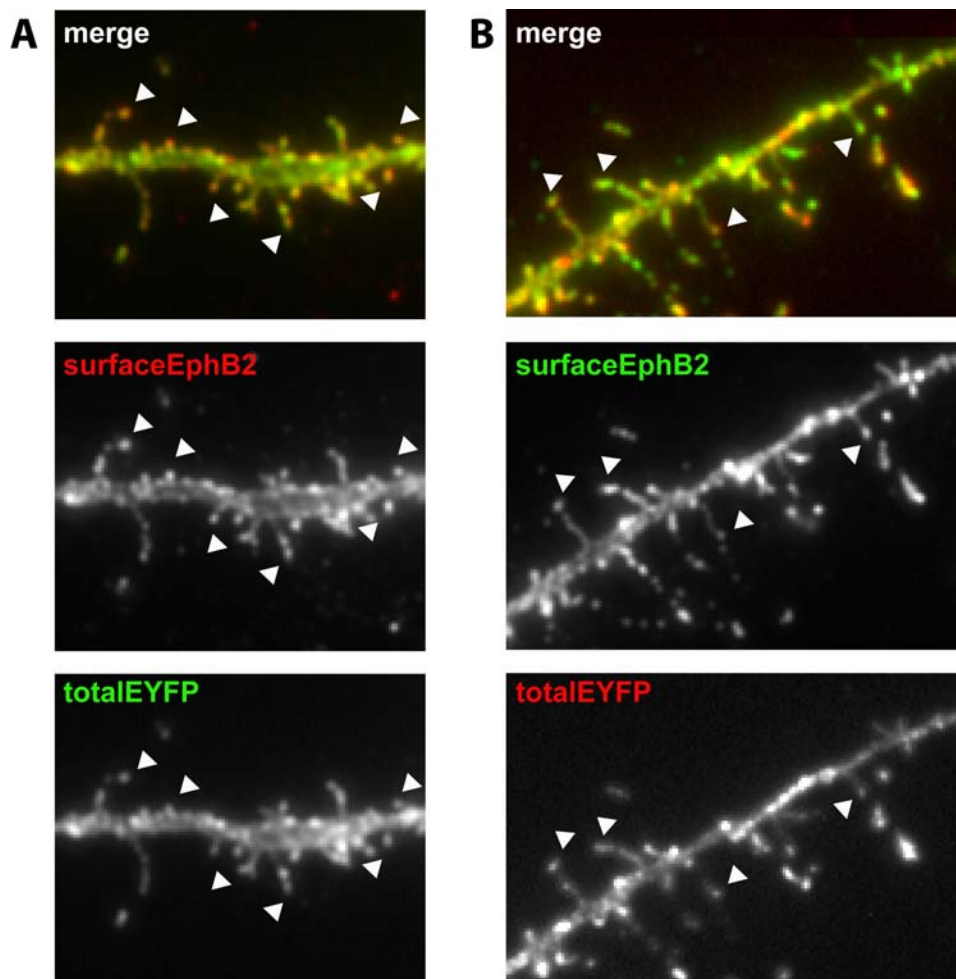


Figure 6.13. **EphB2 receptors are located at the surface of filopodia and other dendritic protrusions.** 13-day-old cultured hippocampal neurons were transfected with EphB2-C1-EYFP expression constructs. Two days later, cultures were fixed and immunostained with antibodies against EphB2 to reveal surface expression of endogenous and fluorescently tagged EphB2 receptors (middle panel, surfaceEphB2). After permeabilization, the total distribution of the transiently expressed EphB2-C1 was visualized with an antibody directed against the intracellular EYFP of EphB2-C1-EYFP receptor (**lower panel, totalEYFP**). The merge of the two signals with anti-EphB2 surface stainings in red (**A**) or green (**B**) and total anti-EYFP stainings in green (**A**) or red (**B**) is shown in the **upper panel (merge)**. Arrowheads indicate the surface expression of EphB2 receptor in filopodia and other dendritic protrusions. 63-times magnification.

6.1.8. Cytoplasmic clusters of fluorescently tagged EphB2 receptors

Besides the surface localization, EphB2 receptors were also localized in the cytoplasm of the neuron. To visualize the cytoplasmic distribution of fluorescently tagged EphB2 receptors in neurons, hippocampal cultures were transfected and immunostained as described previously (for more details, see caption of figure 6.14). A comparison of the totalEYFP staining with the

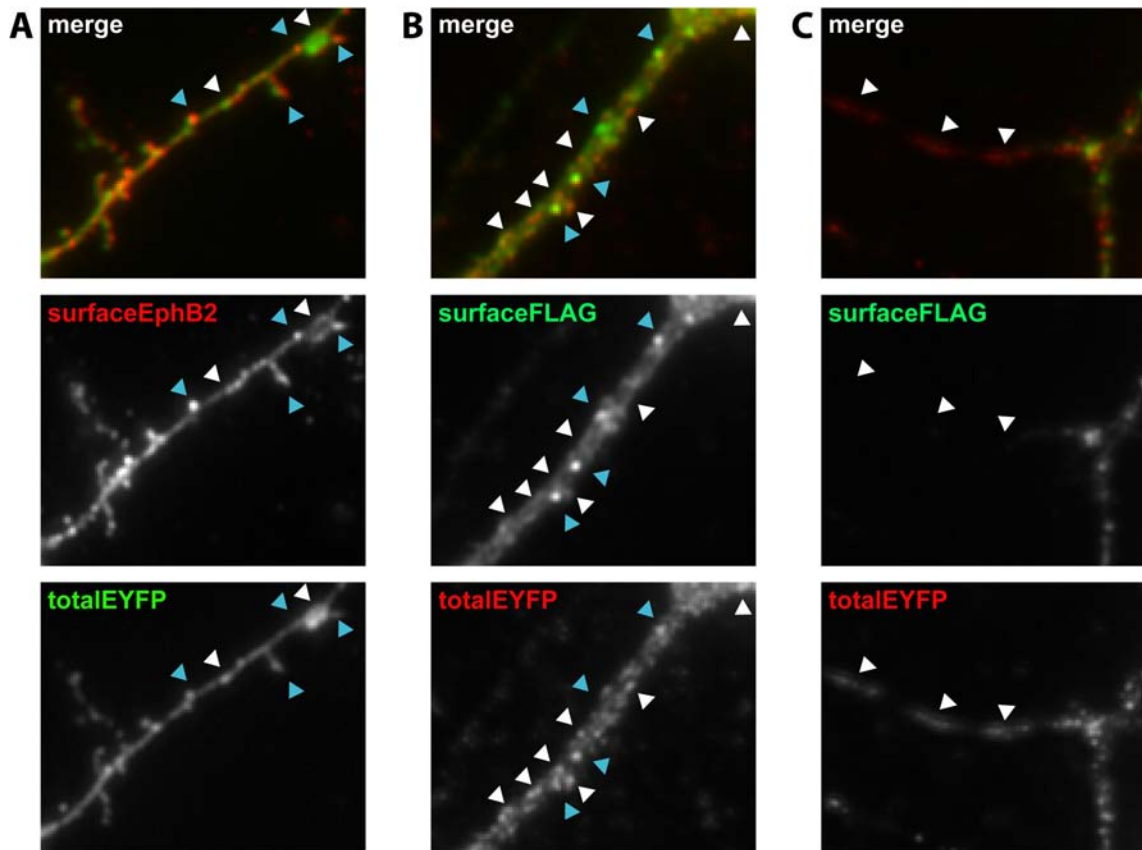


Figure 6.14. **Cytoplasmic clusters of fluorescently tagged EphB2 receptors in neurites.** 15-day-old hippocampal neurons expressing EphB2-C1 for 2DIV were immunostained after fixation with antibodies against the endogenous and transiently expressed EphB2 receptors (**A, middle panel, surfaceEphB2**) or the N-terminal FLAG-epitope of EphB2-C1 proteins (**B-C, middle panel, surfaceFLAG**). After permeabilization the fluorescently tagged EphB2 receptors were stained with antibodies against EYFP (**A-C, lower panel, totalEYFP**). The merge of the two signals with total EphB2 surface stainings in red (**A**) or Flag staining in green (**B-C**) and total anti-EYFP stainings in green (**A**) or red (**B-C**) is shown in the **merge** of the **upper panel**. Blue arrowheads indicate surface expression of EphB2 receptors. White arrowheads indicate cytoplasmic clusters of EphB2 receptors along the dendrite. 63-times magnification.

surface immunolabelling revealed that numerous EphB2-EYFP clusters appeared exclusively after permeabilization (white arrowheads in Figure 6.14). Thick dendritic branches proximal to the cell body showed numerous little cytoplasmic clusters along the dendrite (Figure 6.14B, totalEYFP). However, thinner arborization distal to the cell body displayed less clusters (Figure 6.14A, totalEYFP).

Combining these immunostaining results with later observations from the live-cell imaging experiments (see Live cell imaging of tagged EphB2 receptors), indicates that the punctuate pattern throughout the cytoplasm represents vesicle trafficking. These vesicles containing

either internalized receptors from the cell surface or secretory vesicles carrying newly synthesized EphB2-C1 proteins on route to the plasma membrane.

6.2. Live cell imaging of tagged EphB2 receptors

The aim of the following studies was to investigate (i) if there are trafficking vesicles of fluorescent EphB2 receptors in transfected neurons and (ii) if the impaired kinase activity or the C-terminal truncation of the EphB2-C1 protein has any effects (in comparison to the full-length EphB2-C1 receptor) observed during live-cell imaging. Two additional EphB2-C1 receptors were therefore generated: a kinase-deficient and a C-terminal truncated version of the fluorescently tagged EphB2-C1 protein (Figure 6.15). Both of these proteins are kinase-deficient and act as a dominant-negative receptor.

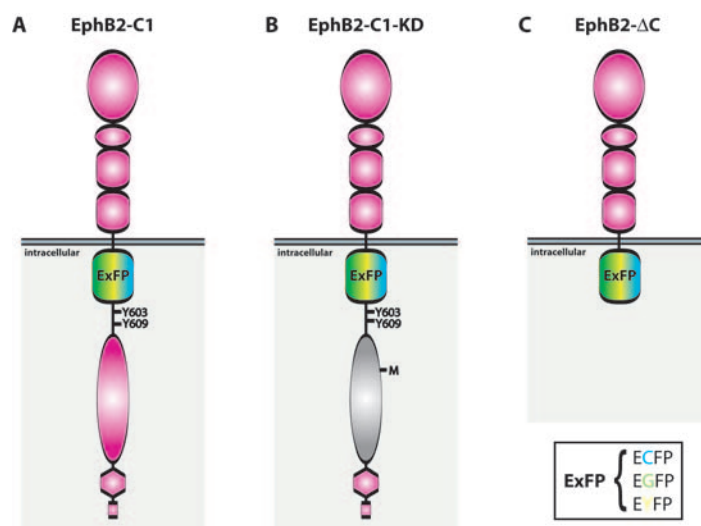


Figure 6.15. **Schematic diagram of the EphB2-C1 variants.** Two additional variants of the EphB2-C1 fusion protein (**A**, **EphB2-C1**) were created: a kinase-inactive EphB2-ExFP receptor (**B**, **EphB2-C1-KD**) and a C-terminal truncated version (**C**, **EphB2-ΔC**).

Young and old primary hippocampal cultures were transfected with expression constructs coding for EphB2-C1-EYFP (Figure 6.16-17, left column; supplementary information on CD-Rom, movie 1 and 4), EphB2-C1-KD-EYFP (Figure 6.16-17, middle column; supplementary information on CD-Rom, movie 2 and 5) or EphB2-ΔC-EYFP (Figure 6.16-17, right column; supplementary information on CD-Rom, movie 3 and 6). Neuronal cultures were imaged by acquiring fluorescence images at a frequency of 1 frame per minute. In addition, prior to starting time lapse microscopy, a phase contrast image was taken (Figure 6.16-17, upper panel).

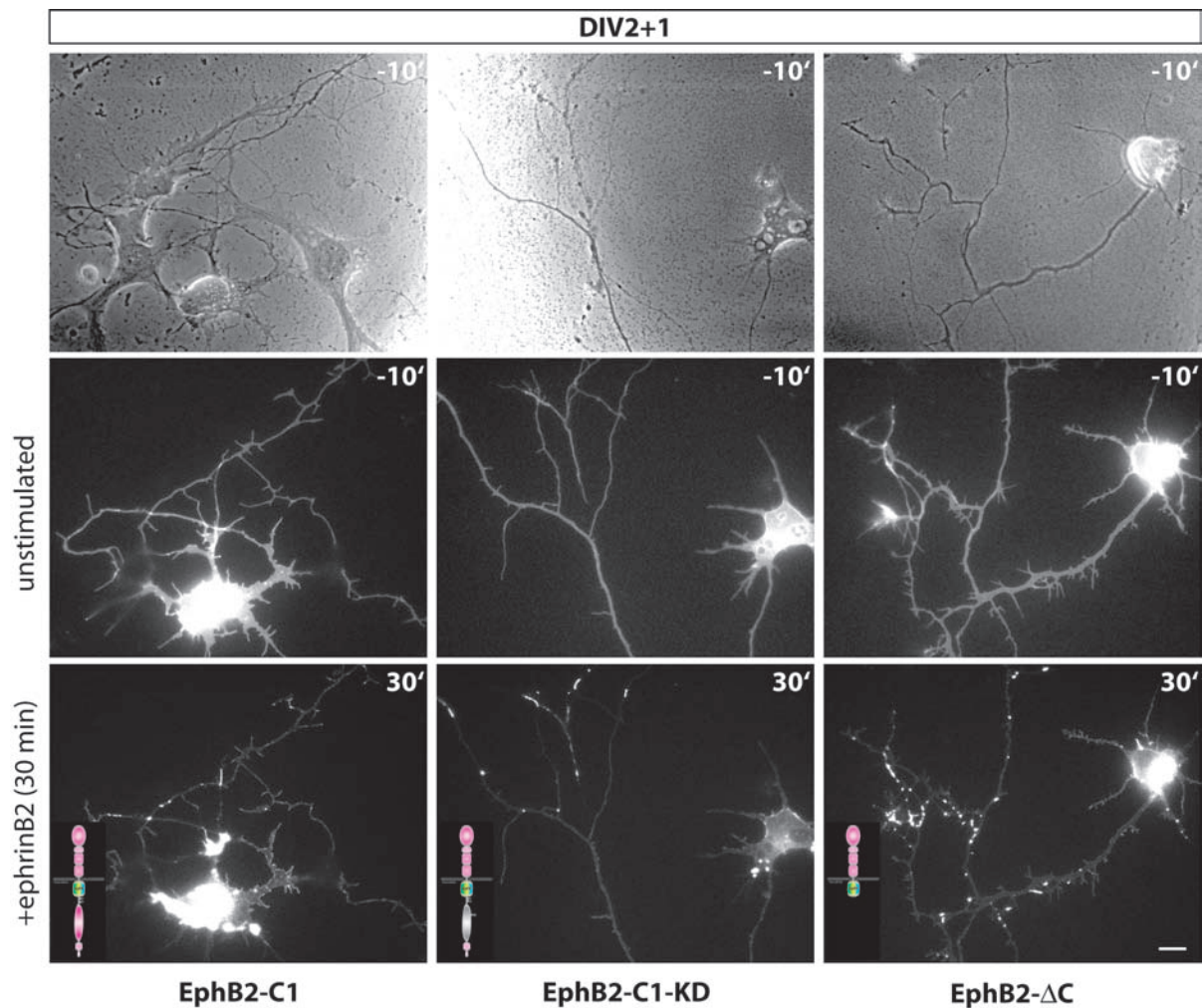


Figure 6.16. Comparison of unstimulated versus ephrinB2-stimulated young neurons (DIV2+1) expressing one variant of EphB2-C1-EYFP during live-cell imaging. 2-day-old primary hippocampal cultures were transfected with expression constructs encoding either EphB2-C1-EYFP (left column; supplementary information on CD-Rom, movie 1), EphB2-C1-KD-EYFP (middle column; supplementary information on CD-Rom, movie 2) or EphB2- Δ C-EYFP (right column; supplementary information on CD-Rom, movie 3). After 1DIV, transfected neurons were imaged by time lapse microscopy at 1 frame per min. The upper and middle panels show phase contrast and fluorescence images 10 minutes before stimulation (-10'), respectively. After 10 min, preclustered ephrinB2-Fc was added. The lower panel shows fluorescent images 30 min after ephrinB2-Fc stimulation (30'). Note the accumulation of bright fluorescent clusters upon stimulation with ephrinB2-Fc. Time points of imaging are indicated in upper right corners. Scale bar = 10 μ m.

Before stimulation with ephrinB ligands, young transfected neurons revealed fast moving vesicles along the neuron. In addition to these moving vesicles, neurons displayed a more homogeneous distribution of fluorescently tagged EphB2-C1 receptors along dendrites and

axons. After adding the preclustered ephrinB2-Fc, cluster formation was visible within a few minutes. In addition, the fluorescent intensity of the plasma membrane was enhanced due to the recruitment of fluorescently tagged EphB2 receptors to the cell surface, thereby altering the homogeneous fluorescence of the young unstimulated neuron. On addition of the ligand, vesicular trafficking was no longer detectable, presumably due to the insertion of the EphB2 receptors into the cell membrane. The initially formed clusters increased with time and sometimes neighbouring clusters merged to form larger clusters. In most cases these clusters were static, only occasionally they did displayed movement. This was observed in all neurons, independent from the expressed EphB2-C1 variant (Figure 6.16).

In contrast, older neurons displayed numerous static clusters prior to stimulation. In addition, these more mature neurons did not show a strong homogeneous distributed fluorescence before stimulation as observed with young neuronal cultures. However, mature neuronal cultures displayed a much higher number of moving vesicles along both dendrites and axons. Similar to the young cultures, addition of the preclustered ephrinB2-Fc resulted in fast cluster formation and brighter fluorescence on the plasma membrane. In contrast to young neuronal cultures, stimulation induced a large number of smaller sized cluster. In addition, the vesicular trafficking slowed and sometimes even stopped (Figure 6.17). Moreover, neither the kinase-inactive nor the C-terminal truncated version of the fluorescently tagged EphB2 receptor showed other effects in transfected neuronal cultures (Figure 6.16-17).

In addition, the velocities of trafficking vesicles in more mature hippocampal neurons expressing one variant of EphB2-C1 receptors were calculated using the so-called "track points tool" of the Metamorph software. The average velocity of vesicles was $0.88 \mu\text{m}/\text{sec}$ in dendrites and $2.90 \mu\text{m}/\text{sec}$ in axons. These velocities are in the range of reported velocities of fast axonal transport ($4.6 \mu\text{m}/\text{sec}$, Kandel et al. (2000)) and of trafficking vesicles in dendrites ($0.77 \mu\text{m}/\text{sec}$, Guillaud et al. (2003)).

In addition, a series of hippocampal cultures of other ages were transfected with the EphB2-C1 variants. Time lapse imaging of these neuronal cultures never showed additional effects (data not shown). In summary, independently from the expressed EphB2-C1 variant and the age of the culture, fluorescently tagged EphB2 receptors were highly dynamic and were transported in vesicles along dendrites and axons in transfected hippocampal cultures. These fast moving fluorescent vesicles were detectable in all transfected neurons, whereas young transfected neurons displayed less trafficking vesicles compared to the older cultures. Young hippocampal cultures showed some stable EphB2 clusters and trafficking vesicles along the neurites, older cultures display many static clusters and many trafficking vesicles. Independently from

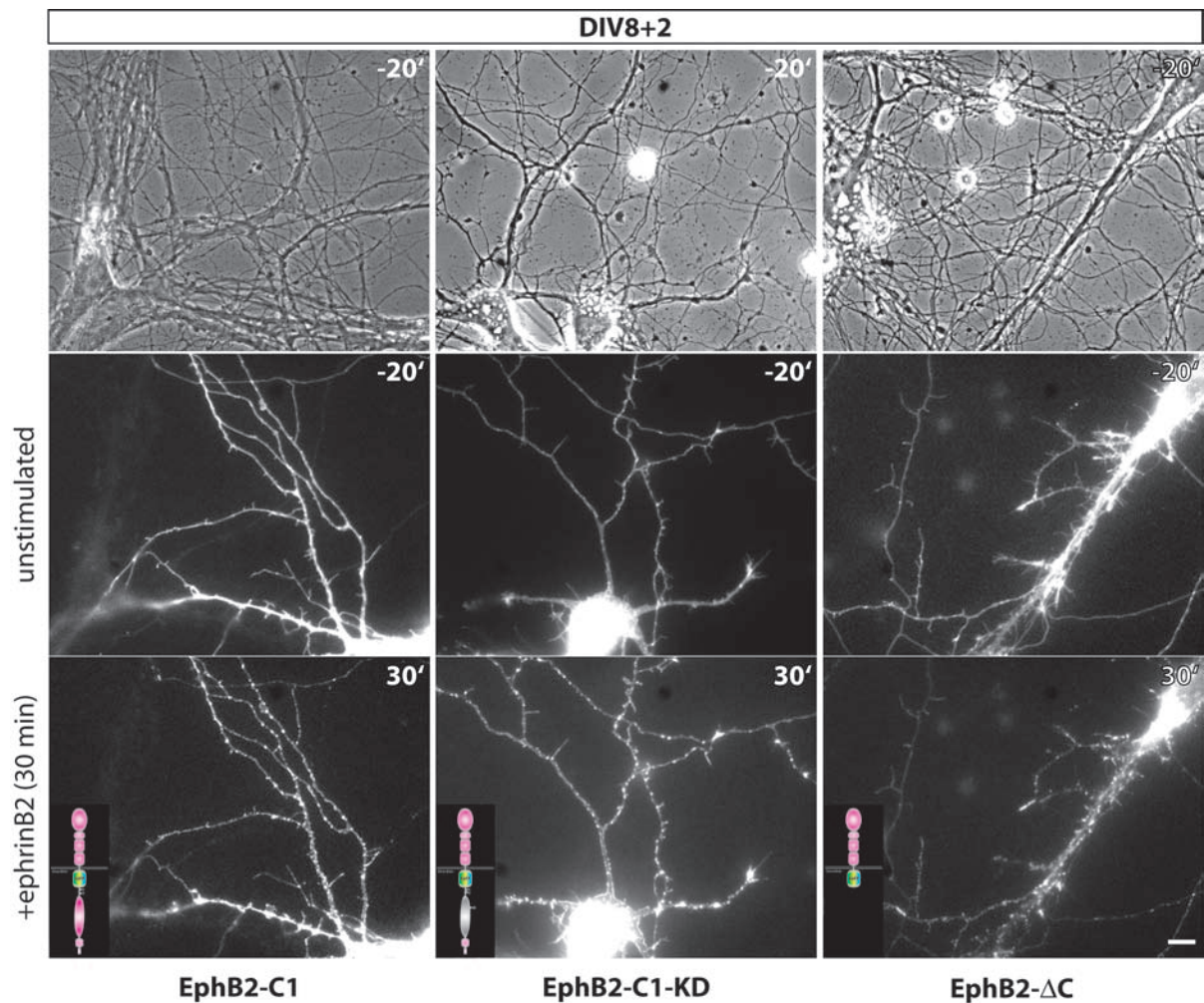


Figure 6.17. Comparison of unstimulated versus ephrinB2-stimulated more mature neurons (DIV8+2/3) expressing one variant of EphB2-C1-EYFP during live-cell imaging. Dissociated hippocampal cultures were transfected at DIV8 with expression constructs encoding either EphB2-C1-EYFP (left column; supplementary information on CD-Rom, movie 4), EphB2-C1-KD-EYFP (middle column; supplementary information on CD-Rom, movie 5) or EphB2- Δ C-EYFP (right column; supplementary information on CD-Rom, movie 6). After 2-3DIV, transfected neurons were imaged by time lapse microscopy at 1 frame/min. The upper and middle panel show phase contrast and fluorescence images 20 min before stimulation (-20'), respectively. After 20 min, preclustered ephrinB2-Fc was added. The lower panel shows fluorescent images 30 min after stimulation (30'). Note the accumulation of bright fluorescent clusters in these images. Time points of imaging are indicated in upper right corners. Scale bar = 10 μ m.

the age of the neurons, the number of moving vesicles decreased, sometimes even stopped, after adding preclustered ephrinB ligands (Figure 6.18). This suggests that the moving vesicles were most likely recruited to the plasma membrane. This would also explain the increased

6. Results

overall fluorescence intensity of the plasma membrane after adding preclustered ligands. The immunostaining results and the observed effects of the live-cell imaging suggest that EphB2 receptors are mainly localized (i) on the surface of neurons and (ii) in cytoplasmic vesicles trafficking along neuronal protrusions.

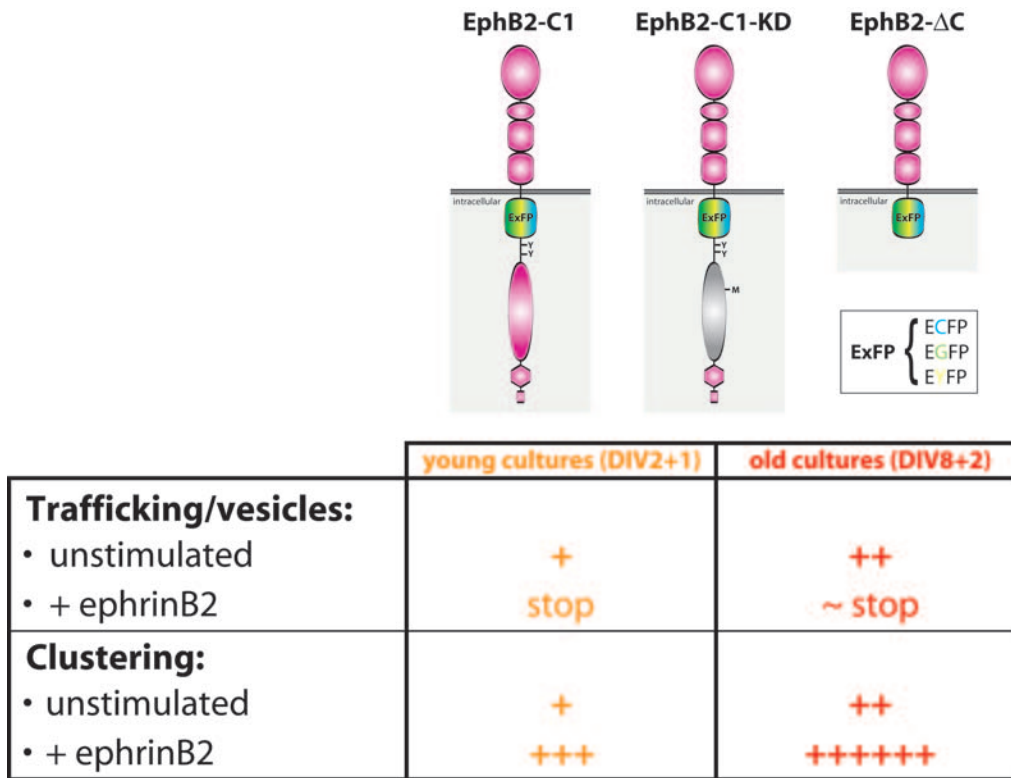


Figure 6.18. Summary of the effects observed during live-time imaging of young and more mature hippocampal neurons expressing one variant of the different EphB2-C1 receptors. Young hippocampal cultures expressing one variant of EphB2-C1 showed trafficking vesicles along the neuron and some stable large EphB2 clusters upon ephrinB2-Fc stimulation. In contrast to young cultures, more mature hippocampal cultures display many trafficking vesicles along dendrites and axons and many static clusters after ephrinB2 stimulation. The trafficking of the vesicles slowed down, sometimes even stopped, after stimulation with preclustered ephrinB-Fc.

6.3. Generation and analysis of transgenic mice expressing one variant of EphB2-C1-EYFP under the control of the Thy-1.2 expression cassette

In order to observe the dynamics and localization of fluorescently tagged EphB2 receptors in the hippocampus *in vivo*, a second approach was taken and *EphB2-C1-EYFP* transgenic mice were generated. An advantage of using an *in vivo* approach avoids the time-consuming calcium phosphate transfection method. This method worked well in relatively young neurons as described previously; however, transfection of very mature neurons is very challenging, due to the low transfection efficiencies, which dramatically decrease with neuronal age. *EphB2-C1-EYFP* transgenic mice would therefore give the possibility to study in more detail very old EphB2-C1-EYFP expressing neurons *in vivo* and *in vitro*.

For this the full-length, kinase-deficient and C-terminal truncated EphB2-C1-EYFP were placed under the control of the Thy-1.2 expression cassette. This expression cassette was chosen because of its unique expression properties: (i) The neuron-specific elements from the *thy-1.2* gene drives strong constitutive expression of transgenes specifically in neurons. Outside the nervous system, only weak expression of the transgene has been reported in the lung (Caroni, 1997). (ii) Transgenic mice expressing multiple spectral variants of EGFP under the control of the Thy-1.2 expression cassette (*thy1-ExFP*) that has been previously generated by Feng et al. (2000) revealed that in some lines only occasional isolated neurons were labelled in different subregions of the brain. With regard to imaging, sparsely labeled neurons allow clear identification of single neurons and their associated dendritic spines and to study the dynamics and localization of EphB2-C1-EYFP variants at these structures. From the *thy1-ExFP* transgenic mice it is known that each of these independently generated transgenic lines express the transgene in a unique, heritable expression pattern (Feng et al., 2000). The offspring of each transgenic founder must therefore be analyzed for the expression of each of the fluorescent EphB2 versions concerning its distribution within the brain region of interest – the hippocampus – and the population and density of affected cells there.

6.3.1. Patterns of transgene expression

41 independent transgenic lines were generated: 22 for the full-length (line A-N, P-W), 8 for the kinase-dead (line Ka-Kh) and 11 for the truncated version (line Da-Dk) of the EphB2-C1-EYFP receptor. The full-length EphB2-C1 transgenic lines were consecutively named in alphabetical order. In case of the kinase-deficient and the truncated EphB2 version a K (abbreviation for **K**inase-dead) or a D (abbreviation for **D**elta-C) was added, respectively.

6.3.1.1. Full-length EphB2-C1-EYFP (line A-N, P-W)

21 founders of the 22 independent transgenic lines expressing full-length EphB2-C1-EYFP driven by the Thy1.2 expression cassette gave offspring. Only 18 lines showed fluorescence in the brain, of which three lines yielded low expression levels and were excluded from further analysis. Compared to one of the *thy1-YFP* transgenic mice (line YFP-2Jrs) from Joshua R. Sanes, which express only the cytoplasmic EYFP protein under the control of the Thy1.2 expression cassette (Feng et al., 2000), the fluorescence was weak in these 15 remaining transgenic lines. The six lines with the strongest fluorescent signal (A, E, J, M, R and W) were selected and analyzed in more detail (Figure 6.19).

The transgenic lines A, E and J yielded a comparable expression pattern. The fluorescently tagged EphB2-C1 receptors were present in the perforant fiber pathway, the mossy fiber pathways and in pyramidal cells of the CA1 region. In contrast, pyramidal cells of the CA3 region showed only a faint or no expression of the full-length EphB2-EYFP receptor. Remarkably, the mossy fiber axons of the granule cell of these three lines showed a strong fluorescence.

The line M and W also yielded a fluorescent signal in the perforant fiber pathway. In contrast, these lines displayed no or only a faint fluorescence in the mossy fiber axons of the granule cell and only a weak homogeneous fluorescence in the CA1 region (Figure 6.19, compare G-H & K-L with A-F). Interestingly, neurons of CA3 region in the hippocampus of the transgenic line M showed a stronger signal than in the CA1 region (Figure 6.19, G-H & K-L with A-F).

Moreover, lines A and J displayed the brightest signal of immunostaining and fluorescence among the six transgenic mouse lines.

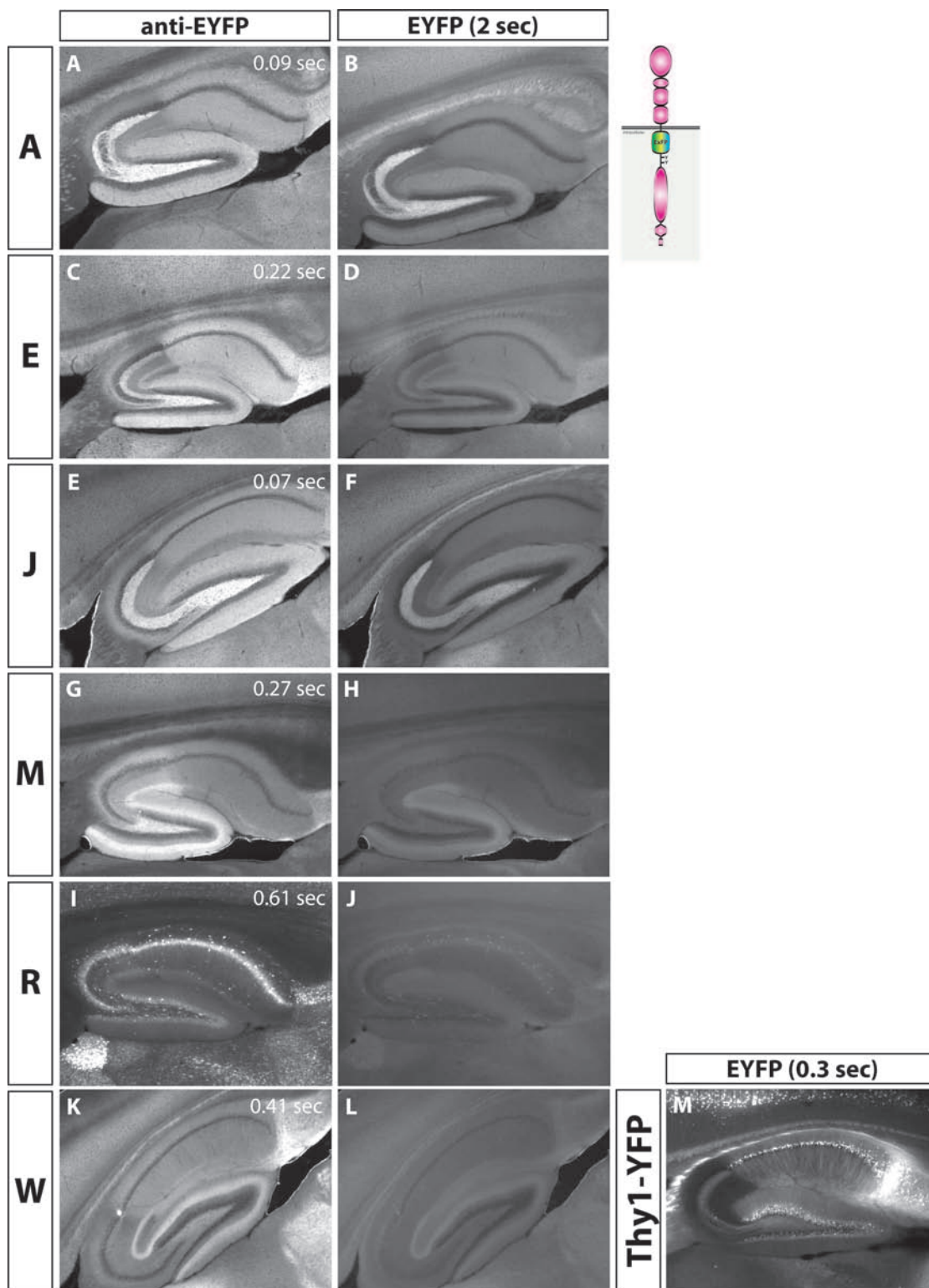
Remarkably, in only one line – the R line – labeling was largely confined to single neurons (Figure 6.19I-J and 6.20). Unfortunately, however, the fluorescent signal in this line was too weak for imaging in slices (Figure 6.19J) and only after an anti-EYFP immunostaining the sparse expression of EphB2-C1-EYFP receptors became clearly visible in all regions of the hippocampus (Figure 6.20A-D). In addition, other regions, such as the cortex, also showed isolated EphB2-C1-EYFP expressing neurons after immunostaining against EYFP (Figure 6.20E-F).

6.3.1.2. Kinase-dead EphB2-C1-EYFP (line Ka-Kh)

Six founders of the eight independent transgenic lines Ka-Kh expressing the kinase-dead EphB2-C1-EYFP under the control of the regulatory elements of Thy1.2 gave offspring. Adults from each line were analyzed, from which five founder mouse lines were fluorescent. The four lines with the brightest fluorescent signal were further analyzed in more detail (Figure 6.21). None of these lines yielded a sparse expression pattern of the fluorescently tagged kinase-deficient EphB-C1 receptor. All lines displayed a homogeneous expression pattern. All regions of the hippocampus were labeled in the transgenic line Ke (Figure 6.21C-D). The two lines Kf and Kh showed, apart from the homogeneous distribution of the transgenic protein in the DG and CA1 region of the hippocampus that granule cells of the DG sent bright fluorescent mossy fibers to the pyramidal cells in CA3 region (Figure 6.21E-H). Interestingly, the transgenic mouse line Kc possessed additional fluorescent pyramidal cell of the CA3 region (Figure 6.21A-B and I-J).

Figure 6.19. **Transgene expression in the hippocampal formation of adult *thy1-EphB2-C1-EYFP* mice.** Analysis of six independent transgenic lines of adult mice expressing EphB2-C1-EYFP under the control of the Thy-1.2 expression cassette (line A (A-B), line E (C-D), line J (E-F), line M (G-H), line R (I-J) and line W (K-L)) and for comparison of the *thy1-YFP* mouse (line YFP-2Jrs (M)). (A-L) Images of each line were taken from the same cryosection of a fixed transgenic brain. The exposure time of each section was always 2 sec for the EYFP-fluorescence (**right column, EYFP (2 sec)**); and in case of the anti-EYFP immunostaining the exposure time is displayed in the upper right corner of each image (**left column, anti-EYFP**). (M) The exposure time of the section of the *thy1-YFP* transgenic mouse was 0.3 sec. 5-times magnification.

6. Results



6.3.1.3. C-terminal truncated EphB2-C1-EYFP (line Da-Dk)

Among the eleven founders (lines Da-Dk) expressing the C-terminal truncated EphB2-C1-EYFP receptor under the control of the Thy1.2 expression cassette, six lines gave offspring. Analysing the offspring of these six transgenic mouse lines revealed that three lines were fluorescent, but only the lines Df and Dj yielded an intense fluorescent signal (Figure 6.22). In both lines neurons of the DG and the CA1 region were labeled homogeneously. Remarkably, in images of the Df line a sharp border in fluorescence was clearly visible between the CA3 region and the CA1 region of the hippocampus. This boundary was also visible in images of

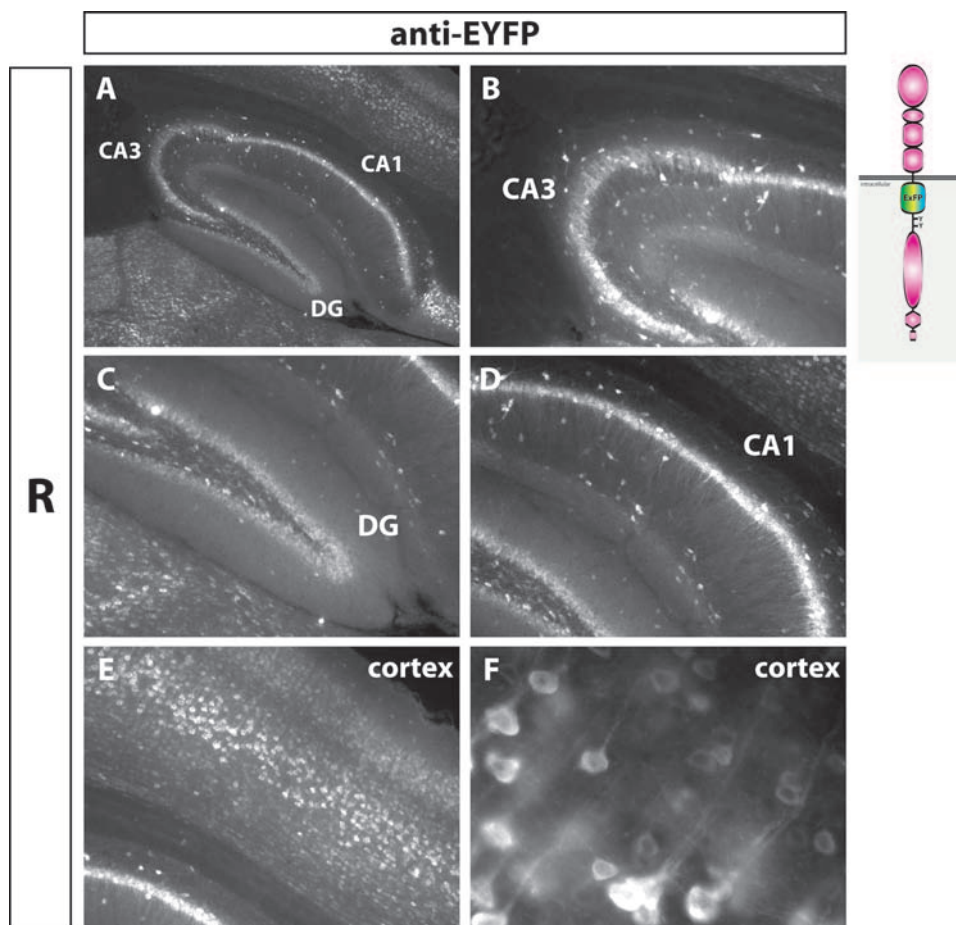


Figure 6.20. **Sparse expression of EphB2-C1-EYFP in the adult transgenic mouse line R.** Analysis of the independent transgenic line R of an adult mouse brain expressing EphB2-C1-EYFP under the control of the Thy-1.2 expression cassette (line R (A-F)). Images were taken from anti-EYFP immunostained cryosections (A-F) of a fixed brain. (A) shows the hippocampus. (B-D) Higher magnification of the hippocampus showing the CA3 (B) and CA1 regions (C) and the dentate gyrus (DG) (D) of (A). (E-F) Different magnifications of the cortical region. Magnifications: 5-times (A), 10-times (B-E) and 63-times (F).

6. Results

the Dj line, however, not as clear as in the Df line (Figure 6.22A-D, white arrowheads). Therefore, in contrast to the Df line, neurons of the transgenic mouse line Dj expressed low levels of transgenic proteins in the CA3 region of the hippocampus. In addition, only in the Df mouse line axons of the mossy fiber pathway displayed an intense fluorescent signal. This signal in the axons was not detectable in the Dj line.

In summary, all analyzed transgenic mouse lines, apart from line R, showed a homogeneous distribution of the transgenic protein mainly in the DG and CA1 region of the hippocampus independent from whether the transgenic mouse expressed either a full-length, a kinase-deficient or a C-terminally truncated fluorescently tagged EphB2 receptor. Surprisingly, the fluorescent intensity of the transgenic protein was not very high in all transgenic lines. Only one line yielded a sparse expression of full-length EphB2-C1-EYFP in neurons, but with weak

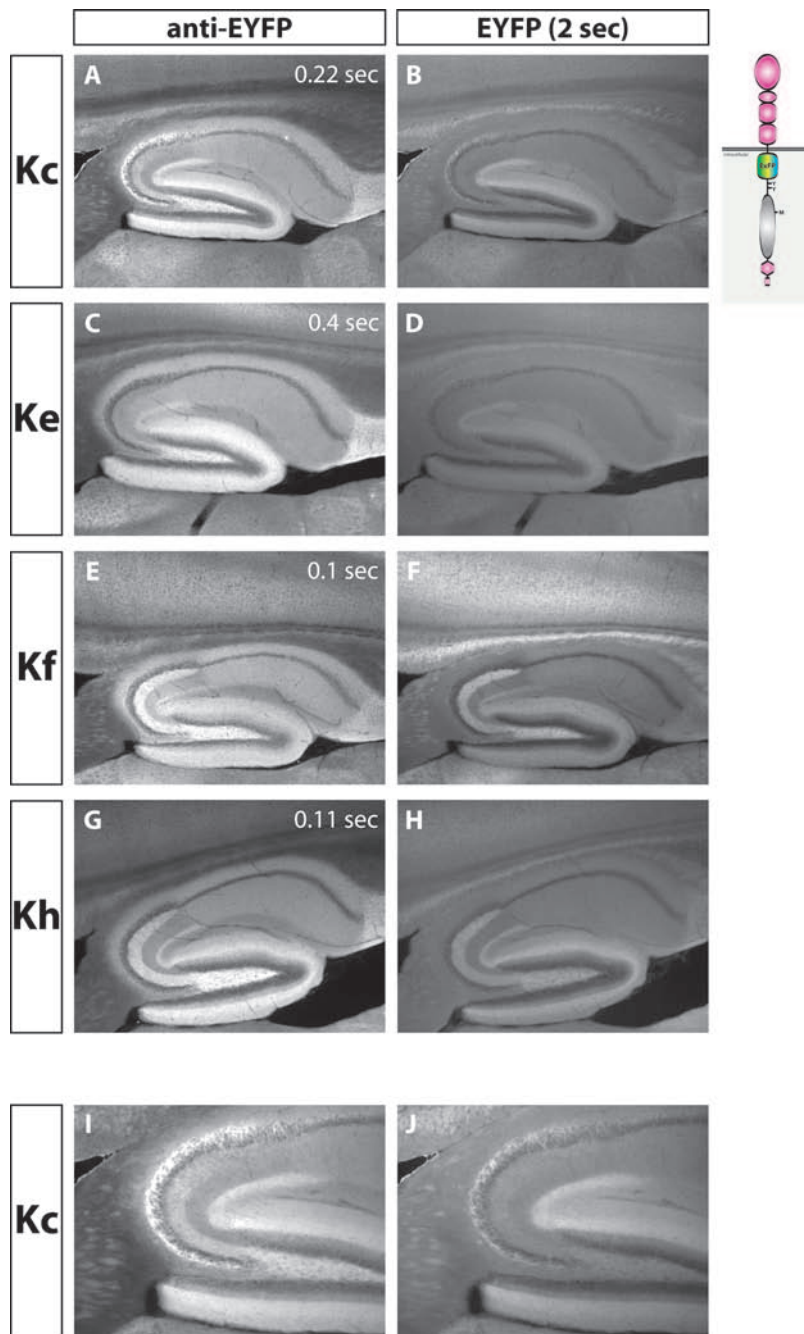


Figure 6.21. Expression pattern of kinase-deficient EphB2-C1-EYFP in the hippocampal formation of adult transgenic mice. Analysis of four independent transgenic lines of adult mice expressing kinase-deficient EphB2-C1-EYFP under the control of the Thy-1.2 expression cassette (line Kc (A-B, I-J), line Ke (C-D), line Kf (E-F) and line Kh (G-H)). Images of each line were taken from the same cryosection of a fixed brain from the adult transgenic mouse. The exposure time of each section was always 2 sec for the EYFP-fluorescence (right column, EYFP (2 sec)); and in the case of the anti-EYFP immunostaining the exposure time is displayed in the upper right corner of each image (left column, anti-EYFP). Magnification: 5-times (A-H) and 10-times (I-J).

6. Results

fluorescence.

After realizing that in almost all lines the fluorescent signal was too homogeneous for imaging in brain slices, primary hippocampal cultures were prepared from the lines with a bright fluorescent signal (line A and J). The aim was to investigate whether these cultures could be useful for time lapse microscopy, but unfortunately the intensity of the fluorescence was still too weak for live-cell imaging (data not shown).

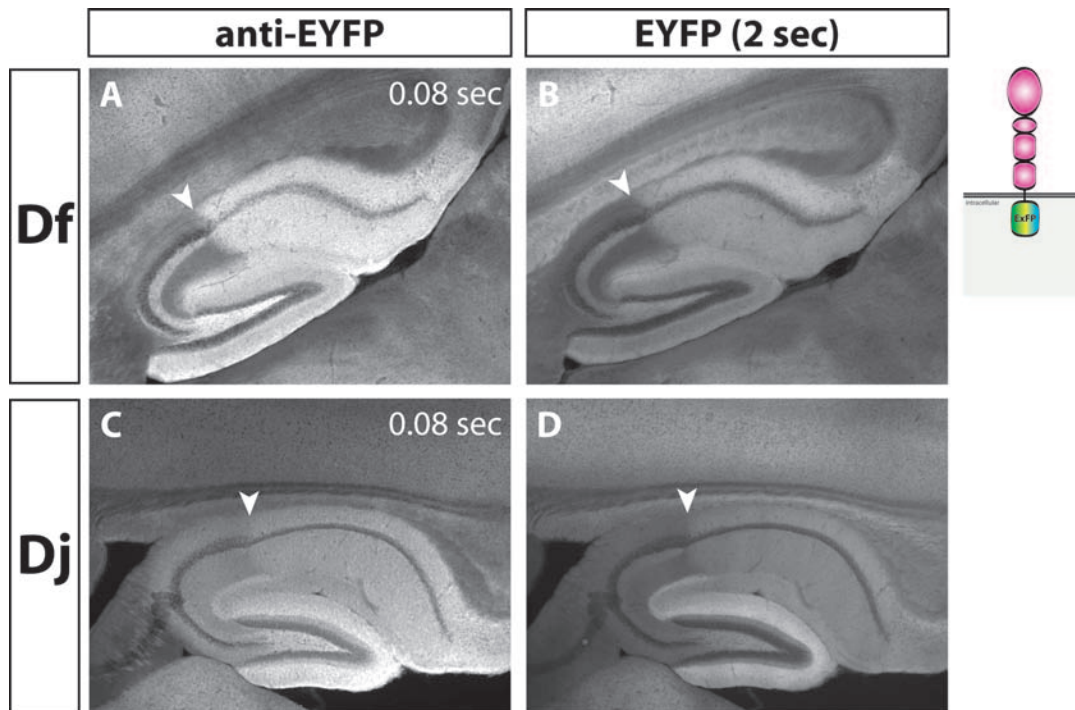


Figure 6.22. **Expression pattern of C-terminal truncated EphB2-C1-EYFP in the hippocampal formation of adult transgenic mice.** Analysis of two independent transgenic lines of adult mice expressing C-terminal truncated EphB2-C1-EYFP under the control of the Thy-1.2 expression cassette (line Df (A-B) and line Dj (C-D)). Images of each line were taken from the same cryosection of a fixed adult transgenic brain. The exposure time of each section was always 2 sec for the EYFP-fluorescence (**right column, EYFP (2 sec)**). The exposure time of the immunostained sections is displayed in the upper right corner of each image (**left column, anti-EYFP**). White arrowheads indicate the transition from the CA3 region to the CA1 region. 5-times magnification.

To determine if the sparse expression pattern of the transgenic mouse line R could yield enough fluorescence for imaging by confocal microscopy, so-called organotypic Gähwiler cultures were made. After two to four weeks in culture, hippocampal slice cultures were imaged, but again, the fluorescent signals were not bright enough for confocal live-cell microscopy (data not shown). Therefore, we did not pursue the original aim of imaging the behaviour of EphB2 proteins in individual neurons, of an intact slice, in these transgenic mice.

6.3.2. *In situ* hybridization data of different transgenic *thy1-EphB2-C1* mice

The analysis of the different transgenic mice expressing one variant of EphB2-C1-EYFP under the control of the Thy1.2 expression cassette revealed that almost all lines showed a homogeneous expression of the transgenic proteins in the DG and CA1 region of the hippocampus. It has been shown that the EphB2 receptor is important in hippocampal LTP (Grunwald et al., 2001). To determine if the overexpression of truncated EphB2 proteins may result in a dominant-negative effect on LTP, we decided to measure LTP in these transgenic mice. An important control was to check the extent of correlation between the transgene expression patterns and their respective mRNA levels. *In situ* hybridization experiments were therefore performed.

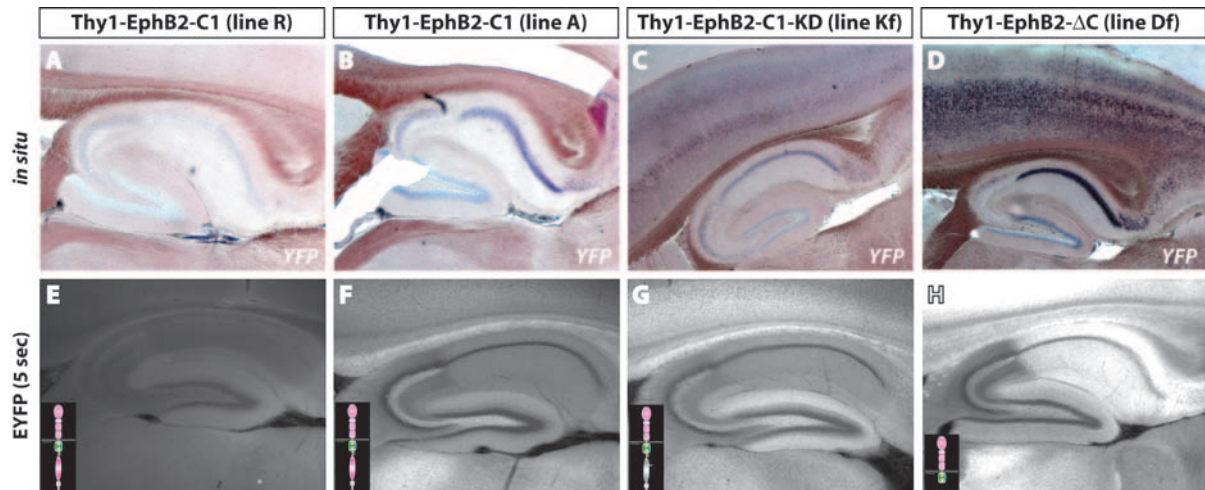


Figure 6.23. Comparison of *in situ* hybridization data with the fluorescent signal of hippocampal section of different transgenic lines. Hippocampal sections of adult transgenic mice expressing either full-length (line R (A, E)), line A (B, F)), kinase-dead (line Kf (C, G)) or C-terminal truncated EphB2-C1-EYFP receptors (line Df (D, H)) were used for *in situ* hybridization analysis using a digoxigenin-labeled antisense probe against EYFP (indicated as YFP (upper panel)). For each line, images were taken from anti-digoxigenin immunostained (upper panel, *in situ*) and fixed-only hippocampal sections (lower panel, EYFP (5 sec)) derived from the same transgenic brain. The exposure time of fluorescent sections was 5 seconds.

The *in situ* hybridization data of the transgenic mice were obtained using a newly generated transgene-specific probe, namely the digoxigenin-labeled antisense probe against the EYFP coding sequence. Three different transgenic mouse lines expressing either full-length (line A), kinase-dead (line Kf) or C-terminal truncated EphB2-C1-EYFP receptors (line Df) driven by Thy-1.2 expression cassette were selected based on (i) similar homogeneous (transgene) expression pattern and (ii) a comparable fluorescent intensity. Adult mice of these transgenic

6. Results

lines were analyzed. In addition, the transgenic *thy1-EphB2-C1* mouse line R displaying the isolated transgene expression in the hippocampus was also examined. To compare the fluorescent signal with the *in situ* hybridization data of the same brain, one hemisphere was used for each experiment (Figure 6.23).

The *in situ* hybridization analysis confirmed the expression pattern of transgenic EphB2-C1 proteins of fixed anti-GFP immunostained sections (Figure 6.19-22): a weak expression pattern in the hippocampus was consistent with a weak mRNA level of the transgene and *vice versa*. The EphB2-C1-EYFP mRNA of the transgenic line R was barely detectable in the hippocampus, consistent with the sparse expression of the transgene (Figure 6.23A, E). The lines A, Kf and Df yielded mRNA levels confined to CA1 region and DG. The lines A and Kf displayed a weak transgene expression in the CA3 region, almost absent in line Df (Figure 6.23B-D, F-H). In addition, the line Df showed a very strong expression of the truncated EphB2-C1 receptor in the CA1 region (Figure 6.23D, H).

The binding specificity of the antisense EYFP probe, which was generated from a newly cloned construct, was demonstrated by using the *thy1-YFP* transgenic mouse line YFP-2Jrs (Figure 6.24A-B). Hippocampal sections of this line nicely showed the isolated transgene expression in fixed-only sections and even sparse mRNA positive neurons were visible in the *in situ* hy-

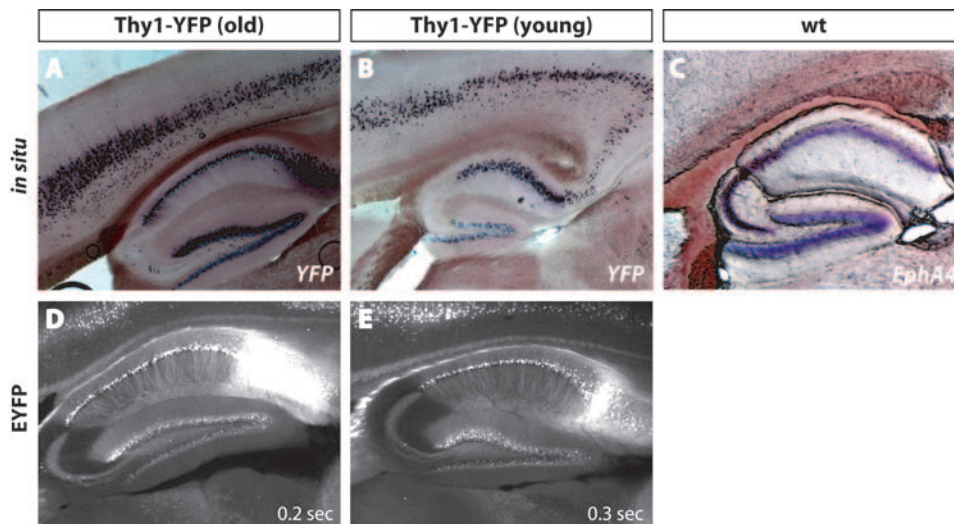


Figure 6.24. *In situ* hybridization analysis of hippocampal sections of *thy1-YFP* transgenic mice and a wild type (wt) animal. *In situ* hybridization analyses (upper panel, *in situ*) of hippocampal sections of the adult *thy1-YFP* transgenic mouse line YFP-2Jrs (A-B) and a wild type mouse (C) using the indicated digoxigenin-labeled antisense probes. Images of the fluorescent signal (lower panel, EYFP) of fixed hippocampal sections of different old *thy1-YFP* transgenic mice (line YFP-2Jrs) (old (D), young (E)). The exposure time of the fluorescent sections is displayed in the lower right corner of these images.

bridization analysis of these sections (Figure 6.24, compare A with D, B with E). An additional control for the *in situ* hybridization procedure was the antisense EphA4 probe, that nicely revealed the previously described mRNA levels from EphA4 in the hippocampus (Figure 6.24C)(Grunwald et al., 2001). In summary, the mRNA levels of the transgene corresponded with the expression patterns of the fluorescently tagged EphB2-C1 variants in all four transgenic mouse lines.

6.3.3. Overexpression of EphB2-C1 or EphB2- Δ C in transgenic mice does not affect CA3-CA1 hippocampal LTP

With respect to the synapse between CA3 and CA1 neurons, ephrinB2 and ephrinB3 are expressed mainly in postsynaptic CA1 neurons, while the relevant Eph receptors - EphB2 and EphA4 - are expressed both pre- and postsynaptically in the adult hippocampus (Grunwald et al., 2001, 2004). In addition, it has been shown by our group that these proteins – EphB2, EphA4, ephrinB2 and ephrinB3 – are required for hippocampal CA3-CA1 long-term plasticity (Grunwald et al., 2001, 2004), thereby supporting the hypothesis that Eph receptors and ephrins are directly involved in synaptic plasticity of mature synapses.

The *in situ* hybridization data and the analysis of the EYFP-fluorescence of hippocampal sections of the transgenic mouse line Df revealed a very strong signal of transgenic mRNA and protein, respectively (Figure 6.23D, H). This mouse line overexpresses the C-terminal truncated EphB2-C1 receptor at the postsynaptic site of CA1 neurons, thereby possibly interfering with hippocampal plasticity. Assuming that transgenic EphB2 receptors interact with wild type EphB2 proteins at the postsynaptic site of the cell, then the overexpression of truncated EphB2 receptors could have a dominant-negative effect by blocking endogenous EphB2 receptor signalling (heterodimers), thereby causing an effect in LTP. Another possibility causing also a dominant-negative effect could be that the overexpressed truncated EphB2 proteins take away ephrinB ligands, thereby preventing endogenous EphB2 forward signalling. A third possibility is that this overexpression results in a dominant-active effect by the interaction of truncated EphB receptors with the endogenous ephrinBs, thereby increasing the activation of ephrinB reverse signalling and affecting LTP. To assess, whether the overexpression of the C-terminal truncated or the full-length EphB2-C1-EYFP could alter the availability of ephrinBs at the CA3-CA1 synapse, LTP was measured in acute hippocampal slices from transgenic mice (line Df and A) and littermate controls after thetastimulation (TBS). The TB stimulus is known to be efficient in inducing long-lasting LTP (Bliss and Collingridge, 1993).

6. Results

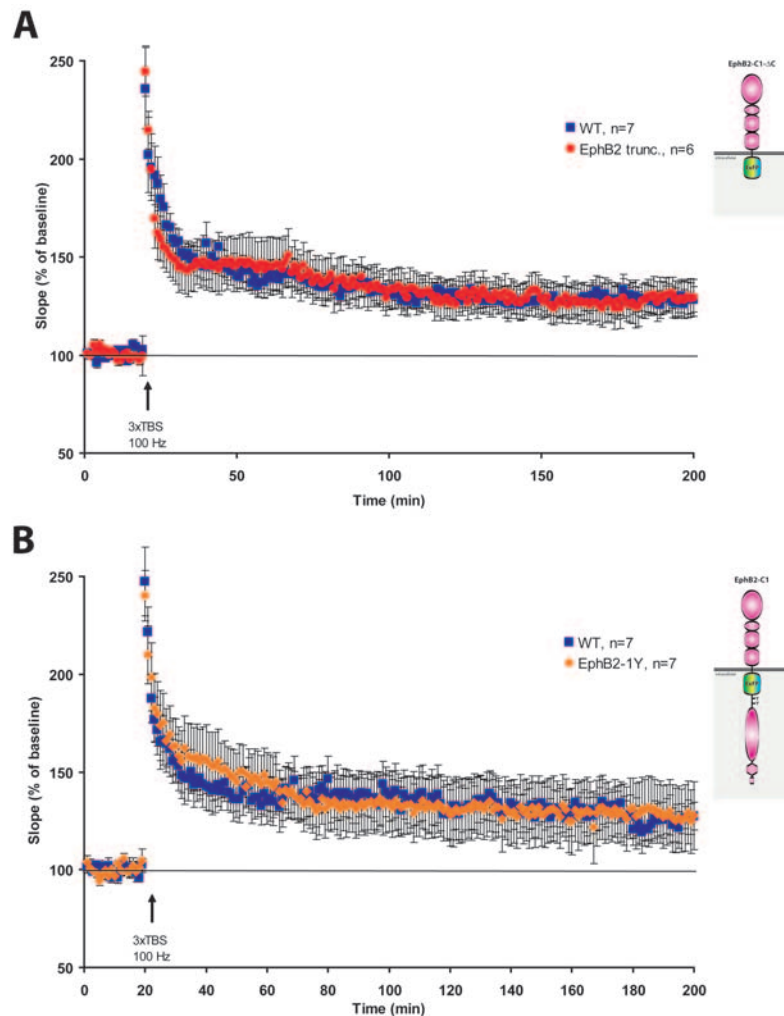


Figure 6.25. **LTP was not affected in hippocampal neurons overexpressing full-length or C-terminal truncated EphB2-C1 in adult transgenic mice.** LTP was induced by stimulation of presynaptic CA3 neurons with theta burst stimulation (TBS, black arrow) in acute hippocampal slices. Transgenic mice expressing EphB2- Δ C-EYFP (line Df, **A**) or full-length EphB2-C1-EYFP (line A, **B**) under the control of the Thy-1.2 expression cassette showed no reduction in early- or late-phase CA3-CA1 LTP compared to littermate controls. Until 180 min after TBS the fEPSP from control and *thy1-EphB2- Δ C-EYFP* (**A**) or *thy1-EphB2-C1-EYFP* (**B**) slices were not significantly different. n=number of slices from 3 (**A**) or 2 (**B**) mice per animal group. Error bars: SEM.

After recording a stable baseline, a TBS was given to the presynaptic CA3 neurons and LTP was recorded from CA1 neurons for up to three hours after stimulation. All electrophysiological experiments were performed by Martin Korte and Volker Staiger in the laboratory of Tobias Bonhoeffer at the Max-Planck Institute of Neurobiology (Martinsried, Germany). All recordings were performed in a strictly blind fashion and the genotypes of the mice were only revealed after final data analysis.

Figure 6.25 shows the summary graphs for all LTP recordings. Hippocampal slices of *thy1-EphB2-C1-EYFP* (full-length EphB2-C1), *thy1-EphB2-ΔC-EYFP* (C-terminal truncated EphB2-C1) and littermate wild type mice showed normal post tetanic potentiation (Figure 6.25). All groups showed clear E- and L-LTP after TBS stimulation with no obvious difference between genotypes.

6.4. Trans(endo)cytosis of EphB2-C1 receptors in primary hippocampal neuronal cultures

Recently our group could show that cell-to-cell contact between EphB- and ephrinB-expressing HeLa cells leads to bi-directional endocytosis, thereby terminating adhesion and enabling cells to detach and separate from each other (Zimmer et al., 2003). In addition, growth cones of very young immature primary neurons of mouse forebrain can take up ephrinB or EphB after stimulation with soluble preclustered ectodomains of ephrinB ligands or EphB receptors fused to Fc fragments and after contact with ligand- or receptor-expressing cell lines (Zimmer et al., 2003).

So far, it is not known (i) if older mature neurons also engage in endocytic events of ephrinB-EphB complexes and if they do so, (ii) what is the cell counterpart in the brain, is it a neuron or a glial cells. Therefore, we decided to investigate whether there is ephrinB- or EphB-triggered transcytosis in mature hippocampal cultures.

6.4.1. Reverse transcytosis of EphB2-C1 receptors in mature primary hippocampal cultures

The aim of the following studies was to investigate whether EphBs and ephrinBs undergo transcytosis in mature neuronal cultures without any “artificial” stimulation, such as soluble preclustered fusion bodies of ephrin/Eph ectodomains with Fc fragments or ligand/receptor-expressing cell lines. To assess this, 14-day-old primary hippocampal cultures were transfected with expression constructs coding for EphB2-C1-EYFP. Two days later, transfected neuronal growth cones were imaged for transcytosis by time lapse microscopy. Figure 6.26B-E shows a sequence of four images taken during a time period of six minutes, showing a neuronal process with its growth cone engaging with other cells in the high-density culture, such as neurons and glial cells. During the first two minutes, a filopodium-like protrusion of the EphB2-C1 expressing neuron showed a small fluorescent cluster of EphB2 on its tip. In sub-

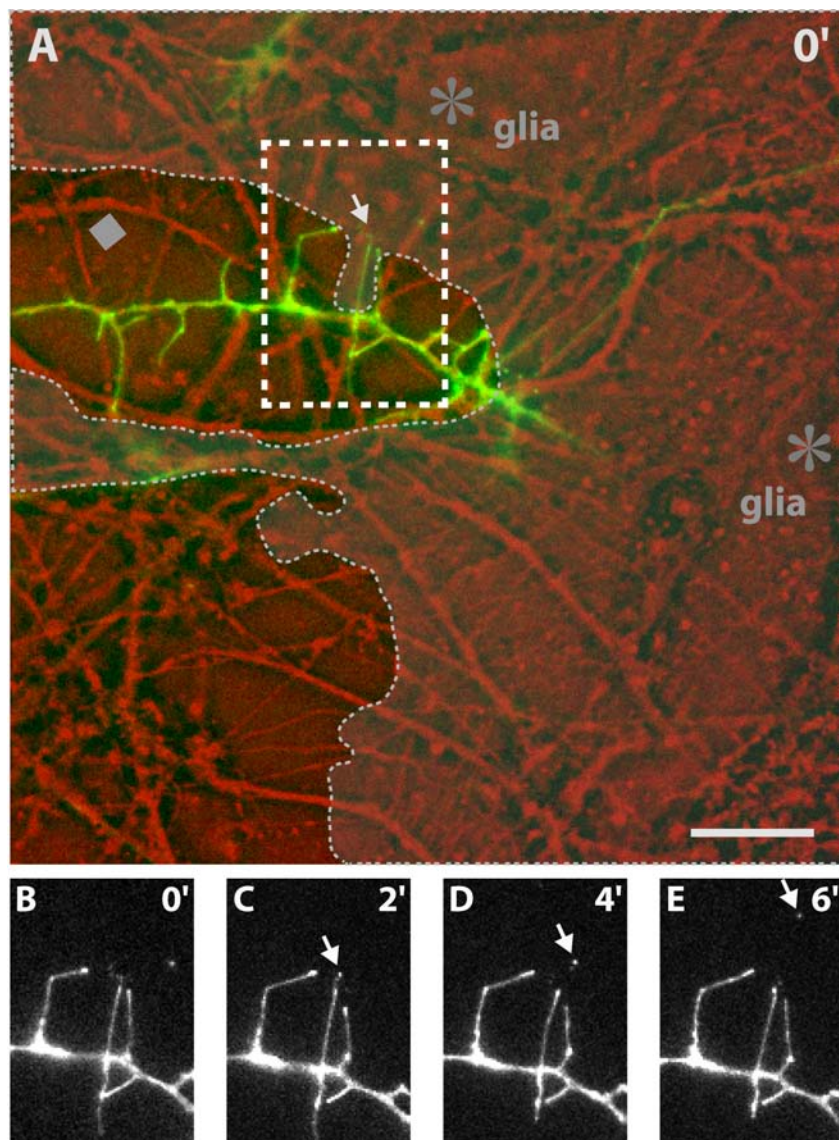


Figure 6.26. **Reverse transcytosis of EphB2-C1-EYFP in a primary neuronal culture during live-cell imaging after neuron-to-cell contact.** (supplementary information on CD-Rom, **movie 8**) A high-density mature 14-day-old primary hippocampal culture was transfected with expression constructs coding for fluorescently tagged EphB2-C1-EYFP receptors. Two days later, transfected neurons were imaged by time lapse microscopy at 1 frame/min. **(A)** Large image shows merge of phase contrast image in red and the EphB2-C1 fluorescence of a transfected neurite and its growth cone in green before the transcytosis. Dashed box indicates the area of transcytosis. Dashed lines and lighter areas indicate outline of glial cells (asterisks). Diamond indicates glia-free area. **(B-E)** Fluorescent images from the area indicated by the dashed box in **A**. Within six minutes a fluorescent cluster is moving away from the middle filopodium-like extension into a neighbouring cell, most-likely a glial cell, after cell-to-cell contact (fluorescent cluster indicated by arrow). Time points of imaging are indicated in upper right corners. Scale bar = 20 μm .

sequent images, this cluster was taken up by another cell, presumably a glial cell and was retrogradely transported (Figure 6.26D-E, arrows). Figure 6.26 displays only six minutes of the total 70 minutes of live-cell imaging (supplementary information on CD-Rom, **movie 8**). A closer look at the movie reveals several interesting events: First, there are several occurrences of transcytosis in the area shown in the figure, especially in the growth cone and in its close proximity. Second, the growth cone and other parts of the neuronal process are partially growing on glial cells (Figure 6.26A, asterisks and dashed lines). These cells are easily recognizable during live-cell imaging because (i) glial cells always display faster cell movement, (ii) their cytoplasm appears different from the neuronal and (iii) they have a flat spread morphology and grow very often underneath the neurons (Figure 6.26A, dashed lines). Third, transcytosis was observed close to areas rich in glial cells. Fourth, filopodia of growth cones and neurites that were not in contact with glial cells only displayed slow movement of filopodia with no obvious transcytosis events (Figure 6.26A, diamond). In contrast, filopodia growing close to or on top of glial cells, very often displayed highly dynamic filopodia accompanied, very often with transcytosis. The neuron-to-cell transcytosis events were also often followed by retraction or even disappearance of filopodia (see also figure 6.28). Last, continuous transcytosis was clearly visible during time lapse imaging of the area shown in figure 6.26B-E; in this case, it appeared that after the contact between the neuronal filopodia and the most-likely glial cell, the glia started to retract, thereby pulling away the filopodia-like protrusion. Very often transcytosis was followed (i) by disconnection of the interacting partners, thus resulting in a retraction or loss of filopodia or (ii) by internalization of the clusters from filopodia still connected to the presumably glial cell.

Figure 6.27 shows another example of transcytosis in mature hippocampal high-density cultures. The white arrows indicate the area of transcytosis with an most-likely astrocyte growing underneath the neuronal process (Figure 6.27, dashed line). In the five successive images taken in a time period of eight minutes the translocation of a fluorescent EphB2 cluster from the tip of the neuronal protrusion was visible. The pink arrow indicates another transcytosis event in close proximity to the same glial cell (supplementary information on CD-Rom, movie 9). The corresponding movie shows several events of transcytosis mainly from two neuronal protrusions (Figure 6.27, arrows). In general the reverse transcytosis events were very fast (within minutes) and were often followed by fast retraction of neuronal protrusions. Furthermore, after cell-to-cell contact EphB2 clusters were internalized from the tip of neuronal protrusions by neighbouring cells and retrogradely transported. The data indicate that the neighbouring cell may be a glial cell or more likely an astrocyte (data not shown). These re-

6. Results

sults show that transcytosis is possible at sites of neuron-to-cell contacts without an “artificial” stimulation in neuronal cultures.

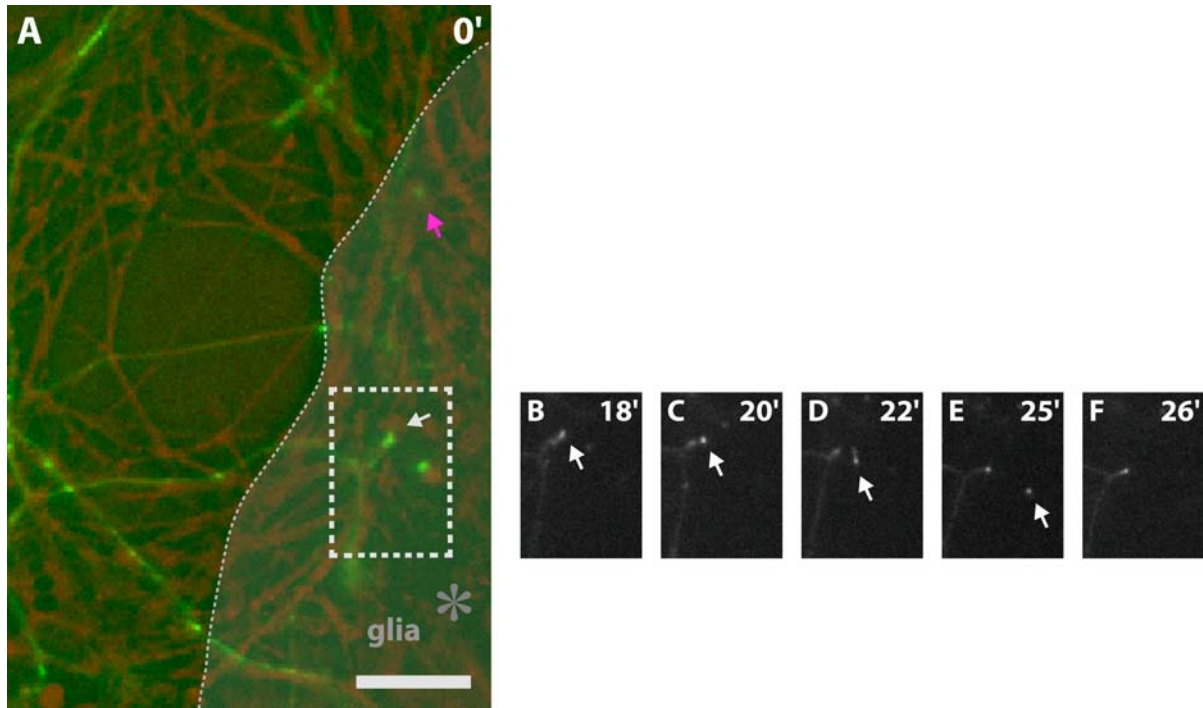


Figure 6.27. Reverse transcytosis of EphB2-C1-EYFP into adjacent cells of a mature primary hippocampal culture during live-cell imaging after neuron-to-cell contact. (supplementary information on CD-Rom, **movie 9**) Similar experiment as shown in figure 6.26. Mature primary high density hippocampal culture was transfected at DIV14 with EphB2-C1-EYFP expression constructs. Two days later, a transfected neuron was imaged by time lapse microscopy at 1 frame per min. **(A)** Merge of phase contrast image in red and the EphB2-C1 fluorescence in green at time point 0 min. **(B-F)** Fluorescent images from the area indicated by the dashed box in **A**, showing the beginning of a transcytosis with the fast translocation of the fluorescent cluster away from the neuronal protrusion within 8 min (indicated by white arrows). Dashed line and lighter area indicate outline of the glial cell (asterisks). Time points of imaging are indicated in upper right corners. Scale bar = 10 μm .

6.4.2. Reverse transcytosis of EphB2-C1-EYFP proteins followed by persistent retraction of the neuronal protrusion

Figure 6.28 shows a sequence of images taken during a time period of ten minutes of an EphB2-C1 transfected high density culture as described earlier. However, in contrast to movie 9 (Figure 6.29), this case the transcytosis was followed by a retraction and persistent disappearance of the neuronal protrusion (see also supplementary information on CD-Rom, movie 8). Again, as mentioned before, the Eph2-C1 expressing neurons only showed events of tran-

scytosis in areas rich in glial cells, indicating again that the transcytosis event is mainly taking place between a neuron and a glial cell (Figure 6.28, dashed lines). The pink arrow indicates other transcytosis events (supplementary information on CD-Rom, movie 10).

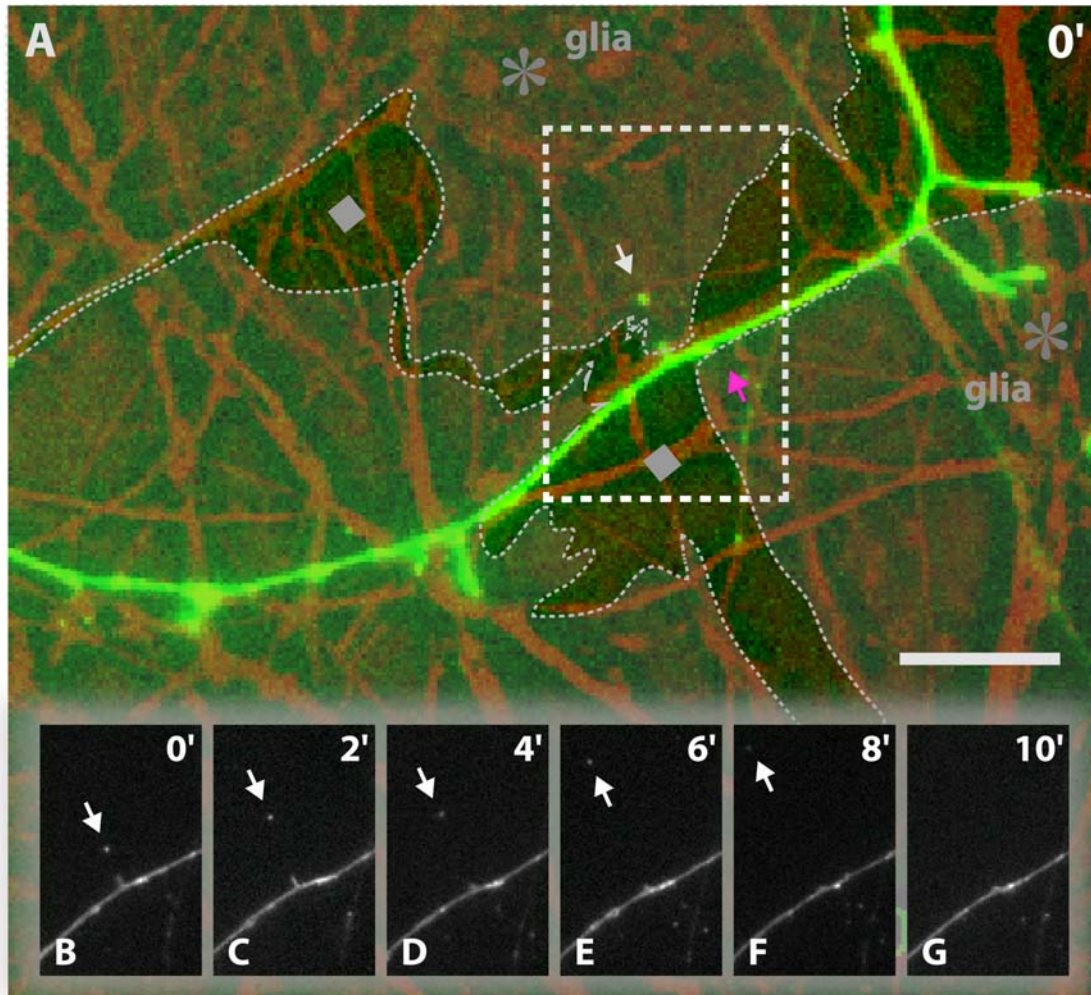


Figure 6.28. Reverse transcytosis of EphB2-C1-EYFP followed by retraction of a neuronal protrusion from the dendritic shaft. (supplementary information on CD-Rom, **movie 10**) A mature primary high-density hippocampal culture was transfected at DIV13 with expression constructs coding for fluorescently tagged EphB2-C1-EYFP. Two days later, the transfected neuron was imaged by time lapse microscopy at 1 frame/min. **(A)** Merge of phase contrast image in red and the EphB2-C1 fluorescence in green before the transcytosis. Dashed box indicates area of transcytosis. **(B-G)** Fluorescent images from the area indicated by the dashed box in **A**. Fluorescent cluster is moving away from the retracting neuronal protrusion (indicated by arrows). Dashed line and lighter areas indicate outline of glial cells (asterisks). Diamonds indicate glia-free areas. Time points of imaging are indicated in upper right corners. Scale bar = 10 μm .

6.4.3. Transcytosis is not a general phenomenon among the Eph and ephrin classes of protein families

Recent data by our group demonstrated that trans-endocytosis can be bi-directional (Zimmer et al., 2003). To address if ephrinB is transcytosed in mature hippocampal cultures, neuronal cultures were transfected at DIV13-14 with expression constructs coding for N-terminal fluorescently tagged ephrinB1 or ephrinB2. This modification has been shown not to interfere with receptor binding or transcytosis (Brückner et al., 1999; Zimmer et al., 2003). Two days later,

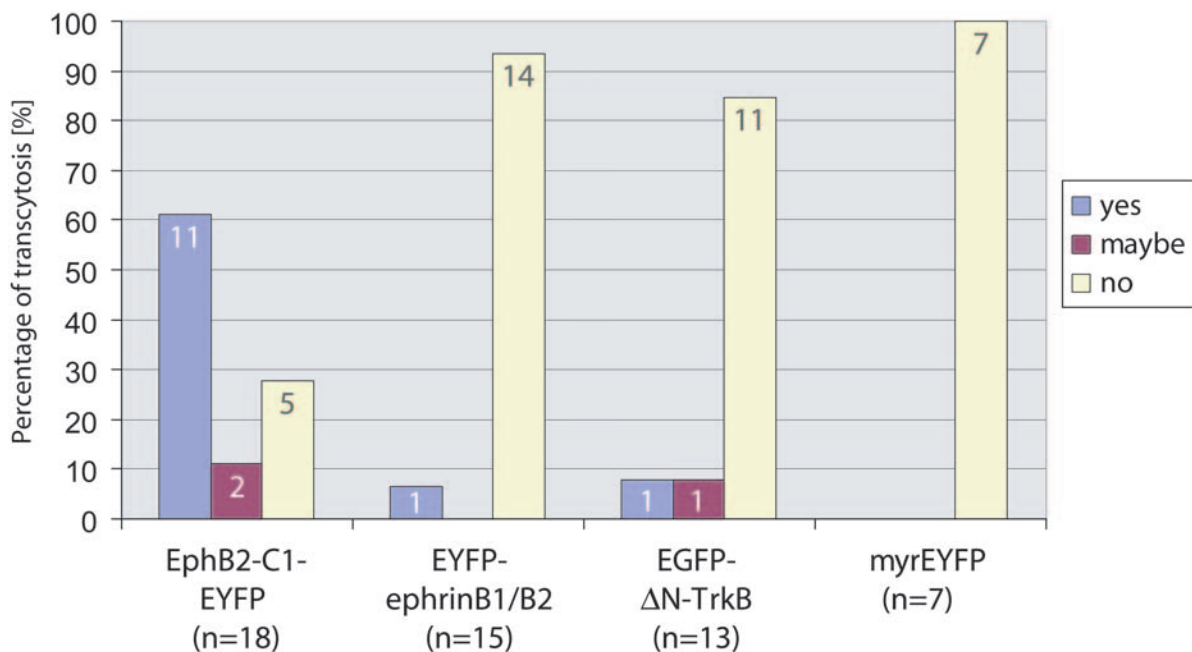


Figure 6.29. **Quantification of percentage of transcytosis in transfected neuronal high-density cultures.** Mature primary hippocampal high-density cultures were transfected at DIV13-15 with expression constructs coding for either EphB2-C1-EYFP, EYFP-ephrinB1, EYFP-ephrinB2, EGFP-ΔN-TrkB or myrEYFP. Two days later, transfected neurons were imaged by time lapse microscopy at 1 frame/min. Each movie was analyzed for transcytosis and counted as negative (no) if no transcytosis was detectable. Movies were counted as positive (yes) if the beginning of the internalization and the fast retrograde translocation of fluorescent clusters were clearly visible. Graph display n=numbers of time lapse recordings used for the analysis.

transfected neuronal cultures were imaged as described before. Each movie was analyzed for transcytosis events and counted as negative (Figure 6.29, no) if no transcytosis event was detectable. Movies were counted as positive (Figure 6.29, yes) if the beginning of the internalization and the fast retrograde translocation of fluorescent clusters were clearly visible. The classification “maybe” was used for ambiguous transcytosis events, e.g. when transcytosis

had seemingly started but then suddenly stopped during retrograde transport. Surprisingly, in only 1 out of 15 cases (= 6.7 %) ephrinB was internalized in a forward manner by glial cells. In contrast, 11 from 18 cases (= 61.1%) showed a clear reverse transcytosis of fluorescent EphB2 clusters, in 5 cases (= 27.8%) no internalization into adjacent cells was detectable and 2 cases (= 11.1%) could not be clearly identified.

To determine if the EphB2 reverse transcytosis is a specific event driven by the exogenous expression of EphB receptors, cultures were transfected with expression constructs coding for either another transmembrane receptor (= the N-terminal truncated EGFP-TrkB receptor) or a membrane targeted version of EYFP (myrEYFP). 84.6% of neurons overexpressing the transmembrane EGFP- Δ N-TrkB receptor showed no internalization of fluorescent TrkB clusters, 7.7% a clear internalization and 7.7% a possible transcytosis. Internalization of fluorescent clusters was never observed when myrEYFP-expressing neurons encountered glial cells. The percentage of transcytosis events for the differently transfected primary hippocampal neurons are summarized in figure 6.29.

In summary, these data suggest that the neuron-to-cell contact of an EphB2-C1 expressing mature neuron and a neighbouring cell, possibly a glial cells, triggers the reverse transcytosis of full-length EphB2 clusters.

6.4.4. Reverse transcytosis of EphB2-C1 in mature primary hippocampal low-density cultures

To have a closer look at the neuron-to-cell interaction during transcytosis, low-density cultures for live-cell imaging were established. Low-density cultures consist of only $\frac{1}{4}$ to $\frac{1}{5}$ of the cell number of high-density cultures; allowing the imaging of single neurons with their single contacts to adjacent cells.

To determine reverse transcytosis in neurons of low-density cultures, mature primary hippocampal cultures were transfected at DIV15 with EphB2-C1-EYFP expression constructs and two days later imaged, acquiring sequentially pairs of fluorescence and phase contrast images at a frequency of 1 frame per minute. In contrast to high-density cultures, the contact between an EphB2-C1 expressing neuronal process and a glial cell was clearly visible in the time lapse recording (Figure 6.30). The glial process was in contact with a filopodium-like protrusion from the axon of the transfected neuron. From the beginning to the end of the time lapse series a fluorescent EphB2 cluster was visible in the glial process (Figure 6.30, white arrows). This cluster was not static and was moving throughout the entire imaging sequence. In the

6. Results

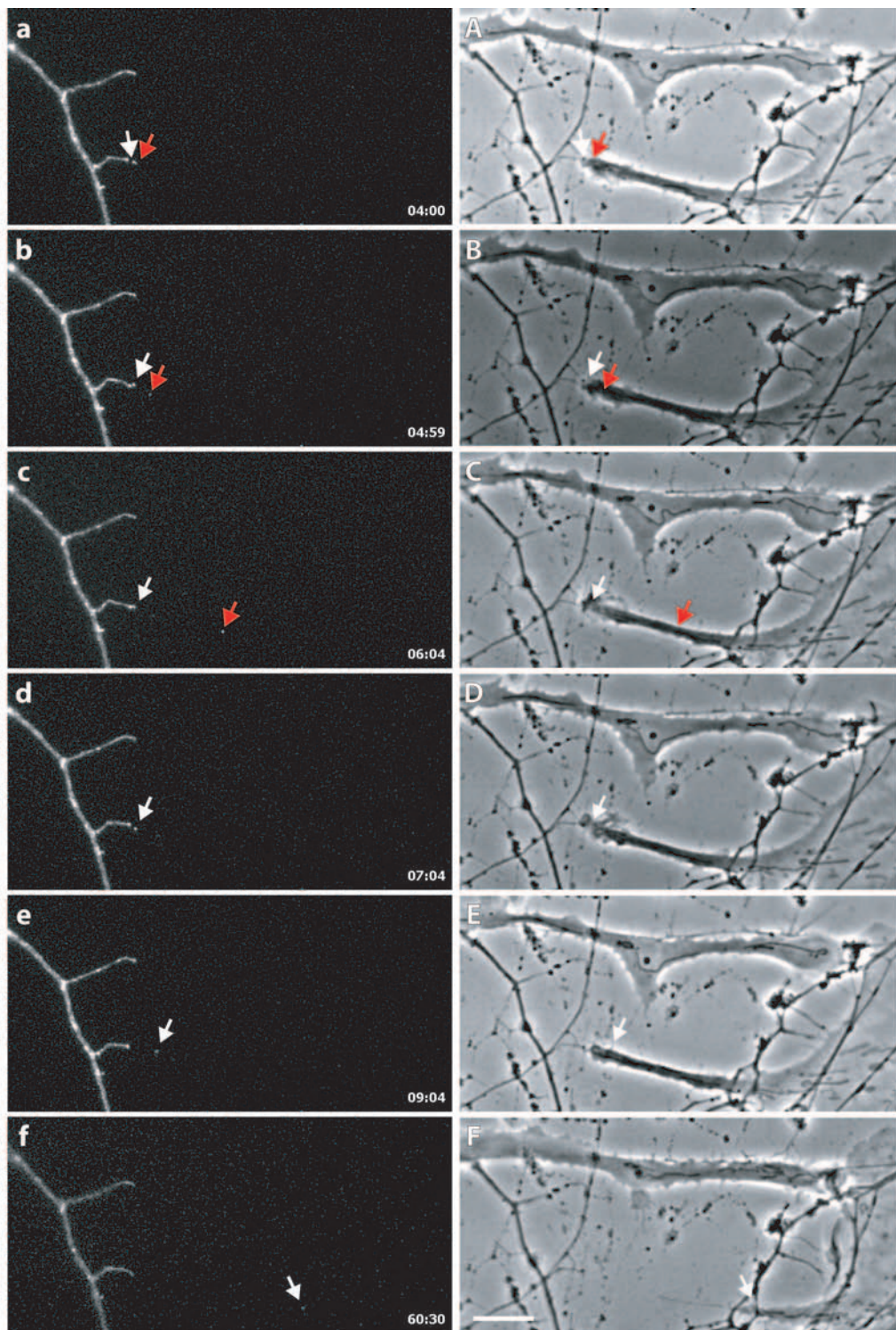


Figure 6.30. **Reverse transcytosis of EphB2-C1-EYFP from an axonal filopodium into a glial process is followed by withdrawal of glia.** (supplementary information on CD-Rom, **movie 11**) A mature primary low-density hippocampal culture was transfected at DIV15 with expression constructs coding for EphB2-C1-EYFP. Two days later, culture was imaged, sequentially acquiring sets of fluorescence and phase contrast images at a frequency of 1 frame per min. Selected pairs of fluorescence and phase contrast images are shown in the **left column (a-f)** and **right column (A-F)**, respectively. Note that after the fast reverse transcytosis of a fluorescent EphB2 cluster (indicated by red arrows **a-c, A-C**) into a possible astrocytic process, the glial cells detaches and withdraws (**E-F**). Time points of imaging are indicated in lower right corners of the fluorescent images. Scale bar = 10 μm .

first 3 minutes it moved towards the neuron (data not shown; supplementary information on CD-Rom, **movie 11**), then for several minutes it remained in close proximity to the filopodial tip (Figure 6.30a-c) and then moved once again towards the glia (similar to a tug-of-war competition between neuronal and glial cell)(Figure 6.30d-f). At the point when the cluster was in the closest proximity to the filopodium a second faint cluster was detectable (Figure 6.20a, red arrow). This EphB2 cluster was reverse transcytosed into the glial process and quickly retrogradely transported during the next two minutes along the process (Figure 6.30b-c, red arrows). After the transcytosis event (Figure 6.30a-c, red arrows) the glial process started to detach (Figure 6.30E) and withdraw (Figure 6.30F), thereby taking away the above mentioned cluster (Figure 6.30e-f, white arrows).

These results demonstrate that the full-length EphB2 receptor expressed in a filopodium of a neuron may be taken up by a glial process through ephrinB reverse endocytosis. Reverse transcytosis of EphB2-C1 into a glial process can sometimes be followed by detachment and withdrawal of the glial cell.

6.5. Supplementary information on CD-Rom

Movie 1-3: Comparison of unstimulated versus ephrinB2-stimulated young neurons expressing one variant of EphB2-C1-EYFP during live-cell imaging. 2-day-old primary hippocampal cultures were transfected with expression constructs encoding either EphB2-C1-EYFP (**Movie 1**), EphB2-C1-KD-EYFP (**Movie 2**) or EphB2- Δ C-EYFP (**Movie 3**). After 1DIV, transfected neurons were imaged by time lapse microscopy taking a fluorescent image at 1 frame per minute. After 10-14 min, preclustered ephrinB2-Fc was added (indicated by a white circle in the upper right corner). Note the fast accumulation of bright and large fluorescent clusters after stimulation with ephrinB2.

Movie 4-6: Comparison of unstimulated versus ephrinB2-stimulated neurons (DIV8+2/3) expressing one variant of EphB2-C1-EYFP during live-cell imaging. Dissociated hippocampal cultures were transfected at DIV8 with expression constructs encoding either EphB2-C1-EYFP (**Movie 4**), EphB2-C1-KD-EYFP (**Movie 5**) or EphB2- Δ C-EYFP (**Movie 6**). After 2-3DIV, transfected neurons were imaged by time lapse microscopy taking a fluorescent image at 1 frame per minute. Preclustered ephrinB2-Fc was added after 20-27 min (indicated by a white circle in the upper right corner). Note the quick accumulation of bright fluorescent clusters and the slowing down of the moving vesicles after stimulation with ephrinB2.

Movie 7: Trafficking of fluorescent vesicles in an EphB2-C1-KD-EYFP expressing neuron. 8-day-old primary hippocampal cultures were transfected with expression constructs encoding EphB2-C1-KD-EYFP. After 2DIV, a transfected neuron was imaged by time lapse microscopy taking a fluorescent image at 1 frame per 3 seconds. The velocity of vesicles was calculated using the Metamorph 6.2 software (Track point tool).

Movie 8: Transcytosis of fluorescently tagged EphB2-C1-EYFP in a primary hippocampal neuronal culture. A 14-day-old primary hippocampal culture was transfected with expression constructs encoding EphB2-C1-EYFP. After 2DIV, the transfected neuron was imaged by time lapse microscopy taking a fluorescent image (left panel) and a bright field image (right panel) at 1 frame per minute. Figure 6.26 shows only plane 27 to 33 of the total 70 planes. Time points of imaging are indicated in the lower right corner.

Movie 9: Transcytosis of fluorescently tagged EphB2-C1-EYFP in a primary hippocampal neuronal culture. A 14-day-old primary hippocampal culture was transfected with expression constructs encoding EphB2-C1-EYFP. Two days later, the transfected neuron was imaged by time lapse microscopy taking a fluorescent image (left panel) and a bright field image (right panel) at 1 frame per minute. Figure 6.27 shows only plane 20 to 26 of the total 60 planes. Time points of imaging are indicated in the lower right corner.

Movie 10: Transcytosis of fluorescently tagged EphB2-C1-EYFP in a primary hippocampal neuronal culture. A 13-day-old primary hippocampal culture was transfected with expression constructs encoding EphB2-C1-EYFP. After 2DIV, the transfected neuron was imaged by time lapse microscopy taking a fluorescent image (left panel) and a bright field image (right panel) at 1 frame per minute. Figure 6.28 shows only plane 6 to 10. Time points of imaging are indicated in the lower right corner.

Movie 11: Transcytosis of fluorescently tagged EphB2-C1-EYFP in a primary hippocampal low-density culture. A 15-day-old primary hippocampal low-density cultures was transfected with expression constructs encoding EphB2-C1-EYFP. After 2DIV, the transfected neuron was imaged by time lapse microscopy taking a fluorescent image (upper panel) and a bright field image (lower panel) at 1 frame per minute (Figure 6.30). Time points of imaging are indicated in the lower right corner of the upper movie.

7. Discussion

My results of the transcytosis experiments will be considered at first. They will be followed by an assessment of the EphB2-ExFP receptors generation and their functionality. Finally, the findings of the *thy1-EphB2-C1-EYFP* transgenic mice of the present study will be discussed.

7.1. Transcytosis of EphB2 in mature neuronal cultures

7.1.1. Overexpression of full-length EphB2-C1-EYFP receptors lead to transcytosis in primary hippocampal cultures

The bi-directional trans-endocytosis of ephrinB-EphB complexes has recently been described as a new mechanism of how the initial high affinity interactions of two transmembrane molecules can be turned into a repulsive response. In cell lines, such as HeLa cells and Swiss 3T3 fibroblasts, this kind of transcytosis leads to cell retraction and detachment (Marston et al., 2003; Zimmer et al., 2003). In addition, stimulation experiments of growth cones of primary immature neuronal cultures with (i) preclustered fusion bodies of B-type ephrin/Eph receptor ectodomains with Fc fragments or (ii) HeLa cells transiently expressing EphB2-C1, could demonstrate that EphB-ephrinB complex internalization is functionally important for axon withdrawal during growth cone collapse (Mann et al., 2003; Zimmer et al., 2003). The data of the study presented here first addressed the phenomenon of transcytosis of EphB or ephrinB clusters in mature hippocampal cultures, deriving with three important observations: (i) mature hippocampal cultures are capable of performing Eph-ephrin transcytosis events, (ii) transient expression of EphB2 (but not of ephrinB) triggers uptake of EphB receptors from neurites and growth cones into neighbouring cells. (iii) These cells are most likely glial cells.

Is transcytosis from the neuron into the interacting cell taking place after cell-to-cell contact in mature hippocampal cultures?

In mature hippocampal cultures, neurons have filopodia-like protrusions on the tip of growth cones and on long neurite shafts. These filopodium-like protrusion form contacts with other

neuronal and non-neuronal cells of the brain. In this study, I could show that these contacts in mature neurons overexpressing fluorescently tagged EphB2 receptors (EphB2-C1) could induce reverse transcytosis of EphB2 clusters from these neurons into neighbouring cells. Since the EYFP-tag is in the cytoplasmic domain of the EphB2-C1 protein, the presence of fluorescent clusters in neighbouring cells strongly indicate that the entire EphB2-C1 molecule was internalized into the encountered cell and not cleaved from the cell surface. So far, it was only demonstrated that immature neurons can uptake ephrinB/EphB from overexpressing HeLa cells after cell-to-cell contact (Zimmer et al., 2003). The endocytosis of the Eph/ephrin complexes in the opposite direction – from the neuron into the neighbouring cell – however, was not observed under these conditions. My finding that transcytosis is taking place in mature hippocampal neurons fits well with the observations done in cell lines and immature neurons at their growth cones: Endocytosis of ephrinB-EphB complexes can occur in a bi-directional fashion in cell lines overexpressing EphB/ephrinB (Zimmer et al., 2003; Parker et al., 2004), whereas prolonged cell-to-cell contact may favour EphB2 forward endocytosis by receptor-expressing cells (Marston et al., 2003; Zimmer et al., 2003). Non-transfected growth cones of a very immature primary mouse forebrain culture showed little EphB2 forward but rather pronounced ephrinB reverse transcytosis into the growth cone after cell-to-cell contact with ephrinB1 and EphB2 transiently expressed in HeLa cells, respectively (Zimmer et al., 2003). Similar results were obtained with young non-transfected primary neurons from embryonic *Xenopus* retina when stimulated with soluble EphB2-Fc or ephrinB1-Fc fusion proteins (Mann et al., 2003). The relative contribution of ephrinB reverse versus EphB forward endocytosis may largely depend on the cellular context, experimental design and expression levels of Eph receptors and their ligands. It has been shown that uni-directional reverse endocytosis alone efficiently switches adhesion to detachment by removal of the ephrin-Eph complexes from the surface (Zimmer et al., 2003).

The experiments presented in this thesis cannot exclude that EphB forward transcytosis into the neuron takes place after an EphB2-C1 expressing neuron encountered another cell of the mature hippocampal culture. In contrast to the growth cones of immature cultures, an internalization from the glial cell into the neuron could not be detected with this experimental design. A future challenge will be to determine bi-directional transcytosis in hippocampal cultures. A potential experiment could be live cell imaging of contacts between e.g. EphB2-C1-EYFP expressing neurons and ECFP-ephrinB expressing glial cells revealing the possible occurrence of EphB2-mediated forward endocytosis into neurons of primary hippocampal cultures.

Findings by Spacek and Harris (2004) in the CA1 region of the mature rat hippocampus indicate that there is more transcytosis taking place from neuronal protrusions into astrocytic processes as *vice versa*. My results also suggest a preferential transcytosis from neuronal protrusions into most likely glial cells. However, in the mature hippocampus Spacek and Harris (2004) could also observe neuron-to-neuron internalization: double-membrane structures (spinules) emerged from spine heads (62%) were invaginated into axons (~90%) rather than astrocytic processes (~8%). So far, I could not reliably detect such kind of neuron-to-neuron transcytosis in EphB2-C1 overexpressing hippocampal cultures because the neuronal identity of the uptaking cell could not be confirmed.

Is there ephrinB triggered reverse transcytosis from the neuron into the neighbouring cell?

My experiments showed that transient expression of EphB2 but not ephrinB1/B2 in neurons triggers transcytosis events into the interacting neighbouring cell after cell-to-cell contact. In primary hippocampal neurons transiently express EphB2 receptors, clusters of EphB2 were preferentially transcytosed into neighbouring cells. Surprisingly, neurons transfected with plasmids coding for the ligand – ephrinB1 or ephrinB2 – did not clearly induce transcytosis. A possible explanation of this observation could be that the ligands for the EphB2 receptor – ephrinBs and ephrinA5 – are endogenously expressed in the uptaking cell, whereas all Eph receptors of ephrinB1/B2 are absent or only weakly expressed. These results implicate that mainly ephrin-mediated reverse transcytosis is taking place between neurons and neighbouring cells. The identity of the uptaking cell has not been verified yet, but the shape and the behaviour of these cells during live cell imaging strongly suggests that they are glial cells as will be discussed later.

Which cell types express Eph receptors and their ligands in the mature hippocampus?

Neuron-to-cell interaction mediated by EphB2s and their ligands leads to transcytosis into the neighbouring cell, potentially a glial cell. In neurons, EphB2 mRNA has been detected at high levels in all regions of the hippocampus, while ephrinB2/B3 mRNAs were absent or barely detectable in the CA3 region of the hippocampus. EphrinB1 mRNA was also barely detectable in the CA1 region, in contrast to the dentate gyrus. EphrinB2 mRNA was mostly confined to CA1 and weakly present in the dentate gyrus (Grunwald et al., 2001). The overall expression of EphB2 in the hippocampus could indicate that transcytosis might potentially be a general phenomenon within the hippocampal formation.

Little is known about the expression patterns of ephrin ligands and Eph receptors in glial

cells. A previous study reported that ephrinA3 displayed the highest hippocampal expression among ephrinAs and is expressed in astrocytic processes of the adult hippocampus (Murai et al., 2003). Another study reported that EphA4 expression in astrocytes was upregulated after spinal cord injury, which inhibits neurite outgrowth in wild type mice (Goldshmit et al., 2004). In addition, data by Conover et al. (2000) identified the presence of ligands of the EphB receptors, such as ephrinB2 and ephrinB3, in astrocytes that ensheath chains of migrating neuroblasts in the adult subventricular zone. Also it has been shown that the ephrinA5 ligand is expressed by astrocytes (Winslow et al., 1995). I tried several immunostainings with antibodies against different B- and A-types of ephrins and Eph receptors on cultured glial cells seeded on coverslips. So far, the majority of these immunostainings looked unspecific, as revealed by control experiments using the secondary antibodies alone (data not shown). However, two immunostainings looked specific and indicate the expression of ephrinB2 and EphA4 in glial cells. Nevertheless, further experiments have to be done to identify the expression patterns of endogenous Eph receptors and their ligands in glial cell in the hippocampal cultures used in this study. To overcome the problems encountered in the immunostainings with primary antibodies, I intend to carry out further immunostainings with fusion proteins of Fc fragments with ectodomains of Eph receptors (Eph-Fc) or ephrin ligands (ephrin-Fc).

What is the identity of the cells that endocytose EphB2 receptors?

As described before, I observed transcytosis between EphB2-C1 expressing neurons and interacting cells. Based on shape, motility and structure, these interacting cells were identified as glial cells, most likely astrocytes.

Nearly one-half of the cells in the human brain are astrocytes (Ullian et al., 2004). In contrast to oligodendrocytes, astrocytes have been described to contribute in regulating spine morphology (Murai et al., 2003), modulating levels of synaptic activity as well as influencing the number of functional synapses (Newman, 2003; Yang et al., 2003) and synaptogenesis in hippocampal neurons (Hama et al., 2004; Ullian et al., 2004). In addition, recent data showed that in the CA1 region of the mature rat hippocampus astrocytes can perform transcytosis or macropinocytosis through double-membrane invaginations emerging from dendrites or axons (so-called spinules). Whereas, thin spines showed more transcytosis in form of spinules into astrocytic processes than mushroom spines (Spacek and Harris, 2004). In addition, it has been shown that fragments of EGFP-labeled plasma membrane from the surface of ephrinB-bearing human umbilical-vein endothelial cells (HUVECs) were removed by adjacent EphB-expressing cells (Marston et al., 2003), suggesting the formation of multivesicular bodies (=

double-membrane structures).

Because of the close association of astrocytes with neurons, the high number of astrocytes in the CNS (Haydon, 2001) and the findings of spinules in astrocytes, it seems to be very likely that reverse transcytosis of EphB receptors can occur between neurons and astrocytes. To confirm the hypothesis that only a specific subtype of glia is involved in neuron-glia transcytosis in the mature hippocampal cultures, immunostainings for a specific marker of astrocytes (e.g. the calcium-binding protein, S-100 β) or oligodendrocytes (e.g. enzyme CNPase) in low density cultures after imaging will be useful (Ghosh and Koenig, 1977; Matthias et al., 2003).

Is the EphB transcytosis event coupled to a change in cell behaviour?

It has previously been shown that contact-triggered EphB activation in HUVECs can stimulate the formation of membrane protrusions, such as lamellipodia and filopodia, exclusively in EphB4-expressing and not in ephrinB-expressing cells (Marston et al., 2003). These events seem to initiate the cells to retract from one another, concomitantly with the endocytosis of the activated EphB receptors and their bound, full-length ephrinB ligands (Marston et al., 2003). Interestingly, the bi-directional transcytosis of ephrinB-EphB complexes can trigger different cellular responses: ephrinB1-overexpressing HeLa cells endocytose efficiently but do not retract, whereas forward endocytosis into cells transiently expressing EphB2 receptors is followed by a lamellipodial retraction response after cell-to-cell contact (Zimmer et al., 2003). Both the Eph-receptor internalization and the subsequent cell retraction events are dependent on actin polymerization in cell lines, which in turn is dependent on Rac signalling within the receptor-expressing cells (Marston et al., 2003). In addition, transcytosis is proposed to destabilize cell contacts and might therefore at least partially contribute to Eph-ephrin regulated cell repulsion (Marston et al., 2003). However, growth cone detachment of immature primary forebrain neurons was impaired after contact with HeLa cells transiently expressing C-terminal truncated EphB2, suggesting that uni-directional ephrinB reverse endocytosis is less efficient (Zimmer et al., 2003).

The data of the present study show that in mature neuronal cultures reverse transcytosis of EphB2-C1 clusters into the cell interacting with the neuron was mainly followed by the detachment and retraction of the filopodia-like protrusion of mature growth cones and of neurites. As mentioned before, with my experimental setup it was not possible to detect bi-directional transcytosis, only the uni-directional transcytosis from the neuron into the neighbouring interacting cell. The above described findings from cell lines suggest that after an EphB2-C1 expressing neuron encounters another ligand-expressing cell, activated ephrinB-EphB clus-

ters are bi-directional – forward and reverse – endocytosed into the neuron and also from the neuron into the other cell (possibly a glial cell), respectively. This would allow the adhesive ligand-receptor interaction to destabilize and enable the cells to detach and the neuronal filopodium-like protrusion to retract, probably involving an actin redistribution mediated by phosphorylated EphB2 proteins.

Dendritic filopodia are discussed to serve as precursors to spines (Dailey and Smith, 1996; Ziv and Smith, 1996). In contrast to spines, filopodia are long, thin structures and display a very dynamic nature. These features indicate an exploratory function of filopodia and only those that successfully capture an axonal terminal became stabilized by transforming into spines (Yuste and Bonhoeffer, 2004). Beside the typical morphological features and the different dynamic nature of filopodia and spines, there is no specific marker that can distinguish filopodia from spines (Yuste and Bonhoeffer, 2004). In addition, EphB receptors can be found in both filopodia and spines. These similarities raise the question if these different dendritic protrusions also display similar cell behaviour, such as repulsion potentially leading to loss of synapses. As the main cytoskeletal element, filamentous actin is highly enriched in spines and filopodia and is necessary for their shape and the motility (Dailey and Smith, 1996; Ethell and Yamaguchi, 1999; Scott and Luo, 2001; Bonhoeffer and Yuste, 2002). The small GTPase Rac1 is important for the formation and maintenance of dendritic spines in cultured pyramidal neurons (Nakayama et al., 2000). It has also been shown that hippocampal neurons in triple *EphB1*, *EphB2*, *EphB3*-deficient mice fail to form spines *in vitro* and develop abnormal immature spines *in vivo*. The actin filament accumulation in spines is disrupted in the triple EphB-deficient hippocampal neurons indicating that the EphBs are responsible for targeting of actin to spines (Henkemeyer et al., 2003). In addition, synaptic EphB receptors have been linked to protrusive responses to ephrinB stimulation. Here activated EphB2 receptors mediate the formation of new actin-rich dendritic spines through Cdc42 and Rac1 activated by their respective exchange factors intersectin and kalirin (Irie and Yamaguchi, 2002; Penzes et al., 2003).

What is the functional relevance of EphB-ephrin transcytosis in cells of the brain?

In contrast to cell lines, in young cortical neurons reverse endocytosis of EphB2 leads to fast detachment and growth cones collapse after contact with HeLa cell transiently expressing EphB2-C1 (Zimmer et al., 2003). Furthermore, growth cones of cultured embryonic *Xenopus* retinal neurons stimulated with unclustered EphB2 ectodomain fusion bodies triggered fast (5-10 min) transient collapse responses concomitant with endocytosed EphB2-Fc molecules.

This suggests that endocytosis provides a fast mechanism for switching off signalling in reverse direction (Mann et al., 2003). In contrast, stimulation with clustered ephrinB1-Fc causes only slow (30-60 min) growth cone collapses and no endocytosis of ephrinB1-Fc molecules into growth cones, suggesting that forward signalling does not involve endocytosis of clustered ephrinB1-Fc. Thus reverse EphB-ephrinB complex internalization is functionally important for axon withdrawal during growth cone collapse (Mann et al., 2003; Zimmer et al., 2003). Anyway, it remains to be solved whether the slow withdrawal of glial cells after contact with the dendritic protrusion of the EphB2-C1 expressing neuron in low density cultures as observed in my studies is a specific effect downstream of EphB-ephrinB complex internalization, or not. Interestingly, in high density cultures some glial cells also showed repulsive responses following reverse transcytosis of fluorescent EphB2 clusters (Movies 8-9, supplementary information on CD-Rom). However, due to the high numbers of cell contacts the overall cell movement was diminished in these cultures and probably only glial protrusion withdrew and not the whole glial cell.

Is intracellular signalling of EphB receptors and their ligands important for transcytosis?

It has been shown that the cytoplasmic tails of ephrinB and EphB2 are required for bi-directional endocytosis in cell lines. If one interaction partner is truncated bi-directional transcytosis is always shifted toward uni-directional endocytosis into the cells overexpressing the full-length protein (Zimmer et al., 2003). Additionally, axon detachment of immature cortical neurons from C-terminally truncated EphB2-C1 expressing HeLa cells is delayed compared to full-length EphB2-C1 expressing HeLa cells. This implies that uni-directional ephrinB reverse endocytosis is less efficient and additional EphB2 forward endocytosis is required for proper axon detachment (Zimmer et al., 2003).

As expected from these published data, weakening the EphB2 receptor's ability to signal by C-terminal truncation or blocking the kinase activity in neurons should not impair the ephrinB reverse transcytosis of the neighbouring glial cells. In contrast, it should have a blocking effect on the EphB2-mediated forward endocytosis into neurons. On the other hand, the expression of C-terminal truncated ephrinB in glial cells should block their transcytosis ability and the EphB-mediated forward transcytosis of neurons should not be effected.

Live cell imaging of transfected C-terminally truncated EphB2-C1-EYFP neurons or ephrinB-ECFP glias may shed more light on the importance of the cytoplasmic tails of B-type ephrins and Ephs in neuron-glia transcytosis.

Can the other subfamily of Eph receptors (EphAs) trigger transcytosis?

This study showed that EphB receptors transiently expressed on neuronal protrusions were internalized into the neighbouring cells after cell-to-cell contact. Like the EphA *in situ* hybridization data indicates, EphA4 is expressed at remarkably high levels in all region of the adult mouse hippocampus (Figure 6.24C and Grunwald et al. (2001)), especially at postsynaptic sites in the CA1 area (Murai et al., 2003). As mentioned before, ephrinA3 – an EphA4 ligand – is expressed on astrocytic processes of the adult hippocampus (Murai et al., 2003). Therefore, it would be interesting to determine, whether A-type Eph receptor can be trans-cytosed into neighbouring cells of the primary hippocampal cultures. To address this, (i) stimulation of cultured astrocytes with preclustered EphA-Fc (or ephrinA-Fc), followed by a surface versus total immunostaining of EphA-Fc (or ephrinA-Fc) and (ii) live time imaging with fluorescently tagged EphAs (or ephrinAs) expressed in primary hippocampal cultures could give further insights in neuron-to-glia transcytosis.

7.1.2. What could be the *in vivo* relevance of Eph receptor transcytosis by glial cells?

Surface availability of receptors and termination of signal transduction

Endocytosis of receptor-ligand complexes is a common feature in signal transduction of receptor tyrosine kinases. It is thought to be involved in regulating the surface availability of receptors as well as to be one of the mechanisms to attenuate signal transduction. Internalization of transmembrane proteins into intracellular vesicles often leads to lysosomal degradation or their recycling to the cell membranes (Presley et al., 1997; Walker-Daniels et al., 2002; Conner and Schmid, 2003; Marmor and Yarden, 2004).

However, a growing body of evidence also suggests that endocytosed membrane may be important for intracellular signalling. Receptors may continue to signal after endocytosis as it was shown for internalized EGF and neurotrophin (TrkA) receptors (Kurten, 2003; Weible and Hendry, 2003). EphB2 may therefore also continue signalling: Consistent with this idea is that (i) internalized EphB2 clusters are tyrosine phosphorylated and (ii) EphB receptor forward signalling is independent of rapid protein synthesis and degradation, indicating receptor recycling (Mann et al., 2003; Marston et al., 2003). Comparable to the Trk receptors, endocytic vesicles of ephrin-EphB can possibly be seen as parcels of activated plasmalemma that can propagate transducing signalling locally and to distant parts of the neuron by retrograde transport (Poo, 2001). Remarkably, in the hippocampal cultures used in my experiments (an-

terograde and retrograde) long-range trafficking EphB2-C1 vesicles was also be seen in neurons expressing EphB2-C1.

Pruning of axons in the developing brain

There is accumulating evidence that the interaction between neurons and glial cells are is important for axonal pruning. Transcytosis, which most likely involves the neuron-to-glial cell interaction might also play a central role in the axon pruning process.

Axon pruning is an important process during the development of the nervous system and is involved in establishment and maintenance of functional neuronal circuits. Studies from *Drosophila* mushroom bodies (MBs) and the vertebrate neuromuscular junctions (NMJs) provide fresh insights into the mechanisms of synapse elimination (Awasaki and Ito, 2004; Bishop et al., 2004; Watts et al., 2004). For example, data by Awasaki and Ito (2004) demonstrate that transient disruption of glial function arrests axon pruning, suggesting an instructive role for glia in developmental axon pruning.

There are three important findings pointing towards a role of transcytosis involved during axon pruning: First, during synapse elimination in the developing mammalian NMJ most of the withdrawing axons shed fragments rich in normal synaptic organelles, so-called axosomes, into surrounding glial cells, presumably terminal Schwann cells. Axosomes may be assimilated in the cytoplasm of Schwann cell (Bishop et al., 2004). However, it is not known, if Schwann cells actively dismantle axons or whether they play a passive scavenger role in this process. Second, in the *Drosophila* larvae MBs, γ neurons initially extend axons branches into both the dorsal and medial MB lobes, which are surrounded by several glial cells (Lee et al., 1999; Watts et al., 2004). During metamorphosis, axon branches degenerate prior to the formation of adult connections. This process is coincident with an increase of the number of glial cells surrounding the dorsal and medial lobe. Changes in glia cell number is coincident with blebbing of axons and fragmentation of dendrites. Finally, Watts et al. (2004) could show that the material which is engulfed by glial cells, originates from the degenerating axons undergoing developmental axon pruning rather than debris from apoptotic cells. Taken together, these findings provide the framework for further investigations into the mechanisms underlying axon-to-glia interactions during developmental axon pruning.

Shaping of synapses in the mature brain

Astrocytes have long been known to phagocytose degenerating axonal boutons (Ronnevi, 1978; Seil, 1997) or whole apoptotic neurons (Freeman et al., 2003). Recently, ultra structural

examination of synapses in the mature rat hippocampus revealed that axons and dendrites extend small protrusions into neighbouring neurons and glial cell. Some of these so-called spinules appear to finally end as double-membrane inclusions in the recipient cell, very often astrocytes, due to trans-endocytose or macropinocytose, which does not resemble traditional astrocytic phagocytosis of degenerating or apoptotic neurons, because of the absence of very dark and condensed cytoplasm (Spacek and Harris, 2004). Thin spines show more transcytosis into astrocytic processes than mushroom spines, suggesting a shaping of interactions between newly formed synapses and their perisynaptic glia during synaptic plasticity in the immature and the mature brain (Spacek and Harris, 2004).

The present study shows that *in vitro* after cell-to-cell contact EphB2 receptors on neuronal protrusions were transcytosed from the EphB2-C1 overexpressing neuron into the neighbouring cell, most likely a glial cell. Considering that glial cells completely surround synapses, neuron-glia transcytosis could also be potentially involved in the synapse elimination after LTD in the mature brain. It is not known so far, if ephrinB-EphB mediated transcytosis between glial cells and neurons actually takes place at freshly formed or mature tripartite synapses and what is its role in the regulation of receptor trafficking and synaptic plasticity. Transcytosis should therefore be analyzed in more detail at synapses.

7.2. Generation and analysis of the different fluorescently tagged EphB2 receptors

To better understand the role of EphB2 receptors and to study their trafficking dynamics, insertion and clustering in neurons during cellular interaction, such as synapse formation and synaptic plasticity, the EphB2 receptor was fluorescently tagged at one of the three different positions: (i) at the N-terminus (EphB2-N), (ii) adjacent to the juxtamembrane region (EphB2-C1) or (iii) between the kinase and the SAM domain (EphB2-C2). Transfected Hek293 cells expressing one of the three different EphB2 fusion proteins showed intense fluorescence at the membrane. Compared to ExFP-expressing cells the fluorescently tagged EphB2 receptors were less intensive in fluorescence, but still bright enough for live cell imaging. However, the fluorescence of the EphB2 receptors was comparable to other known N-terminal fusion proteins of ExFP and transmembrane receptors, such as EGFP-ephrinB1 or EGFP- Δ N-TrkB. Therefore, the insertion of the ExFP between two domains of the EphB2 receptor (EphB2-C1, EphB2-C2) behave as commonly used N-terminal and C-terminal ExFP fusion proteins. In addition, biochemical studies revealed that all three versions of these differently tagged EphB2-

ExFP proteins are tyrosine phosphorylated when expressed in Hek293 cells. Compared to the wild type and the two other fluorescently tagged EphB2 receptors, the EphB2-C2 fusion protein showed less tyrosine phosphorylation, indicating that the ExFP insertion between the kinase and the SAM domain seems to affect proper phosphorylation of this EphB2 receptor. One explanation could be that the insertion of the ExFP "domain" changes the protein structure of EphB2, possibly interfering with the usually close proximity of the juxtaposed kinase domains after ligand binding, thereby affecting the trans-phosphorylation of tyrosine residues in the activation segment of the tyrosine kinase domain (Hubbard, 2004). Another explanation could be that the insertion of the fluorescent protein changes the conformation of the receptor in a way that the inactive form is preferred. All three types of fluorescently tagged EphB2 receptors had a similar behaviour in their interaction with known partners, such as NR1 and GRIP2, in cotransfected HEK293 cells.

Surprisingly, the cluster behaviour of the three different EphB2-ExFP fusion proteins was different upon stimulation with preclustered ephrinB ligands in transfected hippocampal neurons. Only the EphB2-C1 fusion protein displayed proper cluster formation in immature neurons upon stimulation with ephrinB while only few clusters if any clusters were detectable in EphB2-N or EphB2-C2 expressing neurons. This indicates that the insertion of the fluorescent protein at the N-terminus or between the kinase and the SAM domain impaired cluster formation. We assumed that the N-terminal fusion of ExFP followed by a linker region to EphB2 would not interfere with the ligand binding because the N-terminal fusion of EGFP with ephrinB1 does not interfere with cluster formation upon EphB2 stimulation (Brückner et al., 1999). However, the N-terminal ExFP fusion to EphB2 resulted in a clearly functionally impaired protein, similar to the EphB2-C2 proteins. The ExFP insertion between these two functional domains – the kinase and the SAM domain – may inhibit cluster formation, most likely because of the interference with the SAM domain which is known to participate in protein-protein interactions.

In contrast to mature neurons, young immature hippocampal EphB2-C1 expressing neurons revealed a more even distribution of EphB2-C1 and only few fluorescent clusters were visible without stimulation. Application of preclustered ephrinB-Fc specifically induced a dramatic increase in cluster size and number in immature and mature cultures. Remarkably, very old neurons (3-4 weeks old) showed a high number of fixed clusters even without exogenous stimulation. In contrast to immature neurons, mature neurons display a higher degree of arborization and a high number of contacts with other neurons, suggesting that these contacts provided ephrinB ligands, which induced EphB2-C1 cluster formation in transfected neurons.

Consistent with this idea, endogenous EphB2 receptors and their ligands have been found to be expressed at the synapse (Torres et al., 1998; Buchert et al., 1999; Dalva et al., 2000; Grunwald et al., 2004) and in 23-day old hippocampal cultures many EphB2-C1 clusters were localized at spine heads in transfected neurons. In addition, EphB2-C1 receptors were also located on the surface of filopodia and other dendritic protrusions in younger neurons (1-2 weeks old).

I also considered the possibility that neuronal electric activity drives EphB clusters or their vesicles to the plasma membrane or even more specific in filopodia, the discussed precursors of spines (Yuste and Bonhoeffer, 2004). To assess this, young and old hippocampal cultures transiently expressing EphB2-C1-EYFP were briefly depolarized by applying a solution containing KCl [50 mM] or glutamate [50 μ M]. These depolarizing stimuli never induced an increase in EphB2-C1-EYFP fluorescence in dendritic protrusions, dendrites or axons (data not shown). In addition, the fluorescent vesicles never showed an obvious effect in their trafficking behaviour during and after stimulation, suggesting that electric activity does not have an effect in the vesicle trafficking and localization of EphB2-C1-EYFP receptors (data not shown). Immunostainings against a dendritic marker revealed that the fluorescent EphB2-C1 receptors were localized in the axon, in the dendritic tree, as well as in the cell body of the transfected hippocampal neuron. The EphB2-C1 proteins were therefore not subcellularly sorted to the dendrite or the axon, when expressed in neurons. Interestingly, beside the postsynaptic localization of EphB there is evidence that these receptors are also present at the presynaptic terminal of neurons (Buchert et al., 1999; Grunwald et al., 2004).

My results show, that besides the membrane inserted EphB2-C1 receptors a big intracellular pool of these fluorescent receptors are trafficking in vesicles along the dendrites and axons, especially in thick dendritic branches. The number of trafficking vesicles increases with the age of the cultures, suggesting that there is possible correlation between receptor trafficking and the organization of postsynaptic membrane. Most likely, these trafficking vesicles carry either endocytosed receptors from the cell surface to degradative compartments or newly synthesized EphB2-C1 proteins on their way to the plasma membrane. Indeed, transfected hippocampal neurons revealed anterograde and retrograde trafficking vesicles during live cell imaging. Application of preclustered ligands induced a fast recruitment of EphB2-C1 receptors to the cell surface within minutes, thereby fluorescently highlighting the neuronal cell membrane. Simultaneously fast cluster formation became visible. Independently from the age of the neurons, the number of moving vesicles decreased, sometimes even stopped after adding the preclustered ligand.

7.3. Transgenic mice expressing EphB2-C1 variants driven by the Thy-1.2 expression cassette

The overexpression of full-length, kinase-deficient or C-terminal truncated EphB2-C1 receptors never showed any obvious effect on cell morphology, vesicle trafficking or protein distribution during live cell imaging or in fixed cultures. A lack of defects may be due to different cell culture densities. In comparison to other studies, our cultures were almost 6× and even up to 10× less dense for the fixed-only cultures and for the time lapse imaging, respectively. Presumably, the overexpression of kinase-active, kinase-deficient or C-terminal truncated EphB2-C1 causes only little differences in the number of fluorescent clusters, therefore it would be necessary to quantify cluster formation, this still has to be done. For this quantification of membrane inserted (before permeabilization) versus total (after permeabilization) EphB2-C1 clusters should be counted, otherwise it would not be possible to distinguish trafficking vesicles from fixed clusters.

7.3. Transgenic mice expressing one variant of EphB2-C1 driven by the Thy-1.2 expression cassette

7.3.1. Patterns of transgene expression and their fluorescent intensities

Transgenic mice expressing either the full-length, the kinase-deficient or the C-terminal truncated EphB2-C1-EYFP under the control of the neuron-specific elements from the *thy-1.2* gene were generated. The aim was to observe the dynamics and localization of fluorescently tagged EphB2 receptors in the hippocampus *in vivo*. We generated 41 independent transgenic lines: 22 for the full-length (line A-N, P-W), 8 for the kinase-dead (line Ka-Kh) and 11 for the truncated version (line Da-Dk) of the EphB2-C1 receptor. Among the 41 founders 33 gave offspring: 21 for the full-length (wt), 6 for the kinase-deficient (KD) and 6 for the truncated (Δ C) version of the EphB2 receptor. Analysis of the offspring revealed that 23 transgenic lines showed fluorescence in the brain, 5 lines yielded very low expression levels and were therefore excluded from the analysis. The remaining 18 lines were analyzed in more details. Surprisingly, apart from one transgenic line (line R) all analyzed lines showed a homogeneous labeling mainly in the DG and the CA1 region of the hippocampus. The overall fluorescence of these transgenic lines made imaging of single neurons, or even spines almost impossible. As mentioned previously, only one line – line R – yielded a sparse expression pattern of the fluorescently tagged full-length EphB2-C1 receptor, but unfortunately the fluorescent signal was too weak for imaging by confocal microscopy in hippocampal slices.

In neurons transiently expressing the EphB2-C1 proteins (or other ExFP-tagged transmem-

brane proteins) the fluorescent intensity was less as compared with neurons transiently expressing the “pure” cytoplasmic ExFP proteins, indicating that the fusion of the ExFP protein with these kind of proteins impaired fluorescence intensity of the ExFP. In neurons transiently expressing these ExFP-tagged EphB2 proteins the fluorescent signal was still bright enough for live cell imaging. It is known that dependent from the introduced copy number of the expression construct and the strength of the promoter the transient expression can lead to the production of recombinated protein of sometimes more than 50% of the total produced proteins in the eukaryotic cell. In cultured neurons the transient expression of the different EphB2-C1-EYFP versions under the control of the Thy-1.2 expression cassette displayed comparable fluorescence intensities as under the control of the strong cytomegalovirus (CMV) promoter (data not shown). Therefore, the Thy-1.2 expression cassette should drive comparable expression levels of the different EphB2-C1-EYFP versions. Taken together, this could possibly indicate that the copy number of the transgene in the different variants of the *thy1-EphB2-C1-ExFP* transgenic mice caused either homogeneous distribution of the transgene as observed in 17 lines or the isolated expression pattern as observed in a single line. Whereas, a very low copy number of the transgene led to the sparse transgenic expression and a stable integration of more copies caused a homogeneous expression of the transgene in some regions. In addition, a very low copy number of the transgene could also explain the weak fluorescence intensity of the transgenic protein in the mouse line R.

In addition, it was known from transgenic mice expressing multiple spectral variants of EGFP driven by the Thy-1.2 expression cassette that: first, the expression pattern of the *thy1-ExFP* lines differs greatly among lines. This line-to-line variations in *thy1-ExFP* transgene expression indicates that the variation reflects differences in chromosomal integration site and/or copy number. And second, that at least 10-15 founders from the same construct must be generated to obtain one line with a sparse expression pattern (Table 1 of Feng et al., 2000 and Caroni, 1997; personal communication with P. Caroni). In our approach, however, from 33 fertile founders we only had one line with a sparse expression pattern in the hippocampus. This also indicates that possibly too many copies of the transgene were integrated into the genome, causing a homogeneous expression pattern in the brain.

Expression of ExFP proteins in transgenic Thy-1.2 lines clearly labels neurons and these transgenic mice became a general useful tool for imaging neurons *in vitro* and *in vivo* (Feng et al., 2000; Trachtenberg et al., 2002; Bishop et al., 2004; Nägerl et al., 2004). However, the intensity of the different EphB2-C1-EYFP proteins of our *thy1* transgenic mice lines was overall very weak. Even hippocampal cultures of embryos of heterozygote and homozygote mouse

lines with the brightest fluorescent intensity revealed signals that were too weak for live cell imaging. We therefore decided not to follow this direction any further.

7.3.2. Overexpression of full-length or C-terminal truncated EphB2-C1-EYFP receptor does not affect synaptic plasticity

The LTP analysis of hippocampal slices of transgenic mice expressing full-length (line A) or the C-terminal truncated EphB2-C1-EYFP (line Df) at the CA3-CA1 synapse showed no effect on LTP. Assuming that the transgenic proteins were expressed at the right place – the postsynaptic site of the CA1 neuron – then the additional expression of truncated or full-length EphB2-C1 receptors did not influence the synaptic transmission of these transgenic mice. This might suggest that there is no cis interaction of ephrinBs and EphBs at the postsynaptic site. Another possibility could be that in our approach the mouse strain background was not the most suitable. Mouse strain backgrounds can affect LTP analysis, e.g. no stable baseline, LTP can not be induced or is not lasting long (personal communication with M. Korte). To reduce genetic heterogeneity usually F4 offspring of the backcrossed knockout or transgenic mice were used for LTP analysis. Our transgenic mice were generated in a FVB strain and progeny of the first backcross (F1) with C57/Black6 females was used for LTP analysis. LTPs could be induced in these mice, but they showed a relatively low level of LTP in comparison to other mouse strains. Possibly, a weak effect on LTP by the transgene could not be detectable with this approach. Another more simpler explanation could be that the transgenic proteins were not at the correct place in the synapse, because the *in situ* hybridization data and the immunostainings against ExFP of fixed and permeabilized slices only indicated the general localization of the mRNAs and the EphB2-C1 protein in the neuron, respectively. Whether the different EphB2-C1 transgenic proteins are inserted into the neuronal cell membrane and can be found at the synapse as well as in transient expressing primary hippocampal cultures was not analyzed. *In situ* hybridization analysis of hippocampal sections of these heterozygous transgenic mice showed a very strong signal in the CA1 region of the hippocampus in case of the C-terminal truncated EphB2-C1 receptor (line Df), indicating a very strong overexpression of the transgenic protein in these neurons. However, we can not rule out the possibility that too little truncated EphB2-C1 protein in these heterozygous transgenic mice was expressed in the synapse or at the cell membrane to block endogenous EphB2 receptors.

Another explanation based on the freshest finding in the Eph/ephrin field by our group could be a recently demonstrated postsynaptic role for ephrinBs in hippocampal plasticity, whereas

7. Discussion

ephrinB2 and ephrinB3 are required for CA3-CA1 hippocampal LTP (Grunwald et al., 2004). With respect to the CA3-CA1 synapse, ephrinB2 and ephrinB3 are expressed mainly in postsynaptic CA1 neurons, while the relevant Eph receptors – EphB2 and EphA4 – are expressed both pre- and postsynaptically in the adult hippocampus (Grunwald et al., 2001, 2004). Importantly, both EphB2 and EphA4 receptors show signalling-independent requirement in long-term plasticity (Grunwald et al., 2001; Henderson et al., 2001; Grunwald et al., 2004), suggesting reverse signalling by postsynaptic ephrinBs. Assuming that the ephrinBs are the key player in synaptic plasticity of mature synapses and they do not interact with EphB receptors in cis, then the overexpression of EphB2 at the postsynaptic site of the CA1 neuron would have no effect in synaptic plasticity.

Bibliography

- Aoki, M., Yamashita, T., and Tohyama, M. (2004). EphA receptors direct the differentiation of mammalian neural precursor cells through a mitogen-activated protein kinase-dependent pathway. *J Biol Chem*, 279(31):32643–50.
- Awasaki, T. and Ito, K. (2004). Engulfing action of glial cells is required for programmed axon pruning during *Drosophila* metamorphosis. *Curr Biol*, 14(8):668–77.
- Banker, G. and Goslin, K., editors (1998). *Culturing Nerve Cells*. A Bradford Book, The MIT Press, Cambridge, Massachusetts London, England, 2nd edition.
- Barker, P. A., Hussain, N. K., and McPherson, P. S. (2002). Retrograde signaling by the neurotrophins follows a well-worn *trk*. *Trends Neurosci*, 25(8):379–81.
- Bartley, T., Hunt, R., Welcher, A., Boyle, W., Parker, V., Lindberg, R., Lu, H., Colombero, A., Elliott, R., and Guthrie, B. (1994). B61 is a ligand for the ECK receptor protein-tyrosine kinase. *Nature*, 368(6471):558–60.
- Battaglia, A. A., Sehayek, K., Grist, J., McMahon, S. B., and Gavazzi, I. (2003). EphB receptors and ephrin-B ligands regulate spinal sensory connectivity and modulate pain processing. *Nat Neurosci*, 6(4):339–40.
- Beattie, E. C., Stellwagen, D., Morishita, W., Bresnahan, J. C., Ha, B. K., Zastrow, M. V., Beattie, M. S., and Malenka, R. C. (2002). Control of synaptic strength by glial TNF α . *Science*, 295(5563):2282–5.
- Bergles, D., Diamond, J., and Jahr, C. (1999). Clearance of glutamate inside the synapse and beyond. *Curr Opin Neurobiol*, 9(3):293–8.
- Bettler, B. and Mulle, C. (1995). Review: neurotransmitter receptors. II. AMPA and kainate receptors. *Neuropharmacology*, 34(2):123–39.

- Bi, G. and Poo, M. (1998). Synaptic modifications in cultured hippocampal neurons: dependence on spike timing, synaptic strength, and postsynaptic cell type. *J Neurosci*, 18(24):10464–72.
- Binns, K., Taylor, P., Sicheri, F., Pawson, T., and Holland, S. (2000). Phosphorylation of tyrosine residues in the kinase domain and juxtamembrane region regulates the biological and catalytic activities of Eph receptors. *Mol Cell Biol*, 20(13):4791–805.
- Bishop, D. L., Misgeld, T., Walsh, M. K., Gan, W.-B., and Lichtman, J. W. (2004). Axon branch removal at developing synapses by axosome shedding. *Neuron*, 44(4):651–61.
- Bliss, T. and Collingridge, G. (1993). A synaptic model of memory: long-term potentiation in the hippocampus. *Nature*, 361(6407):31–9.
- Bliss, T. and Lomo, T. (1973). Long-lasting potentiation of synaptic transmission in the dentate area of the anaesthetized rabbit following stimulation of the perforant path. *J Physiol*, 232(2):331–56.
- Bonhoeffer, T. and Yuste, R. (2002). Spine motility. Phenomenology, mechanisms, and function. *Neuron*, 35(6):1019–27.
- Bossing, T. and Brand, A. H. (2002). Dephrin, a transmembrane ephrin with a unique structure, prevents interneuronal axons from exiting the Drosophila embryonic CNS. *Development*, 129(18):4205–18.
- Boyer, C., Schikorski, T., and Stevens, C. (1998). Comparison of hippocampal dendritic spines in culture and in brain. *J Neurosci*, 18(14):5294–300.
- Béïque, J.-C. and Andrade, R. (2003). PSD-95 regulates synaptic transmission and plasticity in rat cerebral cortex. *J Physiol*, 546(Pt 3):859–67.
- Brambilla, R., Schnapp, A., Casagrande, F., Labrador, J., Bergemann, A., Flanagan, J., Pasquale, E., and Klein, R. (1995). Membrane-bound LERK2 ligand can signal through three different Eph-related receptor tyrosine kinases. *EMBO J*, 14(13):3116–26.
- Brückner, K., Labrador, J. P., Scheiffele, P., Herb, A., Seeburg, P., and Klein, R. (1999). EphrinB ligands recruit GRIP family PDZ adaptor proteins into raft membrane microdomains. *Neuron*, 22(3):511–24.

- Brückner, K., Pasquale, E., and Klein, R. (1997). Tyrosine phosphorylation of transmembrane ligands for Eph receptors. *Science*, 275(5306):1640–3.
- Brown, D. and London, E. (1998). Functions of lipid rafts in biological membranes. *Annu Rev Cell Dev Biol*, 14:111–36.
- Brown, D. and London, E. (2000). Structure and function of sphingolipid- and cholesterol-rich membrane rafts. *J Biol Chem*, 275(23):17221–4.
- Buchert, M., Schneider, S., Meskenaite, V., Adams, M., Canaani, E., Baechi, T., Moelling, K., and Hovens, C. (1999). The junction-associated protein AF-6 interacts and clusters with specific Eph receptor tyrosine kinases at specialized sites of cell-cell contact in the brain. *J Cell Biol*, 144(2):361–71.
- Burke, P., Schooler, K., and Wiley, H. (2001). Regulation of epidermal growth factor receptor signaling by endocytosis and intracellular trafficking. *Mol Biol Cell*, 12(6):1897–910.
- Bushong, E. A., Martone, M. E., and Ellisman, M. H. (2003). Examination of the relationship between astrocyte morphology and laminar boundaries in the molecular layer of adult dentate gyrus. *J Comp Neurol*, 462(2):241–51.
- Bushong, E. A., Martone, M. E., and Ellisman, M. H. (2004). Maturation of astrocyte morphology and the establishment of astrocyte domains during postnatal hippocampal development. *Int J Dev Neurosci*, 22(2):73–86.
- Cajal, R. (1888). Estructura de los centros nerviosos de las aves. *Rev Trim Histol Norm Pat*, 1:1–10.
- Caroni, P. (1997). Overexpression of growth-associated proteins in the neurons of adult transgenic mice. *J Neurosci Methods*, 71(1):3–9.
- Castillo, P., Malenka, R., and Nicoll, R. (1997). Kainate receptors mediate a slow postsynaptic current in hippocampal CA3 neurons. *Nature*, 388(6638):182–6.
- Chimini, G. and Chavrier, P. (2000). Function of Rho family proteins in actin dynamics during phagocytosis and engulfment. *Nat Cell Biol*, 2(10):E191–6.
- Chin-Sang, I., George, S., Ding, M., Moseley, S., Lynch, A., and Chisholm, A. (1999). The ephrin VAB-2/EFN-1 functions in neuronal signaling to regulate epidermal morphogenesis in *C. elegans*. *Cell*, 99(7):781–90.

- Chittajallu, R., Vignes, M., Dev, K., Barnes, J., Collingridge, G., and Henley, J. (1996). Regulation of glutamate release by presynaptic kainate receptors in the hippocampus. *Nature*, 379(6560):78–81.
- Choi, S. and Park, S. (1999). Phosphorylation at Tyr-838 in the kinase domain of EphA8 modulates Fyn binding to the Tyr-615 site by enhancing tyrosine kinase activity. *Oncogene*, 18(39):5413–22.
- Collingridge, G., Kehl, S., and McLennan, H. (1983). Excitatory amino acids in synaptic transmission in the Schaffer collateral-commissural pathway of the rat hippocampus. *J Physiol*, 334:33–46.
- Conner, S. D. and Schmid, S. L. (2003). Regulated portals of entry into the cell. *Nature*, 422(6927):37–44.
- Conover, J., Doetsch, F., Garcia-Verdugo, J., Gale, N., Yancopoulos, G., and Alvarez-Buylla, A. (2000). Disruption of Eph/ephrin signaling affects migration and proliferation in the adult subventricular zone. *Nat Neurosci*, 3(11):1091–7.
- Contractor, A., Rogers, C., Maron, C., Henkemeyer, M., Swanson, G. T., and Heinemann, S. F. (2002). Trans-synaptic Eph receptor-ephrin signaling in hippocampal mossy fiber LTP. *Science*, 296(5574):1864–9.
- Contractor, A., Swanson, G., Sailer, A., O’Gorman, S., and Heinemann, S. (2000). Identification of the kainate receptor subunits underlying modulation of excitatory synaptic transmission in the CA3 region of the hippocampus. *J Neurosci*, 20(22):8269–78.
- Cowan, C. and Henkemeyer, M. (2001). The SH2/SH3 adaptor Grb4 transduces B-ephrin reverse signals. *Nature*, 413(6852):174–9.
- Cowan, C., Yokoyama, N., Bianchi, L., Henkemeyer, M., and Fritsch, B. (2000). EphB2 guides axons at the midline and is necessary for normal vestibular function. *Neuron*, 26(2):417–30.
- Dai, Y. (1999). *Drosophila melanogaster* ephrin mrna, complete cds. *GenBank/EMBL/DDBJ*, pp. AF216287.
- Dailey, M. and Smith, S. (1996). The dynamics of dendritic structure in developing hippocampal slices. *J Neurosci*, 16(9):2983–94.

- Dalva, M., Takasu, M., Lin, M., Shamah, S., Hu, L., Gale, N., and Greenberg, M. (2000). EphB receptors interact with NMDA receptors and regulate excitatory synapse formation. *Cell*, 103(6):945–56.
- Danbolt, N. (2001). Glutamate uptake. *Prog Neurobiol*, 65(1):1–105.
- Davy, A., Gale, N., Murray, E., Klinghoffer, R., Soriano, P., Feuerstein, C., and Robbins, S. (1999). Compartmentalized signaling by GPI-anchored ephrin-A5 requires the Fyn tyrosine kinase to regulate cellular adhesion. *Genes Dev*, 13(23):3125–35.
- Davy, A. and Robbins, S. (2000). Ephrin-A5 modulates cell adhesion and morphology in an integrin-dependent manner. *EMBO J*, 19(20):5396–405.
- Daw, M., Chittajallu, R., Bortolotto, Z., Dev, K., Duprat, F., Henley, J., Collingridge, G., and Isaac, J. (2000). PDZ proteins interacting with C-terminal GluR2/3 are involved in a PKC-dependent regulation of AMPA receptors at hippocampal synapses. *Neuron*, 28(3):873–86.
- de Hoop, M. J., Meyn, L., and Dotti, C. (1998). *Culturing Hippocampal Neurons and Astrocytes from Fetal Rodent Brain*, volume 1. Cell Biology: A laboratory Handbook, second edition.
- Dingledine, R., Borges, K., Bowie, D., and Traynelis, S. (1999). The glutamate receptor ion channels. *Pharmacol Rev*, 51(1):7–61.
- Dodelet, V. and Pasquale, E. (2000). Eph receptors and ephrin ligands: embryogenesis to tumorigenesis. *Oncogene*, 19(49):5614–9.
- Doyle, D., Lee, A., Lewis, J., Kim, E., Sheng, M., and MacKinnon, R. (1996). Crystal structures of a complexed and peptide-free membrane protein-binding domain: molecular basis of peptide recognition by PDZ. *Cell*, 85(7):1067–76.
- Ehrlich, I. and Malinow, R. (2004). Postsynaptic density 95 controls AMPA receptor incorporation during long-term potentiation and experience-driven synaptic plasticity. *J Neurosci*, 24(4):916–27.
- El-Husseini, A., Schnell, E., Chetkovich, D., Nicoll, R., and Brecht, D. (2000). PSD-95 involvement in maturation of excitatory synapses. *Science*, 290(5495):1364–8.
- Eph Nomenclature Committee (1997). Unified nomenclature for Eph family receptors and their ligands, the ephrins. *Cell*, 90(3):403–4.

- Ethell, I., Irie, F., Kalo, M., Couchman, J., Pasquale, E., and Yamaguchi, Y. (2001). EphB/syndecan-2 signaling in dendritic spine morphogenesis. *Neuron*, 31(6):1001–13.
- Ethell, I. and Yamaguchi, Y. (1999). Cell surface heparan sulfate proteoglycan syndecan-2 induces the maturation of dendritic spines in rat hippocampal neurons. *J Cell Biol*, 144(3):575–86.
- Feng, G., Mellor, R., Bernstein, M., Keller-Peck, C., Nguyen, Q., Wallace, M., Nerbonne, J., Lichtman, J., and Sanes, J. (2000). Imaging neuronal subsets in transgenic mice expressing multiple spectral variants of GFP. *Neuron*, 28(1):41–51.
- Fiala, J., Feinberg, M., Popov, V., and Harris, K. (1998). Synaptogenesis via dendritic filopodia in developing hippocampal area CA1. *J Neurosci*, 18(21):8900–11.
- Finne, E. F., Munthe, E., and Aasheim, H.-C. (2004). A new ephrin-A1 isoform (ephrin-A1b) with altered receptor binding properties abrogates the cleavage of ephrin-A1a. *Biochem J*, 379(Pt 1):39–46.
- Flanagan, J. and Vanderhaeghen, P. (1998). The ephrins and Eph receptors in neural development. *Annu Rev Neurosci*, 21:309–45.
- Flint, A., Maisch, U., Weishaupt, J., Kriegstein, A., and Monyer, H. (1997). NR2A subunit expression shortens NMDA receptor synaptic currents in developing neocortex. *J Neurosci*, 17(7):2469–76.
- Freeman, M. R., Delrow, J., Kim, J., Johnson, E., and Doe, C. Q. (2003). Unwrapping glial biology: Gcm target genes regulating glial development, diversification, and function. *Neuron*, 38(4):567–80.
- Freund, T. and Buzsáki, G. (1996). Interneurons of the hippocampus. *Hippocampus*, 6(4):347–470.
- Fujii, S., Saito, K., Miyakawa, H., Ito, K., and Kato, H. (1991). Reversal of long-term potentiation (depotentiation) induced by tetanus stimulation of the input to CA1 neurons of guinea pig hippocampal slices. *Brain Res*, 555(1):112–22.
- Gale, N., Holland, S., Valenzuela, D., Flenniken, A., Pan, L., Ryan, T., Henkemeyer, M., Strebhardt, K., Hirai, H., Wilkinson, D., Pawson, T., Davis, S., and Yancopoulos, G. (1996). Eph receptors and ligands comprise two major specificity subclasses and are reciprocally compartmentalized during embryogenesis. *Neuron*, 17(1):9–19.

- Gao, P., Yue, Y., Zhang, J., Cerretti, D., Levitt, P., and Zhou, R. (1998a). Regulation of thalamic neurite outgrowth by the Eph ligand ephrin-A5: implications in the development of thalamocortical projections. *Proc Natl Acad Sci U S A*, 95(9):5329–34.
- Gao, W., Shinsky, N., Armanini, M., Moran, P., Zheng, J., Mendoza-Ramirez, J., Phillips, H., Winslow, J., and Caras, I. (1998b). Regulation of hippocampal synaptic plasticity by the tyrosine kinase receptor, REK7/EphA5, and its ligand, AL-1/Ephrin-A5. *Mol Cell Neurosci*, 11(5-6):247–59.
- George, S., Simokat, K., Hardin, J., and Chisholm, A. (1998). The VAB-1 Eph receptor tyrosine kinase functions in neural and epithelial morphogenesis in *C. elegans*. *Cell*, 92(5):633–43.
- Gerety, S., Wang, H., Chen, Z., and Anderson, D. (1999). Symmetrical mutant phenotypes of the receptor EphB4 and its specific transmembrane ligand ephrin-B2 in cardiovascular development. *Mol Cell*, 4(3):403–14.
- Ghosh, S. and Koenig, E. (1977). Isolation of non-myelin plasma membranes unique to white matter. *Biochim Biophys Acta*, 470(1):104–12.
- Goetze, B., Grunewald, B., Kiebler, M. A., and Macchi, P. (2003). Coupling the iron-responsive element to GFP—an inducible system to study translation in a single living cell. *Sci STKE*, 2003(204):PL12.
- Goldshmit, Y., Galea, M. P., Wise, G., Bartlett, P. F., and Turnley, A. M. (2004). Axonal regeneration and lack of astrocytic gliosis in EphA4-deficient mice. *J Neurosci*, 24(45):10064–73.
- Grunwald, I., Korte, M., Wolfer, D., Wilkinson, G., Unsicker, K., Lipp, H., Bonhoeffer, T., and Klein, R. (2001). Kinase-independent requirement of EphB2 receptors in hippocampal synaptic plasticity. *Neuron*, 32(6):1027–40.
- Grunwald, I. C., Korte, M., Adelmann, G., Plueck, A., Kullander, K., Adams, R. H., Frotscher, M., Bonhoeffer, T., and Klein, R. (2004). Hippocampal plasticity requires postsynaptic ephrinBs. *Nat Neurosci*, 7(1):33–40.
- Guillaud, L., Setou, M., and Hirokawa, N. (2003). KIF17 dynamics and regulation of NR2B trafficking in hippocampal neurons. *J Neurosci*, 23(1):131–40.
- Haj, F. G., Verveer, P. J., Squire, A., Neel, B. G., and Bastiaens, P. I. H. (2002). Imaging sites of receptor dephosphorylation by PTP1B on the surface of the endoplasmic reticulum. *Science*, 295(5560):1708–11.

- Hall, A. and Nobes, C. (2000). Rho GTPases: molecular switches that control the organization and dynamics of the actin cytoskeleton. *Philos Trans R Soc Lond B Biol Sci*, 355(1399):965–70.
- Hama, H., Hara, C., Yamaguchi, K., and Miyawaki, A. (2004). PKC signaling mediates global enhancement of excitatory synaptogenesis in neurons triggered by local contact with astrocytes. *Neuron*, 41(3):405–15.
- Harris, K. (1999). Structure, development, and plasticity of dendritic spines. *Curr Opin Neurobiol*, 9(3):343–8.
- Harris, K., Jensen, F., and Tsao, B. (1992). Three-dimensional structure of dendritic spines and synapses in rat hippocampus (CA1) at postnatal day 15 and adult ages: implications for the maturation of synaptic physiology and long-term potentiation. *J Neurosci*, 12(7):2685–705.
- Harris, K. and Stevens, J. (1989). Dendritic spines of CA 1 pyramidal cells in the rat hippocampus: serial electron microscopy with reference to their biophysical characteristics. *J Neurosci*, 9(8):2982–97.
- Hattori, M., Osterfield, M., and Flanagan, J. (2000). Regulated cleavage of a contact-mediated axon repellent. *Science*, 289(5483):1360–5.
- Haydon, P. (2001). GLIA: listening and talking to the synapse. *Nat Rev Neurosci*, 2(3):185–93.
- Hebb, D. (1949). *The Organization of Behavior; a Neuropsychological Theory*. Wiley-Interscience, New York. reprinted by Lawrence Erlbaum Associates, 2002.
- Henderson, J., Georgiou, J., Jia, Z., Robertson, J., Elowe, S., Roder, J., and Pawson, T. (2001). The receptor tyrosine kinase EphB2 regulates NMDA-dependent synaptic function. *Neuron*, 32(6):1041–56.
- Henkemeyer, M., Itkis, O. S., Ngo, M., Hickmott, P. W., and Ethell, I. M. (2003). Multiple EphB receptor tyrosine kinases shape dendritic spines in the hippocampus. *J Cell Biol*, 163(6):1313–26.
- Henkemeyer, M., Orioli, D., Henderson, J., Saxton, T., Roder, J., Pawson, T., and Klein, R. (1996). Nuk controls pathfinding of commissural axons in the mammalian central nervous system. *Cell*, 86(1):35–46.
- Hering, H., Lin, C.-C., and Sheng, M. (2003). Lipid rafts in the maintenance of synapses, dendritic spines, and surface AMPA receptor stability. *J Neurosci*, 23(8):3262–71.

- Himanen, J., Rajashankar, K., Lackmann, M., Cowan, C., Henkemeyer, M., and Nikolov, D. (2001). Crystal structure of an Eph receptor-ephrin complex. *Nature*, 414(6866):933–8.
- Himanen, J.-P., Chumley, M. J., Lackmann, M., Li, C., Barton, W. A., Jeffrey, P. D., Vearing, C., Geleick, D., Feldheim, D. A., Boyd, A. W., Henkemeyer, M., and Nikolov, D. B. (2004). Repelling class discrimination: ephrin-A5 binds to and activates EphB2 receptor signaling. *Nat Neurosci*, 7(5):501–9.
- Himanen, J.-P. and Nikolov, D. B. (2003). Eph signaling: a structural view. *Trends Neurosci*, 26(1):46–51.
- Hindges, R., McLaughlin, T., Genoud, N., Henkemeyer, M., and O’Leary, D. D. M. (2002). EphB forward signaling controls directional branch extension and arborization required for dorsal-ventral retinotopic mapping. *Neuron*, 35(3):475–87.
- Hirai, H., Maru, Y., Hagiwara, K., Nishida, J., and Takaku, F. (1987). A novel putative tyrosine kinase receptor encoded by the eph gene. *Science*, 238(4834):1717–20.
- Hock, B., Böhme, B., Karn, T., Feller, S., Rübsamen-Waigmann, H., and Strebhardt, K. (1998a). Tyrosine-614, the major autophosphorylation site of the receptor tyrosine kinase HEK2, functions as multi-docking site for SH2-domain mediated interactions. *Oncogene*, 17(2):255–60.
- Hock, B., Böhme, B., Karn, T., Yamamoto, T., Kaibuchi, K., Holtrich, U., Holland, S., Pawson, T., Rübsamen-Waigmann, H., and Strebhardt, K. (1998b). PDZ-domain-mediated interaction of the Eph-related receptor tyrosine kinase EphB3 and the ras-binding protein AF6 depends on the kinase activity of the receptor. *Proc Natl Acad Sci U S A*, 95(17):9779–84.
- Holder, N. and Klein, R. (1999). Eph receptors and ephrins: effectors of morphogenesis. *Development*, 126(10):2033–44.
- Holland, S., Gale, N., Mbamalu, G., Yancopoulos, G., Henkemeyer, M., and Pawson, T. (1996). Bidirectional signalling through the EPH-family receptor Nuk and its transmembrane ligands. *Nature*, 383(6602):722–5.
- Hollmann, M. and Heinemann, S. (1994). Cloned glutamate receptors. *Annu Rev Neurosci*, 17:31–108.
- Horner, P. J. and Palmer, T. D. (2003). New roles for astrocytes: the nightlife of an ‘astrocyte’. La vida loca! *Trends Neurosci*, 26(11):597–603.

- Huai, J. and Drescher, U. (2001). An ephrin-A-dependent signaling pathway controls integrin function and is linked to the tyrosine phosphorylation of a 120-kDa protein. *J Biol Chem*, 276(9):6689–94.
- Hubbard, S. R. (2004). Juxtamembrane autoinhibition in receptor tyrosine kinases. *Nat Rev Mol Cell Biol*, 5(6):464–71.
- Husi, H., Ward, M., Choudhary, J., Blackstock, W., and Grant, S. (2000). Proteomic analysis of NMDA receptor-adhesion protein signaling complexes. *Nat Neurosci*, 3(7):661–9.
- Irie, F. and Yamaguchi, Y. (2002). EphB receptors regulate dendritic spine development via intersectin, Cdc42 and N-WASP. *Nat Neurosci*, 5(11):1117–8.
- Johnson, L., Noble, M., and Owen, D. (1996). Active and inactive protein kinases: structural basis for regulation. *Cell*, 85(2):149–58.
- Kalo, M. and Pasquale, E. (1999). Multiple in vivo tyrosine phosphorylation sites in EphB receptors. *Biochemistry*, 38(43):14396–408.
- Kandel, E. (2001). The molecular biology of memory storage: a dialogue between genes and synapses. *Science*, 294(5544):1030–8.
- Kandel, E. R., Schwartz, J. H., and Jessell, T. M., editors (2000). *Principles of Neural Science*. McGraw-Hill, fourth edition edition.
- Kang, J., Jiang, L., Goldman, S., and Nedergaard, M. (1998). Astrocyte-mediated potentiation of inhibitory synaptic transmission. *Nat Neurosci*, 1(8):683–92.
- Katz, L. (1987). Local circuitry of identified projection neurons in cat visual cortex brain slices. *J Neurosci*, 7(4):1223–49.
- Katz, L. and Shatz, C. (1996). Synaptic activity and the construction of cortical circuits. *Science*, 274(5290):1133–8.
- Kauer, J., Malenka, R., and Nicoll, R. (1988). NMDA application potentiates synaptic transmission in the hippocampus. *Nature*, 334(6179):250–2.
- Kennedy, M. (1998). Signal transduction molecules at the glutamatergic postsynaptic membrane. *Brain Res Brain Res Rev*, 26(2-3):243–57.

- Klein, R. (2001). Excitatory Eph receptors and adhesive ephrin ligands. *Curr Opin Cell Biol*, 13(2):196–203.
- Klein, R. (2004). Eph/ephrin signaling in morphogenesis, neural development and plasticity. *Curr Opin Cell Biol*, 16(5):580–9.
- Krull, C., Lansford, R., Gale, N., Collazo, A., Marcelle, C., Yancopoulos, G., Fraser, S., and Bronner-Fraser, M. (1997). Interactions of Eph-related receptors and ligands confer rostro-caudal pattern to trunk neural crest migration. *Curr Biol*, 7(8):571–80.
- Kullander, K. and Klein, R. (2002). Mechanisms and functions of Eph and ephrin signalling. *Nat Rev Mol Cell Biol*, 3(7):475–86.
- Kullander, K., Mather, N., Diella, F., Dottori, M., Boyd, A., and Klein, R. (2001). Kinase-dependent and kinase-independent functions of EphA4 receptors in major axon tract formation in vivo. *Neuron*, 29(1):73–84.
- Kurten, R. C. (2003). Sorting motifs in receptor trafficking. *Adv Drug Deliv Rev*, 55(11):1405–19.
- Laake, J., Slyngstad, T., Haug, F., and Ottersen, O. (1995). Glutamine from glial cells is essential for the maintenance of the nerve terminal pool of glutamate: immunogold evidence from hippocampal slice cultures. *J Neurochem*, 65(2):871–81.
- Lackmann, M., Oates, A., Dottori, M., Smith, F., Do, C., Power, M., Kravets, L., and Boyd, A. (1998). Distinct subdomains of the EphA3 receptor mediate ligand binding and receptor dimerization. *J Biol Chem*, 273(32):20228–37.
- Laming, P., Sykova, E., Reichenbach, A., Hatton, G., and Bauer, H. (1998). *Glial cells: their role in behaviour*. Cambridge UP, Cambridge, UK.
- Lee, T., Lee, A., and Luo, L. (1999). Development of the *Drosophila* mushroom bodies: sequential generation of three distinct types of neurons from a neuroblast. *Development*, 126(18):4065–76.
- Li, Z. and Sheng, M. (2003). Some assembly required: the development of neuronal synapses. *Nat Rev Mol Cell Biol*, 4(11):833–41.
- Lin, D., Gish, G., Songyang, Z., and Pawson, T. (1999). The carboxyl terminus of B class ephrins constitutes a PDZ domain binding motif. *J Biol Chem*, 274(6):3726–33.

- Lledo, P., Zhang, X., Südhof, T., Malenka, R., and Nicoll, R. (1998). Postsynaptic membrane fusion and long-term potentiation. *Science*, 279(5349):399–403.
- Lu, Q., Sun, E., Klein, R., and Flanagan, J. (2001). Ephrin-B reverse signaling is mediated by a novel PDZ-RGS protein and selectively inhibits G protein-coupled chemoattraction. *Cell*, 105(1):69–79.
- Man, H., Lin, J., Ju, W., Ahmadian, G., Liu, L., Becker, L., Sheng, M., and Wang, Y. (2000). Regulation of AMPA receptor-mediated synaptic transmission by clathrin-dependent receptor internalization. *Neuron*, 25(3):649–62.
- Mann, F., Miranda, E., Weinl, C., Harmer, E., and Holt, C. E. (2003). B-type Eph receptors and ephrins induce growth cone collapse through distinct intracellular pathways. *J Neurobiol*, 57(3):323–36.
- Mann, F., Ray, S., Harris, W., and Holt, C. (2002). Topographic mapping in dorsoventral axis of the *Xenopus* retinotectal system depends on signaling through ephrin-B ligands. *Neuron*, 35(3):461–73.
- Marmor, M. D. and Yarden, Y. (2004). Role of protein ubiquitylation in regulating endocytosis of receptor tyrosine kinases. *Oncogene*, 23(11):2057–70.
- Marston, D. J., Dickinson, S., and Nobes, C. D. (2003). Rac-dependent trans-endocytosis of ephrinBs regulates Eph-ephrin contact repulsion. *Nat Cell Biol*, 5(10):879–88.
- Matthias, K., Kirchhoff, F., Seifert, G., Hüttmann, K., Matyash, M., Kettenmann, H., and Steinhäuser, C. (2003). Segregated expression of AMPA-type glutamate receptors and glutamate transporters defines distinct astrocyte populations in the mouse hippocampus. *J Neurosci*, 23(5):1750–8.
- Matus, A., Brinkhaus, H., and Wagner, U. (2000). Actin dynamics in dendritic spines: a form of regulated plasticity at excitatory synapses. *Hippocampus*, 10(5):555–60.
- Miao, H., Wei, B., Peehl, D., Li, Q., Alexandrou, T., Schelling, J., Rhim, J., Sedor, J., Burnett, E., and Wang, B. (2001). Activation of EphA receptor tyrosine kinase inhibits the Ras/MAPK pathway. *Nat Cell Biol*, 3(5):527–30.
- Miller, M. and Peters, A. (1981). Maturation of rat visual cortex. II. A combined Golgi-electron microscope study of pyramidal neurons. *J Comp Neurol*, 203(4):555–73.

- Montgomery, J. M. and Madison, D. V. (2004). Discrete synaptic states define a major mechanism of synapse plasticity. *Trends Neurosci*, 27(12):744–50.
- Mulkey, R. and Malenka, R. (1992). Mechanisms underlying induction of homosynaptic long-term depression in area CA1 of the hippocampus. *Neuron*, 9(5):967–75.
- Muller, D. and Lynch, G. (1988). Long-term potentiation differentially affects two components of synaptic responses in hippocampus. *Proc Natl Acad Sci U S A*, 85(23):9346–50.
- Murai, K. K., Nguyen, L. N., Irie, F., Yamaguchi, Y., and Pasquale, E. B. (2003). Control of hippocampal dendritic spine morphology through ephrin-A3/EphA4 signaling. *Nat Neurosci*, 6(2):153–60.
- Murai, K. K. and Pasquale, E. B. (2003). 'Eph'ective signaling: forward, reverse and crosstalk. *J Cell Sci*, 116(Pt 14):2823–32.
- Murai, K. K. and Pasquale, E. B. (2004). Eph receptors, ephrins, and synaptic function. *Neuroscientist*, 10(4):304–14.
- Nakayama, A., Harms, M., and Luo, L. (2000). Small GTPases Rac and Rho in the maintenance of dendritic spines and branches in hippocampal pyramidal neurons. *J Neurosci*, 20(14):5329–38.
- Nedergaard, M., Ransom, B., and Goldman, S. A. (2003). New roles for astrocytes: redefining the functional architecture of the brain. *Trends Neurosci*, 26(10):523–30.
- Newman, E. A. (2003). New roles for astrocytes: regulation of synaptic transmission. *Trends Neurosci*, 26(10):536–42.
- Nägerl, U. V., Eberhorn, N., Cambridge, S. B., and Bonhoeffer, T. (2004). Bidirectional activity-dependent morphological plasticity in hippocampal neurons. *Neuron*, 44(5):759–67.
- Nichols, B. and Lippincott-Schwartz, J. (2001). Endocytosis without clathrin coats. *Trends Cell Biol*, 11(10):406–12.
- Norenberg, M. and Martinez-Hernandez, A. (1979). Fine structural localization of glutamine synthetase in astrocytes of rat brain. *Brain Res*, 161(2):303–10.
- Oates, A., Lackmann, M., Power, M., Brennan, C., Down, L., Do, C., Evans, B., Holder, N., and Boyd, A. (1999). An early developmental role for eph-ephrin interaction during vertebrate gastrulation. *Mech Dev*, 83(1-2):77–94.

- Ogata, K. and Kosaka, T. (2002). Structural and quantitative analysis of astrocytes in the mouse hippocampus. *Neuroscience*, 113(1):221–33.
- Orioli, D. and Klein, R. (1997). The Eph receptor family: axonal guidance by contact repulsion. *Trends Genet*, 13(9):354–9.
- Palmer, A. and Klein, R. (2003). Multiple roles of ephrins in morphogenesis, neuronal networking, and brain function. *Genes Dev*, 17(12):1429–50.
- Palmer, A., Zimmer, M., Erdmann, K. S., Eulenburg, V., Porthin, A., Heumann, R., Deutsch, U., and Klein, R. (2002). EphrinB phosphorylation and reverse signaling: regulation by Src kinases and PTP-BL phosphatase. *Mol Cell*, 9(4):725–37.
- Papa, M., Bundman, M., Greenberger, V., and Segal, M. (1995). Morphological analysis of dendritic spine development in primary cultures of hippocampal neurons. *J Neurosci*, 15(1 Pt 1):1–11.
- Parker, M., Roberts, R., Enriquez, M., Zhao, X., Takahashi, T., Cerretti, D. P., Daniel, T., and Chen, J. (2004). Reverse endocytosis of transmembrane ephrin-B ligands via a clathrin-mediated pathway. *Biochem Biophys Res Commun*, 323(1):17–23.
- Pawson, T. and Scott, J. (1997). Signaling through scaffold, anchoring, and adaptor proteins. *Science*, 278(5346):2075–80.
- Penzes, P., Beeser, A., Chernoff, J., Schiller, M. R., Eipper, B. A., Mains, R. E., and Huganir, R. L. (2003). Rapid induction of dendritic spine morphogenesis by trans-synaptic ephrinB-EphB receptor activation of the Rho-GEF kalirin. *Neuron*, 37(2):263–74.
- Peters, A., Palay, S., and Webster, H. (1991). *The fine structure of the nervous system. Neurons and their supporting cells*. Oxford University Press, 3. edition.
- Pfrieger, F. and Barres, B. (1997). Synaptic efficacy enhanced by glial cells in vitro. *Science*, 277(5332):1684–7.
- Pin, J. and Duvoisin, R. (1995). The metabotropic glutamate receptors: structure and functions. *Neuropharmacology*, 34(1):1–26.
- Plattner, R., Kadlec, L., DeMali, K., Kazlauskas, A., and Pendergast, A. (1999). c-Abl is activated by growth factors and Src family kinases and has a role in the cellular response to PDGF. *Genes Dev*, 13(18):2400–11.

- Poo, M. (2001). Neurotrophins as synaptic modulators. *Nat Rev Neurosci*, 2(1):24–32.
- Pow, D. and Robinson, S. (1994). Glutamate in some retinal neurons is derived solely from glia. *Neuroscience*, 60(2):355–66.
- Presley, J., Mayor, S., McGraw, T., Dunn, K., and Maxfield, F. (1997). Bafilomycin A1 treatment retards transferrin receptor recycling more than bulk membrane recycling. *J Biol Chem*, 272(21):13929–36.
- Ronnevi, L. (1978). Origin of the glial processes responsible for the spontaneous postnatal phagocytosis of boutons on cat spinal motoneurons. *Cell Tissue Res*, 189(2):203–17.
- Scannevin, R. and Huganir, R. (2000). Postsynaptic organization and regulation of excitatory synapses. *Nat Rev Neurosci*, 1(2):133–41.
- Schlessinger, J. (2000). Cell signaling by receptor tyrosine kinases. *Cell*, 103(2):211–25.
- Scott, E. and Luo, L. (2001). How do dendrites take their shape? *Nat Neurosci*, 4(4):359–65.
- Scully, A., McKeown, M., and Thomas, J. (1999). Isolation and characterization of Dek, a *Drosophila* eph receptor protein tyrosine kinase. *Mol Cell Neurosci*, 13(5):337–47.
- Seil, F. (1997). Serial changes in granulo-prival cerebellar cultures after transplantation with granule cells and glia: a timed ultrastructural study. *Neuroscience*, 77(3):695–711.
- Shamah, S., Lin, M., Goldberg, J., Estrach, S., Sahin, M., Hu, L., Bazalakova, M., Neve, R., Corfas, G., Debant, A., and Greenberg, M. (2001). EphA receptors regulate growth cone dynamics through the novel guanine nucleotide exchange factor ephexin. *Cell*, 105(2):233–44.
- Shank, R., Bennett, G., Freytag, S., and Campbell, G. (1985). Pyruvate carboxylase: an astrocyte-specific enzyme implicated in the replenishment of amino acid neurotransmitter pools. *Brain Res*, 329(1-2):364–7.
- Shatz, C. (1996). Emergence of order in visual system development. *Proc Natl Acad Sci U S A*, 93(2):602–8.
- Sheng, M. (2001). Molecular organization of the postsynaptic specialization. *Proc Natl Acad Sci U S A*, 98(13):7058–61.

- Shi, S., Hayashi, Y., Esteban, J., and Malinow, R. (2001). Subunit-specific rules governing AMPA receptor trafficking to synapses in hippocampal pyramidal neurons. *Cell*, 105(3):331–43.
- Shi, S., Hayashi, Y., Petralia, R., Zaman, S., Wenthold, R., Svoboda, K., and Malinow, R. (1999). Rapid spine delivery and redistribution of AMPA receptors after synaptic NMDA receptor activation. *Science*, 284(5421):1811–6.
- Simard, M., Arcuino, G., Takano, T., Liu, Q. S., and Nedergaard, M. (2003). Signaling at the gliovascular interface. *J Neurosci*, 23(27):9254–62.
- Simons, K. and Ikonen, E. (1997). Functional rafts in cell membranes. *Nature*, 387(6633):569–72.
- Simons, K. and Toomre, D. (2000). Lipid rafts and signal transduction. *Nat Rev Mol Cell Biol*, 1(1):31–9.
- Songyang, Z., Fanning, A., Fu, C., Xu, J., Marfatia, S., Chishti, A., Crompton, A., Chan, A., Anderson, J., and Cantley, L. (1997). Recognition of unique carboxyl-terminal motifs by distinct PDZ domains. *Science*, 275(5296):73–7.
- Spacek, J. and Harris, K. M. (2004). Trans-endocytosis via spinules in adult rat hippocampus. *J Neurosci*, 24(17):4233–41.
- Stapleton, D., Balan, I., Pawson, T., and Sicheri, F. (1999). The crystal structure of an Eph receptor SAM domain reveals a mechanism for modular dimerization. *Nat Struct Biol*, 6(1):44–9.
- Stein, V., House, D. R. C., Brecht, D. S., and Nicoll, R. A. (2003). Postsynaptic density-95 mimics and occludes hippocampal long-term potentiation and enhances long-term depression. *J Neurosci*, 23(13):5503–6.
- Takasu, M. A., Dalva, M. B., Zigmond, R. E., and Greenberg, M. E. (2002). Modulation of NMDA receptor-dependent calcium influx and gene expression through EphB receptors. *Science*, 295(5554):491–5.
- Thanos, C., Goodwill, K., and Bowie, J. (1999). Oligomeric structure of the human EphB2 receptor SAM domain. *Science*, 283(5403):833–6.
- Torres, R., Firestein, B., Dong, H., Staudinger, J., Olson, E., Huganir, R., Brecht, D., Gale, N., and Yancopoulos, G. (1998). PDZ proteins bind, cluster, and synaptically colocalize with Eph receptors and their ephrin ligands. *Neuron*, 21(6):1453–63.

- Toth, J., Cutforth, T., Gelinas, A., Bethoney, K., Bard, J., and Harrison, C. (2001). Crystal structure of an ephrin ectodomain. *Dev Cell*, 1(1):83–92.
- Trachtenberg, J. T., Chen, B. E., Knott, G. W., Feng, G., Sanes, J. R., Welker, E., and Svoboda, K. (2002). Long-term in vivo imaging of experience-dependent synaptic plasticity in adult cortex. *Nature*, 420(6917):788–94.
- Ullian, E., Sapperstein, S., Christopherson, K., and Barres, B. (2001). Control of synapse number by glia. *Science*, 291(5504):657–61.
- Ullian, E. M., Christopherson, K. S., and Barres, B. A. (2004). Role for glia in synaptogenesis. *Glia*, 47(3):209–16.
- Ullrich, A. and Schlessinger, J. (1990). Signal transduction by receptors with tyrosine kinase activity. *Cell*, 61(2):203–12.
- van der Geer, P., Hunter, T., and Lindberg, R. (1994). Receptor protein-tyrosine kinases and their signal transduction pathways. *Annu Rev Cell Biol*, 10:251–337.
- Vignes, M., Clarke, V., Parry, M., Bleakman, D., Lodge, D., Ornstein, P., and Collingridge, G. (1998). The GluR5 subtype of kainate receptor regulates excitatory synaptic transmission in areas CA1 and CA3 of the rat hippocampus. *Neuropharmacology*, 37(10-11):1269–77.
- Volterra, A., Magistretti, P., and Haydon, P. (2002). *The Tripartite Synapse: Glia in Synaptic Transmission*. Oxford University Press.
- Waagepetersen, H., Qu, H., Schousboe, A., and Sonnewald, U. (2001). Elucidation of the quantitative significance of pyruvate carboxylation in cultured cerebellar neurons and astrocytes. *J Neurosci Res*, 66(5):763–70.
- Wahl, S., Barth, H., Ciossek, T., Aktories, K., and Mueller, B. (2000). Ephrin-A5 induces collapse of growth cones by activating Rho and Rho kinase. *J Cell Biol*, 149(2):263–70.
- Walikonis, R., Jensen, O., Mann, M., Provance, D., Mercer, J., and Kennedy, M. (2000). Identification of proteins in the postsynaptic density fraction by mass spectrometry. *J Neurosci*, 20(11):4069–80.
- Walker-Daniels, J., Riese, D. J., and Kinch, M. S. (2002). c-Cbl-dependent EphA2 protein degradation is induced by ligand binding. *Mol Cancer Res*, 1(1):79–87.

- Wang, X., Roy, P., Holland, S., Zhang, L., Culotti, J., and Pawson, T. (1999). Multiple ephrins control cell organization in *C. elegans* using kinase-dependent and -independent functions of the VAB-1 Eph receptor. *Mol Cell*, 4(6):903–13.
- Watts, R. J., Schuldiner, O., Perrino, J., Larsen, C., and Luo, L. (2004). Glia engulf degenerating axons during developmental axon pruning. *Curr Biol*, 14(8):678–84.
- Weible, M. and Hendry, I. (2003). What is the importance of multivesicular bodies in retrograde axonal transport in vivo? *J Neurobiol*, 58(2):230–43.
- Wenthold, R., Petralia, R., J. I. B., and Niedzielski, A. (1996). Evidence for multiple AMPA receptor complexes in hippocampal CA1/CA2 neurons. *J Neurosci*, 16(6):1982–9.
- Wilkinson, D. (2001). Multiple roles of EPH receptors and ephrins in neural development. *Nat Rev Neurosci*, 2(3):155–64.
- Winslow, J., Moran, P., Valverde, J., Shih, A., Yuan, J., Wong, S., Tsai, S., Goddard, A., Henzel, W., and Hefti, F. (1995). Cloning of AL-1, a ligand for an Eph-related tyrosine kinase receptor involved in axon bundle formation. *Neuron*, 14(5):973–81.
- Wisden, W. and Seeburg, P. (1993). A complex mosaic of high-affinity kainate receptors in rat brain. *J Neurosci*, 13(8):3582–98.
- Wybenga-Groot, L., Baskin, B., Ong, S., Tong, J., Pawson, T., and Sicheri, F. (2001). Structural basis for autoinhibition of the Ephb2 receptor tyrosine kinase by the unphosphorylated juxtamembrane region. *Cell*, 106(6):745–57.
- Yang, Y., Ge, W., Chen, Y., Zhang, Z., Shen, W., Wu, C., Poo, M., and Duan, S. (2003). Contribution of astrocytes to hippocampal long-term potentiation through release of D-serine. *Proc Natl Acad Sci U S A*, 100(25):15194–9.
- Yu, A., Drejer, J., Hertz, L., and Schousboe, A. (1983). Pyruvate carboxylase activity in primary cultures of astrocytes and neurons. *J Neurochem*, 41(5):1484–7.
- Yu, H., Zisch, A., Dodelet, V., and Pasquale, E. (2001). Multiple signaling interactions of Abl and Arg kinases with the EphB2 receptor. *Oncogene*, 20(30):3995–4006.
- Yuste, R. and Bonhoeffer, T. (2004). Genesis of dendritic spines: insights from ultrastructural and imaging studies. *Nat Rev Neurosci*, 5(1):24–34.

- Ziff, E. (1997). Enlightening the postsynaptic density. *Neuron*, 19(6):1163–74.
- Zimmer, M., Palmer, A., Köhler, J., and Klein, R. (2003). EphB-ephrinB bi-directional endocytosis terminates adhesion allowing contact mediated repulsion. *Nat Cell Biol*, 5(10):869–78.
- Zisch, A., Kalo, M., Chong, L., and Pasquale, E. (1998). Complex formation between EphB2 and Src requires phosphorylation of tyrosine 611 in the EphB2 juxtamembrane region. *Oncogene*, 16(20):2657–70.
- Zisch, A. and Pasquale, E. (1997). The Eph family: a multitude of receptors that mediate cell recognition signals. *Cell Tissue Res*, 290(2):217–26.
- Zisch, A., Pazzagli, C., Freeman, A., Schneller, M., Hadman, M., Smith, J., Ruoslahti, E., and Pasquale, E. (2000). Replacing two conserved tyrosines of the EphB2 receptor with glutamic acid prevents binding of SH2 domains without abrogating kinase activity and biological responses. *Oncogene*, 19(2):177–87.
- Ziv, N. and Smith, S. (1996). Evidence for a role of dendritic filopodia in synaptogenesis and spine formation. *Neuron*, 17(1):91–102.
- Zukerberg, L., Patrick, G., Nikolic, M., Humbert, S., Wu, C., Lanier, L., Gertler, F., Vidal, M., Etten, R. V., and Tsai, L. (2000). Cables links Cdk5 and c-Abl and facilitates Cdk5 tyrosine phosphorylation, kinase upregulation, and neurite outgrowth. *Neuron*, 26(3):633–46.

8. Acknowledgements

I would like to express special thanks to Tobias Bonhoeffer and Rüdiger Klein for giving me the opportunity to carry out my Ph.D. work in a great scientific environment. I sincerely appreciate their support and interest in my work, the constructive and critical discussions. I am especially grateful for the freedom I had during my thesis work, this allowed me to develop my own thoughts and interests. All this made my stay in their laboratories a great experience.

I would like to thank my committee members, Magdalena Götz and Albrecht Kossel, most sincerely for their interest, critical discussion, suggestions and encouragement. Additionally, I want to thank Albrecht Kossel for introducing me to the “world of neurons” and their cultures and especially for the fast and conscientious correction of this thesis and the helpful suggestions and comments.

Special thanks to my collaborators, especially Manuel Zimmer for his interest in the EphB-/ephrinB-ExFP fusion proteins, as well as Volker Staiger and Martin Korte, for their experimental contribution to this work and their support and interest. I want to thank Benedikt Berninger, Pico Caroni and Michael Greenberg for kindly providing DNA constructs (EGFP-DN-TrkB, wt EphB2 and the Thy1.2 expression cassette).

Special thanks are dedicated to Luca Dolce, John Bailey, Clara Eßmann and Sidney Cambridge for critically reading this thesis and constructive comments.

I want to thank my colleagues for the nice and relaxed atmosphere in the laboratory. The different characters, nationalities and temperaments always provided an interesting environment. Especially, I am grateful to Luca Dolce, Joaquim Egea, Clara Eßmann, Oliver Griesbeck, Laura Knott, Taija Mäkinen, Archana Mishra, Stefan Weinges and Manuel Zimmer, for their help, nice conversations and friendships.

8. Acknowledgements

I am grateful to Max Sperling for his availability in solving technical problems and always giving quick solutions.

I sincerely appreciated the scientific suggestions and endless scientific discussions of my Ph.D. fellows, especially Martin Wienisch and Bernhard Götze.

I want to thank Liane Meyn for introducing me to the secrets of glial cultures and for providing glial cultures and many liters of MEM-HS medium.

Special thanks to all the people of the service units at the Max-Planck-Institute, especially Michael Bösl, Maite Rodriguez-Manzaneque and Anna Dengler, who supported me with their professional and efficient work.

And many thanks to everyone who helped in any way contributing to this Ph.D. thesis.

I particularly acknowledge, Henning Lauterbach, for critically reading this thesis as a non-neurobiologist, his encouragement and his affectionate care when I was in need.

Finally, I want to thank my parents and my sisters, as well as my best friends, who supported and encouraged me during all this time, they deserve my deep gratitude.

A. Curriculum vitae

Personal data

Name	Jenny Köhler
Date of Birth	1st of October 1973
Place of Birth	Hanau, Germany
Nationality	German

Education

since 03/2005	Continuation of the Ph.D. project
03/2001-02/2005	Ph.D. thesis at the Max-Planck-Institute of Neurobiology, Munich, Germany, Dept. PD Dr. R. Klein & Prof. Dr. T. Bonhoeffer
04/2000	Diploma degree ("sehr gut")
04/99-03/2000	Diploma thesis at the Max-Planck-Institute of Immunobiology, Freiburg, Germany, Dept. Prof. Dr. M. Reth Thesis title: "The control of activation of B-cells by intracellular signal molecules."
10/1994-10/2000	Study of biology, Albert-Ludwigs-University, Freiburg, Germany major: Immunobiology minors: Neurobiology, Genetics, Neuropathology
09/1993-06/1994	Training as a chemistry technician

A. Curriculum vitae

06/1993

Baccalaureate (Abitur) at Lichtenberg-Oberstufen-Gymnasium,
Bruchköbel, Germany